

~~FEAR 88~~

30130

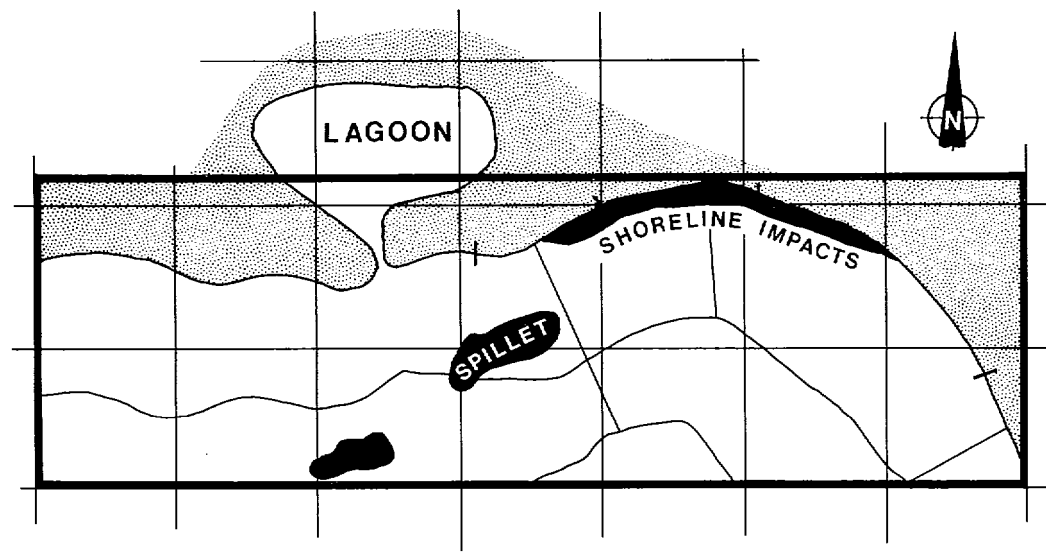
OCS STUDY MMS 88-0032

Final Report

DEVELOPMENT, TESTING AND VERIFICATION OF AN OIL SPILL SURF ZONE MASS TRANSPORT MODEL

Prepared for:

Minerals Management Service
Anchorage, Alaska



Prepared By:

Coastal Science &
Engineering, Inc.
Columbia, SC

Applied Science.
Associates, Inc.
Narragansett, RI

And

E-Tech, Inc.
Narragansett, RI

3690



REGISTERED

Final Report

OCS Study, MMS 88-0032

DEVELOPMENT, TESTING, AND VERIFICATION OF AN
OIL SPILL SURF-ZONE MASS-TRANSPORT MODEL

Prepared by:

Principal Investigators:

Mark Reed¹
Timothy W. Kana²
Erich R. Gundlach³

¹Applied Science Associates, Inc.
70 Dean Knauss Drive
Narragansett, RI 02882-1143

²Coastal Science & Engineering, Inc.
P.O. Box 8056
Columbia, SC 29202

³E-Tech, Inc.
70 Dean Knauss Drive
Narragansett, RI 02882

Contract No. 14-12-0001-30130

Alaska OCS Region
Minerals Management Service
949 East 36th Avenue, Room 110
Anchorage, AK 99508-4302

[CSE'87-88 R-12]
June 1988

Disclaimer: *The opinions, findings, conclusions or recommendations expressed in this report are those of the authors and do not necessarily reflect the views of the U.S. Department of the Interior, nor does mention of trade names or commercial products constitute endorsement or recommendation for use by the Federal Government.*

This study was funded by a contract between the Minerals Management Service and Coastal Science & Engineering, Inc. (CSE) with subcontracts between CSE and Applied Science Associates, Inc. (ASA) and Battelle New England Research Laboratory (Phase 1) and E-Tech, Inc. (Phase 11).

Study Participants: Phase II

Present Affiliation

Timothy W. Kana, Ph. D., Project Director	Coastal Science & Engineering, Inc.
Mark Reed, Ph. D., Co-Principal Investigator	Applied Science Associates, Inc.
Erich R. Gundlach,* Ph. D., Co-Principal Investigator	E-Tech, Inc.
Malcolm L. Spaulding, Ph. D., Reviewer	Applied Science Associates, Inc.
Katherine Jayko, M. S., Research Assistant	Applied Science Associates, Inc.
Will Knauss, B. A., Research Assistant	Applied Science Associates, Inc.
J. Steven Dingman, Ph. D., Research Associate	Coastal Science & Engineering, Inc.
Eric Anderson, M. S., Research Associate	Applied Science Associates, Inc.
Christopher P. Jones, P. E., Research Assistant	Coastal Science & Engineering, Inc.
William C. Eiser, M. S., Research Assistant	Coastal Science & Engineering, Inc.
Mark L. Williams, B. S., Field/Laboratory Assistant	Coastal Science & Engineering, Inc.
Heyward Robinson, B. S., Field Assistant	South Carolina Coastal Council
D. Bryan Stone, A. S., Field Assistant/Graphics	Coastal Science & Engineering, Inc.
Support Staff: D.R. Sangster, R. Elmore, B. Frame	Coastal Science & Engineering, Inc.

[*Former principal. Coastal Science & Engineering, Inc.]

ABSTRACT

This report describes phase II of a multiyear project to develop and test a probabilistic coastal zone oil spill (COZOIL) model for use by the Minerals Management Service (MMS). The report is divided into sections covering description of model algorithms, description and results of field surveys at a test site along Bristol Bay, flexibility of the model to implement various input data and user options, results of model tests for waves in the field study area, and results of model tests using prototype data from the *Amoco Cadiz* oil spill. Appendices include a Users' Manual with the model code in FORTRAN 77 (under separate cover) and observational data from the field site at Port Heiden (this volume).

The purpose of the project was to develop a generic, computer-based model for the simulation of oil spills entering the surf zone, impacting a shoreline, and transforming through time as a result of physical and chemical processes. COZOIL, therefore, builds on previous oil-spill trajectory and fates models which typically end with contact at the coastline.

The present model includes explicit representations of as many known, active processes as possible, partitioning oil quantities among air, water surface, water column and the substrate/ ground water systems in or near the surf zone. Eight shoreline types (e.g., smooth rocky, sand, marsh, and tidal lagoon) with varying oil holding capacities and seven oil types encompassing a range of viscosities can be simulated. Processes and fates simulated include:

Processes

- Winds - deterministic from a time-series or stochastic simulation
- Waves - modified CERC model RCPWAVE incorporating refraction, diffraction, breaking, height, and phase transformations
 - Wave runup and setup - from procedures outlined in CERC (1984)
 - Currents - tidal, wind-driven, and wave-induced including Reed et al. (1980), Longuet-Higgins (1970); Stive and Wind (1982)

Oil Fate - Offshore

- Spreading - Mackay et al. (1980)
- Evaporation - Payne et al. (1984)
- Entrainment/Dissolution - Audunson (1979) or Spaulding et al. (1982)
- Emulsification - Mackay et al. (1980)
- Advection - Instantaneous sum of currents at slick centroid

Oil Fate - Surf Zone

- Spreading - onshore/offshore balanced by wind stress: a longshore by usual processes
- Entrainment - same as offshore
- Advection - Longuet-Higgins (1970) radiation stress

Oil Fate Onshore

- Foreshore surface - function of shoreline type, foreshore slope, backshore width
- Sediment/groundwater system - standard fluid/sediment algorithms
- Removal from surface by wave overwash - empirical relation of Thibodeaux (1977)
- Erosion/Accretion - Sunamura and Horikawa (1974)
- Evaporation - same as water surface
- Reflotation - can be combined with succeeding spilletts
- De-watering - estimated first-order process from stranded mousse

The model outputs include boiling-point-cut information, overall mass balance, and line plots showing the location of surface and alongshore oil distribution. Other physical parameters such as the depth and shoreline grids and wave and current fields can be displayed. COZOIL is inherently deterministic with respect to results from any single simulation. Stochastic oil-distribution estimates are produced by combining the results of multiple simulations using a statistical analysis processor at the end of a test.

COZOIL was tested against prototype data for wave predictions using the Bristol Bay field data (Port Heiden) obtained by the study team in August-September 1986. Results indicate the model produces realistic approximations of wave height, wave period, and approach angle from a local or offshore wind field (details contained in section 5.0). Three tests were also performed against data from the 1978 *Amoco Cadiz* oil spill off Brittany, France. Tests were conducted at three scales or levels of grid resolution:

- 1) A relatively detailed, small area (mesoscale, 20x40 km) near the wreck site.
- 2) A large area (macroscale, 100x175 km) encompassing virtually the entire shoreline impact area.
- 3) The same large area with additional detail near the spill site.

The detailed, mesoscale test case generally overestimated the quantity of oil onshore but produced the general variance and distribution of oil. Model and prototype differences are considered to be due to the complexity of the shoreline in question and limitations of the hydrodynamic algorithms at these spatial scales. The macroscale test cases provided less resolution because of grid cell size but reproduced the overall distribution of offshore and onshore oil quite well. The mass balance of onshore oil realistically depicts the actual spill case and compares well with observations (section 6.0).

While improvements to COZOIL can be made in the future as additional prototype data and new algorithms are developed, the present model successfully links a large number of physical process and oil fates models in a straightforward manner. COZOIL is designed to be used interactively on a PC and allow users to perform oil spill simulations in a wide range of coastline settings.

TABLE OF CONTENTS

	Page
ABSTRACT	i
TABLE OF CONTENTS	
List of Figures	vi
List of Tables	vii
List of Symbols	viii
1.0 INTRODUCTION	1
1.1 Relation to Recent Onshore Oil-Spill Models	3
1.2 Conceptual Design of the COZOIL Model	4
2.0 DESCRIPTION OF MODEL Algorithms	7
2.1 COZOIL Model System Overview	7
2.2 Physical Environmental Concepts and Algorithms	13
2.2.1 Grid System	13
2.2.2 Coastal Reach System	16
2.2.3 Wind	18
2.2.4 Waves	19
Wave transformation outside the surf zone	20
Wave transformation inside the surf zone	23
Wave runup and setup	25
2.2.5 Currents	26
2.3 Oil Fate Concepts and Algorithms	30
2.3.1 Offshore	30
Spreading	30
Evaporation	31
Entrainment/Dissolution	32
Emulsification	32
Advection	34
2.3.2 Surf Zone	35
Spreading	35
Entrainment	38
Advection	38
2.3.3 Onshore	39
Deposition on foreshore surface	39
Deposition on backshore	39
Entry into sediment/groundwater system	39
Direct penetration of oil into sediments	43
Removal of surface oil by wave overwash	43
Removal from the sediment/groundwater system	45
Evaporation	49
Refloating	49
De-watering (de-emulsification)	49

3.0	DESCRIPTION OF FIELD ACTIVITIES	51
3.1	Geographic Setting	54
3.2	Physical Process Measurements	57
3.2.1	General Sampling Scheme	57
3.3	Results	62
3.3.1	Geomorphic Data	62
3.3.2	Beach Sediment Data	69
3.3.3	Winds	70
3.3.4	Tides	70
3.3.5	Coastal Processes	70
3.3.6	Suspended-Sediment Measurements	77
	Effect of suspended sediment on spilled oil	84
3.4	Wind and Wave Hindcast	86
3.4.1	Methodology	86
3.4.2	Case 1 – Wind and Wave Field, September 6-10, 1986	88
	Onshore wind direction observed at beach and offshore station locations	88
	Description of event	88
	Notes on the hindcast analysis	88
	Notes on deep-water wave hindcast versus observed onshore breaking waves	90
3.4.3	Case 2 – Wind and Wave Field, August 22-28, 1986	91
	Onshore wind direction observed at beach and offshore station locations	91
	Description of event	91
	Notes on the hindcast analysis	91
3.4.4	Case 3 – Wind and Wave Field, August 12-20, 1986	95
	Description of event	95
3.4.5	Supplemental Data	99
4.0	FLEXIBILITY OF MODEL FOR PROBLEM-SOLVING	103
4.1	Basic Options	103
4.2	Petroleum Selection and Preweathering Option	103
4.3	User-Specified Parameters	104
4.4	Spill Input Parameters	104
4.5	Shoreline Definition Parameters	105
4.6	Nearshore Process Data Sets	106
4.7	Other Model Features	107
5.0	RESULTS OF ANALYSIS OF MODEL ACCURACY	108
5.1	Model Tests: Waves Off Port Heiden, Alaska	108
5.2	Sensitivity Analysis	119
5.2.1	Spreading in the Surf Zone	119
5.2.2	Penetration Rates	119
5.2.3	Retention of Oil in Groundwater System	120
5.2.4	Whole-Model Sensitivity Tests	120

6.0 AMOCO CADIZ HINDCAST	135
6.1 Introduction	135
6.2 Model Input Data	138
6.3 Summary of Oil Distribution Data	147
6.4 Results	151
6.4.1 Mesoscale Test Case	151
Offshore and onshore distribution.....	151
Dynamic mass balances of oil quantity.....	155
Grid cell analysis.....	157
6.4.2 Macroscale Test Case	159
Offshore and onshore distribution.....	159
Dynamic mass balances of oil quantity.....	161
6.4.3 Macroscale Test Case with Additional Detail	161
Offshore and onshore distribution.....	161
Dynamic mass balances of oil quantity.....	164
6.5 Conclusions	166
7.0 COMPATIBILITY OF COZOIL WITH RELATED MMS TRANSPORT MODELS	168
8.0 SUMMARY AND CONCLUSIONS	169
REFERENCES	173

APPENDICES

- I. User's Manual with model documentation code (under separate cover)
- II. Field Survey Data
 - A. Beach Profiles
 - B. Contour Movement Summaries
 - C. Profile Volumetric Changes
 - D. Beach Sand Analysis Graphs
 - E. Wind Speed and Direction
 - F. Suspended Sediment in the Surf Zone

LIST OF FIGURES

	Page	
1.1	COZOIL mass transfer pathways in the coastal zone	6
2.1	COZOIL model system schematic	9
2.2	Schematic of model initialization procedures	10
2.3	Schematic of topographical/geological initialization procedures	11
2.4	Schematic of procedures for specification of environmental data	12
2.5	Example COZOIL model study area, showing bathymetry and division of shoreline into reaches	14
2.6	Definition of input parameters for coastal reaches (except coastal ponds)	15
2.7	Example specification of inshore distance for reaches 1, 4 and 5	17
2.8	The convention for wave angle determination	22
2.9	Schematic of oil slick driven against the shore by wind	36
2.10	Schematic of beach groundwater system	42
2.11	Relationship of sediment grain size to porosity, specific yield, and specific retention (from Todd, 1959)	48
3.1	Port Heiden field study location and measurement stations	52
3.2	Beach and inshore contours near stations 9-16	58
3.3	Surf-zone grid at station 10 for coastal process measurements	60
3.4	Sketch map of Port Heiden showing principal morphological features	63
3.5	Beach profile at station 10 showing principal features	65
3.6	Winds at Port Heiden air station and the beach (August 16-September 11, 1986)	71
3.7	Predicted tides at Port Heiden for August and September 1986	72
3.8	Sampling arrangement for suspended-sediment measurements in the surf zone	78
3.9	Typical suspended-sediment concentration at the breakpoint under plunging waves at high-tide stages	82
3.10	Typical suspended-sediment concentration in the surf zone under spilling waves at low-tide stages	83
5.1	Study area for wave-hindcast model tests	110
5.2	Digital land/water grid for Port Heiden model-testing area	111
5.3	Depth grid for Port Heiden model-testing area	112
5.4	Model wave-breaking matrix for input conditions of September 8, 1986.	117
5.5	Wave-height matrix for each grid cell for September 8th input conditions	118
5.6a,b	Onshore-offshore foreshortening of a 100-m³ oil slick under influence of various onshore wind speeds	121
5.7a-b	Penetration depth as a function of time for various petroleum	122
5.7c	Penetration depth as a function of time for various petroleum	123
5.8a-f	Petroleum retention in sediments for various values of the partition coefficient K	124
5.9a,b	Overall mass balance for Prudhoe Bay crude oil coming ashore on a sand beach	130
5.9c,d	Mass balance for oil associated with the coastline in Figure 5.9 (a, b)	131
5.10	Overall mass balance for Prudhoe Bay crude oil coming ashore on an eroding peat scarp	132
5.11	Overall mass balance for Prudhoe Bay crude oil coming ashore on a tidal mudflat	132
5.12	Overall mass balance for Prudhoe Bay crude oil coming ashore on a gravel beach	133
5.13	Overall mass balance for Prudhoe Bay crude oil coming ashore on a cobble beach	133
5.14	Overall mass balance for Prudhoe Bay crude oil coming ashore on smooth rock or seawall	134
6.1	<i>Amoco Cadiz</i> hindcast study areas	136
6.2	Estimated cumulative release of oil from the <i>Amoco Cadiz</i>	137
6.3	Temperature and winds from Brest airport during <i>Amoco Cadiz</i> spill	140
6.4	Representative shoreline profiles from Gundlach and Hayes (1978)	145
6.5	Modeled coastline for three test cases	146
6.6	Distribution of offshore and onshore oil for mesoscale test case	152
6.7	Observed distribution of <i>Amoco Cadiz</i> oil - Aber Benoit to St. Cave	154
6.8	Dynamic mass balances for oil in the mesoscale test case	156

6.9	Comparison of simulated oil quantity within individual cells	158..
6.10	Distribution of offshore and onshore oil for the macroscale test case	160
6.11	Dynamic mass balances for oil in the macroscale test case	162
6.12	Distribution of offshore and onshore oil for the macroscale, detailed test case	163
6.13	Dynamic mass balances for oil in the macroscale, detailed test case	165

LIST OF TABLES

2.1	Default values for partitioning of oil removed from the beach face by action of waves	45
3.1	General description of survey stations at Port Heiden	62
3.2	Average widths for the beach face and low-tide portions of Port Heiden profiles	66
3.3	Beach unit-width volumes for each station at representative contour intervals	68
3.4	Summary grain-size statistics for beach sediments	69
3.5	Summary of coastal-process measurements obtained at station 10	75
3.6	Station 10 profile slopes and morphology for August 20, 1986	84
3.7	Comparison of hindcasted offshore and onshore winds for September 6-10, 1986	89
3.8	Hindcasted offshore and observed onshore waves for September 6-10, 1986	90
3.9	Comparison of hindcasted offshore and onshore winds for August 22-28, 1986	93
3.10a	Locally generated, hindcasted offshore waves for August 22-28, 1986	93
3.10b	Hindcasted deep-water waves and decayed waves for August 22-28, 1986	93
3.10c	Onshore breaking waves for August 22-28, 1986	94
3.11	Comparison of hindcasted offshore winds and onshore winds for August 12-20, 1986	96
3.12a	Locally generated, hindcasted offshore waves for August 12-20, 1986	97
3.12b	Hindcasted deep-water waves and decayed waves for August 12-20, 1986	98
3.12c	Onshore breaking waves for August 12-20, 1986	98
3.13	Hindcasted offshore and measured onshore winds during miscellaneous dates	100
3.14a	Locally generated, hindcasted offshore waves for miscellaneous dates	101
3.14b	Hindcasted deep-water waves and decayed waves for miscellaneous dates	101
3.14c	Observed onshore breaking waves for miscellaneous dates	102
5.1	Model input parameters for coastal topography at Port Heiden	109
5.2	Results of model tests of waves for September 6-10, 1986	113
5.3	Results of model tests of waves for August 22-28, 1986	113
5.4	Results of model tests of waves for August 12-20, 1986	114
5.5	Statistical summary of model test results for wave angle	115
5.6	Statistical summary of model test results for wave height	115
5.7	COZOIL model input parameters for the single-reach test cases	127
5.8	Reach specification parameters for single-reach COZOIL model test	127
6.1	COZOIL input parameters for <i>Amoco Cadiz</i> hindcast	139
6.2	Summary of boiling point characteristics of Murban, Abu Dhabi crude	139
6.3	Coastal reach parameters for mesoscale test case	142
6.4	Coastal reach parameters for macroscale test case	143
6.5	Coastal reach parameters for macroscale, detailed test case	144
6.6	Quantity of oil measured at <i>Amoco Cadiz</i> monitoring stations	148
6.7	Summary of oil quantity for mesoscale test case	149
6.8	Summary of oil quantity for entire <i>Amoco Cadiz</i> spill site	150

LIST OF SYMBOLS

A	spill area	MG	mean grain size
C_1	constant	P	porosity
C_2	constant	P_i	vapor pressure for boiling point i
C_a	adsorbed concentration	Q	mass flux
C_{wa}	water-accommodated concentration	R	gas constant, mean slick radius
C_{ss}	sediment concentration	R^*	random variate
CD	stress coefficient	R_e	Reynolds number
CT	total concentration	v_d	drag velocity at depth d
D	slick diameter, diffusivity	R_s	surface drag velocity
d_{50}	50th percentile sediment size	R_w	wave runup height
D_H, D_V	horizontal, vertical diffusion coefficients	r_T	slick radius transverse to shoreline
F	wind fetch length	S_c	Schmidt number
F_c	organic fraction of sediment	S_n	net wave setup
F_{evap}	fraction evaporated	S_Y	specific yield
F_i	sediment carbon fraction, fractional slick component	T	temperature
F_s	spreading force	T	wave period
F_w	wind force	T_a	temperature air
F_{wa}	mass removed per tidal cycle	t_b	breaking wave period
F_{Wc}	fractional water content of emulsion	t_D	decayed wave period
F_{wc_0}	initial fractional water content	t_k	environmental temperature
G_o	erosion/accretion parameter	T_{ps}	tide period
H	wave height	T_s	temperature sea surface
h_b	wave height at breaking	T_w	significant wave period
H_o	wave height in deep water	U	wind velocity component (+x)
H_s	significant wave height	U_g	geostrophic wind speed
H_{rms}	root-mean-squared wave height	US	surface wind speed
h_D	decayed wave height	V	wind velocity component (+y), slick volume, slick velocity
h_A	a constant	v_b	wave-breaking velocity
h_B	a constant	v_{LS}	longshore transport velocity in the surf zone
K_p	partition coefficient	$v_{l/2}$	longshore current speed at the mid-surf position
L	wave length, surf-zone width, longshore coastal cell dimension	v_{max}	maximum tidal current amplitude
L_o	deep-water wavelength	v_R	random velocity component
M	molecular weight	v_T	tidal velocity
M_i	mass of oil in beach segment i	v_w	wind-driven current velocity
M_{wa}	water-accommodated mass	W	wind speed

v_N	normal component of wind velocity	α_b	wave breaker angle with the shoreline
W_r	reference wind speed	β	offshore bottom slope, offshore wave approach direction
		δ	average slick thickness
a	constant	ϕ	velocity potential, tidal phase lag
b	constant	γ	proportionality constant
c	wave celerity	θ	angle of wave crest with bathymetric contour
c_g	wave group celerity	θ_c	contour angle
c_o	deep-water wave celerity	θ_o	deep-water wave direction
CD	drag coefficient	κ	energy dissipation coefficient
cp	oil viscosity units (centipoise)	μ	oil viscosity
d	mean water depth over the fetch	μ_o	reference oil viscosity
f	earth rotation rate	ρ	oil density
f_i	fractional slick component	ρ_a	air density
g	gravitational acceleration	ρ_{oil}	oil density
h	water depth at point of interest in surf zone, mean surf zone depth, mean slick thickness, mass transfer coefficient	ρ_w	density of water
h_b	water depth at breaking	σ	angular wave frequency, oil/water interracial tension
h_m	mass transfer coefficient	σ_g	graphic standard deviation sediments
h_t	water depth at wave trough	τ	wind stress
k	wave number	$\tau_{xs,xd}$	stress at surface and depth d (+x)
m	beach slope, oil mass	$\tau_{ys,yd}$	stresses at surface and depth d (+y)
mt	metric tons	ω	tidal frequency
m _i	mass of oil with boiling point i	θ	asymptotic transport angle
p	intrinsic sediment permeability		
q_{off}	volumetric offshore transport rate		
s	wave phase function		
t	time		
u	water velocity component (+x)		
u_o, v_o	initial water velocity components		
u_{oo}, v_{oo}	asymptotic water velocity components		
v	water velocity component (+y)		
v_p	penetration velocity		
x	Cartesian coordinate		
y	Cartesian coordinate		
z	depth		

NOTE: Occasionally, the same symbol is used for different variables (e. g., T = temperature; wave period). This only occurs where the applications in the model are independent and such use is consistent with existing practice.

1.0 INTRODUCTION

This report describes phase II of a multiyear project to develop and test a probabilistic coastal zone oil spill (CO ZOIL) model for use by the Minerals Management Service (MMS). Phase I (CSE/ASA/BAT, 1986)* encompassed an evaluation of component algorithms and models of nearshore currents, sediment transport, and oil weathering to determine the most appropriate and workable combination for use in a unified COZOIL model. Phase II involved model development, testing, verification, and documentation. Part of this work entailed a field study of littoral processes at a representative site in Alaska. These field data were used to verify nonoil processes and parameters which affect the transport of oil along the shoreline. Phase II also included a test of the model against data from the *Amoco Cadiz* oil spill.

Section 2.0 of this report is a detailed description of the model algorithms. These include formulations for:

- 1) Dynamic processes which move the oil from an offshore location to and along the shoreline.
- 2) Physical parameters which define the grid system and boundary conditions.
- 3) Oil-fates algorithms which relate to the transformation of oil quantity and quality in the surf zone or along the shoreline.

Oil-fates algorithms include spreading, evaporation, entrainment/dissolution, emulsification, deposition, entry into sediments/groundwater system, and removal from the shoreline. To the extent possible, previously formulated and tested algorithms for particular processes were incorporated into the model. Other related MMS-sponsored models and studies have also been considered in formulation of the COZOIL model in order to maintain compatibility.

The model formulation outlined in section 2.0 is supplemented by a copy of the users' manual in Appendix I and the model documentation in Appendix I-A (both under separate cover). The model has been developed for application on a personal computer (PC, IBM compatible). The user's manual is included in Appendix 1.

*CSE (Coastal Science & Engineering, inc.: principal investigator). ASA (Applied Science Associates kc.: associate investigator).
BAT (Battelle New England Marine Research Laboratory; associate investigator).

Section 3.0 presents results of a six-week field survey at Port Heiden, Alaska, on Bristol Bay. The field survey was designed to collect prototype shoreline, sediment, and littoral process (waves, winds, and currents) data for use in testing the COZOIL model. Fieldwork was conducted in late summer 1986 to obtain prototype data during the ice-free season. Summary results in section 3.0 are supplemented by detailed data in Appendix II.

Section 4.0 addresses the flexibility of the model for problem-solving. The model has been set up to allow users the option of specifying certain input parameters at the terminal (e.g., type of oil, grid system, etc.), calling up data sets as available (e.g., winds, tides, waves, shoreline segments), and/or leaving the model to apply default values. Section 4.0 outlines how the model can be adapted for areas with limited data or areas where large data sets are available. The COZOIL model has been designed for use in a wide range of applications, operating in either "stand-alone" mode (by creating estimates of process parameters) or in a "mainframe" mode whereby the model can draw on hydrodynamic and meteorological outputs from external models or data bases.

Section 5.0 addresses the results of analysis of model accuracy and sensitivity. Included are results of tests comparing winds and waves at the Bristol Bay field study site. Section 6.0 includes a test application of the COZOIL model using *Amoco Cadiz* study data. The *Amoco Cadiz* spill in 1978 is one of the best studied in terms of measuring oil quantities impacting the shoreline. It also represents a spill occurring along a fairly complex and variable shoreline. Tests were completed for representative shoreline reaches and oiling periods.

Section 7.0 addresses the compatibility of the COZOIL model with related MMS transport models. Finally, section 8.0 offers a summary and recommendations for future work.

1.1 RELATION TO RECENT ONSHORE OIL SPILL MODELS

Oil spill trajectory and fates models typically follow a surface slick until it contacts a coastline, at which time the simulation ceases. The coastal zone oil spill model (COZOIL) described here is designed to simulate oil spill fates both before and after a coastal contact.

Two statistical regression models have been developed previously to attempt to correlate length of affected coastline with oil spill size (Ford, 1985; Seip et al., 1986). By converting to log-log space, Ford (1985) was able to explain about 65 percent of the total variance in coastline affected using latitude and volume as the independent variables. The percent explained would presumably be considerably reduced in nontransformed space. Seip et al. (1986) found no correlation between shore length damaged and the amount of oil spilled. Results of these efforts show the statistical approach to be relatively unsatisfactory for this problem.

Seip et al. (1986) have also constructed a highly parameterized computational model for estimating length of shoreline affected following an oil spill. The model uses the amount of oil nearshore, the littoral area, and a wave parameter (i. e., rough or smooth) as the primary input parameters. Four types of shoreline, distinguished by a saturation density or holding capacity, are identified--smooth rocks, boulders or cobble, sand, and mudflats. First-order removal rates are estimated for each shoreline type. Removal from the water surface via evaporation, entrainment, and advection out of the study area is also included as a single, first-order decay process. Results of the simple computational model appear somewhat better than those for the regression model. The major weakness of the model by Seip et al. is that it includes no physical or chemical processes, except as represented by input parameters. The model, therefore, cannot account for tides, complex topographies, wind direction and shifts, wave diffraction/refraction, longshore transport. effect of changing oil viscosity, compression of oil slicks against the shoreline, and so forth. Although the model is probably of limited use in many specific situations, it may prove useful in the more general applications of oil spill contingency planning, for which it was developed.

1.2 CONCEPTUAL DESIGN OF THE COZOIL MODEL

The COZOIL model has been designed to include explicit representations of as many of the known active processes as possible. Multiple discrete batches of oil, or spinets, are used to represent the surface slick. Spinets are circular while offshore but become elliptical upon contact with the shoreline. The amount of onshore/offshore foreshortening is governed by a balance between wind stress and gravity spreading forces, and is accompanied by alongshore spreading of the spinet. Evaporated hydrocarbons are given no spatial representation, but are simply accumulated from all sources during the simulation.

Entrained oil offshore is represented by discrete particles which are advected by the local currents. Inside the surf zone, entrained oil takes on a continuous representation, discretized by alongshore grid cell. Transport in the surf zone is governed by a classical radiation stress formulation. Incorporation of water into surface oil (emulsification) is simulated offshore. De-emulsification (de-watering) is allowed to occur for oil which is on the foreshore or backshore.

Oil coming ashore may be deposited on the foreshore or the backshore or be carried into coastal lagoons, ponds, or fjords. Oil on the foreshore penetrates into the underlying sediments at a rate dependent on sediment grain size and oil viscosity, and to a depth modulated by the groundwater system. Oil may also be carried into the beach/groundwater system by wave overwash. Reflotation of surface oil occurs during rising tides. These mass transfer pathways are shown schematically in Figure 1.1.

Oil which is spilled offshore may be transported by winds and waves into the surf zone. Once in the surf zone, oil on the water surface or in the water column can be transported alongshore, or back offshore. Oil on the water surface can also be deposited on the foreshore beach or backshore surfaces, depending on the water surface height. Oil which has been deposited on the backshore is subject to continued evaporation and may be removed during subsequent high-water events. Oil on the foreshore surface may also penetrate into the sediments, eventually reaching the groundwater system. Removal from the beach groundwater system occurs due to flushing during ebb tides. All of these coastal processes are computed up and down the modeled coastline as long as oil is present.

The model is inherently deterministic with respect to results of any single simulation. Stochastic oil-distribution estimates are produced by combining the results of multiple simulations, each of which is driven by a separate weather scenario. Wind

and temperature are computed stochastically by the model, using statistical parameters supplied by the user. COZOIL includes a statistical analysis subroutine that produces a summary at the end of the series of stochastic simulations.

Details of the algorithms contained in COZOIL are described in section 2 of this report.

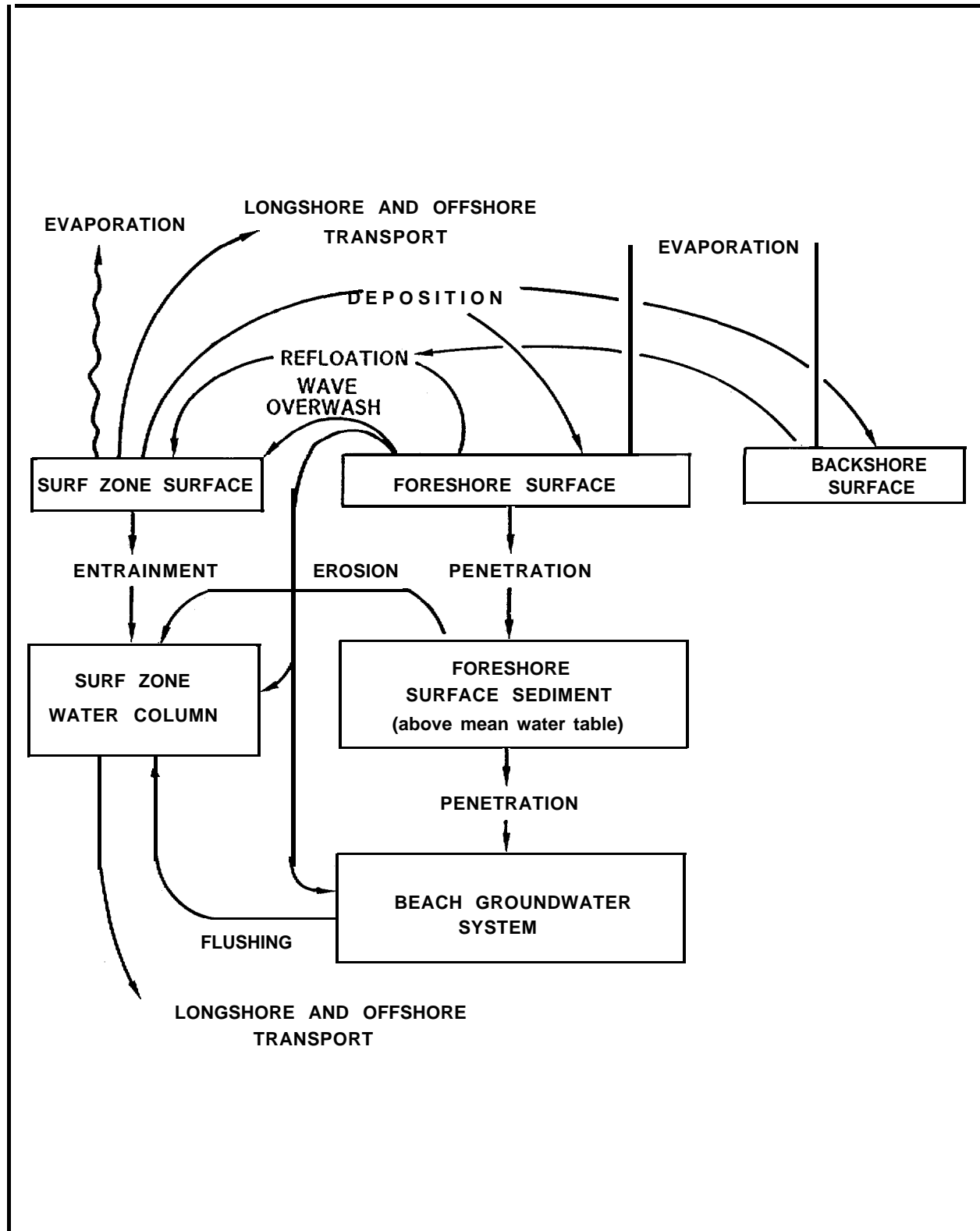


FIGURE 1.1. COZOIL mass transfer pathways in the coastal zone.

2.0 DESCRIPTION OF MODEL ALGORITHMS

In this chapter, we present an overview of COZOIL, including initialization procedures. Details of these procedures, and instructions for application and use of the model, are given in the users' manual (Appendix I). The mathematical algorithms used in the model will be described here; the actual FORTRAN 77 code is listed in Appendix I-A.

2.1 COZOIL MODEL SYSTEM OVERVIEW

The COZOIL model can be conceptually divided into a set of initialization processes, followed by computational and output routines (Fig. 2.1). During initialization, the spill scenario is established, including specification of oil type, spill size and duration, simulation duration, and study area topography and geology.

Details of the initialization process are shown schematically in Figure 2.2. The program leads the user through initialization via a series of queries. An option between verbose (i.e., complete) and abbreviated output is open to the user at program startup. The option selected affects only the amount and detail of output produced by the model, with no effect on the actual computations performed. The most complex portion of the initialization process is the establishment of the geophysical environment within which the simulation will take place. The flow of logic for this section of the program is shown in Figure 2.3. To allow for input errors and facile alteration of the simulation environment, an iterative loop has been built into this section of the program. Thus, the user can alter the originally specified set of coastal reach parameters, whether they were obtained interactively or from an external file.

The second important part of the model initialization process centers on the specification of the environmental data used to drive the simulation. The steps followed are shown in Figure 2.4. First, the user must either direct the model to access an existing wind data set or input a new time-series. If a stochastic series of simulations is to be performed, the model will request means and standard deviations for wind speed, direction, and air temperature. The model then requests the name of an existing tidal current data set or sufficient data to create one. A wind-driven current data set is then created by the model from the wind record, if the user does not specify an existing data set. Finally, the model either computes waves from the wind record or accesses a wave time-series from an external file.

Model output is controlled by the program itself; the user controls only the time interval between outputs to the screen and to data storage files. Outputs at the end of each time interval include boiling-point cut information by surface spinet and coastal reach, an overall mass balance, and line plots showing the location of surface spinets and the alongshore distribution of hydrocarbons. COZOIL also tells the user when new environmental data is being read into the model and shows the results of ensuing wave height and angle computations. If the user elects the abbreviated output option, much of this secondary information is suppressed.

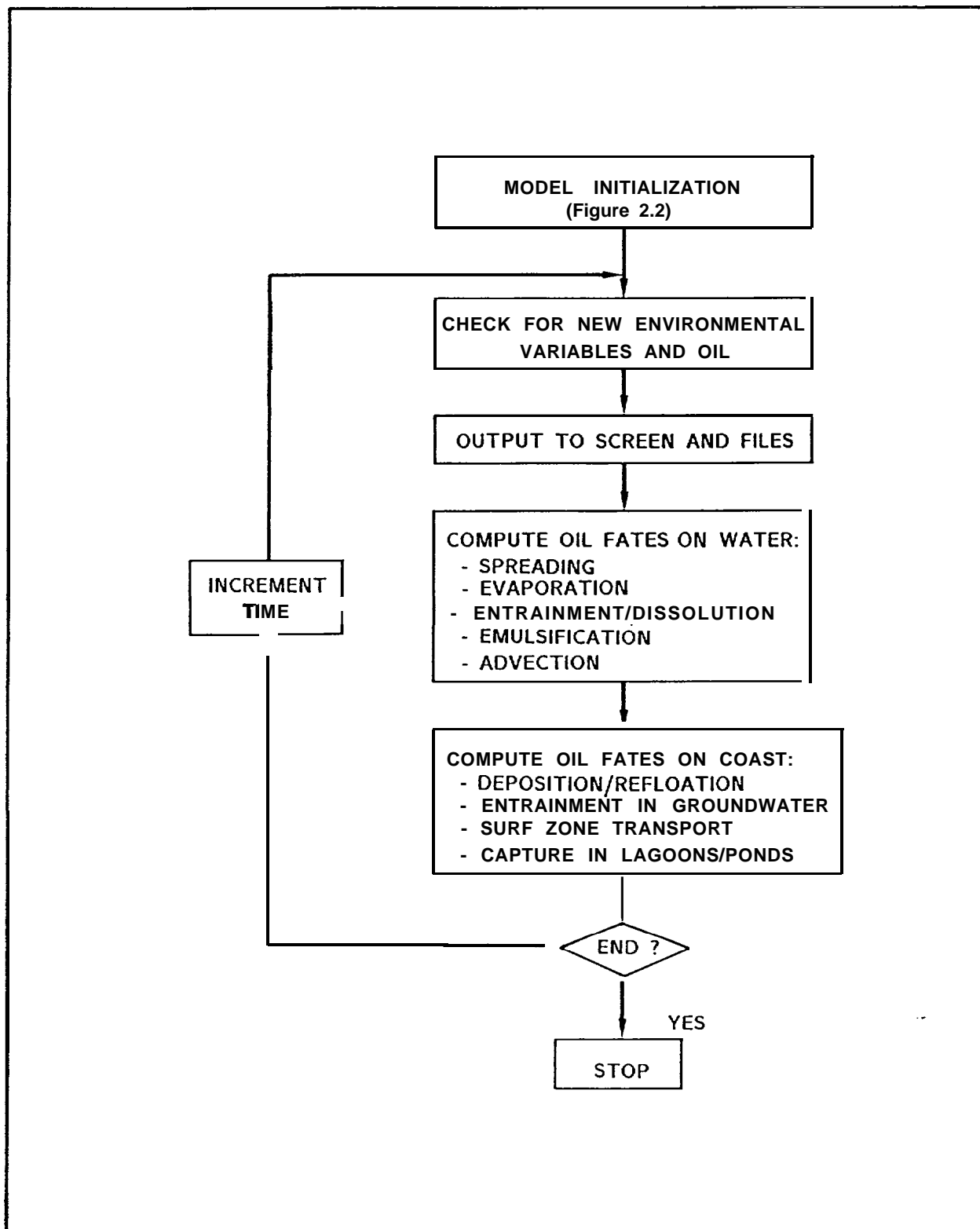


FIGURE 2.1. COZOIL model system schematic.

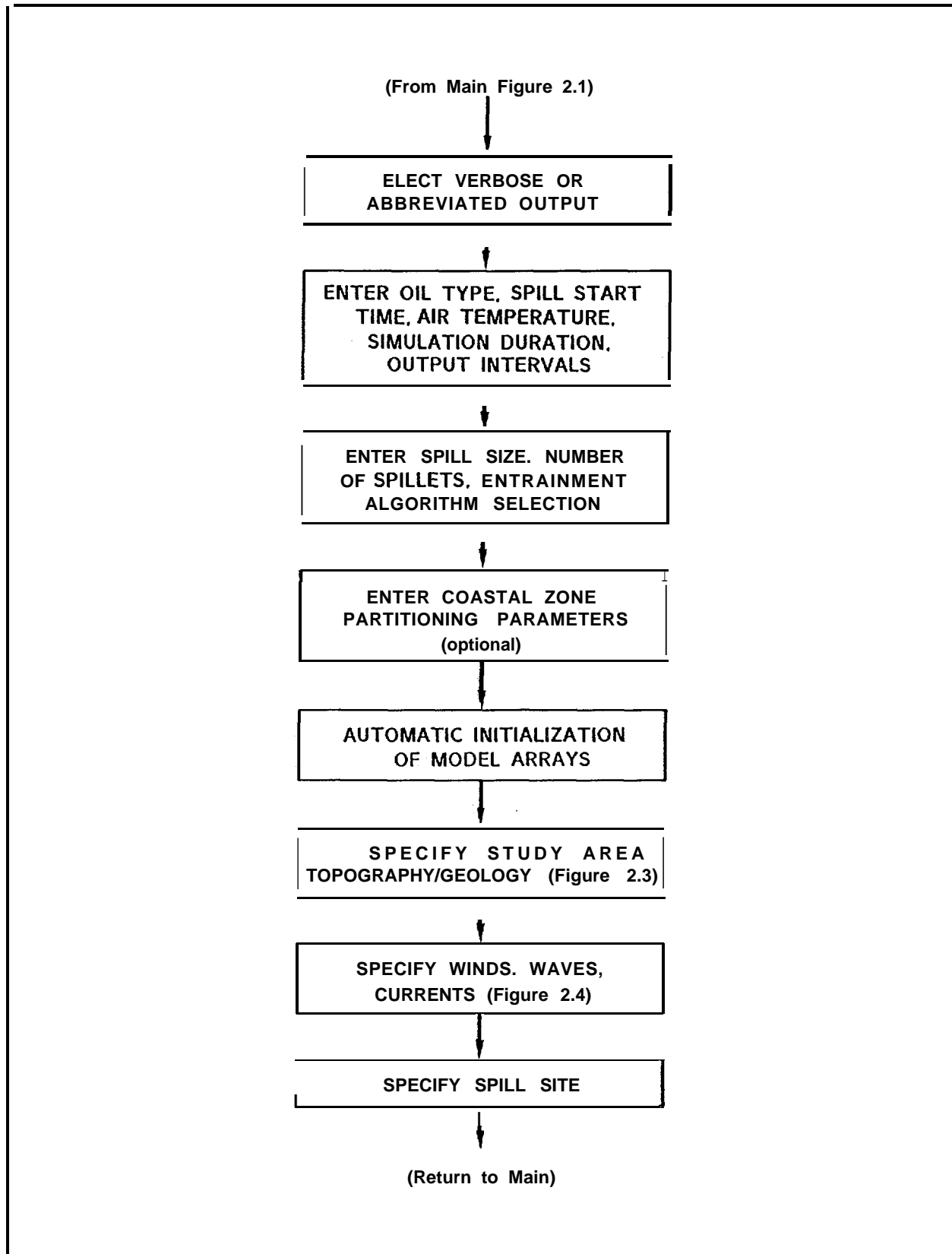


FIGURE 2.2. Schematic of model initialization procedures.

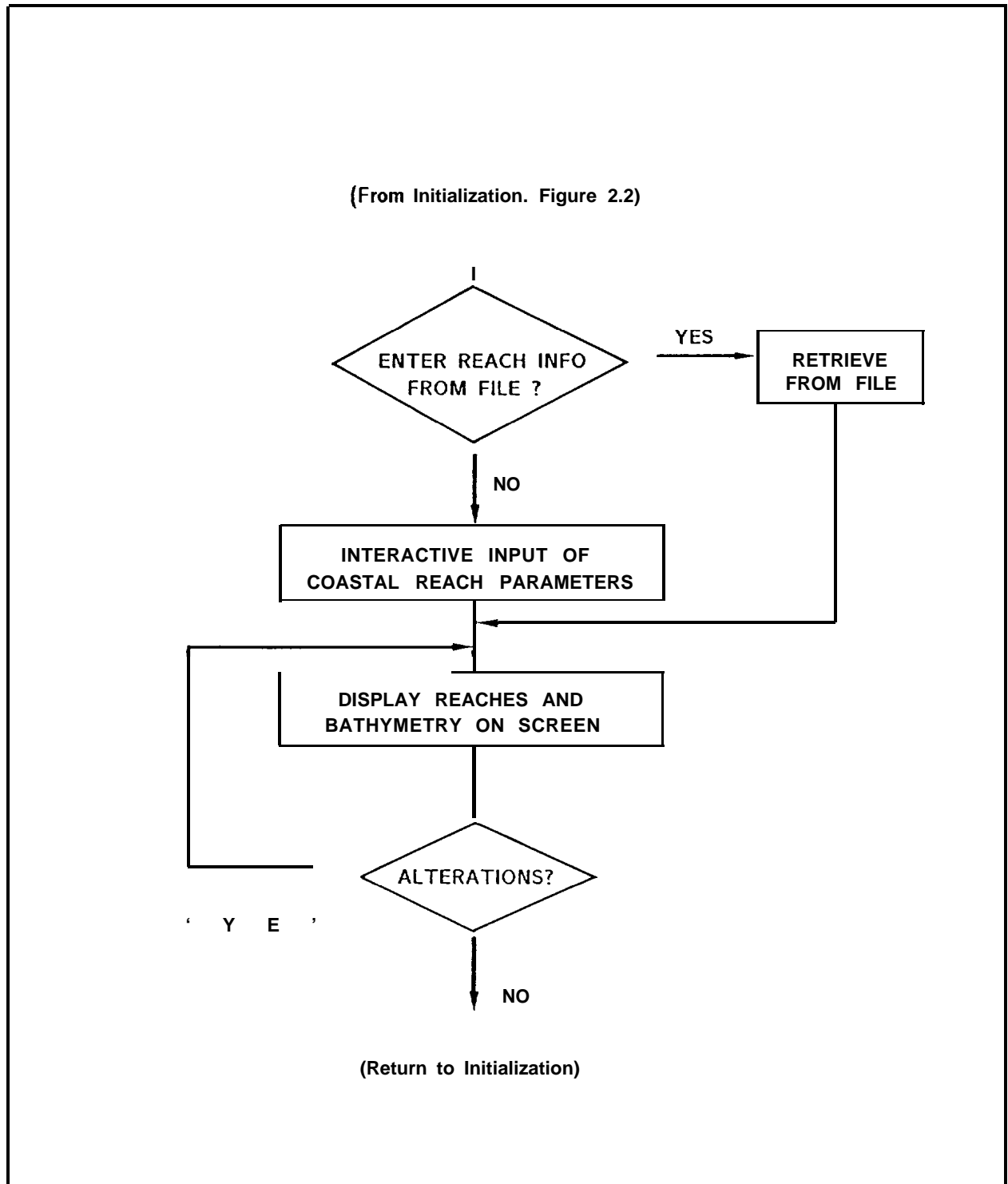


FIGURE 2.3. Schematic of topographical/geological initialization procedures.

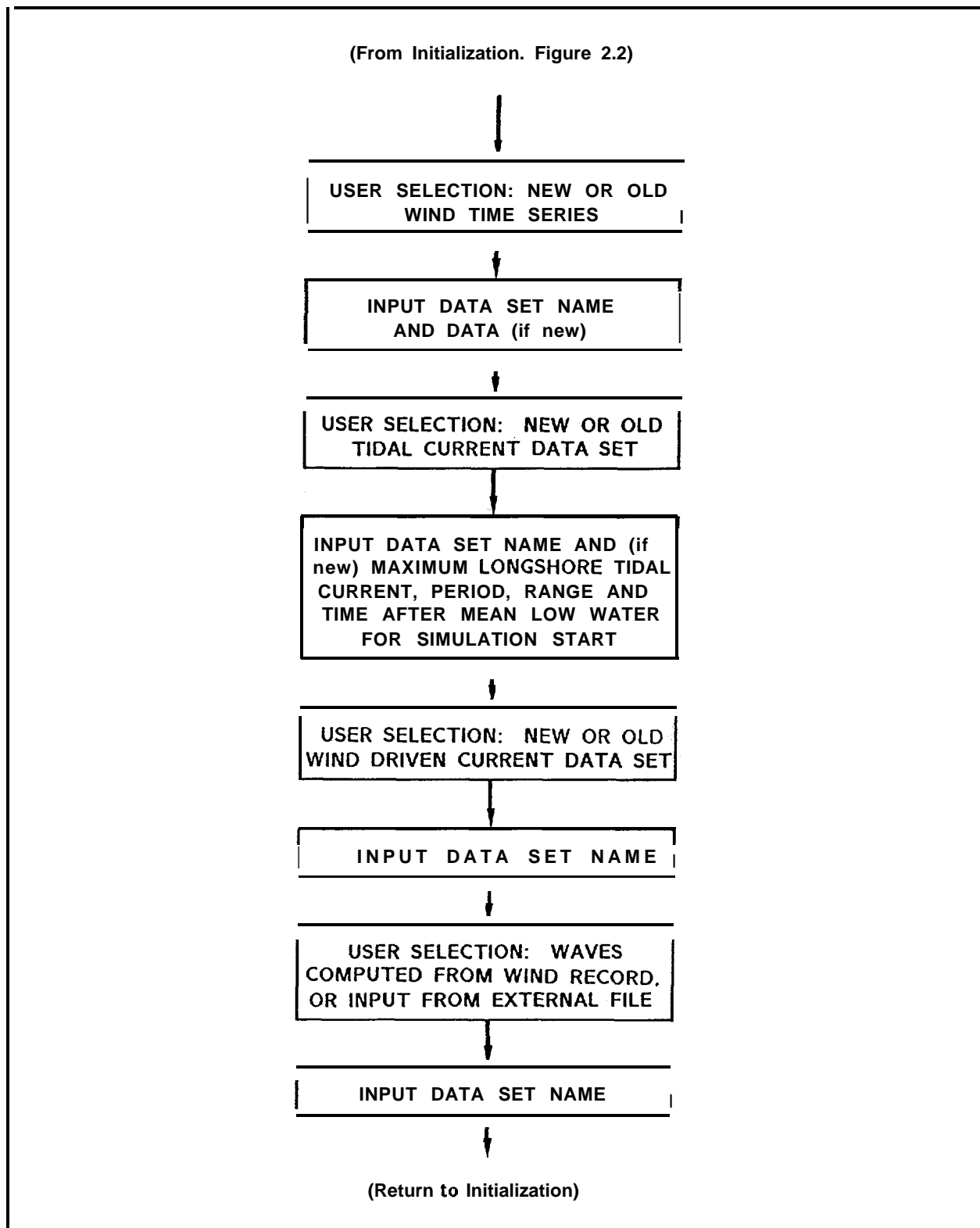


FIGURE 2.4. Schematic of procedures for specification of environmental data.

2.2 PHYSICAL ENVIRONMENTAL CONCEPTS AND ALGORITHMS

Discussed in this section are the physical concepts embodied in the model, including the grid system, the specification of coastal reaches and bathymetry, as well as wind, wave, and current data inputs.

2.2.1 Grid System

The COZOIL model runs on a rectangular grid system oriented such that the first subscript (I) runs from west to east and the second (J) from south to north (Fig. 2.5). Thus the origin of the grid is located at the lower left corner of the COZOIL model study area and is at the lower left corner of grid cell (1,1) in the model code.

The dimensions of a single grid cell are a function of the specified size of the study area and the dimension of the governing arrays in the model. In our example of Figure 2.5, the study area is about 20 km by 70 km. If the code is compiled with a 10x10 grid system, then the grid-cell size for this case will be 2,000 m onshore/offshore (east/west) and 7,000 m alongshore (north/south). At these study-area and array sizes, no reaches shorter than 7,000 m north/south (or 2,000 m east/west) will be resolved. To increase the resolution (i.e., achieve a smaller grid-cell size), one should either decrease the study area size or re-compile the model with larger arrays.

There are two model arrays that appear in the model output. The first contains land/water codes:

Type 1: Below mean low water (MLW) and offshore (code 0).

Type 2: Intertidal (coded by reach number).

Type 3: Below MLW and adjacent to an intertidal cell (coded by reach number, but negative).

Type 4: Land cells above mean high water plus wave runup/setup (code 99).

From the definitions above and those in Figure 2.6, it can be seen that the lower end of the beach foreshore coincides with the intersection between positive and negative coded cells (types 2 and 3 above).

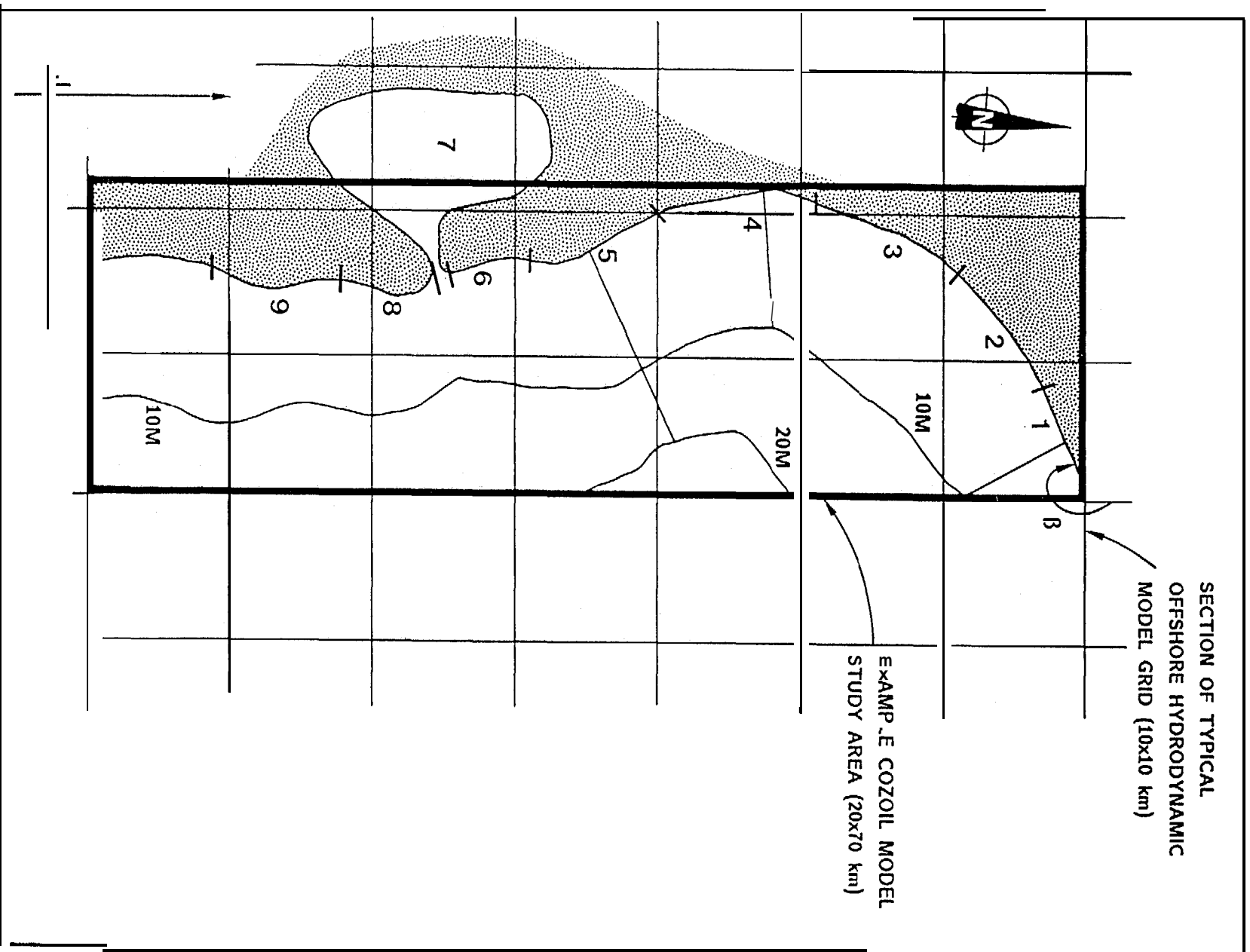


FIGURE 2.5. Example COZOIL reaches.

study area showing bathymetry and division of shoreline into reaches.

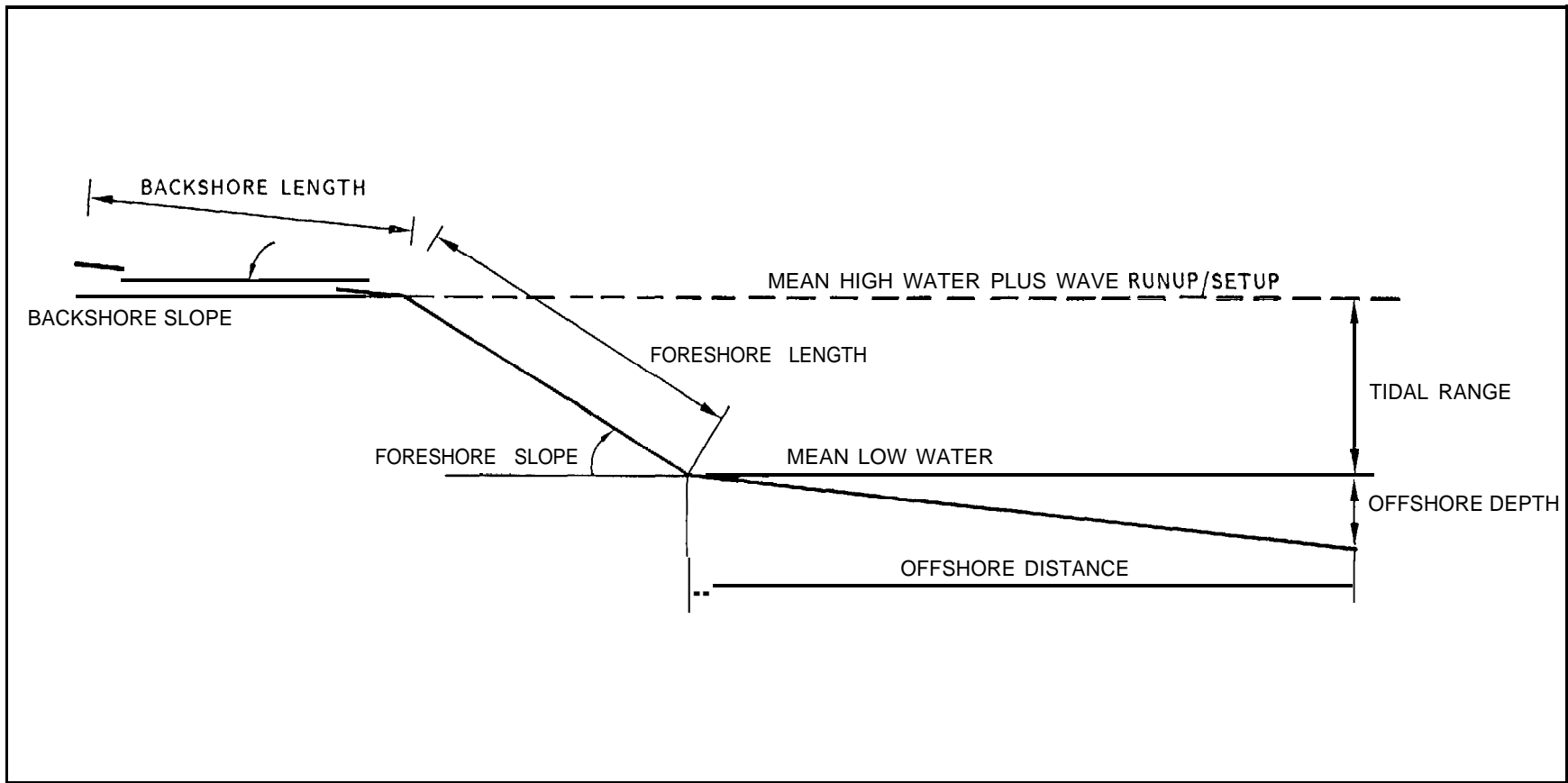


FIGURE 2.6. Definition of input parameters for coastal reaches (except coastal ponds),

As opposed to offshore and coastally adjacent cells (types 1 and 3 above) the onshore/offshore dimension of intertidal cells (type 2) is determined by input values of the foreshore plus backshore distances. Thus these "flooding boundary" cells are of variable width from one reach to the next to accommodate, for example, extensive tidal mudflats which may be located next to eroding bluffs with very little exposed intertidal area.

The second array of interest contains the bathymetric values. Here land cells are coded with a '-1', while other cells contain the water depth at that location at MLW. The computation of the bathymetry is discussed in the following section, since it is governed by reach parameters supplied by the user.

2.2.2 Coastal Reach System

There are eight types of reaches defined in the present version of the COZOIL model:

- | | |
|----------------------------------|-----------------------------------|
| 1) Smooth rocky shore or seawall | 5) Gravel beach |
| 2) Cobble beach | 6) Tidal (mud) flat |
| 3) Eroding peat scarps | 7) Marsh |
| 4) Sand beach | 8) Coastal pond, lagoon, or fjord |

For each of reach types 1-7, there are eight parameters required by the model:

- | | |
|--------------------------|--------------------------------|
| 1) Reach length (m) | 5) Backshore slope (rise/run) |
| 2) Backshore width (m) | 6) Foreshore slope (rise/run) |
| 3) Foreshore width (m) | 7) Offshore depth (m) |
| 4) Offshore distance (m) | 8) Reach orientation (degrees) |

The identification of parameters 2-7 is given in Figure 2.6. The foreshore is defined to extend from the MLW line to the berm. The backshore extends from the berm to the dunes, cliffs, or first permanent onshore vegetation. Parameter 8, reach orientation, is measured in degrees clockwise from true north, standing at the beginning of the reach with water on the left. Thus in our example case, Figure 2.5, reach 1 is at the top of the figure and has an orientation β of about 240° .

Figure 2.7 shows examples of specifications for the offshore distance (parameter 4 above). This distance and the offshore depth (parameter 7) are used to determine the mean bathymetric slope for this reach. The model uses linear interpolation among the offshore depths specified for all reaches to create a discretized representation of the study area bathymetry. For reach type 8, the model requests six parameters:

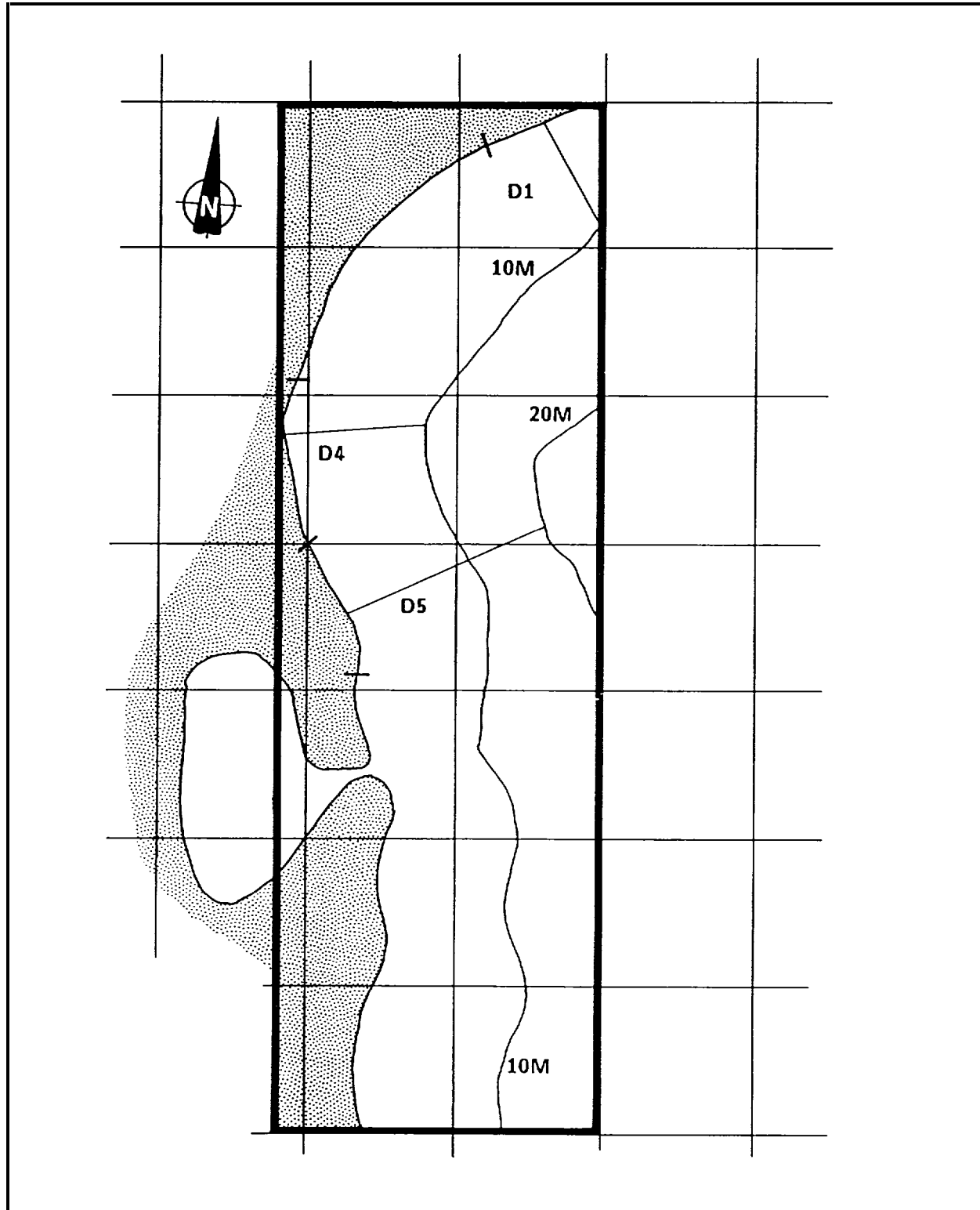


FIGURE 2.7. Example specification of inshore distances for reaches 1, 4, and 5 (see Fig. 2.5 for reach locations).

- | | |
|--|---|
| 1) Pond surface area (m ²) | 4) Tidal range inside the pond (m) |
| 2) Breachway (entrance) width (m) | 5) Fractional flushing value (per tidal cycle) |
| 3) Breachway (entrance) depth (m) | 6) Freshwater inflow rate to pond (m ³ /see) |

Flow into and out of coastal ponds and lagoons is computed by simple conservation of mass principles, assuming uniform velocities over the entrance cross-section and neglecting phase lags inside and outside the pond.

Sometimes a lagoon can be represented in COZOIL by including its actual coastal features in the coastal reach system. Such explicit representation is preferable to a reach type designation of '8', since more realistic transport and transformation processes will be included. Whether or not such explicit representation is possible depends upon the grid-cell size relative to the coastal features being resolved. Features which are close together (e.g., opposite shores of a river) will tend to "overwrite" each other in the representation. If in doubt, a simple trial including the explicit representation should be attempted. If the feature is too small to resolve, COZOIL will inform the user of this fact.

2.2.3 Wind

The model assumes a uniform wind field over the study area. Since study areas are generally expected to be small (e. g., 100 km alongshore and 1-20 km offshore), spatial variability in the wind field generally will be difficult to resolve from typically available data.

For a deterministic run, the user may either input a wind time-series manually or direct the model to access a prepared data set. Wind data sets from nearby land stations are appropriate for input to COZOIL, as opposed to offshore oil spill models. Thus for most applications, there will be an abundance of historical data.

For a series of stochastic simulations, COZOIL allows either zeroth or first-order Markov processes. (The order of a Markov process refers to the number of previous values of the stochastic variable which are correlated to the next value.) For a zeroth order process COZOIL requests means and standard deviations for wind speed, wind direction, and air temperature. The model assumes that both wind direction and air temperature are normally distributed; wind speed is drawn from a Poisson distribution. (Note that the variance and the mean are the same in a Poisson distribution.) The procedure neglects autocorrelations in the stochastic wind record, but greatly increases the ease of application.

To perform stochastic simulations with a first-order Markov process, the user must supply a full Markov matrix. The form of this matrix is described in detail in the user's manual for COZOIL. In overview, the matrix has eight directional components, each with five speed intervals. The matrix is therefore of dimension 41x41, to include the calm wind condition. Use of the first-order Markov option provides more realistic wind time-series than the zeroth-order option:

- 1) Correlations between speed and direction are maintained.
- 2) Non-Poisson (e.g., bimodal) wind speed and nonnormal wind direction distributions are more accurately represented.
- 3) Temporal correlations in the wind record are more accurately reflected in the simulation.

2.2.4 Waves

The user can direct the model to compute waves from the wind record or to read in a wave time-series from a prepared file. In either case, the inputs to the computational model are wave height (m), wave period (see), and direction of propagation. These values are assumed by the model to apply at the offshore (open) boundaries. If the user elects to compute waves from the wind record, the model uses the shallow-water, wave-forecasting equations recommended by the U.S. Army Corps of Engineers Shore Protection Manual (CERC, 1984):

$$\frac{gH_s}{w'} = 0.283 \tanh \left[0.530 \left(\frac{gd}{w^2} \right)^{3/4} \right] \tanh \left\{ \frac{0.00565 \left(\frac{gF}{w^2} \right)^{1/2}}{\tanh \left[0.530 \left(\frac{gd}{w^2} \right)^{3/4} \right]} \right\} \quad (2.1)$$

$$\frac{gT_w}{w} = 7.54 \tanh \left[0.833 \left(\frac{gd}{w^2} \right)^{3/8} \right] \tanh \left\{ \frac{0.00379 \left(\frac{gF}{w^2} \right)^{1/3}}{\tanh \left[0.833 \left(\frac{gd}{w^2} \right)^{3/8} \right]} \right\} \quad (2.2)$$

$$\frac{gt}{W} = 5.37 \times 10^2 \frac{\left[\frac{gT_w}{w} \right]^{7/3}}{\left[\frac{gt}{W} \right]} \quad (2.3)$$

where g = gravitational acceleration (9.81 m/sec²).

H_s = significant wave height (m).

w = wind speed (m/sec).

d = water depth (m).

F = wind fetch (m).

T_w = significant wave period (sec).

t = wind duration (sec).

Refraction, diffraction, wave height, and phase transformations are computed using a modified version of the CERC linear wave propagation model RCPWAVE (Ebersole et al., 1986). The theoretical basis of this model, condensed from the source document, is described below.

Wave transformation outside the surf zone

The velocity potential function for linear, monochromatic, plane waves can be represented by the expression:

$$\phi = ae^{is} \quad (2.4)$$

where $a(x,y)$ = wave amplitude function equal to $gH(x,y)/2\sigma$.

$H(x,y)$ = wave height.

σ = angular wave frequency ($2\pi/T$); T = wave period.

$s(x,y)$ = wave phase function.

Here the velocity potential function only describes the forward scattered wave field. No considerations are given to wave reflections. By substituting this expression for the velocity potential into the "mild slope equation" (Smith and Sprinks, 1975) and solving the real and imaginary parts separately, two equations can be derived (Berkhoff, 1976):

$$\frac{1}{a} \left\{ \frac{\partial^2 a}{\partial x^2} + \frac{\partial^2 a}{\partial y^2} + \frac{1}{cg} \left[\nabla a \cdot \nabla \left(\frac{c}{g} \right) \right] \right\} k^2 - |\nabla s|^2 = 0 \quad (2.5)$$

$$\nabla^* (a^2 c c_g \nabla s) = 0 \quad (2.6)$$

where c is wave celerity (wave speed), c_g is wave group celerity, and the symbol ∇ denotes the horizontal gradient operation.

Together, these equations describe the combined refraction and diffraction process. The governing equations are solved using a finite-difference operator. Model input includes values of the deep-water wave height H_0 , direction θ_0 , and period T of waves to be simulated. It also includes specification of the bottom bathymetry throughout the grid. The wave number, which is related to the wave period and the local water depth through the dispersion relation, is computed at every cell. Wave number is used as an initial guess for the magnitude of the wave phase function gradient. The wave celerity c (at any point in question) and the group velocity C_g are functions of the wave period and wave number. Therefore these variables can be calculated at each cell. From Snell's law:

$$\frac{\sin \theta}{c} = \frac{\sin \theta_0}{c_0} \quad (2.7)$$

where c_0 is the deep-water wave celerity (defined to be $gT/2\pi$), an estimate of the local wave angle is calculated everywhere. This estimate assumes that the bottom contours are parallel with the shoreline. If the bottom bathymetric contours make a known nonzero angle with the shoreline, a better first guess for the wave angles can be computed. The new approximation is:

$$\theta = -\sin^{-1} \left| \frac{\sin(\theta_0 - \theta_c)}{\frac{c_0}{c}} \right| + \theta_c \quad (2.8)$$

where θ_c defines the contour angle. The local wave angle, deep-water wave angle, and contour angle follow the angle convention shown in Figure 2.8.

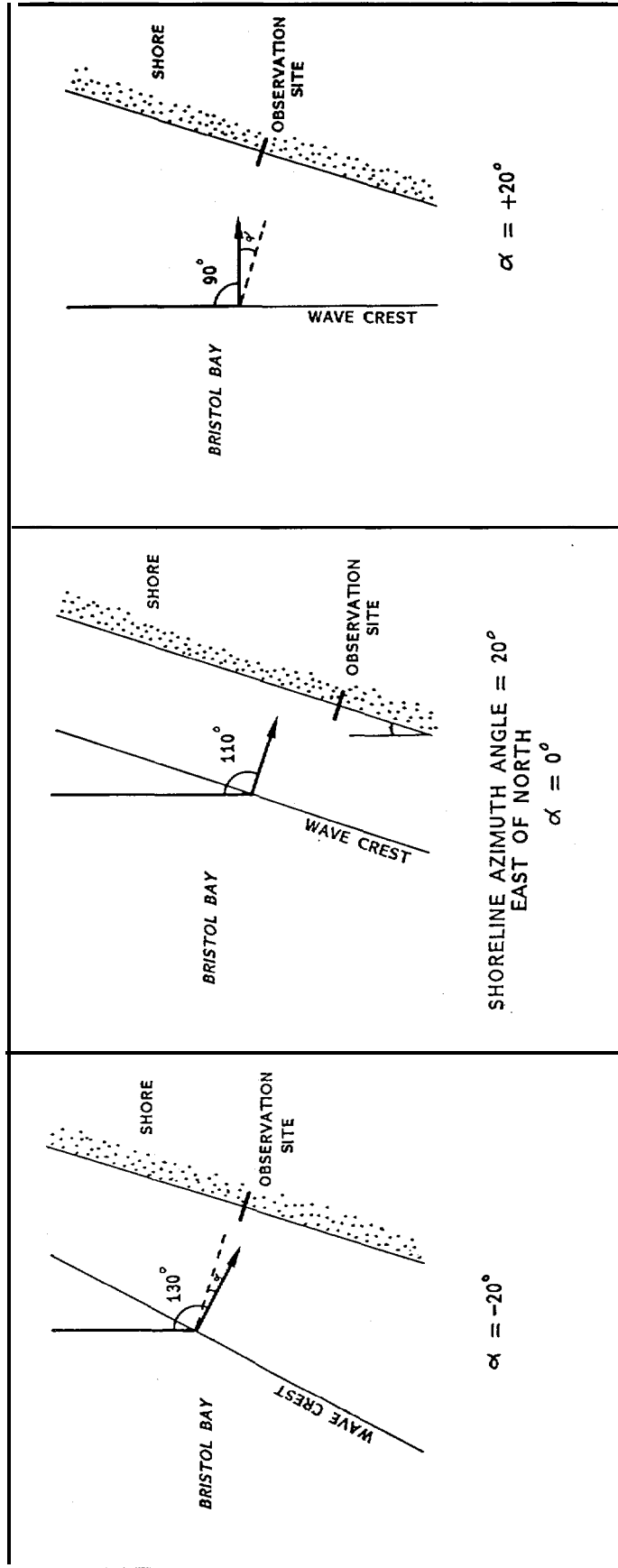


FIGURE 2.8. The convention for wave angle determination. Azimuths are in degrees True.



Wave transformation inside the surf zone

Waves approaching the very nearshore zone tend to steepen and eventually break because of decreasing water depths. Shoreward of this breaking point, dissipative energy losses due to turbulence strongly influence the wave height. Linear theory allows neither for prediction of the breaker location nor for wave transformation across the surf zone. Instead, empirical and approximate methods must be used to describe the breaking process.

Based on the review of wave-breaking criteria by Iwata and Sawaragi (1982), the authors of RCPWAVE use the criterion of Weggel (1972):

$$H_b = \frac{bh_b}{1 + \frac{ba}{gT^2}} \quad (2.9)$$

where $a = 43.75 [1 - e^{(-19 m)}]$.

$b = 1.56 [1 + e^{(-19.5 m)}] - 1$.

$m =$ beach slope.

Once the incipient breaking point is defined, a mechanism is needed to transform the breaking wave across the surf zone. Historically, the wave height has been assumed to be proportional to the local water depth throughout the surf zone. The constant of proportionality was assumed to be about 0.8. Field and laboratory data have shown that this approximation consistently overestimates actual wave heights within the surf zone (Dally, 1980; Thornton and Guza, 1982).

The transformation algorithm selected for use in RCPWAVE (Dally et al., 1984) uses the hydraulic jump energy loss to approximate losses across the entire surf zone. Through analogy with energy flux in a channel, the following equation is postulated:

$$\frac{\partial \left(H^2 c_g \right)}{\partial x} = \frac{-\kappa}{h} \left[H^2 c_g - \left(\gamma^2 h^2 c_g \right)_s \right] + D \quad (2.10)$$

where κ = rate of energy dissipation coefficient (set equal to 0.2 in RCPWAVE).

$(\gamma^2 h^2 c_g)_s$ = stable level of energy flux that the transformation process seeks to attain.

h = local water depth (m).

H = wave height (m).

γ = proportionality coefficient (set equal to 0.4 in RCPWAVE).

This surf-zone, wave-transformation model can be incorporated into the conservation-of-wave-energy equation by adding the dissipation term D to the right-hand side, representing dissipation in the direction of wave propagation. In vector notation, the energy equation becomes:

$$\nabla \cdot \left[a^2 c c_g \nabla s \right] = \frac{-\kappa}{h} \left[a^2 c c_g |\nabla s| - \left[\frac{g}{2\sigma} \gamma^2 h c c_g |\nabla s| \right] s \right] \quad (2.11)$$

This equation can be thought of as being valid both inside and outside the surf zone. Outside, the coefficient κ is zero.

For computation of wave phase transformations within the surf zone, diffraction effects are assumed to be negligible. Therefore, the wave number k is assumed to accurately represent the magnitude of the wave-phase function gradient. The linear wave theory assumption that the waves are irrotational also will be assumed to remain valid inside the surf zone. Consequently, wave angles inside the surf zone are computed in the same manner as used outside the surf zone.

Comparisons between model results and observed data were used to verify the model. Both laboratory and field data were used in these tests. The ability of RCPWAVE to simulate wave transformation outside the surf zone was checked using data collected during a laboratory experiment conducted by Berkhoff et al. (1982) and using prototype data obtained during a field experiment at the CERC Field Research Facility in Duck, North Carolina. Only laboratory data were used to verify the surf-zone, wave-transformation part of the model. These data were collected during one-dimensional flume tests performed by Horikawa and Kuo (1966) and Isumiya (1984). Both experiments considered only breaking of monochromatic plane waves. The former experiment investigated wave transformation on a plane beach only; the latter involved tests using plane, stepped, and barred beaches. These comparisons are discussed in detail in Ebersole et al. (1986).

Wave runup and setup

COZOIL also includes a procedure for computing wave runup. The vertical height above the still-water level to which incident waves will run up a beach face depends on the shape, roughness, and permeability of the beach, as well as characteristics of the wave. A comprehensive theoretical description of this process is not available due to the large number of variables involved (CERC, 1984). In addition, most laboratory tests have been performed for smooth impermeable slopes.

Based on the graphical procedures outlined in CERC (1984), the following approximate-curve fit has been obtained:

$$R_w = 1.5 H_o \exp \left[\frac{-295 H_o}{g T_w^2} \right] \quad (2.12)$$

in which R_w = vertical runup distance (m).
 H_o = deep-water wave height (m).
 T_w = significant wave period (sec).
 g = gravitational acceleration (m/sec^2).

COZOIL also incorporates a wave setup computation based on radiation stress concepts (CERC, 1984). The net wave setup, S_n , at the coast is the wave setup minus the setdown:

$$S_n = 0.15 h_b - \left[\frac{g^{1/2} H_o^2 T_w^2}{64 \pi h_b^{3/2}} \right] \quad (2.13)$$

The depth of water at the breaker point is computed from:

$$b = \frac{b}{b - \frac{aH_b}{gT_w^2}} \quad (2.14)$$

where the coefficients a and b are as given for equation (2.9).

2.2.5 Currents

COZOIL uses tidal, wind-driven, and wave-induced currents to perform transport calculations. With the exception of the wave-induced currents used inside the surf zone, these data sets can be input directly by the user or accessed from external files. Wave-induced currents are computed inside the model as the simulation proceeds.

To compute tidal currents, the model requests two parameters, tidal period and maximum tidal current amplitude, from the user. The latter parameter can be obtained approximately from "local knowledge" (e.g., fishermen), from a current-meter record, coastal pilot handbook, or charts. The model assumes that tidal currents are parallel to the coast (a reasonable assumption nearshore) and proceeds to compute the mean longshore direction from the input reach information. The tidal currents, V_T , are then simulated as:

$$V_T = V_{max} \sin(\omega t + \phi) \quad (2.15)$$

where V_{max} = maximum tidal current amplitude.

$$\omega = 2\pi/T_{ps} \text{ (per hour).}$$

$$T_{ps} = \text{tidal period (hours).}$$

$$t = \text{time (hours).}$$

$$\phi = \text{user input tidal phase lag at simulation start (radians).}$$

Tidal currents are 90 degrees out of phase with tidal height. The mid-tide level corresponds to maximum current velocities, whereas high and low tides correspond to minimum velocities. COZOIL incorporates a simple model (Reed et al., 1980) to provide an estimate of the wind-driven currents in the study area. This model incorporates the following assumptions:

- 1) Uniform currents over an upper mixed layer of constant depth.

- 2) No flow in the vertical.
- 3) No surface setup.

It should be noted that this model is not a particularly good one to use near shorelines since it ignores the surface slope terms and, therefore, is less than ideal for inclusion in COZOIL. Other two-dimensional hydrodynamic models with realistic bathymetric and free-surface effects are too demanding in terms of CPU requirements for inclusion in COZOIL at present. However, data sets derived from such hydrodynamic models with more realistic boundary conditions will give more reliable results.

The governing equations for the slab flow model are:

$$\frac{du}{dt} = fv + \frac{\tau_{xs}}{\rho_w d} - \frac{\tau_{xd}}{\rho_w d} \quad (2. 16a)$$

$$\frac{dv}{dt} = fu + \frac{\tau_{ys}}{\rho_w d} - \frac{\tau_{yd}}{\rho_w d} \quad (2. 16b)$$

which have the solution:

$$u(t) = \exp\left[-\frac{R_d t}{d}\right] \left[\cos(ft) [U_0 - u_{\infty}] + \sin(ft) [v_0 - v_{\infty} + u_{\infty}] \right] \quad (2. 17a)$$

$$v(t) = \exp\left[-\frac{R_d t}{d}\right] \left[\cos(ft) [V_0 - v_{\infty}] - \sin(ft) [u_0 - u_{\infty} + v_{\infty}] \right] \quad (2. 17b)$$

where R_d = drag velocity at the depth d (0.001 m/sec).

d = depth (m) of wind-driven flow (average study area depth).

f = earth rotation rate (radians/sec).

u_0, v_0 = water velocity (m/sec) components at start of wind input ($t=0$).

u_{∞}, v_{∞} = asymptotic water velocity (m/sec) components at $t = \infty$.

The asymptotic velocity components are given by:

$$u_{\infty} = \frac{\left(\frac{\rho_a}{\rho_w}\right) R_s (R_d U + dfV)}{d^2 + d^2 f^2} \quad (2.18a)$$

$$v_{\infty} = \frac{\left(\frac{\rho_a}{\rho_w}\right) R_s (R_d V + dfU)}{d^2 + d^2 f^2} \quad (2.18b)$$

where ρ_a, ρ_w = air and water density, respectively.

R_s = surface drag velocity (0.01 m/sec).

U, V = wind velocity components (m/sec).

The asymptotic transport angle is then:

$$\theta = \tan^{-1} \left[\frac{df}{d} \right] \quad (2.19)$$

to the right of the wind in the northern hemisphere. The model uses the mean depth of the study area for the depth d . For a 5-m/sec wind and a mean depth of 5 m, the asymptotic wind-driven current is about 5 cm/sec, 25° to the right, achieved after about six hours: for a mean depth of 10 m, the asymptotic current is about 4 cm/sec at 45° after about eight hours (Reed et al., 1980).

The wind-driven flows are not applied inside the surf zone and are therefore most relevant with regard to transport of subsurface entrained oil offshore. Since this transport has little effect on the ultimate disposition of oil along the coastline, further improvements on this aspect of COZOIL are given relatively low priority.

A potential future improvement, representing a compromise between the slab flow model now used in COZOIL and a full two-dimensional model, would be to incorporate the one-dimensional mode of Hubertz (1987). This model would be an improvement for straight shorelines, but may be problematic for complex coastal configurations since conservation of mass from one reach to the next would not be assured.

Subsurface advection in the surf zone is assumed to be dominated by the wave-induced current in the water column, with wind effects superimposed for surface slicks. The model uses the radiation stress theory of Longuet-Higgins (1970) as modified empirically by CERC (1984). The longshore velocity V_{LS} is given in terms of the breaker height H_b , the angle between breaker crest and shoreline α_b , and the beach slope m as:

$$V_{LS} = 20.7 m \left[\frac{g H_b}{d} \right]^{1/2} \sin 2\alpha_b \quad (2.20)$$

The direction of transport (i.e., to the left or to the right) is given by the angle α_b relative to the shoreline.

A seaward return flow in the surf zone compensates for the shoreward mass flux above the level of the wave troughs. The effect of this return flow is to transport oil in the surf-zone water column to the water column offshore. COZOIL incorporates the work by Stive and Wind (1982, 1986), whereby the offshore volumetric flux rate per unit length of beach is given by:

$$q_{off} = 0.1 \left(\frac{g}{d} \right)^{1/2} H h_t \quad (2.21)$$

where h_t = the depth up to the wave trough level (m).

d = mean water depth (m).

H = wave height (m).

The mass of oil in the surf zone of reach i which is removed to the offshore per time-step Δt is then:

$$\Delta M_i = \frac{M_i q_{off} \Delta t}{Lh} \quad (2.22)$$

where M_i = the total mass (ret) of oil entrained in the surf-zone water column.

L = the width (m).

h = the mean depth (m) of the surf zone of reach i .

2.3 OIL-FATE CONCEPTS AND ALGORITHMS

Offshore, outside the surf zone. COZOIL employs numerical concepts for oil spill fates simulation developed previously (Mackay et al., 1980; Reed et al., 1980; Payne et al., 1984a, b; Spaulding et al., 1986). Inside the surf zone, many additional concepts have been incorporated--in some cases, without strong empirical evidence for values of the necessary parameters. In such cases, the user is given optional control over parametric values.

2.3.1 Offshore

Spreading

Spreading of a surface slick is computed according to the gravity-viscous formulation of Fay (1971) and Houtt (1972), as modified by Mackay et al. (1980). An oil slick can be conceptualized as consisting of thick and thin (i. e., sheen) portions. Mackay et al. (1980) use the gravity/viscous formulation to describe spreading of the thick portion of the slick, while the thin portion spreads according to the viscous/surface tension formulation. Since most of the mass is associated with the thick slick, only that portion of the modified formulation is included here. As discussed below, neglecting the larger surface area covered by sheen makes comparison with observations of slick size difficult. The rate of change of surface area, A (m^2), with time, t (see), is:

$$\frac{dA}{dt} = K_A A^{1/3} \frac{V}{A} \cdot 4/3 \quad (2.23)$$

Here, V is slick volume (m^3). The constant K_A is set to 150 (see-i) in COZOIL. This is the value suggested by Mackay et al. (1980), although their analysis was performed in the absence of any mass-loss processes such as evaporation or dispersion. These processes can account for over 50 percent of the total mass spilled over a time period of a few days to a week. Any analysis which assumes the volume V in equation (2.23) to be constant over time periods of several days is therefore bound to result in significant error. In fact, the areal coverage as computed from equation (2.23) is in general at least two orders of magnitude below the observed data accumulated by Ford (1983). This latter document is unclear, however, with regard to how much open water or sheen-covered water is included in the areal estimates for specific spills,

making comparisons difficult at best. Equation (2.23) is explicitly used only to compute the surface area covered by relatively thick oil: results from this equation would therefore be considerably lower than observations which do not account for patchiness of thick oil slicks.

Evaporation

Evaporation of hydrocarbons from a surface slick is computed using the methods of Payne et al. (1984 b). The parent oil is represented by a series of constituents differentiated by boiling point, density, and molecular weight. The mass transfer rate from the slick for the i^{th} constituent is:

$$\frac{dm_i}{dt} = \frac{K_B P_i A f_i M_i}{RT} \quad (2.24)$$

where P_i = vapor pressure (atm) of i^{th} constituent.

A = slick area (m^2).

f_i = fraction of remaining slick consisting of constituent i .

M_i = molecular weight (g/mole) of constituent i .

R = gas constant ($8.206 \times 10^{-5} \text{ atm} \cdot \text{m}^3/\text{mole} \cdot \text{K}$)

T = environmental temperature "K.

Since the water-surface temperature effectively controls the air temperature near the water surface, either can be used in COZOIL. The mass transfer coefficient K_B is that of Mackay and Matsugu (1973):

$$K_B = 0.029 W^{0.78} D^{-0.11} S_c^{-0.67} \sqrt{\frac{M_i + 29}{M_i}} \quad (2.25)$$

where W = wind speed (m/hr).

D = slick diameter (m).

Following Mackay et al. (1980), we use a Schmidt number S_c for cumene, 2.7. The molecular weight term in equation (2.25) is a correction for diffusion in air (Liss and Slater, 1974).

Entrainment/Dissolution

Entrainment and dissolution represent the only offshore pathways for removal of mass from a surface slick other than evaporation. Unlike evaporation, entrainment is assumed to occur equally across all boiling point constituents of the oil. Dissolution is not modeled explicitly as a process separate from entrainment of oil particles or globules into the water column.

The user has two options for oil entrainment algorithms. The first is that proposed by Audunson (1979) and modified by Spaulding et al. (1982a). The mass transfer rate (per day) is:

$$\frac{dm}{dt} = 0.4 \frac{m^{1/2}}{W_{ol}} \left[\frac{W}{W_{ol}} \right]^2 \quad (2. 26)$$

where m = mass of spinet (ret)

W = wind speed (m/sec).

t = time (days) since spinet release.

W_{ol} = reference wind speed (8.5 m/sec).

The second alternative algorithm is that proposed by Mackay et al. (1980), which gives a mass transfer rate (per hour) of

$$\frac{dm}{dt} = \frac{0.11m(1+W)^2}{1 + 50\mu^{0.5}\delta\sigma} \quad (2. 27)$$

where μ = dynamic viscosity of oil (cp).

δ = slick thickness (m).

σ = oil/water interracial tension (dyne/cm).

Emulsification

The emulsification viscosity μ (cp) is allowed to increase for petroleum products according to a "mousse formation" algorithm, also from Mackay et al. (1980). The rate of incorporation of water into the slick is:

$$\frac{dF_{wc}}{dt} = 2 \times 10^{-6} (W + \left[\frac{1 - F_{wc}}{C_1} \right]) \quad (2.28)$$

where F_{wc} = fraction of water in oil.

W = wind speed (m/sec).

$OC_1 = 0.7$ for crude oils and heavy fuel oils (Mackay et al., 1982).

Gasoline, kerosene, and light diesel fuel are assumed not to form emulsions with water (Payne and Phillips, 1985). The resultant viscosity μ of the oil in the slick is then computed using the Mooney (1951) equation:

$$\frac{\mu}{\mu_o} = \exp \left\{ \frac{2.5 F_{wc}}{1 - 0.65 F_{wc}} \right\} \quad (2.29a)$$

in which μ_o is the viscosity of the parent oil. The effect of evaporation on viscosity is modeled as:

$$\mu = \mu_o \exp \left\{ C_2 F_{\text{evap}} \right\} \quad (2.29b)$$

where F_{evap} is the fraction evaporated from the slick. C_2 varies in value between about 1 and 10 (Mackay et al., 1982). The model uses C_2 equal to one for jet fuel and light diesel fuel, and C_2 equal to ten for other petroleum products.

The viscosity varies with temperature according to the de Guzman-Andrade equation (Perry and Chilton, 1973), as incorporated by curve fit into the CERCLA Type A Natural Resource Damage Assessment Model (Reed et al., 1988):

$$\mu = \mu_o \exp \left[\frac{8770}{T_k} - 29.41 \right] \quad (2.30)$$

where μ_o = reference viscosity (cp) at 25° (298°K).

μ = temperature-corrected viscosity (cp).

T_k = environmental temperature (°K).

Advection

Offshore oil at the water surface is transported by the instantaneous sum of currents at the slick centroid. An additional transport at the surface is included to reflect wind and wave effects. Thus the net instantaneous slick transport velocity V is:

$$V = \vec{V}_T + \vec{V}_W + 0.03 \vec{W} + \vec{V}_{LS} \quad (2.31)$$

The tidal and wind-driven velocity components, V_T and V_W , are bilinearly interpolated within the grid system. Local velocities are defined at the midpoints of the side of grid cells. The longshore velocity V_{LS} is applied only to oil inside the surf zone.

Subsurface oil is represented offshore by discrete particles entrained from surface slicks. The initial location of a particle is at a random location under the source slick, at a depth z , given by:

$$z = 0.5(1 + R^*)H \quad (2.32)$$

where R^* = random variate $[-1 \leq R^* \leq 1]$.

H = wave height.

Subsequent transport of the particle is by the superposition of interpolated horizontal velocities, plus random components in both the horizontal and the vertical. The random components are computed (Reed et al., 1980) as:

$$R^* = \frac{R}{\sqrt{A}} \quad (2.33)$$

The diffusivity D is selected from the pair (D_H, D_V) , depending on whether a horizontal or vertical random walk step is being computed. The values of D_H and D_V are taken as 10 and $0.01 \text{ m}^2/\text{sec}$, respectively (Okubo, 1971; Csanady, 1973).

The offshore subsurface transport of entrained oil is largely irrelevant to the ultimate fate of oil along the coastline. This facility has been included to give the eventual users of COZOIL a more complete simulation capability, and it can be optionally "turned off" by the user to increase model operation speed.

2.3.2 Surf Zone

Spreading

Spreading of surface slicks in the surf zone can occur in both onshore/offshore and longshore directions. Transverse to the shoreline, compression of the slick occurs due to wind and wave/current forces on the slick and impedance to forward motion by the shoreline. (If the wind is offshore, the slick will be transported away from the coast, and the following discussion does not apply).

Buist and Twardus (1984) and Buist (1987) present data for the equilibrium thickness of small (<1 kg) oil slicks spreading against wind in a windtunnel. Their definition of the equilibrium thickness is that thickness at which the spreading and wind forces balance. At this point, the acceleration of the slick edge is zero, but the velocity in general is nonzero. Investigation of the dynamic behavior of the equation for the one-dimensional spreading used by Buist and Twardus (1984) shows that the location of the slick edge oscillates in time, such that the equilibrium thickness as defined by these authors occurs when the velocity of the slick edge is a maximum (i.e., when the acceleration is zero and the thickness itself is changing most rapidly). Their analysis, therefore, is not useful for the COZOIL model in which winds are, in general, unsteady and coastal slicks are constantly changing mass and shape. We therefore have performed a more detailed analysis which is based on certain simplifying assumptions:

- 1) Oil slick thickness is uniform across the slick.
- 2) Tendency of a slick to spread remains a function of area and thickness, as offshore.
- 3) Tendency to compress is proportional to the onshore wind stress on the slick.
- 4) Circulation of oil within the slick is negligible.

Little error is introduced as a result of assumption (1) relative to the thick slick/thin slick conceptualization, since over 90 percent of the mass is associated with the thick slick (Mackay et al., 1980). Assumption (2) simply reflects the parameterization of the spreading process (equation 2.23), wherein the mean effects of chemical composition and environmental processes are represented by a single rate parameter.

For an infinitesimal element of oil (Fig. 2.9), we assume that the spreading force in the onshore-offshore direction is balanced by the wind stress. In the alongshore direction, spreading occurs as usual.

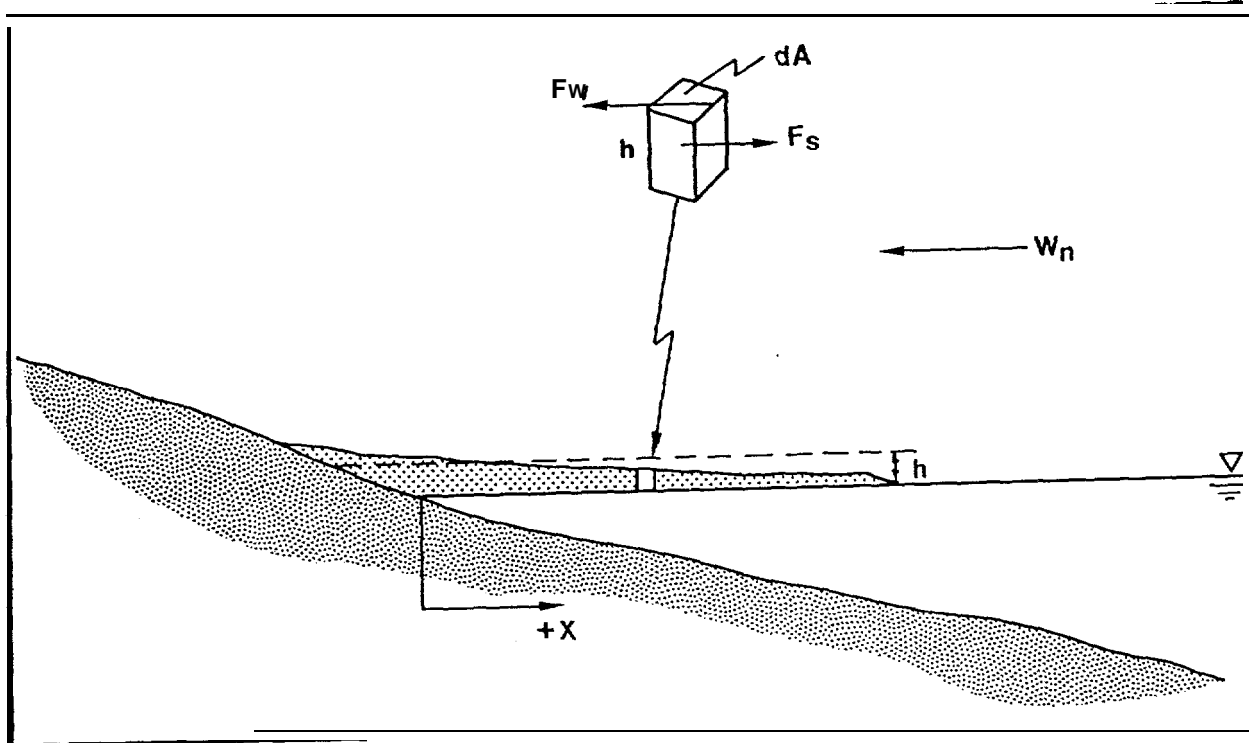


FIGURE 2.9. Schematic of oil driven against the shore by the wind. Spreading/contracting transverse to the shoreline is the resultant of the wind force F_w and the spreading force F_s .

From equation (2.23), we have:

$$\frac{dA}{dt} = 2\pi R \frac{dR}{dt} = K_A A^{1/3} \delta^{4/3} \quad (2.34)$$

where δ is the mean slick thickness and R is mean slick radius. Then the rate of change of the radius due to the spreading force is:

$$\frac{dR}{dt} = 0.5K_A \delta^{4/3} \pi^{-2/3} R^{1/3} \quad (2.35)$$

If the volume of the slick is constant (i.e., we neglect evaporation, entrainment, and emulsification during a computational time-step), then the rate of change of the thickness δ in terms of the radius R is:

$$\frac{dh}{dt} = -\frac{2\delta}{R} \frac{dR}{dt} \quad (2.36)$$

and the acceleration of the slick edge, due to spreading forces only, still is:

$$\frac{d^2R}{dt^2} = \frac{-1.5 K_A \delta^{4/3} \pi^{-2/3} R^{-1/3} dR}{dt} \quad (2.37)$$

Here we see that the spreading force opposes the spreading velocity. The wind stress due to a wind speed W_N on an element of our ideal slick of uniform thickness is then:

$$T = \rho_a C_D W_N^2 dA \quad (2.38)$$

in which ρ_a = density of air (kg/l).

C_D = stress coefficient.

dA = area element (m^2).

W_N = wind speed normal to and directed towards the coast (m/sec).

The spreading force plus the wind stress force (Fig. 2.9) give the net acceleration of the element:

$$\rho_{oil} \delta dA \frac{d^2R}{dt^2} - \rho_a C_D W_N^2 dA = \rho_{oil} \delta dA \frac{d^2R_T}{dt^2} \quad (2.39)$$

where we have used R to denote radial changes due to spreading alone, as before, and R_T for the net radial change transverse to the shoreline. Then:

$$\frac{d^2R_T}{dt^2} = \frac{d^2R}{dt^2} - \frac{\rho_a C_D W_N^2}{\rho_{oil} \delta} \quad (2.40)$$

We are interested here in a methodology which will allow us to estimate the foreshortening of a slick in the onshore/offshore direction, with continued spreading along here. We therefore adopt the convenience of allowing the slick to become elliptical, with the major axis alongshore and the spreading velocity of the major radius given by equation (2.35). The dynamics of the minor radius of the slick, oriented transverse to the shoreline, are then governed by equation (2.40), the major axis by equation (2.23) recast in terms of mean slick radius rather than area. The dynamic

behavior of the minor axis of a 100-m³ oil slick under the influence of various onshore wind speeds is discussed in section 5.2.1.

Entrainment

Entrainment of oil from a surface slick inside the surf zone is computed using the same algorithm as was specified by the user outside the surf zone.

Advection

Advection in the surf zone is assumed to be dominated by the wave-induced current in the water column, with wind effects superimposed for surface slicks. The model uses the radiation stress theory of Longuet-Higgins (1970) as modified empirically by CERC (1984). The longshore velocity V_{LS} is given in terms of the breaker height H_b , the angle between breaker crest and shoreline α_b , and the beach slope m as:

$$V_{LS} = 20.7 m \left(g H_b \right)^{1/2} \sin 2\alpha_b \quad (2.41)$$

The direction of transport (i.e., to the left or to the right) is given by the angle α_b relative to the shoreline.

A surf-zone "subcell," with a width equal to the then-current surf-zone width, is associated with each coastal cell. A fraction F_i of the mass of oil, m_i , which is in surf-zone cell i , is transported into an adjacent surf-zone cell each time-step:

$$F_i = \frac{V_{LS} \Delta t}{\Delta L} \quad (2.42)$$

in which V_{LS} = the longshore transport velocity (m/sec) for this coastal cell (equation 2.41).

ΔL = the longshore coastal cell dimension (m).

Δt = the time-step (sec).

Whether the transport is into the prior ($i-1$) or the subsequent ($i+1$) surf-zone cell depends on the incident wave angle α_b .

2.3.3 Onshore

Deposition on foreshore surface

An oil slick which has contacted the shoreline may deposit oil on the foreshore if the water level (tide height plus wave setup and runup) does not exceed the foreshore height associated with that reach. First, the model checks to determine that an empirical "holding thickness" (CSE/ASA/BAT, 1986; Gundlach, 1987) has not been exceeded for the coastal cell in which contact has occurred. When the tide is falling, the ratio of the newly exposed beach face to the onshore/offshore radius of the slick determines the fraction of the slick which is deposited, if the holding thickness has not been reached.

Oil deposited on a previously clean foreshore carries with it the characteristics of the parent slick--viscosity, density, and boiling-point constituents. As additional oil comes ashore at the same location, perhaps from the same or another spinet, the oil on the foreshore surface takes on the weighted average values of the above characteristics. If, for example, a mass of new oil is added which equals 10 percent of the mass already present, then the new characteristics will be 10/110, or about 9 percent those of the new oil, and 91 percent those already present. This represents an assumption of complete mixing and is consistent with assumptions made elsewhere in the model.

Deposition on **backshore**

If the water height exceeds the input foreshore height, then a slick in contact with the shoreline will deposit oil on the backshore. As on the foreshore, the fraction of the slick which is deposited is determined by the ratio of newly exposed backshore to slick width and is again limited by a maximum holding thickness.

Entry into sediment/groundwater system

Observational evidence from several major oil spills (particularly the *Arrow* in Canada and the *Amoco Cadiz* in France) indicates that oil, in association with the groundwater within beaches, may persist for several years. Vandermeulen and Gordon (1976) reported observations of oil associated with groundwater resulting from the *Arrow* oil spill in Nova Scotia. An estimate of the general level of oil released from the sediments was presented, indicating runoff losses in the parts-per-billion range.

Self-cleaning of incorporated oil was estimated to take as much as 170 years, indicating the possible long-term nature of the problem.

Study of the *Amoco Cadiz* oil spill indicated that numerous beaches and tidal flats contained polluted groundwater long after the beach surface was free of oil. A survey in August 1986, 8.5 years after the spill, revealed that contaminated groundwater still was present in some sheltered (and very soft) mudflat areas and associated with remaining cleanup trenches. "On beaches, in contrast to mudflats, the most common areas for oil-contaminated groundwater to be found were at the base of the beach (slightly above the toe of the beach) or along the upper part of the low-tide terrace. These areas generally conformed to the surface waters of the zone of saturation. On mudflats, oil was incorporated within the soft, water-saturated sediments wherever substantial surface concentrations of oil had occurred.

The processes governing oil incorporation and movement within beach sediments and groundwater are not fully understood. However, by utilizing a series of formulations originally developed to predict fluid transport through land-based groundwater systems, it is possible to develop a computer-simulation model depicting penetration into beaches and subsequent removal or flushing of oil from this system.

The two concepts of wettability and capillarity are relevant here. Relative to oil, water is a "wetting fluid" [i.e., the adhesive forces between the fluid and the sediment exceed the cohesive forces within the fluid (Convery, 1979)]. Wettability is a relative term, defined technically as a balance among the relevant surface tension forces. A pressure difference exists across the interface between two immiscible fluids in a porous medium. The curvature of the interface reflects the magnitude of this pressure difference, called the capillary pressure. This pressure is a measure of the tendency of the sediment to draw in the wetting fluid (water) and to repel the nonwetting fluid (oil).

Three different regimes of fluid saturation can be distinguished (Convery, 1979). At very low saturations, the wetting fluid exists as *pendular* rings around grain contacts within the porous medium. These rings of fluid are completely isolated from one another, except perhaps for a thin film of wetting phase that coats the grain surface. This film, present at extremely low saturations, occurs on surface adsorption sites on the sediments. The film has a monomolecular thickness and may be continuous or discontinuous. Hydraulic pressures cannot be transmitted through the wetting

fluid in the pendular regime. since it is not continuous. In our analysis, the wetting fluid is water and the nonwetting fluid is oil.

If the saturation of the wetting phase increases. the pendular rings expand and coalesce. so that flow of the wetting phase is possible. Coincidental with this development is a decrease in the saturation of the nonwetting phase. This saturation regime is labeled funicular. The phase distribution and flow behavior of fluids in the funicular regime are complex and are strongly a function of the saturation history of the porous medium.

With increasing saturation of the wetting phase, the nonwetting phase eventually becomes discontinuous. Commonly, droplets of the nonwetting phase become isolated in the larger pores of the medium. The nonwetting phase is in a condition of insular saturation. Nonwetting phase droplets become mobile only if a pressure discontinuity exists across them within the wetting phase to force them through capillary restrictions. Otherwise, the droplets are immobile and remain trapped within the pores. The insular drops will impede flow of the wetting phase to some extent.

In our analysis, we will identify only two regimes, the pendular and the insular, occurring at the foreshore surface in the presence of oil and in the zone of saturation, respectively (Fig. 2.10). Thus. we neglect some interfering complexities, such as pore blockage by oil in the funicular regime, allowing the characteristics of the oil to control flow computations at the foreshore surface and water to control within the beach.

In the present analysis, it is assumed that oil deposited on the beach foreshore may enter the sediment/groundwater system in two ways--the first by direct penetration and the second by transport in wave overwash. The former process is simulated using standard fluid/sediment flow algorithms. The second process assumes that waves breaking and overwashing oil on the foreshore will carry with them dissolved and particulate ("water-accommodated") oil. This water-accommodated oil is assumed to travel into the sediments with. and at the same rate as, the water itself. Once within the groundwater system, the transport of oil is assumed to be governed by flushing of the groundwater and equilibrium partitioning kinetics between the adsorbed and water-accommodated phases.

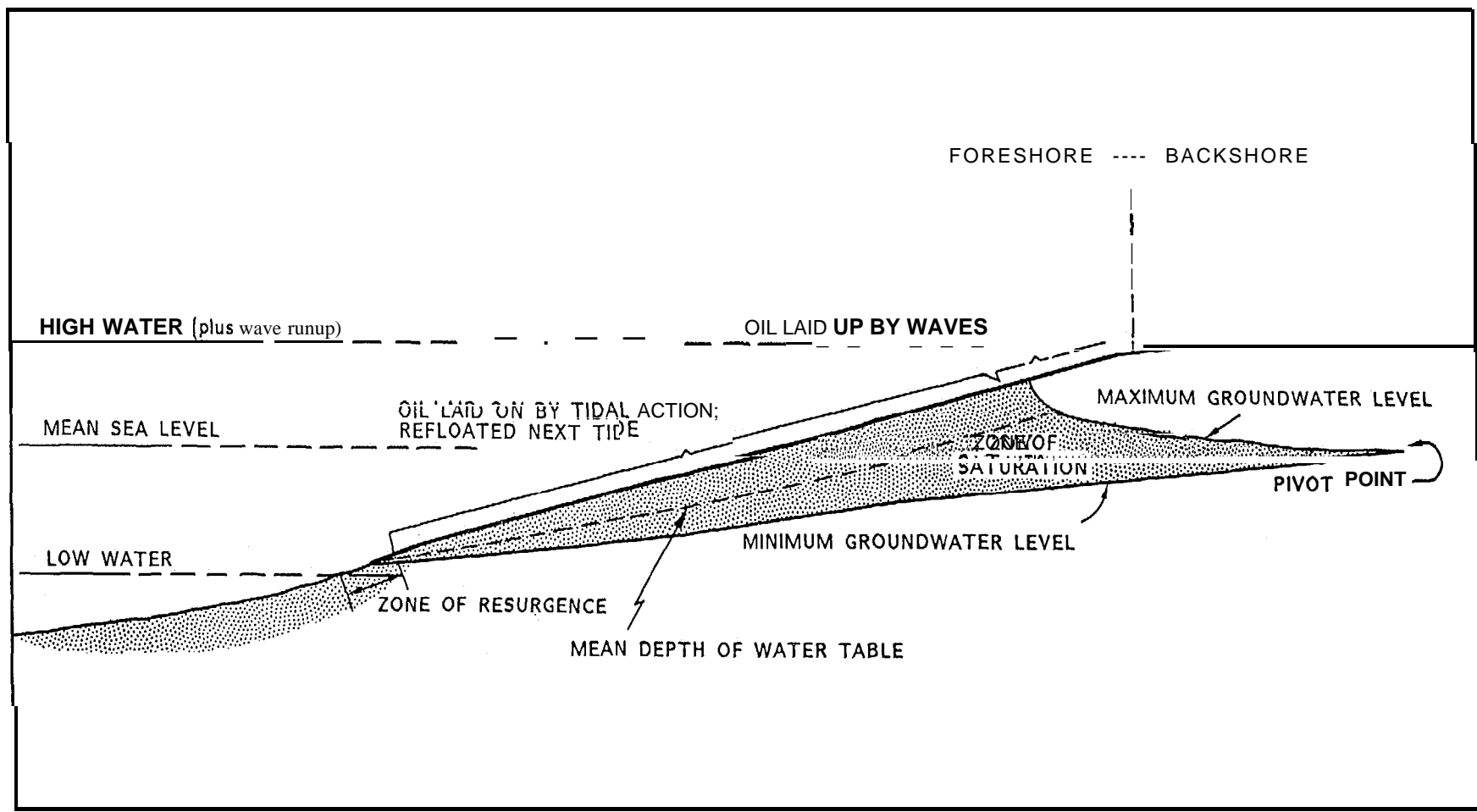


FIGURE 2.10. Schematic of beach groundwater system.

Direct penetration of oil into sediments

The flow of oil from a surface deposit into the underlying sediments can then be approximated by Darcy's law:

$$v_p = \frac{pg\rho \left(\frac{dh}{dl} \right)}{\mu} \quad (2.43)$$

where v_p = flow velocity (m/sec).

p = intrinsic permeability of the sediment (m^*).

g = gravitational acceleration (m/sec^2).

ρ = oil density (kg/m^3).

μ = dynamic viscosity ($N\text{-sec}/m^2$).

$\frac{dh}{dl}$ = pressure head gradient (m/m).

The intrinsic permeability is computed with an equation from Krumbeyn and Munk (1943):

$$p = 7.6 \times 10^{-10} (MG)^2 e^{-1.31\sigma_g} \quad (2.44)$$

in which MG = mean grain size (mm).

σ_g = inclusive graphic standard deviation (ϕ units).

The depth of penetration during a time-step Δt is then, to first order, $v_p \Delta t$. The mass flux Q is:

$$Q = A\rho v_p \Delta t \quad (2.45)$$

Here, A is the surface area covered with oil.

Removal of surface oil by wave overwash

Observations by Owens et al. (1983, 1987) suggest that wave exposure is an important parameter for the rate of oil removal from the beach surface. An expression is therefore required for the rate at which oil is removed from the parent slick on the foreshore and carried into the underlying sediments or returned to the active surf zone by wave action. We hypothesize that the governing variables are wave-breaking velocity V_b , exposed oil surface area A , oil viscosity μ and density ρ , and turbulent

diffusivity in the surf-zone D_v . Then the mass-transfer coefficient will be a function of the dimensionless groups:

$$R_e = \frac{\rho V_b L}{\mu}$$

$$S_c = \frac{\mu}{\rho D_v}$$

where R_e and S_c are the Reynolds and Schmidt numbers, respectively. The characteristic length L is taken as the square root of the exposed area A . The velocity of water falling from the crest of a breaking wave of height H_b onto the beach is:

$$V_b = \sqrt{2gH_b} \quad (2.46)$$

if frictional losses are neglected. The associated turbulent diffusivity is:

$$D_v = \frac{b^2}{T} \quad (2.47)$$

where T is the wave period (Harris et al., 1962). Based on an empirical relationship (Thibodeaux, 1977, 1979), the mass transfer coefficient for relatively insoluble high density ($\rho > 1$) substances can be approximated by:

$$h = 0.36 \left(\frac{\rho V_b L}{\mu} \right)^{0.8} \left(\frac{\mu}{\rho D_v} \right)^{0.33} \frac{D_v}{L} \quad (2.48)$$

Equation (2.48) is an empirical relationship developed for relatively low Reynolds number flows on river bottoms. Surf-zone Reynolds numbers are considerably higher, such that equation (2.48) appears to give unreasonably high removal rates. The rate coefficient, 0.36, in equation (2.48) is replaced by 0.0001 in COZOIL based on observed oil removal rates (Gundlach, 1987). The actual mass removal rate is then:

$$\frac{dm}{dt} = \rho hA \quad (2.49)$$

The mass removed from the oil on the foreshore surface by wave overwash is not all carried into the groundwater. Some fraction is carried back into the surf zone with the retreating wave. This oil in the surf zone is then further partitioned between the water column and the water surface, depending on the size range of the oil particles relative to the surf-zone turbulence. Lacking empirical values for these partitioning coefficients, the model supplies a set of default values based on best estimates of the authors (Table 2.1) and allows the user to alter them if desired. The default values neglect direct entry from the beach surface to the surf-zone water column, since this avenue is already represented via surface oil.

TABLE 2.1. Default values for partitioning of oil removed from the beach face by the action of waves. The oil removed is partitioned among the beach groundwater, the surf-zone surface, and the surf-zone water column in the following proportions.

	Reach Type						
	1 Smooth Rocks	2 Cobble	3 Eroding Peat Scarp	4 Sandy Beach	5 Gravel Beach	6 Tidal Flat	7 Marsh
Groundwater	0.000	0.100	0.100	0.100	0.100	0.050	0.050
Surface	0.900	0.900	0.900	0.900	0.900	0.950	0.950
Water Column	0.100	0.000	0.000	0.000	0.000	0.000	0.000

Removal from the sediment/groundwater system

Oil in the beach groundwater system probably exists in three phases. The first is a pendular phase, in which oil is the primary fluid within the sediment pores and may preclude penetration of water. If the oil in this phase has a relatively low viscosity, it may actually ride up and down on the rising and falling water table, as hypothesized by McLaren (1985) for diesel fuel in a gravel/sand beach. The second phase is droplets, which may adhere to sediment particles or become trapped within sediment pores. The third is a dissolved phase, whose transport is governed by movement of the groundwater itself.

Oil which has penetrated the surface sediments via equation (2.45) and remains above the mean water table (Fig. 2.10) may be removed to the surf zone if the beach

is subject to erosion by the present wave field. A basic assumption here is that the presence of the oil will not appreciably alter erodability of the beach sediments. Following Sunamura and Horikawa (1974), COZOIL incorporates a dimensionless erosion/accretion parameter G_o :

$$G_o = \frac{\left(\frac{H_o}{L_o}\right) \tan \beta^{0.27}}{\left(\frac{D_{50}}{L_o}\right)^{0.67}} \quad (2. 50)$$

where H_o = deep-water wave height (m).

L = deep-water wave length (m).

P_O = offshore bottom slope.

D_{50} = size of 50th percentile of sediment sample (m),

Beach erosion is assumed to occur for $G_o > 18$, accretion for $G_o < 4$, and equilibrium in between, [Note that CERC (1984) introduces some errors relative to the original document in reporting these limiting values.]

Relatively little is actually known regarding the details of oil behavior within the beach groundwater system. The following facts have been established through observation and experiment:

- 1) Both low and high viscosity petroleums can enter the groundwater system in significant quantities and remain detectable for years afterwards (Vandermeulen and Gordon, 1976; Harper et al., 1985; McLaren, 1985).
- 2) Release of oil from groundwater appears to occur primarily at low tide (McLaren, 1985; Gundlach, pers. comm.).

The COZOIL model incorporates a relatively simple representation of oil in the beach groundwater system, a representation which none-the-less reproduces the observed behavior relatively well. The oil is partitioned between two phases, one of which is trapped by the sediments (an "adsorbed." phase) and one which is transported with the groundwater (a "water-accommodated" phase). We assume the

equivalent to an equilibrium partitioning between oil in the adsorbed and water-accommodated phases (e.g., Thibodeaux, 1979):

$$\frac{C_a}{C_{wa}} = K_{\rho} C_{ss} F_c \quad (2.51)$$

in which C_a and C_{wa} are the concentrations of oil in the groundwater which are adsorbed and water-accommodated, respectively. K_{ρ} is the partition coefficient; C_{ss} is the sediment concentration; and F_c is the fraction of the sediment which is composed of organic matter. From the fact that $C_a + C_{wa} = C_T$, the total concentration, equation (2.51), can be rewritten as:

$$C_{wa} = \frac{C_T}{1 + K_{\rho} C_{ss} F_c} \quad (2.52)$$

The mass removed per tidal cycle is then:

$$F_{wa} = \frac{S_y M_{wa}}{P} \quad (2.53)$$

in which M_{wa} is the total water-accommodated mass, and S_y and P are the specific yield and porosity of the sediment (Fig. 2.11).

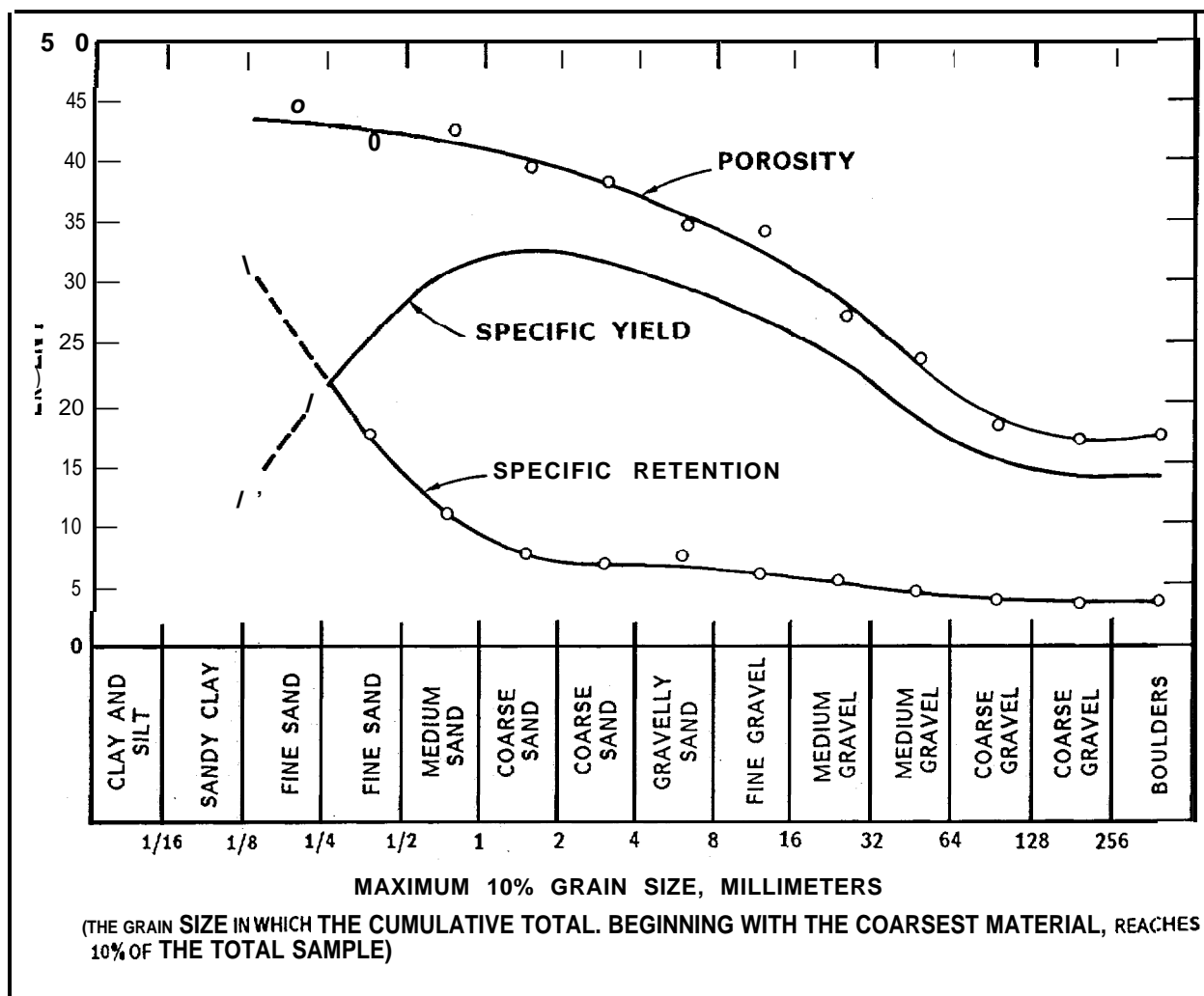


FIGURE 2.11. The relationship of sediment grain size to porosity, specific yield, and specific retention of an oil (from Todd, 1959).

The retentive behavior of this system of equations is discussed in section 5.2.3 for several values of the partition coefficient K_p in each of three distinct beach sediment types. As discussed above, oil in beach groundwater systems remains detectable for several years at least. The sensitivity study in section 5.2.3 suggests that a reasonable value for K_p is about 1,000. The user can adjust this value at will.

Evaporation

Evaporation on the foreshore follows the same computational procedures as on the water surface. Surface oil entering coastal lagoons or deposited on the backshore evaporates at the mean rate for oil on the beach during each time-step. This approximate procedure conserves both computer storage and processing time, while retaining a realistic evaporation rate governed by the composition of the oil spilled.

Refloatation

Oil on the beach face (foreshore surface) or on the backshore which has not penetrated the sediments may be refloated on a rising tide. As oil is refloated from the foreshore surface, it is combined with an existing spinet if one is present at that coastal location. In this case, the characteristics of the spinet become the mass-weighted characteristics of the spinet plus the newly refloated oil. If a spinet does not exist at the coastal cell where refloatation is occurring, a new spinet may be formed.

De-watering (de-emulsification)

Water which has become incorporated into oil during the process of emulsification may be released from oil/water mousse deposited on the beach face. The rate of release, or de-emulsification, is dependent on the stability of the mousse. Stability is in turn a function of several factors (Payne and Phillips, 1985). Natural emulsifying agents (such as asphaltene, waxes, and porphyric complexes) must be present. Viscosity also is important, since higher viscosities will tend to hinder movement of water within the mousse. Specific gravity, water content, and age of the emulsion may also contribute to stability. Detailed investigations by Berridge et al. (1968a,b) evaluated mousse formation and stability for several crude oils and five petroleum products. In general, the crude oils investigated formed relatively stable emulsions,

whereas the refined products (e.g., diesel, kerosene, gasoline) did not form emulsions at all. The set of characteristics governing emulsion stability, however, appears to be sufficiently complex as to warrant a separate study. No quantitative rate data have been located in the published literature. Here, we simply assume a first-order process for the loss of water from stranded mousse:

$$F_{Wc} = F_{Wc_0} e^{-bt} \quad (2.54)$$

where F_{Wc} = fraction of water in oil at time t .

F_{Wc_0} = initial fraction of water in oil.

b = constant.

The model is initialized with b equal to 0.058 per hour, giving an emulsion half life of 12 hours on land. The user then has the option of modifying this parameter.

3.0 DESCRIPTION OF FIELD ACTIVITIES

In keeping with the overall purpose of the study to develop, verify, and apply a probabilistic model of spilled oil in the surf zone, a field study of surf-zone processes was completed. A requirement of the project was to test the COZOIL model with prototype data from the Bristol Bay area. Therefore, a field site was chosen for evaluation and testing during the ice-free summer season. For obvious reasons, such field surveys were limited to measurement of physical characteristics and processes at a particular site and did not include any tests involving the release of oil. Because of this limitation, it was decided at the end of phase I of the present project to revise the original scope of work and use the case history of the *Amoco Cadiz* spill in Brittany, France, for additional model testing. To accomplish this work, the original proposal for a 12-week field deployment in Bristol Bay was reduced to six weeks, and the remaining time and budget was applied to a study of the *Amoco Cadiz*. The present section of the report addresses field activities in Bristol Bay. Section 6.0 will address the review and testing of *Amoco Cadiz* prototype data which included shoreline oiling rates.

Selection of the field site was based on previous knowledge of Bristol Bay with respect to sediment type, coastal morphology, availability of shelter and transportation, general wave climate, and operation costs. It was selected in consultation with MMS and NOAA's CSEAP scientists after a reconnaissance in April 1986. Study personnel (Gundlach) had worked in Alaska several times during the past decade and obtained detailed, low-altitude photographic records of the Bristol Bay shore. These records were used in preparation of an environmental sensitivity index (ESI) report to NOAA (Michel et al., 1982). Port Heiden (Fig. 3.1) was chosen as the most suitable setting for the field survey because of logistics, exposure to a range of wave and tide conditions, and the occurrence of a reasonably straight section of beach. For various reasons, the Port Heiden site was superior to candidate sites at Cold Bay, Port Moller, Bear Lake, and King Salmon, and was considered representative of the Bristol Bay shoreline.

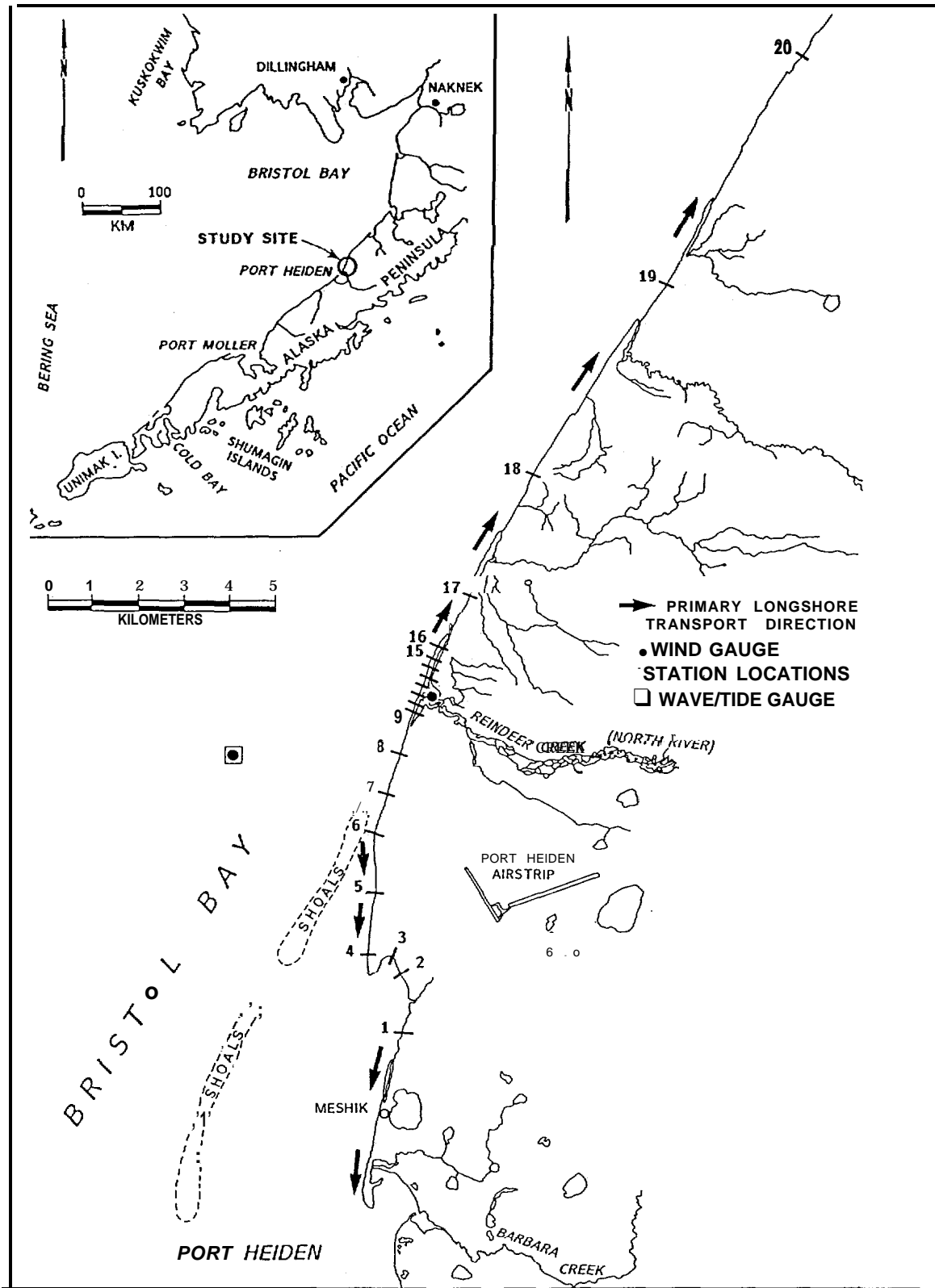


FIGURE 3.1 Field study site for measurement of coastal processes and physical characteristics at Port Heiden. Monitoring stations were established along the shoreline as shown. A grid centered near station 10 was established for the most intensive surf-zone measurements. Access to stations 17-20 was limited because of Reindeer Creek which discharges between stations 16 and 17. Lodging and laboratory facilities were set up at the Port Heiden airstrip.

Basing and transportation were convenient at the Port Heiden Air Station. Other logistical advantages included availability of space to set up a laboratory for processing suspended-sediment samples and assembling field instruments. Surplus tower sections were available for installation of a beach weather station which could be checked against the air station record several kilometers inland. Fishing vessels with booms were available for deployment of offshore instrumentation. Upon review of these advantages over other sites, the COTR approved Port Heiden as the field site for coastal process monitoring during a six-week period in 1986. The field deployment began 3 August and was scheduled to coincide with the transition period from moderate to high (relative to Bristol Bay) wave energy conditions which tends to occur in August.

The principal purpose of field data collection was to obtain input data for testing, modification, and verification of the COZOIL model. Since we were not able to field-test using an actual oil spill, field data collected were restricted to coastal processes, shoreline variations, sediment type, and sediment transport estimates. Because of the relatively remote setting of the site, data collection was designed to be nondependent on sophisticated power systems and was performed at a level commensurate with the budget available. The following section outlines the field-sampling design, data collection methodology, and backup or contingency plan for field equipment.

3.1 GEOGRAPHIC SETTING

Port Heiden is a tide-dominated estuary along the north shore of the Alaska peninsula approximately 200 km from the apex of Bristol Bay. The northeast shoreline at the entrance to the Port is a elastic beach and barrier spit composed of basaltic sands transported into Port Heiden. Several kilometers east of the entrance, sand transport reverses and moves dominantly toward the northeast into the Bristol Bay embayment. A large tidal delta (indicated approximately by shoals on Fig. 3.1) appears to control the transport reversal. These general trends are based on distinctive morphology of spits and eroding bluffs along the shoreline east of Port Heiden where the present field surveys were focussed. Primary exposure of the site is to waves propagating into Bristol Bay from the Bering Sea from the northwest.

Tides in the area are mixed, semidiurnal with a mean range of 8.5 ft (2.6 m) and a diurnal range of 12.3. ft (3.7 m) (USDC, 1986). However, peak astronomic tides exceed 18 ft (5.5 m). Tidal currents off the entrance to Port Heiden average 1.0 knot (0.51 m/s) on the flood and ebb (USDC, 1976). Tidal currents increase markedly during peak, or fortnightly, spring tides due to resonance in Bristol Bay.

Wave energy at Port Heiden consists principally of swell propagating into Bristol Bay and refracting around shoals at the entrance before reaching shore. Deep-water waves are modified by locally generated winds which produce more complicated wave spectra (based on field observations during the present study). Wave energy is reported to be greatest in late summer although no data were available for Port Heiden prior to our field deployment. Ice cover in Bristol Bay reduces fetches much of the year and, therefore, reduces mean wave energy substantially below levels observed during summer months. An earlier study of waves off the Seward Peninsula (Chukchi Sea) describes similar seasonal trends (Kozo,1985).

The shoreline east of Port Heiden consists of an alluvial plain of volcanic sediments eroded from the Alaska Range approximately 30 km inland. Meshik River is the largest river draining into the area. The mouth of the river broadens into a shallow tide-dominated estuary (Port Heiden) which has a complex network of braided drainage channels with longitudinal bars exposed at low tide. Width of the estuary exceeds 10 km near the entrance. Offshore of Port Heiden, a broad ebb-tidal delta and associated shoals have formed, extending upwards of 5 km into Bristol Bay. For the most part, shoals are subtidal. The influence of the ebb-tidal delta extends at least 8 km north of the village of Meshik shown on Figure 3.1. Shoals of the delta

can be seen at low tide off stations 6 and 7 indicating this is the approximate northern terminus of the tidal delta. This can also be delineated approximately on NOS chart 16343 for the area. Although basaltic sands dominate in the sediments, ejects from volcanic eruptions has left layers of pumice at discrete horizons. These can be seen where coastal bluffs are exposed along the shore. Coarse stream gravel also occurs above sea level in recent deposits along bluffs, possibly indicating tectonic uplift in the area. as well as long-term erosion of the coastal plain.

During our reconnaissance of the area, we noted the occurrence of 20-40 m high bluffs containing stream gravel and ejects at several points along the shoreline including areas around stations 6, 18, and 20 (Fig. 3.1). A lag of coarse gravel occurred at the base of bluffs in these localities although the dominant sediment type on the beach is sand. Between eroding bluffs, lower relief dunes occurred which were predominantly composed of sandy sediments. Upland vegetation from the edge of eroding dunes or bluffs is dominated by tundra species of mosses and grasses.

Beaches along the study area consist of a series of storm and lower berms ranging from a few tens of meters in width to over 100 m wide. Given the high-tide range, berm elevations are upwards of 3 m above local mean water level. The beach face tends to be relatively steep (1:15 slope) with a relief approximating the tide range. Slope tapers gently to the low-tide terrace which is ubiquitous in this area and extends on the order of 100-300 m offshore. Complex bar forms, ridge and runnel systems (Hayes, 1972). and irregular topography indicate various modes of beach cycle development (Short, 1979) evolving during the summer season. During overflights and ground inspections in August and September 1986, we observed nearshore cells, rip currents, and wave-breaking being controlled to a certain extent by complex bottom topography. These features were indicative of a transitional surf zone which is highly dissipative at low tide but more reflective at high tide. using terminology of Wright and Short (1983).

Three small streams cross the beach between stations 16 and 17, stations 17 and 18. and stations 18 and 19 (Fig. 3.1). Deflection of the channels toward the north by several hundred meters indicated the predominant drift direction north of Port Heiden's ebb-tidal delta. Tidal prisms for the streams are very small. As a result, the streams discharge as shallow sheet flow across the beach face at low tide. At high tide, depths increased beyond wading depth precluding access north of station 16 from our base camp at the air station.

Except where high bluffs occur and a lag of coarse gravel becomes deposited, the shoreline north of Port Heiden is relatively straight. High bluffs tend to produce minor "headlands" which appear to supply sediment to adjacent beaches and control the overall orientation of the coast. Long, straight sections of beach between the "headlands" suggest wave-energy flux is relatively uniform away from Port Heiden's entrance and not affected by offshore shoals or differential refraction. In contrast, the beach between stations 7 and 1 is sheltered by the ebb-tidal delta of Port Heiden and appears to have more variable wave-energy flux. Drift direction reverses around station 7 and becomes predominantly southward into Port Heiden estuary. This can be inferred from spit growth at station 4 (Fig. 3.1) and the recurved spit south of Meshik village. [Note: The spit at station 4 is not shown on NOS chart 16343 (June 1976 edition) but it was an obvious feature based on the 1986 ground surveys and aerial overflights.] These types of shoreline morphology and drift patterns are common to estuarine entrances.

3.2 PHYSICAL PROCESS MEASUREMENTS

The primary field measurements obtained at Port Heiden during the field deployment were:

- Littoral process measurements.
- Beach sediments and beach morphology, and surf-zone bathymetry.
- Suspended sediment in the surf zone.
- Wind measurements.

Littoral-process measurements include observations of breaking wave height (H_b), wave period (T), breaker angle (α_b), longshore current ($V_{\ell 1/2}$), dimensions of the surf zone, relative water levels, and breaker type. These parameters provide the basic input variables for existing surf-zone transport models, sediment budgets, and empirical models of onshore/offshore motion, suspended-sediment transport, and morphological variation. The following section outlines the specific data-collection scheme and methodology during the field surveys.

3.2.1 General Sampling Scheme

We delineated a *20-km, contiguous section of shoreline for data collection from Port Heiden to the north. This shoreline has a predominant northerly sand-transport direction, as well as a variety of morphological features as previously described. Field measurements consisted of a combination of remote-recorded and visual observations along with surveys of selected shoreline transects. Our primary coastal process and profile station was established about 4 km from the Port Heiden base camp at the airstrip. Designated as station 10, it was the principal data-collection point along the shoreline. Secondary transects and sampling stations were established at various intervals updrift and downdrift (according to local topography, geomorphic character, accessibility, and so on). Stations 9 through 16 were placed at surveyed intervals along the beach measured from station 10. In this fashion, a nearshore grid (Fig. 3.2) was established for mapping surf-zone topography, measuring volumetric changes and detecting longshore transport by means of drifters. Stations 9-13 were spaced at 100-m intervals. Stations 13 to 16 were spaced at 200-m or 300-m intervals. The grid terminated at station 16 before the mouth of Reindeer Creek which drained across the beach about 500 m to the north.

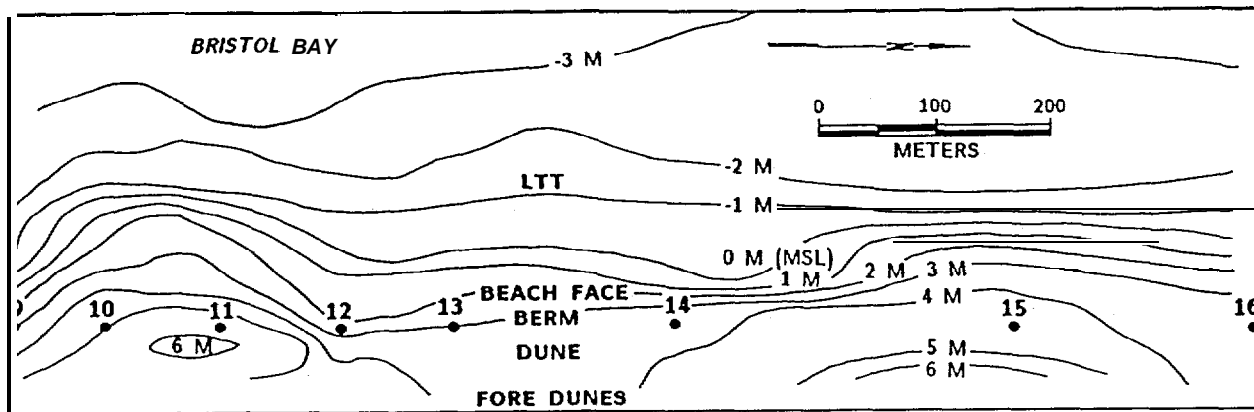


FIGURE 3.2 Beach and inshore contours in the vicinity of stations 9-16 (see Fig. 3.1).

The principal instruments deployed were an offshore wave/tide gauge pressure sensor (Sea Data Model 6.35-12) and an onshore wind gauge (RM Young Model 1). The Sea Data wave/tide sensor was deployed approximately 3 km offshore of station 10 in 12-m water depth (Fig. 3.1). It was deployed by divers from a local fishing vessel, *FV Pat Joy*, and was deployed on the sea floor using a customized tripod anchored by two handset Danforth anchors and about 350 pounds of sandbags tied to the frame. The bottom was firm, sandy silt. Two sets of buoys were used to mark the site of the gauge. The Sea Data was set to sample wave spectra in 15-minute bursts (1.0 Hz) every three hours (dictated by the longevity of batteries). The instrument also was to provide a concurrent record of tide level and an estimate of wave direction based on time-averaged current oscillations at the sensor. Data were to be set to record in situ on magnetic tape and would be reduced after deployment to obtain the necessary wave and tide statistics for use by the model (i.e., H_{rms} , H_s etc.)

Deployment was completed successfully on 16 August, the first available day after receipt and preparation of the equipment and favorable weather conditions. The COTR assisted in the deployment. Retrieval was scheduled for mid September. Upon return to the wave-gauge deployment site, we found the marker buoys gone and made repeated dives over the site in search of a trip line which had been set as a guide along the bottom. On 16 September, we also dragged a 0.5-km² area centered at the deployment coordinates; None of these attempts were successful and we informed the COTR of the lost equipment.

The wind gauge was deployed on a 10-m tower set up at the backshore in the vicinity of station 13, several hundred meters north of station 10. With the exception of a defective recorder problem the first week, a continuous record of wind speed and direction was obtained between 16 August and 11 September.

As required in the original RFP for the project, a backup plan for data collection was implemented. In the case of offshore wave and tide measurements, budget limitations precluded deployment of multiple gauges. Therefore, offshore wave climatology was determined by hindcasting from weather records. Tide estimates were obtained from predicted water levels (USDC, 1986). Methodology and results are given later in this section.

Port Heiden maintains a government weather station near the airstrip which provided backup daily observations for our use. This station was located about 3 km inland and provided comparative data as well as information on microclimatology differences between the two sampling positions.

After an initial mobilization period, coastal-process measurements were completed each day during a mid-tide to high-tide condition at station 10. After establishing a measurement grid of stakes placed across the surf zone (Fig. 3.3), a standardized set of observations were made:

- 1) *Breaking-wave characteristics.* Visually using a calibrated staff placed at the breaker line by a swimmer (for waves up to 1.0 m) or mounted on poles at various fixed positions. Only staffs at the breakpoint were monitored. Dangerous surf conditions (i.e., above 1.5 m) were monitored by visual estimates from the swash zone as close as practicable. During storm-wave conditions, a combination of visual estimates and results from offshore wave hindcast was used to estimate inshore breaking waves. Wave height (H_b) was measured for several discrete waves in a set comparing trough depth and crest depth at the calibrated pole and taking the difference as height. Such visual estimates have been shown to approximate H_s (significant wave height) rather than mean wave height (CERC, 1984). We averaged results for a sequence of waves in a set and generally repeated the procedure during each observation period for several wave sets. On occasion, two observers obtained independent estimates and compared results to arrive at an average.

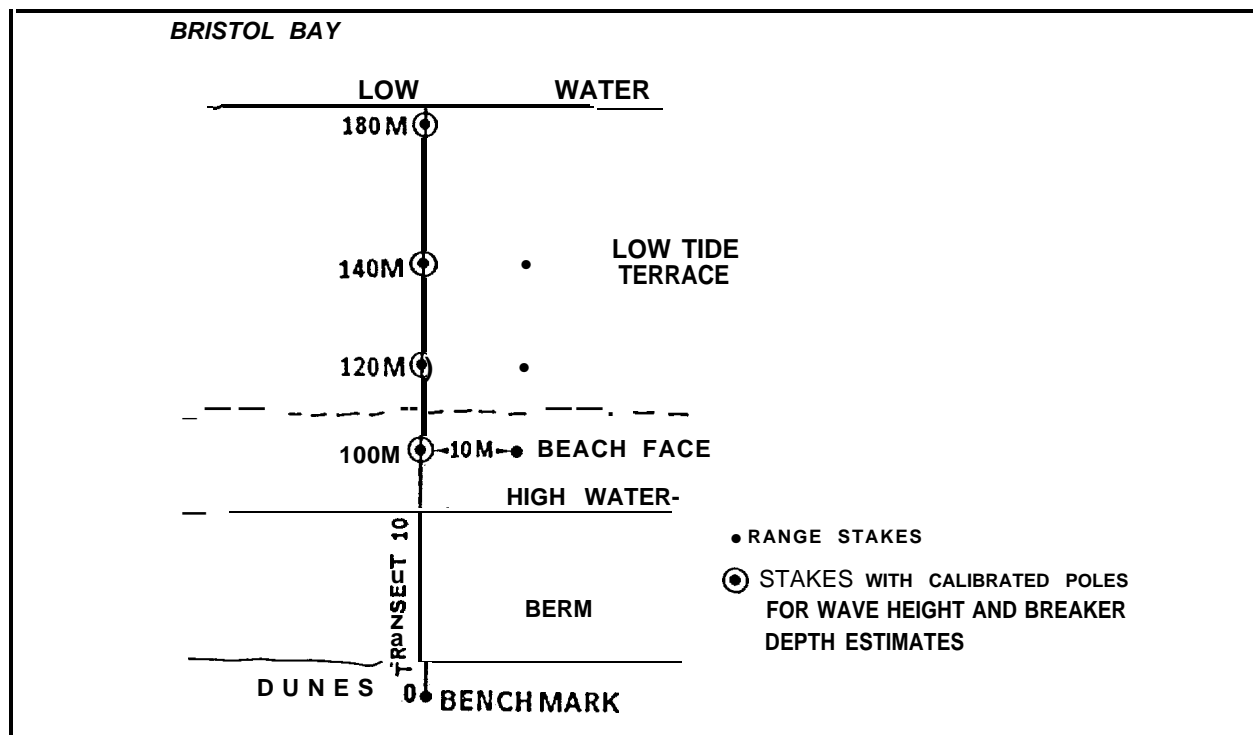


FIGURE 3.3 Surf-zone grid at station 10 for coastal process measurements.

Other parameters measured were water depth at breaking (h_b), breaker type using standard classifications (Galvin, 1968) and documented periodically by photos and height to depth ratios as in Kana (1979), and breaker angle (α_b) (using compass and protractor to mark the angle of the breaker crest with respect to the shoreline). Multiple readings were made to arrive at average values.

- 2) *Longshore currents.* Two techniques were used to estimate longshore-current distribution in the surf zone:
 - a) Portable, electromagnetic flow meter with digital readout (Marsh-McBirney Model 201) moved from place to place at points and depths across the surf zone, each noted with respect to the bottom and mid-surf position (grid stakes were used for reference).
 - b) Slightly buoyant floats released at several points and monitored for distance traveled over time with respect to the longshore and cross-shore direction. Range stakes were used to sight movement of floats past a starting and ending point and to repeat measurements conveniently.

Note: A third technique--injection of nontoxic dye from representative grid points--was attempted on a few occasions but was not successful in delineating current speeds. We believe one reason for this was the predominance of cell circulation established by nearshore bars which persisted during lower wave-energy conditions. At higher wave-energy conditions when longshore currents were well developed, hazardous surf conditions precluded swimmers from injecting dye near the breaker line. Inner and mid surf measurements using floats or the current meter provided consistent results under higher energy conditions, precluding the need for dye.

- 3) *Beach profiles.* Controlled rod-and-level surveys were completed between the backshore and outer surf zone to measure the active profile. Data were sufficiently detailed to compute local slopes at grid points as well as slope at the breakpoint. Profiles were completed approximately weekly at station 10 and less frequently at other stations.

A typical field day included beach surveys near the times of low tide and coastal-process measurements around mid-to-high-tide stage. We referenced a local datum with respect to mean water levels using a U.S. Coast and Geodetic marker at station 10 which was located after contact with the State of Alaska.

During the course of our field deployment, we collected about 150 suspended-sediment samples in the surf zone under breaking wave conditions using an apparatus and technique applied by Kana (1976, 1977). In situ, bulk water samples were obtained using reference points in the surf with control on sample position with respect to the bed, the wave breakpoint, the wave phase, and local slope. The samples were collected under typical wave conditions up to the limiting height and longshore current for swimmers (H_b less than 1.5 m: $V_{\ell 1/2}$ less than 0.5 m/s) with the goal of obtaining representative concentration distributions between the swash zone and area seaward of the breaker line. Samples were transferred to holding jars and filtered in a temporary laboratory at the base camp. Filters with sediment were archived for later computation of concentration.

3.3 RESULTS

3.3.1 Geomorphic Data

Figure 3.4 is a sketch map of shoreline transects and geomorphology of the study area at Port Heiden. The shoreline encompasses several reaches of sandy beaches, broad low-tide terraces, two spits migrating into Port Heiden (sheltered by the ebb-tidal delta of the estuary) and two spits associated with outwash streams north of the air station. Table 3.1 contains a general description of each station.

TABLE 3.1. General description of survey stations at Port Heiden. See Figure 3.4 for approximate location.

Station Number	Description
1	Sheltered beach; mixed sand/light gravel
2	Medium- to coarse-grained sand beach; peat outcrops; washover; freshwater marsh along backshore
3	Sheltered beach; pumice gravel, eroding volcanic ash deposits. broad tidal flat with muddy veneer
4	Recurved spit: sandy beach: multiple ridge-and-runnel systems; longshore transport dominantly toward south
5	Exposed sandy beach: steep beach face: deep berm runnel; sandy low-tide terrace; in lee of ebb-tidal delta
6	Exposed beach: moderate slope; medium- to coarse-grained sand: small gravel lag deposit on berm; near northern terminus of ebb-tidal delta
7	Eroding bluff; narrow beach: erosional profile: cemented sandstone outcrops; mixed sand and gravel
8	Eroding bluff; mixed sand/gravel berm: gravel toe; sandy low-tide terrace
9-16	Sandy exposed beach; cobble/small gravel toe; moderate slope; exposed low-tide terrace of medium- to coarse-grained sand: complex ridge-and-runnel systems; nearshore cells: longshore transport dominantly toward the north
	Spacing between stations: 9-13) 100 m each for a total of 300 m
	13-14) 200 m
	14-15) 300 m
	15-16) 200 m
17	Exposed sand beach: eroding dune: 2 km north of station 10
18	Exposed sand beach; well-developed ridge-and-runnel system: stable dune: eroding bluffs 2 km north of station 18: relief exceeds 30 m: exposed pumice ash fall deposits; eroding buttresses
19	Sandy beach: low dunes: exposed low-tide terrace
20	Sandy beach; low/stable dunes: a "headland" of eroding bluffs occurs about 4 km north of station 20

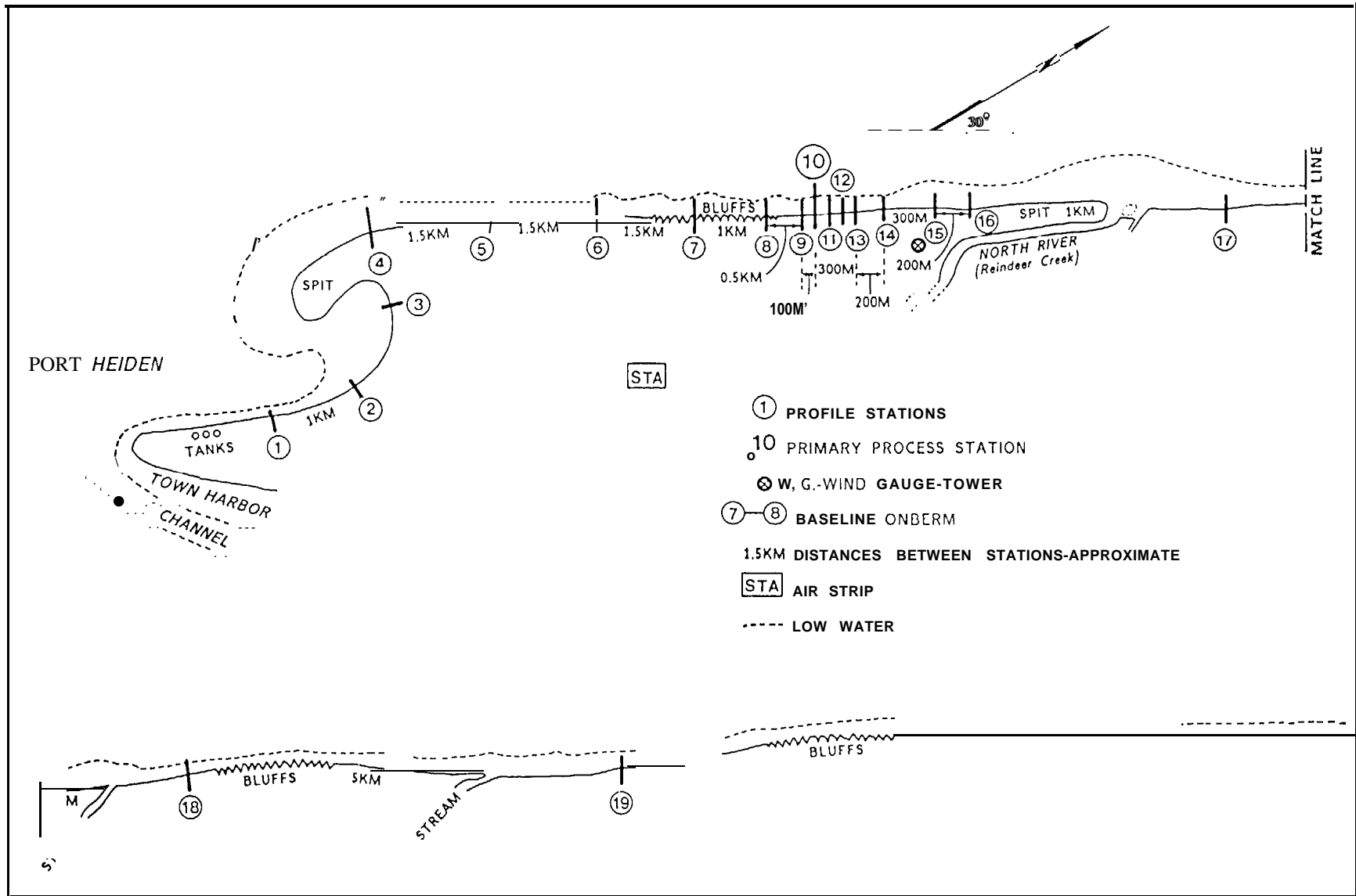


FIGURE 3.4. Sketch map (not to scale) showing principal morphologic features and distances between stations,

Profile transects were established from reference stakes placed in the fore-dunes/bluffs at each station. Using a benchmark in the vicinity of station 10, vertical control was carried to stations 1-16 for leveling to a common datum (approximate mean sea level). The set of profile transects is given in Appendix II-A (this volume). Figure 3.5 contains a representative beach profile from station 10 showing principal morphological features and arbitrary placement of reference stakes. The profile was surveyed five times during the study in order to detect erosion/ accretion events. Local slopes were computed at 5-m intervals for purposes of applying certain surf-zone current or transport estimates and relating local slope to the suspended-sediment sample points. Grid stakes provided static reference points from which timing of wave periods were measured. They also allowed more consistent estimates (using multiple observers) of surf-zone width, wave runup, and other surf features.

Detailed information on beach profile change is given in Appendices II-B and II-C (this volume). Two analyses that were performed on the data were contour-movement summaries and unit volumetric change. The contour-movement summaries provide a measure of representative linear dimensions such as the width of the intertidal zone. Table 3.2 summarizes width of the beach face (berm crest to toe of beach) and low-tide terrace (ending at the survey limit common to the entire data set).

Review of Table 3.2 indicates beach widths are generally lowest along the sheltered stations nearest Port Heiden (stations 1 and 2) or along eroding bluffs (station 7). Widest beach face width occurred at station 4, the primary recurved spit at the north entrance to Port Heiden. Principal reasons for this area being wider is the active accretion which is occurring along the spit whereby multiple ridges and berms are depositing along the shoreface. Stations away from the influence of recurved spits or runnel outlets (e.g., station 15) had relatively consistent beach widths on the order of 75-100 m.

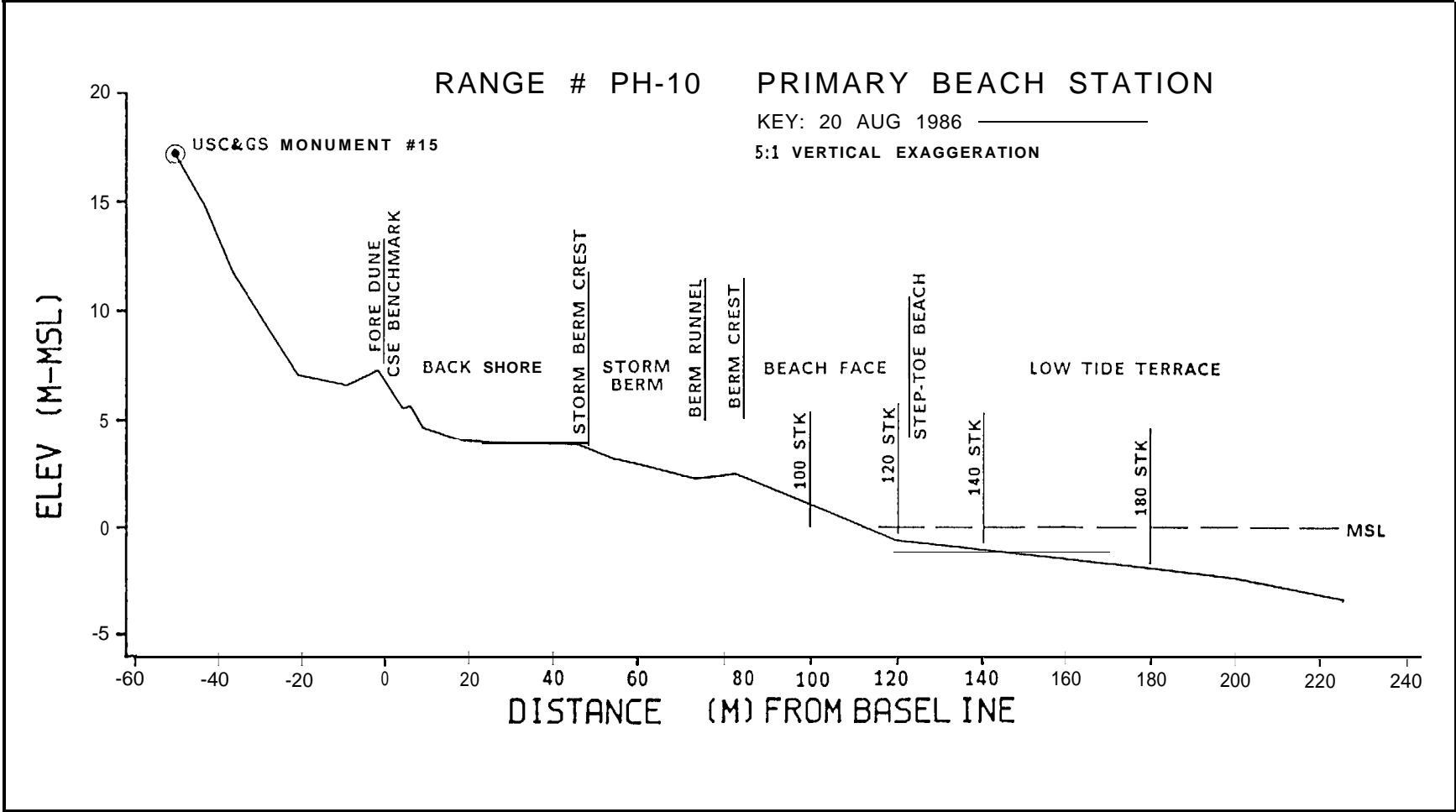


FIGURE 3.5, Representative beach profile for station 10 where most of the littoral process measurements were made.

TABLE 3.2. Summary average beach widths for two representative portions of the profile--beach face measured from the +3.0 m to -0.9 m MSL contour and low-tide beach measured from -0.9 m to -2.4 m. Surveys were completed in English units because of the equipment used and later converted to metric in the office. Missing data indicate datum depth was not achieved as in the case of station 3 which is located at a very wide tidal flat.

Station	Beach Face Width		Low-Tide Width	
	Feet	Meters	Feet	Meters
1	167.9	51.2	171.5	52.3
2	118.4	36.1	234.3	71.4
3	233.3	71.1		
4	979.0	298.4	173.2	52.8
5	362.9	110.6	206.9	63.1
6	276.2	84.2	293.1	89.3
7	146.5	44.7	322.7	98.4
8	301.9	92.0	266.0	81.1
9	210.0	64.0	179.9	54.8
10	250.5	76.3	202.4	61.7
11	259.6	79.1	154.2	47.0
12	317.0	96.6	230.3	70.2
13	324.6	98.9	278.6	84.9
14	260.6	79.4	321.4	98.0
15	148.9	45.4	83.8	25.5
16	263.9	80.4	170.6	52.0
17	311.5	94.9		
18	453.6	138.3	117.7	35.9
19	199.5	60.8	238.1	72.6
20	211.5	64.5	218.4	66.6

Table 3.3 and Appendix II-C contain unit-width volume statistics for each station for various portions of the profile. Unit-width volumes were based on cross-sectional areas and area changes between surveys, applied over a representative (unit) distance along the shoreline. Because surveys were made in English units, detailed data were calculated in English units (yd^3/ft), then converted to metric units (m^3/m). Table 3.3 summarizes the initial beach volumes and the change during the period before the last survey. Total volumes are used to compare the condition of one station against another. Higher unit volumes indicate generally healthier beach conditions. Review of Table 3.3 indicates that station 4, as expected, has the highest unit volume in the active beach zone. In contrast, station 7 (located along eroding bluffs) has one of the lowest unit volumes. Station 15 is anomalously low because it is situated at a runnel outlet which has lowered the beach in the vicinity. Note the results for adjacent stations, 200-300 m away, are 30 percent higher. During the study, a high-energy event occurred in early September. This is reflected in the change rates for the beach face (Lens 2) at stations 3, 4, and 10 which were resurveyed after the storm.

Lenses used were as follows:

Lens 1	top of profile to + 10 ft (3.0 m)	– supratidal beach
Lens 2	+10 ft to 0 ft (3.0 m to 0 m)	— upper beach face
Lens 3	0 ft to -3 ft (0 m to -0.9 m)	– lower beach face
Lens 4	-3 ft to -8 ft (-0.9 m to -2.4 m)	– low-tide terrace

In order to account for different profiles starting at benchmarks located at different points along the profiles, volume calculations were started at the +10 ft (+3.0 m) MSL contour. This forces Lens 1 volumes to be calculated as zero, which is purely a consequence of the analysis scheme used. For subsequent profiles, absolute volume changes and annualized rates of change are determined.

TABLE 3.3. Volumetric summaries for all beach stations, showing initial survey volume and change between first and last surveys. Units are in English (yd³/ft) with metric equivalents (m³/m) in parentheses.

Station	Lens 2		Lens 3		Lens 4		Total	
	Initial	Change	Initial	Change	Initial	Change	Initial	Change
1	26.3 (65.8)	0.2 (0.5)	15.7 (39.3)	0.2 (0.5)	47.4 (118.5)	1.3 (3.3)	89.4 (223.5)	1.7 (4.3)
2	15.3 (38.3)	0.3 (0.8)	10.5 (26.3)	0.6 (1.5)	39.0 (97.5)	1.7 (4.3)	64.8 (162.0)	2.6 (6.5)
3	21.3 (53.3)	-4.6 (-11.5)	16.7 (41.8)	0.1 (0.3)	39.0 (97.5)	38.9 (97.3)	77.0 (192.5)	34.4 (86.0)
4	24.1 (60.3)	-4.9 (-12.3)	22.6 (56.5)	-3.1 (-7.8)	119.9 (299.8)	-1.7 (-4.3)	166.6 (416.5)	-9.7 (-24.3)
5	17.4 (43.5)	1.5 (3.8)	24.0 (60.0)	2.4 (6.0)	95.7 (239.8)	-10.6 (-26.5)	137.1 (342.8)	-6.7 (-16.8)
6	26.8 (67.0)	-2.5 (-6.3)	24.2 (60.5)	1.4 (3.5)	75.2 (188.0)	3.0 (7.5)	126.2 (315.5)	1.9 (4.8)
7	20.2 (50.5)	-- (---)	14.2 (35.5)	--- (---)	58.9 (147.3)	-- (---)	93.3 (233.3)	-- (---)
8	23.8 (59.5)	0.9 (2.3)	26.0 (65.0)	-0.5 (-1.3)	79.6 (199.0)	-0.8 (-2.0)	129.4 (323.5)	-0.4 (-1.0)
9	32.9 (82.3)	-7.0 (-17.5)	20.9 (52.3)	-3.0 (-7.5)	57.2 (143.0)	4.5 (11.3)	111.0 (277.5)	-5.5 (-13.8)
10	41.3 (103.3)	-8.1 (-20.3)	23.0 (57.5)	0.1 (0.3)	67.3 (168.3)	-0.3 (-0.8)	131.6 (329.0)	-8.3 (-20.8)
11	45.4 (113.5)	9.8 (24.5)	26.5 (66.3)	5.5 (13.8)	65.4 (163.5)	19.1 (47.8)	137.3 (343.3)	34.4 (86.0)
12	35.5 (88.8)	3.1 (7.8)	26.2 (65.5)	-2.1 (-5.3)	75.0 (187.5)	4.8 (12.0)	136.7 (341.8)	5.8 (14.5)
13	36.3 (90.8)	-1.6 (-4.0)	27.0 (67.5)	-1.3 (-3.3)	82.4 (206.0)	-0.7 (-1.8)	145.7 (364.3)	-3.6 (-9.0)
14	16.0 (40.0)	5.0 (12.5)	21.0 (52.5)	1.0 (2.5)	71.4 (178.5)	4.5 (11.3)	108.5 (271.3)	10.5 (26.3)
15	21.4 (53.5)	1.0 (2.5)	13.8 (34.5)	1.2 (3.0)	35.2 (88.0)	-0.6 (-1.5)	70.4 (176.0)	1.6 (4.0)
16	34.0 (85.0)	-2.1 (-5.3)	21.9 (54.8)	3.2 (8.0)	64.3 (160.8)	-8.1 (-20.3)	120.2 (300.5)	-7.0 (-17.5)
17	17.2 (43.0)	-- (---)	16.6 (41.5)	--- (---)	79.3 (198.3)	-- (---)	113.1 (282.8)	-- (---)
18	15.3 (38.3)	-- (---)	29.1 (72.8)	-- (---)	94.5 (236.3)	--- (---)	138.9 (347.3)	--- (---)
19	9.0 (22.5)	-- (---)	15.9 (39.8)	-- (---)	50.1 (125.3)	-- (---)	75.0 (187.5)	-- (---)
20	38.5 (96.3)	--- (---)	21.4 (53.5)	--- (---)	52.7 (131.8)	-- (---)	112.6 (281.5)	-- (---)

3.3.2 Beach Sediment Data

Samples of beach sediments were taken at stations 1-7, 10, 16, and 19. At each of these stations, samples were collected from five morphological features in the littoral zone--dune, berm, trough (berm runnel), beach face, and low-tide terrace. Composite samples were prepared for each station incorporating each of the five morphologic areas. Similarly, composites of each morphologic unit from all stations sampled were analyzed. Grain-size distribution curves are given in Appendix II-D (this volume). Summary grain-size statistics are given in Table 3.4.

The results indicate a gradation in grain size occurs along the profile with finest sediments in the dune (medium sand) and low-tide terrace (medium to coarse sand). Coarse sand (*0.9 mm mean diameter) predominates on the berm. Very coarse sand is typical along the beach face. There were also significant longshore variations in the composite distributions between stations ranging from coarse sand at stations 1, 2, 3, and 4 to medium sand at stations 5 and 6. Station 10 was dominated by coarse sand, although a lag deposit of scattered gravel clasts also occurred along the berm. Similarly, coarse gravel occurred in conjunction with medium sand at station 7.

TABLE 3.4. Summary grain-size statistics (graphical) for composite sediment samples collected at representative Port Heiden beach stations. Appendix II-D contains cumulative size-frequency curves based on sieve analyses.

Composite	Mean		Standard Deviation	
	ϕ	mm	ϕ	mm
Station 1	1.128	0.603	1.329	0.505
2	0.780	0.923	1.696	0.950
3	0.837	0.910	1.733	0.955
4	1.193	0.663	1.530	0.660
5	1.323	0.463	0.965	0.295
6	1.527	0.423	1.076	0.310
7	1.940	0.273	0.485	0.090
10	0.367	1.133	1.540	1.085
16	0.560	0.953	1.472	0.870
19	0.506	1.180	1.714	1.270
Dune	1.569	0.367	0.721	0.180
Berm	0.696	0.923	1.626	0.895
Berm trough	0.566	0.893	1.317	0.755
Beach face	0.290	1.500	1.837	1.705
Low-tide terrace	1.247	0.547	1.230	0.450

3.3.3 Winds

Two sets of wind measurements were available for the duration of the field survey. Recordings at the beach station began around 11 August 1986 but due to a malfunctioning recorder were unusable until the new recorder was installed on 15 August. After checking response against a hand-held wind meter and the readings at Port Heiden air station, a continuous record was monitored from 16 August (0000 hrs) through 11 September (1550 hrs). Hourly readings obtained from the CSE strip chart recorder are given in Appendix II-E (this volume). Because of instrument calibration, wind speed is given in miles per hour (mph) with computed metric equivalents.

Winds recorded by NOAA at the Port Heiden air strip were obtained several months after our field deployment. The NOAA record sampled at less frequent and sometimes sporadic intervals. Nevertheless, there was good agreement in phasing of wind events. Figure 3.6 is a time-series of wind speed and direction from the CSE beach station and NOAA's station at the airstrip. One can see the approximate 20 percent difference in wind speed for the two stations. Lower speeds at the airstrip, particularly during storm events, are attributable to friction effects over the land. Both towers were 10 m high, although absolute elevation of the air station is on the order of 50 ft (15 m) higher than the beach station. Wind direction showed relatively good coherence, generally matching direction within several degrees at both stations (Fig. 3.6b).

3.3.4 Tides

With the loss of the wave/tide gauge, tidal elevation was obtained from tide tables. Figure 3.7 contains the tide record for the study period. Diurnal and semidiurnal components are evident in the time-series. Also characteristic of this part of Bristol Bay is the relatively large range ≈ 5.5 m and large variation in fortnightly amplitude. Neap tides for the study period had a range of ≈ 2.0 m.

3.3.5 Coastal Processes

Standard procedures for obtaining visual observations of littoral environment observations have been developed by CERC (Schneider, 1981). Variations on these procedures have been applied in numerous studies of coastal processes including Hayes et al. (1973), Nummedal and Stephen (1976), and Kana (1977). Parameters measured and the procedure for obtaining representative estimates are given below.

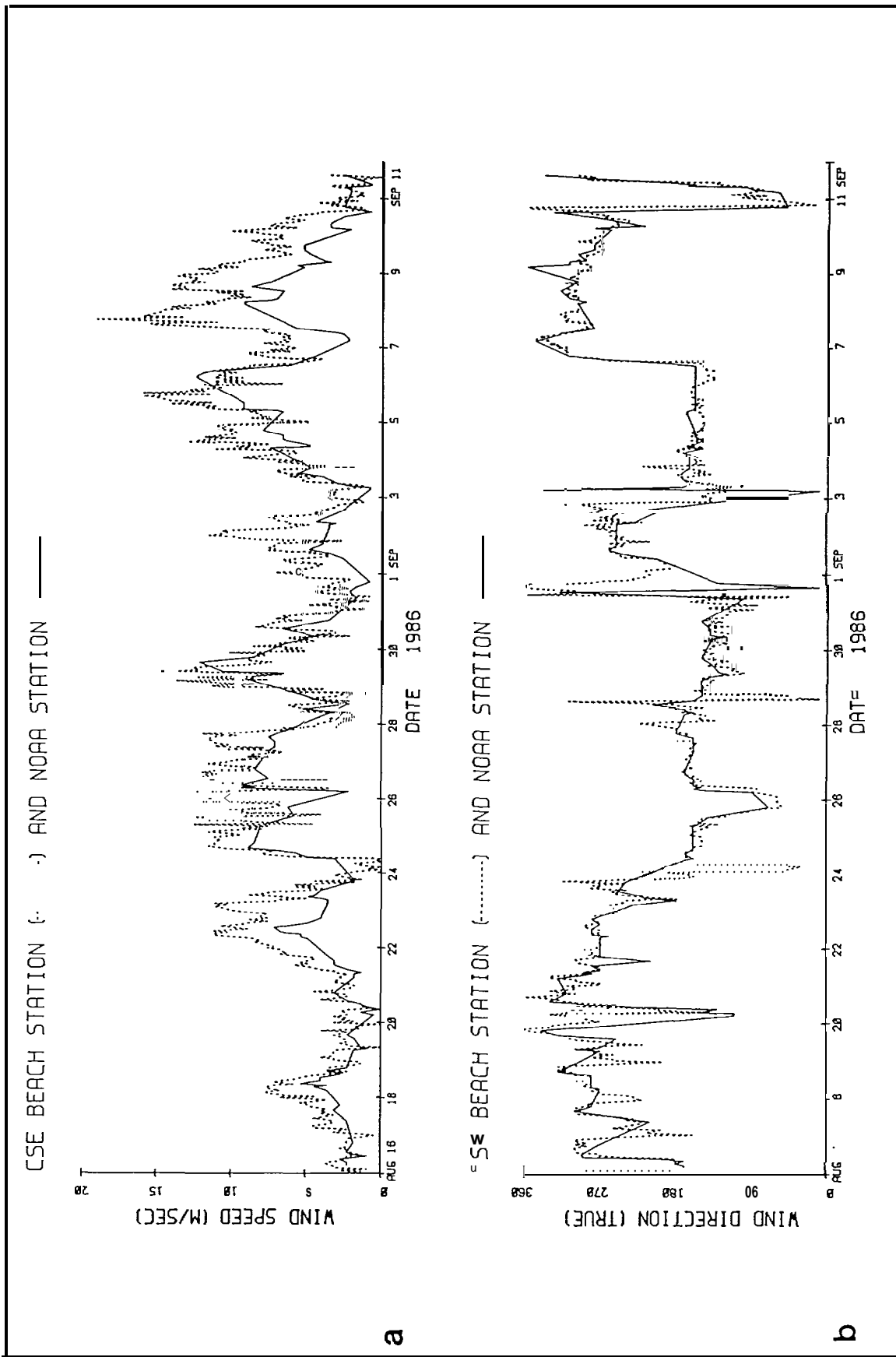


FIGURE 3.6. (a) Wind speed (m/s) between 16 August and September 9 \pm 6 at Port Heiden. (b) Wind ($^{\circ}$ True) for the same period.

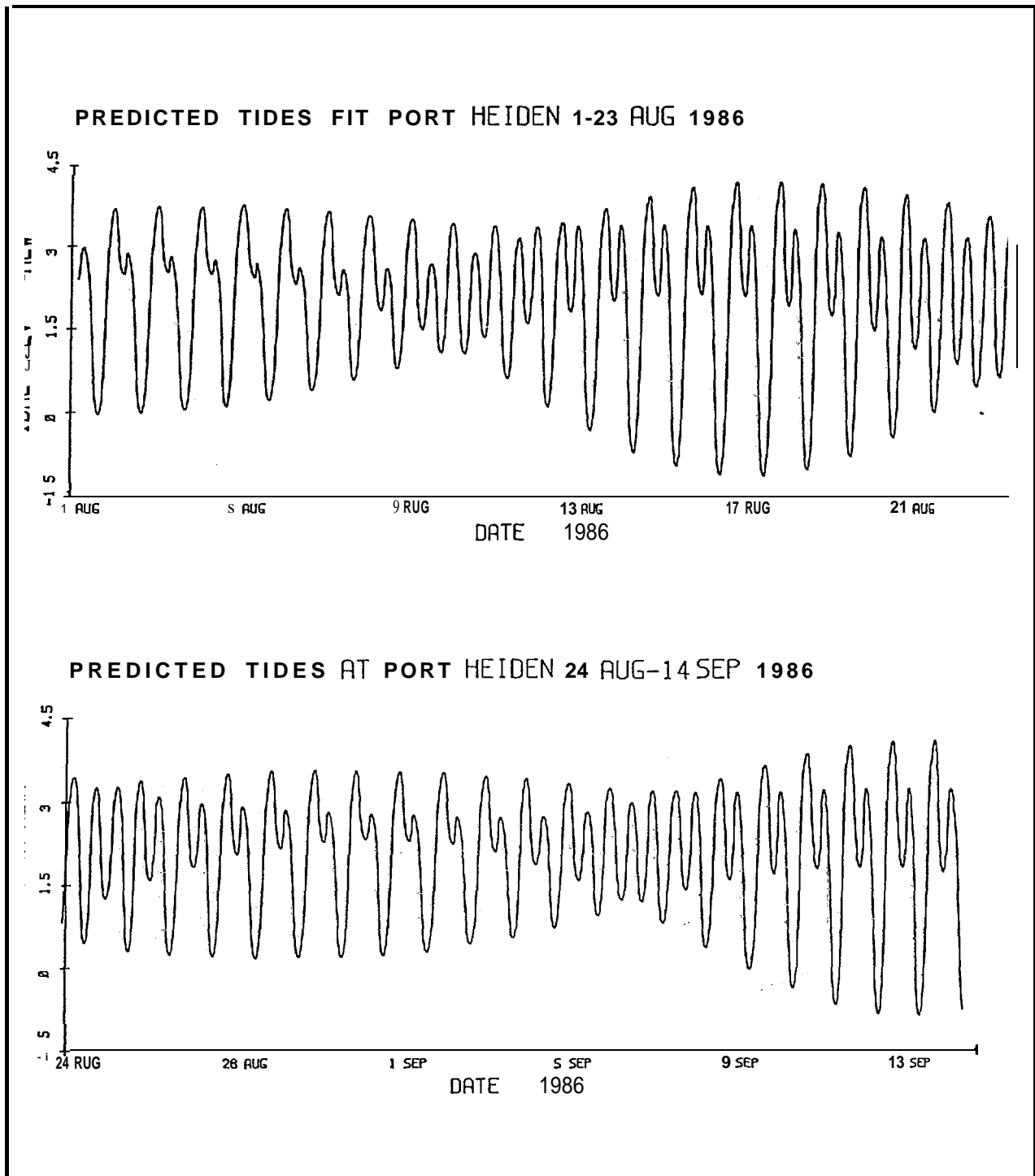


FIGURE 3.7. Predicted tides at Port Heiden during the field survey period. Elevations are given in meters above MLW, converted from English units given in USDC (1986).

Breaker height (H_b) - visually by means of a graduated staff held at the breakpoint by swimmers [waves up to 1.5 m high under moderate longshore current conditions (i.e., <50 cm/s)]. Trough depth and breaking crest height were measured for three to five waves in a set: the difference was computed as wave height for individual waves. Mean of each set was computed and assumed to represent mean significant wave height (H_s) at breaking. For higher energy conditions, reference rods in the surf were used to estimate peak wave crest height and minimum trough depth for a similar series of waves in a set. Observations were made by swimmers as close to the breaker line as possible without undue risk. Such visual estimates were occasionally checked against estimates by onshore observers using binoculars. Under high energy conditions, the surf at Port Heiden tended to have two or more breaker lines coinciding with ridge-and-runnel systems or fluctuating energy levels. Where multiple breakpoints occurred, visual estimates were noted for each zone.

Breaker depth (h_b) - estimated the same way as wave heights with respect to the vertical distance between trough and bed at the breakpoint. For high energy conditions, h_b was estimated at 1.3 times H_b over gentle slopes (or spilling wave conditions) and 1.0 times H_b over steeper slopes (plunging wave conditions).

Breaker angle (a_b) - estimated for several waves in a set by sighting the approach direction of waves using a protractor aligned with the beach azimuth. Experience has shown that an observer facing an approaching wave can detect the angle more easily from the ground than one sighting along crests, if conditions preclude placing swimmers near the breaker line.

Wave period (T) - measured by timing the travel of six successive wave crests past a fixed reference staff and dividing by five to obtain mean period for a set. Procedure was repeated 3-5 times and an average computed from all wave sets. This measure is assumed to represent significant wave period, T_s .

Breaker type - classified qualitatively by visual observations according to the classification schemes of Galvin (1968) or Battjes (1974). Principal wave types are spilling, plunging, collapsing, and surging. The ratio, H_b/h_b , increases from spilling to collapsing type waves (Kana, 1979). Swimmers near the breakpoint observed a sequence of waves noting the degree of vorticity (highest in plunging waves). Occasional photographs or videos were taken to record representative breaker types at various tide stages and breakpoints over the profile.

Surf width - The distance to the outermost breaker line was estimated using fixed ranged poles. The innermost swash line at the same time was marked. Surf width was computed as the difference between the two readings. Surf width increases with wave energy but decreases at higher tide levels because of steepening beach slope.

Longshore current speed ($V_{\ell 1/2}$) - measured at the mid surf position (midway between breaker line and inner swash line), Using arrays of parallel range markers set 10 m or 20 m apart in the longshore direction, slightly buoyant floats were released updrift from the first range markers. As the floats passed the first range, timing began. Travel time was measured until the second set of ranges was passed. Distance traveled over time was reduced to unit values (m/s). This procedure was repeated at least three times and an average value computed. Also noted in the field was onshore/offshore movement of the floats, particularly during periods with small longshore current gradients.

Longshore current direction — recorded in the field as transport to the right or to the left when looking seaward, using standard convention.

The accuracy of littoral process measurements decreases under higher energy conditions for a number of reasons including the difficulty of getting an observer close to the breaker line. We found the practical limits for observations with swimmers were H_b less than 1.5 m and $V_{\ell 1/2}$ less than 0.5 m/s. Higher $V_{\ell 1/2}$ made it difficult to hold position in H_b greater than 1.0 m. Conditions below these energy levels were measurable with a fair degree of confidence. Littoral process measurements are also more consistent in long-crested waves. Short-crested waves, typical where cross-shore wind stress introduces a locally generated "chop" superimposed on deep-water swell or where two or more intersecting wave fields occur, are difficult to measure accurately. One effect of short-crested waves is to break away from a central, "high" point. Since breaking is related to depth, a short-crested wave will begin to break in deeper water at the high point of the crest. Breaking will progress toward shore as the wave shoals and lower parts of the wave reach breaking depth. The perception to an observer is that the wave breaks left and right at two opposing angles. Estimates of α_b therefore must account for this effect. One way of determining if wave approach is at an angle to shore under short-crested wave conditions is to observe the longshore-current gradient. If it is very small, one can assume α_b is negligible. This

was one way the field team checked for consistency in the coastal-process observations.

A summary of daily littoral process measurements and related surf-zone parameters is given in Table 3.5. As Table 3.5 indicates, mean wave heights were generally higher in September.

TABLE 3.5. Summary of coastal-process measurements obtained at station 10.

Code	Definition	Code	Definition
OBS	Observation number	WVTYPE	Visual wave type (S = spilling; P = plunging; C = collapsing)
DATE	Date [month, day, year]	LSCUR	Longshore current velocity (cm/s)
TIME	Time (24-hour clock)	LSDIR	Longshore current direction viewed from shore (1 = to right; 2 = to left)
WINDVEL	Wind velocity (m/see)	ALPHAB	Breaker angle/degree
WINDAZI	Wind azimuth [degrees True]	INSURF	Distance to inner surf line (m)
WVHT	Breaker height (cm)	OUTSURF	Distance to outer surf line (m)
WVDPTH	Breaker depth (cm)	WIDSURF	Width of surf zone (m)
WVPER	Wave period (seconds)		

o	D	T	W	W		w	w	V	V	L	L	A	I	O	w
B	A	I	N	I	W	V	W	P	P	S	S	L	N	U	I
s	E	E	L	z	T	H	R	E	P	U	R	A	R	R	F
1	08/11/86	1530	5.4	160	70	70	6.6	P	93	1					20
2	08/12/86	1500	8.9	230	140		5.3	s	156	1	25	110	210	100	
3	08/13/86	1400	-	250	80	100	5.5	s	60	1	10	160	300	140	
4A	08/14/86	1330	10.3	260	120		7.0	s	77	1	10	200	320	120	
4B	08/14/86	2100	11.2	270	230		7.5	s	100	1	15	60	260	200	
5	08/15/86	1430	4.0	310	110	120	8.0	s	60	2		220	350	130	
6	08/16/86	2100	1.3	310	100	100	8.0	P	35	2	5	110	130	20	
7	08/17/86	1600	3.6	300	50	70	5.8	s	0	-	0	210	300	90	
8	08/18/86	1730	2.2	300	40	50	5.0	s	9	2	0	215	320	105	
9	08/19/86	2000	1.3	330	120	160	7.0	s	38	1	0	170	190	20	
10	08/20/86	2030	4.5	315	130	160	5.5	s	27	2	5	190	210	20	
11	08/21/86	1530	4.5	300	50	60	5.7	s	<3	1	5	100	120	20	
12	08/22/86	1600	8.9	280	100	120	-	s	26	1	10	95	120	25	
13	08/23/86	1210	6.7	250	150	110	1.0	s	-	1	15	80	150	70	
14	08/24/86	1400	10.3	90	130		7.0	P	67	1		110	160	50	
15	08/25/86	1400	4.0	120	50		8.0	s	-		0	130	150	20	
16A	08/26/86	1445	11.2	170	90	90	9.0	P	44	1	3	110	150	40	
16B	08/26/86	1915	9.4	175	50		7.0	c	18	1	8			20	
17	08/27/86	1530	11.2	170	75	90	6.0	P		1	3	115	160	45	
18	08/28/86	1930	0.9	150	100		6.5	P	35	1	5	85	110	25	
19A	08/29/86	1330	9.8	145	20		5.0	c	<3	1	3	170	175	5	
19B	08/29/86	1845	8.0	150	10		5.0	s	10	1		100	105	5	
20A	08/30/86	1315	4.5	150	30	10	6.0	s	<3	2	5	150	160	10	
20B	08/30/86	2050	6.3	125	10	10	8.0	c	10	1	5	110	115	5	

3.3.6 Suspended-Sediment Measurements

Suspended-sediment samples were collected in the surf zone under a range of conditions in order to determine quantities of sand in suspension as a function of surf-zone position, height above the bed, and breaker parameters. The field data reported herein were collected during ten sampling days in August and September 1986. Each sampling period was designed to select particular waves, then simultaneously sample suspended sediment, measure wave process parameters, and record sampling positions with respect to the beach profile. A 2-3 man field team was required to coordinate all of these functions.

A range was established at each experiment site and periodically surveyed to the low-tide breaker line to calculate the beach slope at each sampling point. Stakes were set across the surf zone as reference points for sampling location and wave position. In addition, they provided convenient ranges to monitor longshore currents at the surface by means of slightly buoyant floats. Each suspended-sediment sample was positioned relative to:

- 1) The bed, by means of the sampling apparatus.
- 2) A bench mark on land, by means of the reference stakes.
- 3) The wave breakpoint, by measuring the distance seaward or landward of each array.
- 4) The time of passage of each wave sampled.

Figure 3.8 is a sketch of a typical sampling arrangement. Details of the sampling apparatus and method of operation are given in Kana (1976).

Suspended-sediment samples were collected and recorded by array. An array consists of all samples trapped simultaneously by one sampling apparatus. In most instances, the number of samples per array was two, centered at 10 cm and 40 cm above the bed. The lowermost sample at 10 cm above the bed was designated SS10; the one at 40 cm was SS40, and so on for occasional higher samples. The samplers are "rigged" for operation according to the water depths. When small waves are sampled, only the lowermost bottles are mounted to the support pole. Rigged samplers are then carried into the surf by swimmers.

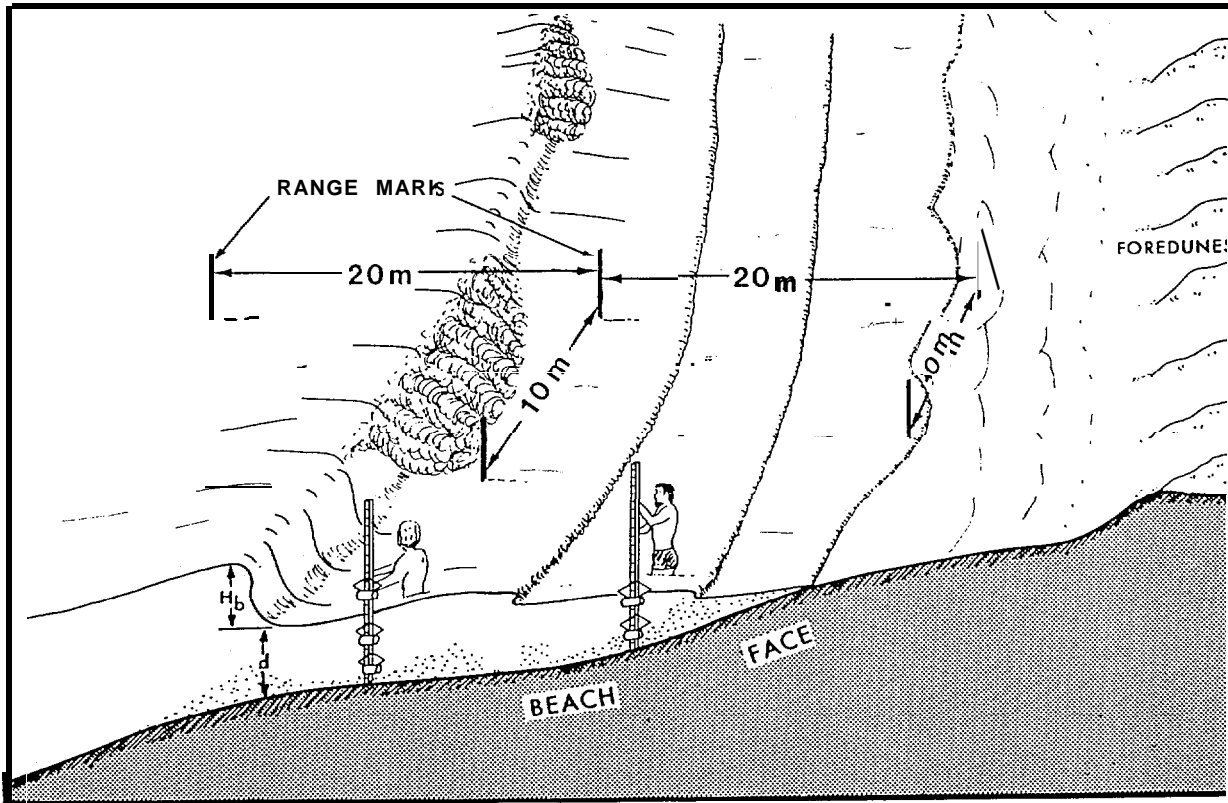


FIGURE 3.8 Sketch of the sampling arrangement showing samplers in place. Operators stood downdrift from sample point holding 'apparatus above bed until sampling instant. Range markers provided reference marks to locate sampling positions and to measure longshore-current velocity and position within the surf zone. [Note: At Port Heiden, we generally used only one sampler at a time.]

Positioning in the surf is determined with respect to the mean breaker line, using reference stakes as guides. Similar to a surfer positioning himself to ride a wave, each operator positions the sampler at a predetermined distance from the breaker line. In general, the seawardmost operator controls the positioning and spacing between arrays and selects the wave. Prior to or after sampling, we measured the breaker height, wave period, and surface longshore-current velocity.

Based on tests conducted during earlier field experiments (Kana, 1977), it was determined that the most consistent results are obtained when the operator stands downdrift of the sampler, faces alongshore, and holds the apparatus away from his body in a vertical position several centimeters above the bed. At the desired sampling instant, the operator steps forward thrusting the device away from his body and into the bed. As the footpad at the heel of the sampler depresses on striking the bed, each water bottle closes automatically.

For the Port Heiden samples, each array was collected at various times (as noted) with respect to passage of the wave bore by the sampler. Results from Kana (1977) and Brenninkmeyer (1976) indicate that, in general, the maximum concentration at a point occurs after the passage of a wave. Thus, the intent of this procedure was to sample at a range of representative times and representative wave conditions before, during, and after the period of maximum concentration. A total of 83 arrays were obtained.

After the water samples are trapped in each collecting bottle, the apparatus is carried ashore for transfer of the suspended-sediment samples to holding jars. Each collecting bottle has a calibrated scale mounted along the side for measuring volume directly in the field. This eliminates the normal transfer into graduated cylinders before filtering. After the volume was measured and recorded, each sample was emptied through a large funnel into a 2-liter Nalgene widemouth jar, then rinsed with distilled water to remove any remaining sediment. The jars were stored in boxes for transfer back to the Port Heiden air station where we set up a laboratory for analysis. The number of samples collected each day was restricted by the number of holding jars available. Generally, 15-25 samples were collected each sample period.

Using up to two samplers in each wave, over 83 individual waves were sampled during the experiment, yielding approximately 150 concentration values. Of these, about two-thirds were collected at the lowermost position, 10 cm above the bed.

In the laboratory, samples were filtered using standard filtering apparatus and techniques to retain the suspended sediment. The filtering system used consisted of a Millipore vacuum pump, ballast jug, and several manifolds of Millipore filtering flasks. Millipore 0.45-p, 45-mm-diameter cellulose filters were used and stored in locking petri dishes.

Since suspended-sediment concentrations can be high in the surf zone, it is necessary to preweigh the filter together with the petri dish to allow for overflow of sediment on the filter. In cases where concentration exceeded 5 g/l, several weighed petri dishes and filters are generally required to retain all of the sample. This is easily accomplished by spooning out the excess sediment from the filter flask and transferring it to a second filter. The combined weights of sediment on the two filters are calculated to determine concentration.

Filtered samples were rinsed three times with distilled water to remove salt, then stored for shipment to CSE. The final laboratory analysis entailed drying the filters and sediment at 70°C, then weighing the petri dish, sediment, and filter. All concentrations were determined as a weight-per-unit volume (grams/liter).

Results of the suspended-sediment sampling are given in Appendix II-F (this volume). Samples were taken under a range of wave and tide conditions encompassing H_b values from 60 cm to 180 cm. Other studies have shown that the primary controls on suspended sediment in the surf zone on sandy beaches are elevation above the bed, breaker type, and local slope (Kana, 1979). Other factors of lesser importance are wave height, wave period, longshore current speed, and distance from the breakpoint or swash zone. High concentrations will occur at plunge points where H_b/h_b is high or the slope is relatively steep. This is related to vortices which reach the bottom and produce bursts of sand from the bed (Miller, 1976; Brenninkmeyer, 1974). It is also affected by the backrush of a wave meeting the incoming wave. Sediment motion is initiated by rolling action during the return flow, facilitating suspension as the next wave breaks. Kana (1979) found that concentration peaks occur near the breakpoint in plunging waves. Spilling waves, however, typically suspend only a fraction of the quantities in plunging waves (regardless of wave height for moderate energy conditions), and there will be a tendency for more uniform concentrations across the surf zone. Other concentration maxima occur in the upper swash zone where Froude numbers are high (upper flow regime).

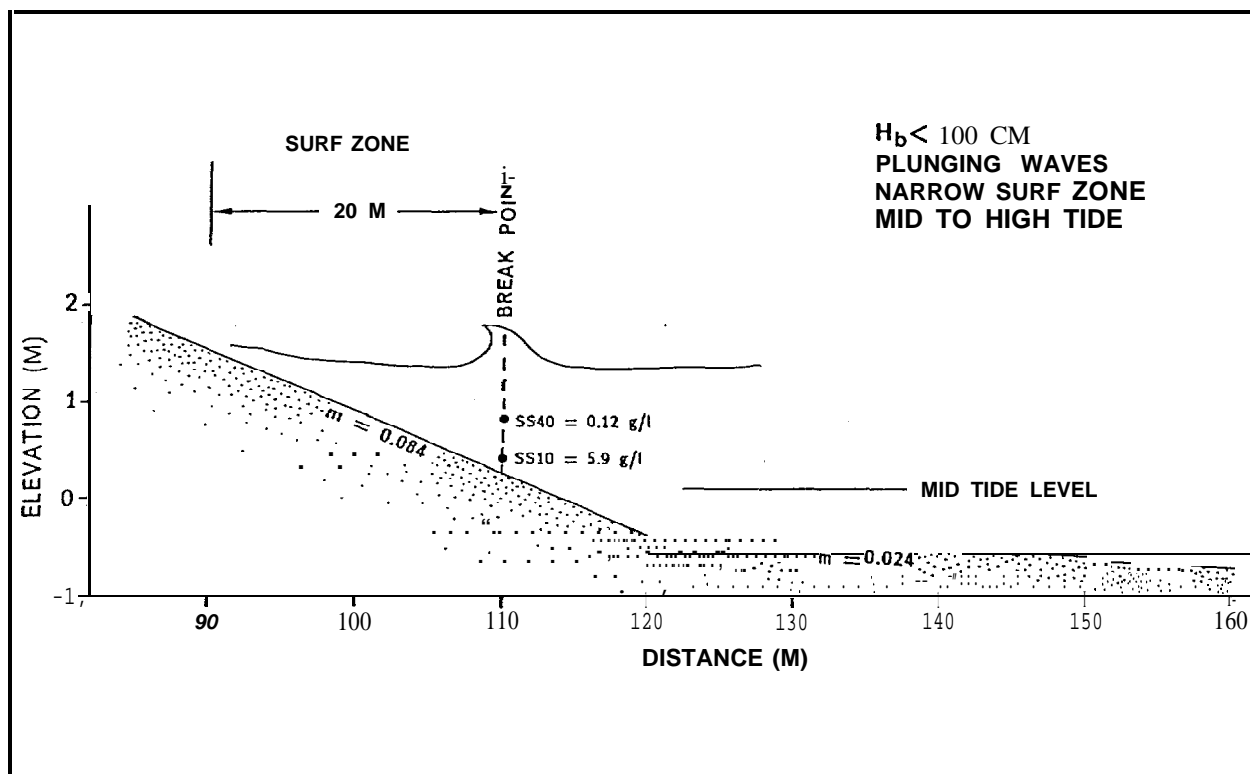
Because the number of suspended-sediment samples collected at Port Heiden was limited to 150, it is not possible to statistically test all the factors affecting suspended-sediment concentration in the area: nor was that the purpose of the study. However, review of the data indicated several primary trends which are consistent with findings in other moderate energy surf environments. Figures 3.9-3.10 have been synthesized from data subsets to illustrate how suspended-sediment tends to vary at Port Heiden under the range of conditions sampled.

Samples collected on 11 and 27 August and 3-6 September represented wave conditions dominated by plunging breakers with H_b less than 100 cm. Twenty-one samples were obtained at 10 cm above the bottom along the middle beach face (between 100 m and 120 m from station benchmarks) where the local slope, m , was 0.084 (Table 3.6). These samples also represented conditions near the breakpoint of the outer breaker line. Fifteen simultaneous samples were collected at 40 cm above

the bed. Figure 3.9 schematically illustrates the results. Typical surf width at mid-to-high tide under H_b less than 100 cm is 20 m for the site. Mean concentration for 10 cm and 40 cm above the bed near the breakpoint was 5.9 g/l and 0.12 g/l, respectively (highest and lowest four samples omitted as outliers). Standard deviation was high for the 10-cm samples (*5.4 g/l). However, this is typical of the wide range of sand concentrations found in the surf zone. The higher samples in the water column decreased exponentially in concentration, consistent with findings in other areas.

In contrast to the above results for "low energy" plunging waves along the beach face, spilling breakers dominated along the low-tide terrace where average slope was 0.024. On 13 and 15 August, suspended-sediment samples were collected over the low-tide terrace under waves up to 160 cm. Figure 3.10 illustrates that surf-zone width was much wider, ranging upwards of 140 m from the outer breaker line to the inner swash zone. Dissipation of wave energy is more gradual under these conditions and suspended-sediment concentration tends to be lower (despite higher wave heights).

One final trend of interest was the typical background levels of suspended sediment. An array of three samples was collected outside the surf zone on 6 September. The results for 10 cm, 40 cm, and 90 cm above the bed were 0.165, 0.084 and 0.047 g/l, respectively. These levels were similar to other random samples in the surf zone between waves breaking under low energy conditions. Thus, background levels for this time of year can be assumed to range from 10^{-1} g/l to 10^{-2} g/e. Inspection of filters indicates that concentrations in this range are dominantly clays or silts.

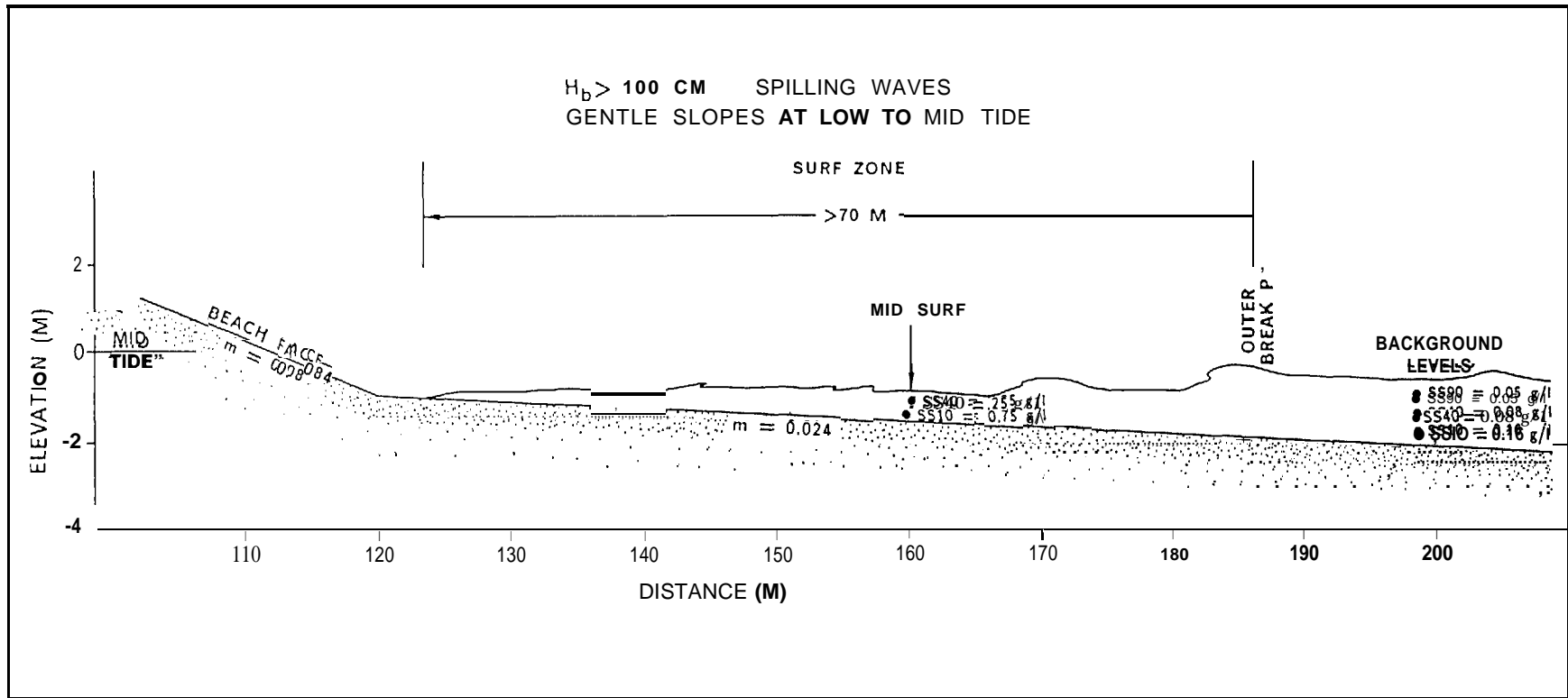


Data Subset (see Appendix III-E) Concentration in g/l.

Array No.	Ss10	SS40	Array No.	Ss10	SS40
A2	16.9		F1		0.15
A4	3.4		F3	1.8	-
A5	1.8		F7		0.2
A6	5.5	0.14	F8	1.3	
A10	6.0		F9	2.1	0.06
A11	8.5	0.11	G2		0.15
E2		0.09	G3	17.9	0.11
E8	2.2		G4	10.6	0.12
E9		0.12	H2	0.9	
E10	0.6		H5b	7.2	
E12	2.8	0.09	H6	11.3	-

NOTE: Highest two and lowest two values within each sample elevation subset were discarded as outliers. Standard Deviation: Ss10 = *5.4 g/l; SS40 = *0.04 g/l.

FIG U RE 3.9 Typical suspended-sediment concentration levels at the breakpoint under moderate energy, plunging waves at mid-to-high tide. Note relatively narrow surf zone and concentrations reaching 10 g/l at 10 cm above the bed.



DATA SUBSET: B1a, B1b, B2a, B2b, B3a, B3b, B4b, B5b, C1 (See Appendix III-E).

STANDARD DEVIATION: SS10 ± 0.48 g/l; SS40 ± 0.07 g/l.

FIGURE 3.10. Typical suspended-sediment concentration levels across a dissipative surf zone (spilling breakers) at mid-to-low tide. Note wider surf zone but significantly lower suspended-sediment concentrations over $H_b > 100$ cm.

TABLE 3.6. Profile slopes and beach morphology computed for station 10 from profile surveys on 20 August 1986.

	Distance (m)	Slope	Notes
Front stake	0	0.31	Foredune
	5	0.00	
	10	0.0625	Base foredune
	15	0.0625	
	20	0.0075	Berm backshore
	25	0.0075	"
	30	0.0075	
	35	0.0075	
	40	0.0075	
	45	0.0075	Storm berm crest
	50	0.0825	
	55	0.0825	
	60	0.035	
	65	0.054	
	70	0.054	
Reference stake	75	0.0	Berm runnel
	80	-0.027	Reverse slope
	85	0.084	Near berm crest
	90	0.084	
	95	0.084	
	100	0.084	Beach face
	105	0.084	
	110	0.084	
	115	0.084	
	120	0.084	Near step
Reference stake	125	0.024	
	130	0.024	
	135	0.024	
	140	0.024	Low-tide terrace
Reference stake	150	0.024	
	160	0.024	
	170	0.024	
	180	0.024	
	190	0.024	
	195	0.024	
	200	0.028	
	205	0.042	Outer breaker zone
210	0.042		
215	0.042	at normal low tide	
	220	0.042	

Effect of Suspended Sediment on Spilled Oil

With respect to the effect of suspended sediment on oil in the surf zone, the following processes are expected to affect transport. First, sand-sized material, which makes up the bulk of suspended sediment, will have an abraiding effect. Oil is not likely to become armored with sand-sized particles until it lays on the bed or becomes beached. After resuspension of tar balls, armored or unarmored with sand, surf-zone

turbulence and sand in suspension will break up oil. This will be more pronounced where sand concentrations are high (i. e., plunging waves on steeper slopes or in the upper flow regime swash zone). Fine-grained sediment in suspension, on the other hand, will adsorb oil. Under low energy conditions, where spilling waves dominate, or in areas outside the surf zone, the principal sediment load consists of a wash load of fine-grained material. Concentrations tend to be at least two orders of magnitude less than the sand concentrations.

The results from Port Heiden indicate that turbulence near the bed is highest under plunging and (probably) collapsing waves, both of which types occur at higher tide stages on steeper slopes. Sediment concentrations in the surf-zone water column decay rapidly above the bottom but reach values that dwarf background levels of suspended sediment. It is presumed that abrasion of oil would be a dominant process under plunging wave conditions because of high concentrations of sand placed in suspension. A large spill entering the surf zone, of course, would damp wave-breaking and probably not induce high concentrations of sand from the bed: therefore, abrasion processes would diminish.

At lower tide stages, wave-breaking occurs on gentler slopes at Port Heiden. As a result, spilling waves predominate over the low-tide terrace. Suspended-sediment concentrations are at least an order of magnitude lower at a comparable point in the surf zone. The effect of suspended sediment on oil under these conditions should be diminished. Abrasion is not expected to be important until oil is advected to the swash zone and begins interacting with the bed during wave uprush and downrush. "Washload" sediments in suspension were found to be in the range 10^{-1} to 10^{-2} g/t in the Port Heiden surf zone. While such fine-grained material has the potential to adsorb oil, it is believed that the magnitude of this process will be exceedingly small in the surf zone in relation to gross quantities advected shoreward into the swash zone and onto the beach face. Incorporation of fine sediment by oil is likely to be insignificant (by mass or volume) in comparison to incorporation of sand-sized material once a spill reaches the inner surf zone or beach. These results suggest that additional partitioning of oil to account for differences in suspended sediment concentration would be exceedingly complex and are not warranted for application in the COZOIL model. The interaction of oil with fine-grained sediments in the surf zone is a process that appears to be dwarfed (in volumetric terms) by other surf-zone processes.

3.4 WIND AND WAVE HINDCAST

A wave hindcast was performed for offshore waves during the period August-September 1986. This was necessitated after loss of the wave gauge off Port Heiden. The hindcast was performed using about 100 synoptic weather charts for the Bering Sea obtained from the National Climatic Center (Asheville, North Carolina). The general procedure for the wave hindcast is given in the Shore Protection Manual (CERC, 1984). It involves determination of surface winds from the geostrophic wind, delineation of fetches, and determination of duration for discrete events which generate waves toward Port Heiden. Using these data, the appropriate deep-water or shallow-water forecasting curves (given in CERC, 1984) are applied to determine H_s and T_s at the downwind end of the fetch. Where applicable, hindcasted waves are decayed from the fetch-generating area to Port Heiden. Three case studies were developed from the hindcast data for testing with the COZOIL model. This section outlines the methodology of the hindcast and presents details of each case study.

3.4.1 Methodology

Weather maps were provided by the National Climatic Center for the Bering Sea/Bristol Bay area at one inch equals 356 statute miles (1 cm = 226 km). Isobars and shorelines were retraced to develop fetch maps for each event. Geostrophic winds were determined for fetches relevant to Port Heiden (i. e., within 30° of the point of interest). Geostrophic winds are a function of isobar spacing and latitude, and can be estimated using nomography in CERC (1984).

The geostrophic wind was corrected to the gradient wind according to the following conventions:

- 1) For anticyclonic curvature of isobars, add 10 percent.
- 2) For cyclonic curvature, subtract 10 percent.
- 3) For moderately curved to straight isobars, no correction was applied.

Surface wind speeds are lower than geostrophic winds and are dependent on the ratio between sea surface temperature and air temperature. We computed the surface wind speed (US) as a function of corrected geostrophic wind speed (U_g) and the sea/air temperature difference ($T_s - T_a$) according to the following factors:

$$\frac{u_s}{U_g} = \begin{array}{l} 0.60 \text{ where } T_s - T_a = \text{negative (stable)} \\ 0.65, \text{ where } T_s - T_a = 0-10^\circ \text{ F } (0-5.5^\circ \text{ C}) \text{ (mildly unstable)} \\ 0.75, \text{ where } T_s - T_a = 11-20^\circ \text{ F } (6-11^\circ \text{ C}) \\ 0.90, \text{ where } T_s - T_a = >20^\circ \text{ F } (>11^\circ \text{ C}) \text{ (very unstable)} \end{array}$$

Generally, a factor of 0.65 was applied in the hindcast for Port Heiden. This is assumed to represent the duration-averaged wind.

Fetches were delineated using general procedures outlined in CERC (1984). A fetch relevant to Port Heiden was assumed to be one where winds have a fairly constant direction and speed, and blow within a *30* angle to either side of the true direction from the end of the fetch to Port Heiden. Once such an area can be delineated on a map, a reasonable length of fetch can be determined by averaging the distances of rays emanating from the point of interest taken from several maps. It was assumed that confidence in the result improves when the wind direction variation remains less than 15*. We considered the wind direction constant from map to map if it varied from the mean less than 30°. We considered the speed constant if it varied from the mean by less than *5 knots (*2.6 m/s). In this procedure, average values for wind speed and direction are used and are assumed constant over the fetch area for a particular duration.

Duration was determined by comparing winds under the above criteria from map to map. It was assumed an event began at the time midway between successive maps and terminated after the last map with the same wind speed and direction at the midway time to the next map.

Waves were estimated using deep-water or shallow-water forecasting curves (CERC, 1984) as appropriate to the depths of water at the end of the fetch, and the significant wave period (wave length). The forecasted waves were checked to distinguish between fetch-limited or duration-limited values. A second check was performed by comparing reduced surface winds to over-water winds measured in the fetch area (where available). Waves were "decayed" between the fetch and Port Heiden using nomography in CERC (1977, SPM earlier edition).

The following sections provide results of three case studies of hindcasted winds and waves compared with onshore observations at Port Heiden.

3.4.2 Case 1 – Wind and Wave Field, September 6-10, 1986

Onshore wind direction observed at beach and offshore station locations

Description of event. The time period encompassed the south to north propagation of a deep low-pressure system [central pressure of 988 millibars (rob)] across the Bering Sea. The storm system was noted to have nicely defined warm, cold, and occluded fronts propagating with the storm. Wind patterns before the frontal passages were generally southeast over the Port Heiden area with intensities averaging well over 20 knots. A sudden wind shift from 165°T (degrees true) to 260°T was observed at Port Heiden between 1400-1500 local standard time (LST) on September 6, and the wind pattern generally remained from the west and northwest for several days. Wind and waves were of small gale conditions during this time period. The winds subsided rather quickly and became light and variable at the Port Heiden beach station after 1600 LST on September 10. An offshore fetch area of light west to northwest winds existed until approximately 2100 LST on September 10 after which the offshore winds became light and variable.

Notes on the **hindcast** analysis. The offshore winds (Table 3.7) are approximate duration-averaged winds at the final extent of the deep-water wave field. This area is located several kilometers offshore. Wind velocities are estimated from weather maps using a conversion from geostrophic winds to approximate 10-meter surface winds following Chapter 3 in the Shore Protection Manual (CERC, 1984). When geostrophic winds are unobtainable, a best-estimate using sparse but available over-water wind observations from the weather maps is performed. Approximate fetch distances for offshore wave generation are also given. The times of observation are based on Alaskan local standard time which is equivalent to Greenwich mean time (GMT) minus nine hours. Instantaneous onshore wind velocities at approximately the same time periods as the offshore winds are also given for the beach wind station. The generation of waves for this case study is a local event directly affecting Port Heiden as opposed to an offshore event in which swells are created and impact the area. Note that the wave periods as measured or observed onshore will tend to be biased toward the predominant swell for the area which precedes the storm event. Hindcast wave periods initially must be short because the prediction is duration limited. Expected swell wave heights and periods for the period of September 6-7 will appear in supplementary tables.

TABLE 3.7. Comparison of hindcasted offshore winds and onshore winds during case study 1.

Date	Hindcasted Offshore Station Winds					Measured Instantaneous Beach Station Winds				
	Time (LST)	Speed (mph)	Speed (m/s)	Direction ("T)	Duration (hrs)	Fetch (km)	Time (LST)	Speed (mph)	Speed (m/s)	Direction ("T)
Sep 6	1500	15.0	6.7	260	6	270	1450	10	4.5	260
	2100	15.4	6.9	290	6	430	2050	20	8.9	315
Sep 7	0300	15.0	6.7	320	6	330	0250	18	8.0	335
	0900	17.3	7.7	300	6	400	0850	15	6.7	320
	2100	25.3	11.3	300	12	320	2050	36	16.1	310
Sep 8	0900	20.3	9.1	300	12	580	0850	20	8.9	300
	2100	18.6	8.3	300	12	450	2050	28	12.5	300
Sep 9	0900	14.5	6.5	290	12	290	0850	21	9.4	300
	2100	14.5	6.5	270	12	320	2050	19	8.5	300
Sep 10	0900	16.1	7.2	280	12	270	0850	15	6.7	255
	2100	14.0	6.3	290	12	270	2050	7	3.1	030

Notes on deep-water wave hindcast versus observed onshore breaking waves. All hindcasted waves are assumed deep-water-generated waves. The resulting waves (Table 3.8) are representative of the significant wave height and significant period and are formulated following the CERC Shore Protection Manual. Direction of breaking waves is relative to the true direction in the direction of wave travel. Azimuth angle of shoreline at our primary coastal process monitoring station is approximately 20° clockwise from North. Thus, a shore-perpendicular breaking wave will be traveling in the direction of IIO" T (see Fig. 2.8 for example convention).

TABLE 3.8. Hindcasted offshore and observed onshore waves during the case study 1 period.

Date	Hindcasted Offshore Waves			Onshore Breaking Waves					
	Time (LST)	H _s (m)	T _s (s)	Direction ("T)	Time (LST)	' _b (m)	T _b (s)	Direction (*T)	Breaker Angle to Shore a
Sep 6	1500	0.82	4.4	80	1335	0.60	8.0	92	18
	2100	0.85	4.5	110	1520	0.70	-	96	14
Sep 7	0300	0.82	4.4	140	1345	1.30	7.2	110	0
	0900	1.01	4.8	120	1525	1.80	6.8	110	0'
	2100	3.05	8.5	120					
Sep 8	0900	2.19	7.5	120	1355	1.20	6.0	110	0
	2100	1.95	7.2	120					
Sep 9	0900	1.28	5.9	110	1705	1.10	6.0	110	0
	2100	1.28	5.9	90					
Sep 10	0900	1.55	6.5	100	1450	1.00	6.9	102	8
	2100	1.13	5.6	110					

3.4.3 Case 2 - Wind and Wave Field, August 22-28, 1986

Offshore wind directions observed at beach and offshore station locations

Description of event. The general weather pattern on 1500 LST, 22 August showed a 992 rnb low centered at approximately 60° N, 170° E. High pressure centered well south of Alaska produced an area of westerly winds over Port Heiden and Bristol Bay. As the storm moved southeast, a southwest fetch area developed in the central Bering Sea. The winds over Port Heiden and surrounding waters "backed" toward the south and south-southeast (Table 3.9). By 0300 LST, 24 August, the low had intensified to 990 mb and was centered approximately 600 miles west of Port Heiden. The counterclockwise circulation around the low generated south to southeast winds over Port Heiden and the offshore waters. An area of west to southwest winds was located just south of the low, and this area remained in nearly the same location for about 12 hours. By 0300 LST, 25 August, the low moved southeast and was located just north of the Aleutian Island chain. The west to southwest wind fetch area disappeared, and the winds over Port Heiden and the eastern portion of the Bering Sea were southeast. Because of this wind pattern, Port Heiden should be influenced by swell-type wave conditions for most of the study period. By 0900 LST, the original low had merged with a second low and moved north and was centered off Port Moller, Alaska. Winds at Port Heiden were still southeast to south but an area of westerly winds began to develop south of the low. The low moved due north, and the westerly fetch area enlarged. However, the winds near Port Heiden were still offshore so that swell-induced waves should be predominant. The storm turned and moved northwest, diminishing in intensity. The western fetch area disappeared, and the wind patterns over Bristol Bay remained southeast to south. This wind pattern induced a wave set-down over the study area and between August 29-31, the shore-breaking waves were observed to be less than one foot (30 cm).

Notes on the **hindcast** analysis. The predominant wave event, as determined from the analysis of the weather maps, appears to be a swell-induced wave traveling from the west or southwest. Following an earlier version of the Shore Protection Manual, the deep-water hindcasted waves generated at the eastern extent of the fetch decayed as they traveled to shore so that their wave height decreased and wave period increased (Table 3.10). Included in the hindcasting tables are the initial deep-water waves, the decay distance from their point of generation to Port Heiden, and the resulting decayed wave height or swell wave height (H_D) and decayed swell wave

period (T_D). Also included is the expected time of travel of these waves and the local time in which these waves are expected at the study area. In general, the fetch locations on these maps were often vague and undefined, and estimates were made assuming the general circulation around low and high pressure areas. One should expect some variability between observed breaking waves and swell-induced waves.

TABLE 3.9. Comparison of hindcasted offshore winds and onshore winds during case study 2. [(1) Locally generated fetch area]

Date	Hindcasted Fetch Winds							Measured Instantaneous Beach Station Winds			
	Time (LST)	Speed (mph)	Speed (m/s)	Direction ("T)	Duration (hrs)	Fetch (k m)	Distance from Port Heiden (km)	Time (1ST)	Speed (mph)	Speed (m/s)	Direction ("T)
Aug 22	1500	17.0	7.6	265	12	340	(1)	1450	21	9.4	290
Aug 23	0300	18.8	8.4	270	12	400	(1)	0250	25	11.2	255
	0300	19.2	8.6	240	12	900	320				
	1500	14.0	6.3	260	12	290	(1)	1450	13	5.8	285
	1500	18.8	8.4	250	12	800	430				
Aug 24	0300	17.0	7.6	250	12	240	800	0250	2	0.9	045
	1500	17.0	7.6	250	12	240	640	1450	22	9.8	160
Aug 26	0900	17.0	7.6	270	6	350	140	0750	22	9.8	150
	1500	17.0	7.6	270	6	360	140	1450	25	11.2	160
Aug 27	0300	17.0	7.6	260	12	210	320	0250	17	7.6	165
	1500	21.0	9.4	260	12	400	370	1450	26	11.6	175
Aug 28	0300	16.0	7.2	250	12	380	320	0250	5	2.2	135
	1500	14.0	6.3	250	12	500	320	1450	5	2.2	310

TABLE 3.10a. Locally generated hindcasted offshore waves during case study 2.

Locally Generated Hindcasted Offshore Waves				
Date	Time (LST)	H _S (m)	T _S (s)	Direction (*T)
Aug 22	1500	5.6	6.8	90
Aug 23	0300	6.4	7.2	90
	1500	3.7	5.6	80

TABLE 3.10b. Hindcasted deep-water waves and decayed waves at Port Heiden during case study 2.

WAVES IN FETCH				DECAYED WAVES AT PORT HEIDEN						
Wave Origin Data				Probable Observance of Swells						
Date of Generation	Time (LST)	H _S (m)	T _S (s)	Date	Time (LST)	Swell Decay Distance (km)	Time of Travel (hrs)	H _D (m)	T _D (s)	Direction ("T)
Aug 23	0300	2.04	7.3	Aug 23	1900	320	16	0.79	9.3	60
	1500	1.98	7.2							
Aug 24	0300	1.83	7.1	Aug 24	1100	430	20	0.70	9.3	70
	1500	1.83	7.1							
Aug 26	0900	1.04	4.8	Aug 26	2100	640	30	0.67	9.3	70
	1500	1.04	4.8		1900	140	10	0.46	6.0	90
Aug 27	0300	1.71	6.8	Aug 27	0100	140	10	0.46	6.0	90
	1500	2.13	7.4		1900	320	16	0.64	8.8	80
Aug 28	0300	1.55	6.5	Aug 28	0800	370	17	0.79	9.6	80
	1500	1.12	5.6		2000	320	17	0.55	8.5	70
				Aug 29	1100	320	20	0.37	7.4	70

TABLE 3.10C. Onshore breaking wave observations during case study 3. [*Estimated]

Onshore Breaking Waves from Visual Observations					
Date	Time (1ST)	H _b (m)	T _b (s)	Direction ("T)	Breaker Angle to Shore ^a
Aug 22	1600	1.0		100	10
Aug 23	1210	1.5	11.0	95	15
Aug 24	1400	1.3	7.0	95*	15*
Aug 25	1400	0.5	8.0	110	0
Aug 26	1445	0.9	9.0	107	3
	1915	0.5	7.0	102	8
Aug 27	1530	0.75	6.0	107	3
Aug 28	1930	1.0	6.5	105	5
Aug 29	1330	0.2	5.0	107	3

3.4A Case 3 – Wind and Wave Field, August 12-20, 1986

Description of event. During the first part of this time period, the study area (including the eastern portion of the Bering Sea) was being influenced by long-fetch southwest winds produced by a strong high-pressure area centered at 50° N. 175°E. As the high-pressure area drifted southeast between 1500 LST, August 12 to 0300 LST, August 14, the winds became more westerly locally and a southwest wind fetch area with strong winds developed in the mid-eastern portion of the Bering Sea (Table 3.11). Thus, the study area would be influenced by possible long-period swells and locally generated waves traveling from the west and southwest. By 0300 LST, August 15, a cold front extending from a low northeast of Port Heiden produced a wind shift to the northwest while the southwest fetch area in the central Bering Sea remained. Local winds generally remained from the west to northwest throughout the rest of the period while the local wave field generally consisted of small-period duration, limited waves traveling from the west and swells moving in from the southwest and west (Table 3.12).

TABLE 3.11. Hindcasted offshore winds and measured onshore winds during case study 3. [(1) Locally generated fetch area. *Port Heiden Airport winds. Beach winds not measured until August 16.]

Date	Hindcasted Fetch Winds							Measured Instantaneous Beach Station Winds			
	Time (LST)	Speed (mph)	Speed (m/s)	Direction ("T)	Direction (hrs)	Fetch (k m)	Distance from Port Heiden (km)	Time (LST)	Speed (mph)	Speed (m/s)	Direction (' T)
Aug 12	1500	15.3	6.8	250	12	960	(1)	1546	20.7	9.3	280*
Aug 13	0300	16.5	7.4	260	12	1280	(1)	0437	15.0	6.7	260*
	1500	18.4	8.2	260	12	800	(1)	1541	19.6	8.8	270*
Aug 14	0300	20.0	8.9	260	12	160	(1)	0450	20.7	9.3	250*
	0300	18.8	8.4	250	12	880	160				
	1500	24.0	10.7	270	12	800	(1)	1541	26.5	11.9	260*
Aug 15	0300	18.3	8.2	290	12	430	(1)	0530	10.3	4.6	290*
	0300	16.5	7.4	240	12	880	560				
	1500	13.0	5.8	305	12	450	(1)	1546	8.1	3.6	310*
	1500	14.1	6.3	250	12	960	320				
Aug 16	0300	15.0	6.7	270	12	640	400	0250	2.0	0.9	180
	1500	17.0	7.6	265	12	400	(1)	1450	5.0	2.2	300
	1500	17.0	7.6	250	12	370	480				
Aug 17	0300	18.8	8.4	260	12	1200	240	0250	6.0	2.7	210
	1500	15.0	6.7	290	12	480	(1)	1450	8.0	3.6	300
Aug 18	0300	13.0	5.8	300	12	350	(1)	0250	17.0	7.6	270
	1500	12.0	5.4	290	12	210	(1)	1450	9.0	4.0	300
Aug 19	0300	13.0	5.8	290	12	350	(1)	0250	7.0	3.1	270
	1500	13.0	5.8	295	12	350	(1)	1450	6.0	2.7	310
Aug 20	0300	12.8	5.7	300	12	320	(1)	0250	5.0	2.2	290
	1500	15.0	6.7	300	12	240	(1)	1450	9.0	4.0	320

TABLE 3.12a. Locally generated hindcast offshore waves during case study 3.

Locally Generated Hindcasted Offshore Waves				
Date	Time (LST)	H _s (m)	T _s (s)	Direction ("T)
Aug 12	1500	1.40	6.3	70
Aug 13	0300	1.62	6.6	80
	1500	1.92	7.0	80
Aug 14	0300	2.19	7.5	80
	1500	2.87	8.3	90
Aug 15	0300	2.13	7.4	110
	1500	0.94	5.1	125
Aug 16	1500	1.68	6.7	85
Aug 17	1500	1.31	6.0	110
Aug 18	0300	0.91	6.0	120
	1500	0.76	4.6	110
Aug 19	0300	0.94	5.1	110
	1500	0.94	5.1	115
Aug 20	0300	0.91	5.1	120
	1500	1.31	6.0	120

TABLE 3.12b. Hindcasted deep-water waves and decayed swell waves at Port Heiden during case study 3.

WAVES IN FETCH				DECAYED WAVES AT PORT HEIDEN						
Wave Origin Data				Probable Observance of Swells						
Date of Generation	Time (LST)	H _s (m)	T _s (s)	Date	Time (LST)	Swell Decay Distance (km)	Time of Travel (hrs)	H _D (m)	T _D (s)	Direction ("T)
Aug 14	0300	1.95	7.2	Aug 14	1300	160	10	0.95	8.6	70
Aug 15	0300 1500	1.58 1.16	6.6 5.7							
Rug 16	0300 1500	1.31 1.68	6.0 6.7	Aug 16	0500 1000	560 320	26 19	0.46 0.40	8.9 7.5	60 70
Rug 17	0300	1.95	7.2	Aug 17	0200 1400 1500	400 480 240	23 23 12	0.43 0.55 0.85	7.8 8.8 8.9	90 70 80

TABLE 3.12c. Observed onshore breaking waves at Port Heiden during case study 3. [*Estimated]

Onshore Breaking Waves from Visual Observations					
Date	Time (LST)	H _b (m)	T _b (s)	Direction ("T)	Breaker Angle to Shore α
Aug 12	1500	1.4	5.3	85	25
Rug 13	1400	0.8	5.5	100	10
Aug 14	1300 2100	1.2 2.3	7.0 7.5	100 95	10 15
Rug 15	1430	1.1	8.0	110*	
Rug 16	2100	1.0	8.0	115	-5
Rug 17	1600	0.5	5.8	110	0
Rug 18	1750	0.4	5.0	110	0
Rug 19	2000	1.2	7.0	110	0
Aug 20	2030	1.3	5.5	115	-5

3.4.5 Supplemental Data

The following data (Tables 3.13-3.15) represent the remaining hindcasted fetch winds and deep-water wave periods for the time periods not included in the three case studies. The same table format is used as in case studies 2 and 3. Beach instantaneous wind velocities are also given. The dates where wave hindcasting could not be performed are also included.

TABLE 3.13. Hindcasted offshore and measured onshore winds during the field study period (1986).
 [(1) Locally generated fetch area. *Winda at Port Heiden Airport. Beach winds unavailable. **Swell-generated waves between September 4 and September 6 may influence wave conditions during case study 1.]

Date	Hindcasted Fetch Winds							Measured Instantaneous Beach Station Winds			
	Time (LST)	Speed (mph)	Speed (m/s)	Direction (°T)	Duration (hrs)	Fetch (k m)	Distance from Port Heiden (km)	Time (LST)	Speed (mph)	Speed (m/s)	Direction (°T)
Aug 10	0300	15.1	6.8	270	12	370	160	0545	11.5	5.1	280*
	1500	13.2	5.9	290	12	250	(1)	1542	9.2	4.1	320 ^s
Aug 11	0300	unresolvable						0452	4.6	2.1	100*
	1500	15.0	6.7	240	12	510	420	1549	15.0	6.7	170*
Aug 12	0300	14.1	6.3	270	12	1200	360	0534	15.0	6.7	280*
	1500	(LST) to Aug 20.1500 (LST): Case Study 3									
Aug 21	0300	unresolvable						0250	7.0	3.1	300
	1500	12.0	5.4	285	12	430	(1)	1450	12.0	5.4	300
Aug 22	0300	17.0	7.6	270	12	290	(1)	0250	18.0	8.1	270
	1500	(LST) to Aug 29 1500 (LST): Case Study 2									
Aug 29	0300	unresolvable						0250	24.0	10.7	140
	1500	unresolvable						1450	19.0	8.5	135
Aug 30	0300	unresolvable						0250	15.0	6.7	140
	1500	unresolvable						1450	19.0	8.5	120
Aug 31	0300	unresolvable						0250	7.0	3.1	145
	1500	15.1	6.8	260	12	650	360	1450	5.0	2.2	350
Sep 1	0300	13.0	5.8	260	12	350	(1)	0250	13.0	5.8	255
	1500	13.0	5.8	290	12	290	(1)	1450	17.0	7.6	300
Sep 2	0300	14.0	6.3	285	12	370	(1)	0250	23.0	10.3	300
	1500	14.0	6.3	290	12	380	(1)	1450	10.0	4.5	285
Sep 3	0300	unresolvable						0250	7.0	3.1	150
	1500	unresolvable						1450	12.0	5.4	140
Sep 4	0300	unresolvable						0250	18.0	8.1	160
	1500	26.0	11.6	270	6	210	960	1450	27.0	12.1	160
Sep 5	0300	28.1	12.6	270	12	320	800	0250	20.0	8.9	150
	1500	24.0	10.7	270	12	640	690	1450	33.0	14.8	150
Sep 6	0300	23.6	10.6	270	12	530	800	0250	21.0	9.4	150
	0900	20.0	8.9	285	6	420	560	0850	26.0	11.6	135
	1500	LST to Sep 10 2100 LST: Case Study 1**									
Sep 11	0300	unresolvable						0250	4.0	1.8	120
	1500	unresolvable						1450	4.0	1.8	280

TABLE 3.14a. Locally generally hindcasted offshore waves at Port Heiden.

Locally Generated Hindcasted Offshore Waves				
Date	Time (LST)	H _s (m)	T _s (s)	Direction ("T)
Aug 10	1500	0.98	5.2	110
Aug 21	1500	0.76	4.6	105
Aug 22	0300	1.71	6.8	90
Sep 1	0300	0.67	4.1	80
	1500	0.94	5.1	110
Sep 2	0300	1.13	5.6	105
	1500	1.13	5.6	110

TABLE 3.14b. Hindcasted deep-water waves and decayed waves at Port Heiden.

WAVES IN FETCH				DECAYED WAVES AT PORT HEI DEN						
Wave Origin Data				Probable Observance of Swells						
Date of Generation	Time (LST)	H _s (m)	T _s (s)	Date	Time (LST)	Swell Decay Distance (k m)	Time of Travel (hrs)	H _D (m)	T _D (s)	Direction (*T)
Aug 10	0300	1.37	6.2	Aug 10	1300	160	10	0.64	7.8	90
Aug 11	1500	1.34	6.1							
Aug 12	0300	1.16	5.7	Aug 12	1200	420	21	0.64	8.2	60
				Aug 13	0100	360	22	0.37	7.5	90
Aug 31	1500	1.37	6.2	Sep 1	1000	360	19	0.46	8.2	80
Sep 4	1500	1.95	6.3							
Sep 5	0300	3.63	9.2							
	1500	2.87	8.3							
Sep 6	0300	2.80	8.2	Sep 6	1100	960	44	0.40	9.1	90
	0900	1.31	5.3		0600	800	27	1.10	12.4	90
					1800	690	27	0.91	11.0	90
				Sep 7	0900	800	30	0.79	11.1	90
					1800	560	33	0.34	7.3	105

TABLE 3.15. Observed onshore breaking waves at Port Heiden. [NOTE: A complete set (13) of measurements was made on September 5 and have been submitted to National Oceanographic Data Center (NODC).]

Onshore Breaking Waves from Visual Observations					
Date	Time (LST)	H _b (m)	T _b (s)	Direction (°T)	Breaker Angle to Shore <i>a</i>
Aug 11	1530	0.70	6.6	---	--
Aug 21	1530	0.50	5.7	105	5
Aug 30	1315	0.30	6.0	115	-5
	2050	0.10	8.0	105	5
Aug 31	1210	0.50	10.0	110	0
	2045	0.30	10.0	107	3
Sep 1	1105	0.80	10.0	100	10
	1830	0.50	4.0	105	5
Sep 2	1420	1.0	6.0	113	-3
	2130	1.0	7.0	110	0
Sep 3	0945	0.75	5.5	102	8
	1155	1.0	5.0	110	0
	2010	0.5	5.0	107	3
Sep 4	1120	0.6	9.5	100	10
	1230	0.9	7.5	100	10
Sep 11	1420	1.6	8.0	107	3

4.0 FLEXIBILITY OF MODEL FOR PROBLEM-SOLVING

The COZOIL model has been designed and implemented for use in a wide range of applications. It can operate as a completely independent ("stand-alone") coastal zone oil spill model on a microcomputer, creating estimates of tidal and wind-driven current and wave fields from user-supplied or stochastic wind time-series. The model can also operate on a minicomputer or mainframe, taking hydrodynamic and meteorological input from external two- or three-dimensional models. In either mode, COZOIL operates from a relatively simple question-answer interactive format, so that the user can easily control and alter model parameters. The effect of these parameters will be discussed below to clarify the extent of model flexibility. Parameters are discussed below in the order in which they appear on the monitor during model execution.

4.1 BASIC OPTIONS

Interactive Option. Enter 'T' to run at the terminal, 'F' to run from a file containing responses to subsequent queries from the interface. A batch job will always require the "F" response. "T" is used primarily to set up or modify a coastline, wind or wave time-series for subsequent simulations. (Note that COZOIL will recognize either upper- or lower-case responses.)

Stochastic Option. A response of "Y" (yes) is followed by a query for the number of stochastic runs to be performed, and will also require wind statistics, rather than a deterministic wind time-series.

Verbose/Abbreviated Option. If the stochastic option is not selected, the user can create a large amount of detailed output by entering 'V'. This level of detail is useful during trial runs of a new problem, to ascertain that topographic and hydrodynamic inputs are correct. In general, the abbreviated option ('A') is used. If a series of stochastic runs is being performed, the model automatically terminates all output except for a few minimal statements to allow the user to measure simulation progress, and the final summary statistics.

4.2 PETROLEUM SELECTION AND PREWEATHERING OPTION

Petroleum Selection. There are seven petroleum types programmed into COZOIL. If the petroleum of interest is not included, the user may refer to Anonymous (1983) to find a close match. The seven types presently available in the model are:

- | | | | |
|---------------------------|-----------------------|----------------------|------------------|
| 1) Prudhoe Bay crude (AK) | 3) Wilmington (CA) | 5) Lake Chicot (LA) | 7) Jet fuel JP.5 |
| 2) Cook Inlet (AK) | 4) Murban (Abu Dhabi) | 6) Light diesel fuel | |

Prewea thering Option. This option allows the user to reduce the percentage contributions (by volume) of each boiling point fraction to the whole oil, effectively "pre-evaporation." The user may also "pre-emulsify" the oil by entering the fraction of water-in-oil at simulation start.

Resolution of Boiling Point Fractions. The number of boiling point fractions used in a simulation can be reduced from the number provided by the program library. This reduction in resolution allows the model to execute more rapidly, and if not too severe, results in virtually the same evaporative losses as with the full range of boiling point fractions. The model compresses the number of fractions" by combining adjacent fractions (e.g.. 1 and 2, 3 and 4, 5 and 6, etc.) until the desired number of fractions is achieved. The characteristics of adjacent fractions are combined by linear mass-weighted averaging. To determine whether enough resolution has been retained in the definition of the oil, the user should run two 4- or 5-day simulations, one with the "compressed" oil, and one with the complete representation, and compare the mass balances. If they are significantly different, then more fractions must be retained.

4.3 USER-SPECIFIED PARAMETERS

Environmental Temperature. The user enters an air or water surface temperature in degrees centigrade for the time of the simulation.

Simulation Duration. When first setting up and testing a new simulation, this parameter should be set at one day or less. When it has been determined that the model inputs are correct, the full duration should be entered. There is no inherent time limit for simulations.

Output Intervals. Output intervals to the screen can be controlled separately for the first 24 hours of a simulation versus the full duration. This allows observation of mass-balance changes which occur relatively rapidly at first, and more slowly there after.

4.4 SPILL INPUT PARAMETERS

Spill Size. This is the total amount of oil (barrels) which is to be released. If the oil has been preweathered, this is the total amount of weathered oil to be released.

Number of Spinets. This is the number of discrete batches of oil, each of equal mass, into which the spill will be divided. The model will release spinets at the input release interval (below). Thus the release rate is linear in time. A parameter in the FORTRAN common, NSPMX, controls the maximum number of spinets which will be represented in the model at any one time. The number of input spinets is not limited by NSPMX since the model contains an array compression subroutine to combine overlapping and neighboring spinets, making space in the array for new entries.

Entrainment Algorithms. Either of the two entrainment algorithms described in section 2 can be invoked. The Audunson/Spaulding algorithm entrains oil at a rate which decreases exponentially with time. The Mackay algorithm couples the rate to oil viscosity and slick thickness.

Subsurface Oil Transport. Transport of oil entrained in the water column is computed with a Lagrangian marker particle submodel. Selection of this option invokes the Lagrangian subroutines, and causes the model to run more slowly since more computations are being performed each time step. The mass balance may also be affected, since oil which is in the water column may be transported out the open boundaries of the model.

Stand-Alone Option. The stand-alone option ('1') is selected for independent runs of the model. The dependent option ('2') is used when COZOIL is operated in conjunction with the offshore oil spill, hydrodynamic, and weather models. Oil and hydrodynamic input files must exist for successful operation in the dependent mode.

Spinet Release Interval. The user enters a release interval which, multiplied by the number of discrete spinets to be released, defines the duration of the release.

4.5 SHORELINE DEFINITION PARAMETERS

Beach Interaction Parameters. COZOIL contains a number of parameters which affect the rates of oil incorporation and release from various sediment types. The parameters over which the user has direct control are:

- 1) Partitioning of oil removed from the beach surface by waves.
- 2) Specific yield.
- 3) Porosity.
- 4) Carbon fraction.
- 5) Adsorbed/water-accommodated partition coefficient.

Definition of Coastal Reaches. When first setting up a problem, it is recommended that a preliminary interactive run be performed for the sole purpose of establishing a data file for coastal reach definitions. Since the number of individual entries required may be relatively large, errors will often need to be identified and corrected. This process is best kept separate from actual simulations of oil spills. After entering 'T' (for "terminal") in response to the first query, enter '1' followed by "return" about 20 times. This will bring the program past all subsequent queries until the request for a reach definition file. At this point, the user instructs the model to allow entry of reach parameters from the terminal. COZOIL then leads the user through the process of reach definition.

Saving Reach Definition Files. The answer to this question should be 'Y' if the reaches have just been defined, or any of the reach parameters have been altered. Otherwise, the answer should be "N" to avoid creating a series of redundant files.

4.6 NEARSHORE PROCESS DATA SETS

Wind Data Sets. A wind data set can be created by a preliminary run of COZOIL, and stored in a file for subsequent model runs. If the stochastic option is invoked, the model will request mean wind speed and mean direction and standard deviation. A stochastic time-series is then created by the model. Wind speed is assumed to follow a Poisson distribution: wind direction is assumed to be normally distributed.

Tidal Data Sets. Given velocity amplitude and tidal period, COZOIL can create an approximate tidal data set based on the assumption that the flow is parallel to the mean coastal direction. COZOIL can also be directed to use tidal velocity data sets created by earlier runs of the model, or by an external hydrodynamic model. Note that in the latter case, the hydrodynamic output must be properly resolved onto the COZOIL model grid.

Wind-driven Data Sets. COZOIL incorporates a simple wind-driven current model which can be invoked by selection of this option. Alternatively, COZOIL will use a data set prepared by an external hydrodynamic model. Declining this election or entering a file name of "NONE" will allow the model to run without wind-driven effects in the water column.

Wave Data Set Options. The user can elect to have waves computed from the wind record, to create a new wave data set, or to access a data set created earlier by this or another wave generation model.

Inclusion of Wave-Diffraction Effects. If the user chooses to include wave-diffraction effects, the model will run noticeably slower for most applications. However, the inclusion of diffraction effects appears to give more realistic and consistent results. It is therefore suggested that diffraction effects be neglected while preliminary model tests for a new application are being performed, with diffraction included for final simulations.

4.7 OTHER MODEL FEATURES

Initial Location of Spinets Entering the Model. In stand-alone mode, the user must locate the spill source (inside the model domain) in kilometers to the right (east) and up (north) from the lower left corner of the gridded model domain. The location is shown by an asterisk on the first study area map following the mass-balance information at time 0, thus allowing the user to verify that the input location is correct. If the model computes that the input distances place the spill site on shore, the model will write a message to this effect to the screen, and stop.

Resolution of Coastal Mass Output Histogram. The model creates a histogram showing the distribution of oil along the coast by coastal cell. At default, the histogram is scaled by the total mass to be spilled. Thus if all the spilled mass were to come ashore at one coastal cell, the model would draw a maximum length "line" (row of 60 asterisks) beside that coastal cell number in the histogram. The discrete nature of the display then dictates that all coastal cells with more than zero mass but less than 1/60th of the total mass will show only one asterisk. If a spill is of long duration, it is probable that the mass will be widely distributed along the coast. In this case, the resolution of the histogram can be increased by reducing the maximum fraction of the total mass which is expected to appear on any one coastal cell. Some experimentation will reveal a reasonable level of reduction for each case.

Emulsification Parameters. Both the limiting fraction of water-in-oil and the de-emulsification (de-watering) half-life parameters are user-adjustable. The model displays its default values, allowing the user the option of changing them. If, for example, it is known that a particular oil forms a very stable emulsion with water, then the user may wish to increase the de-watering half life accordingly.

5.0 RESULTS OF ANALYSIS OF MODEL ACCURACY

5.1 MODEL TESTS: WAVES OFF PORT HEIDEN, ALASKA

The wave-refraction, shoaling, and breaking components of COZOIL were evaluated by comparison with field observations taken along the southern shore of Bristol Bay during August and September 1986. It should be noted that the original version of this section of the code has also been tested by the originators (Ebersole et al., 1986). Three sets of field data were selected for test purposes--August 12-20 (case III), August 22-29 (case II), and September 6-10 (case I). Due to the loss of the wave gauge during the field study, the study team has been forced to hindcast the offshore waves necessary as input to CO ZOIL. Although observational data are available for periods other than those listed above, they occur during transient weather events that introduced additional uncertainties into the wave hindcast results. The time periods selected therefore represent the most reliable data for model testing.

Table 5.1 shows the model input parameters used to specify the coastal topography of the study area (Fig. 5.1). All reaches are sand, with an evenly sloping bottom which reaches a depth of 6 m below mean low water (MLW) at a distance of 2 km offshore. The test cases were run on a 40x40 grid system, giving a grid size of 260 m east-west (approximate onshore-offshore) and 460 m north-south (along-shore). The digital land/water grid is shown in Figure 5.2. Here, "O" designates a cell which is below MLW; '99' designates a cell on dry land; a positive integer identifies a coastal cell associated with a specific reach; a negative integer identifies the adjacent water cell. The boundary between a negative and a positive cell is the MLW line. The depth grid is shown in Figure 5.3. The depths are in meters, rounded to the nearest whole. Negative values identify land cells.

Results of model tests are shown in Tables 5.2, 5.3, and 5.4 for test cases I, II, and III respectively. In several situations, specifically at low tidal levels with relatively large (>1 m) waves at the offshore boundary, waves begin to break several grid cells offshore in the model. A wave which experiences successive breaking events as it approaches shore goes through a series of transformations, from higher to lower heights. In these cases, Tables 5.2 through 5.4 contain the wave heights one grid cell (260 m) offshore, since reported heights reflect observations with wave staffs out in the surf zone, rather than wave heights at the beach face. These latter heights would in general be much smaller.

TABLE 5.1. Model parameters for shoreline reaches at Port Heiden.

Segment	Station	Length (m)	Degrees from North	Backshore (m)	Backshore Slope	Foreshore (m)	Foreshore Slope
1	1	1500	13.3	38.4	0.028	128.4	0.048
2	2	1050	339.2	23.8	-0.015	161.0	0.040
3	3	800	217.2	1.0		110.1	0.048
4	4	1200	360.0	118.9	0.001	265.2	0.024
5	5	1250	5.2	47.9	0.007	332.3	0.022
6	6	1200	3.4	12.5	0.070	221.0	0.030
7	7	950	21.0	1.0		190.2	0.034
8	8	950	21.0	17.7	0.048	222.9	0.034
9	10	1450	24.0	38.1	0.027	179.3	0.042
10	16	1150	20.3	64.3	-0.016	232.0	0.029
11	17	2150	21.0	26.2	0.042	173.8	0.034
12	18	4100	33.0	12.8	0.016	191.2	0.034

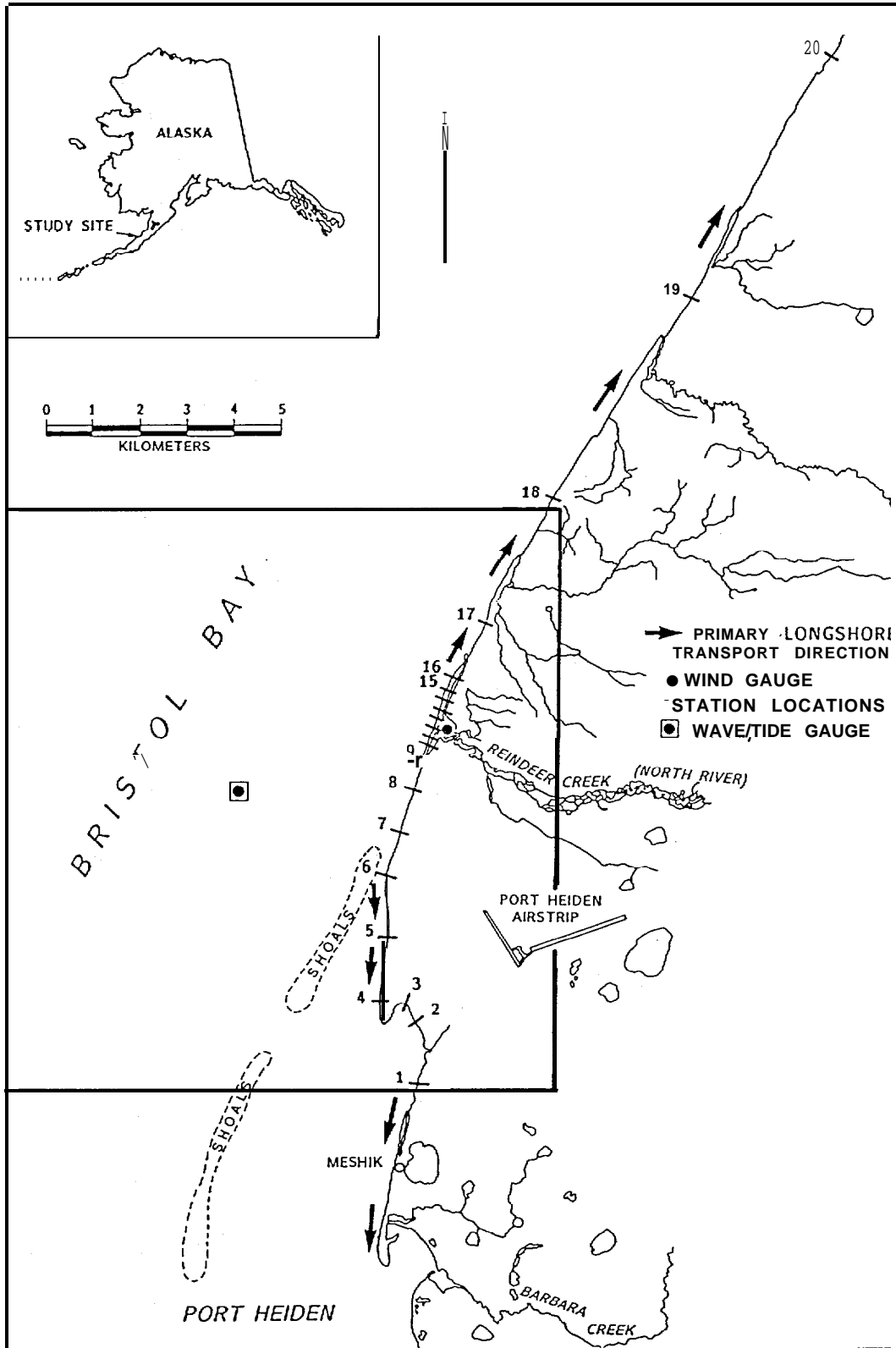


FIGURE 5.1. Study area for wave hindcast model tests.

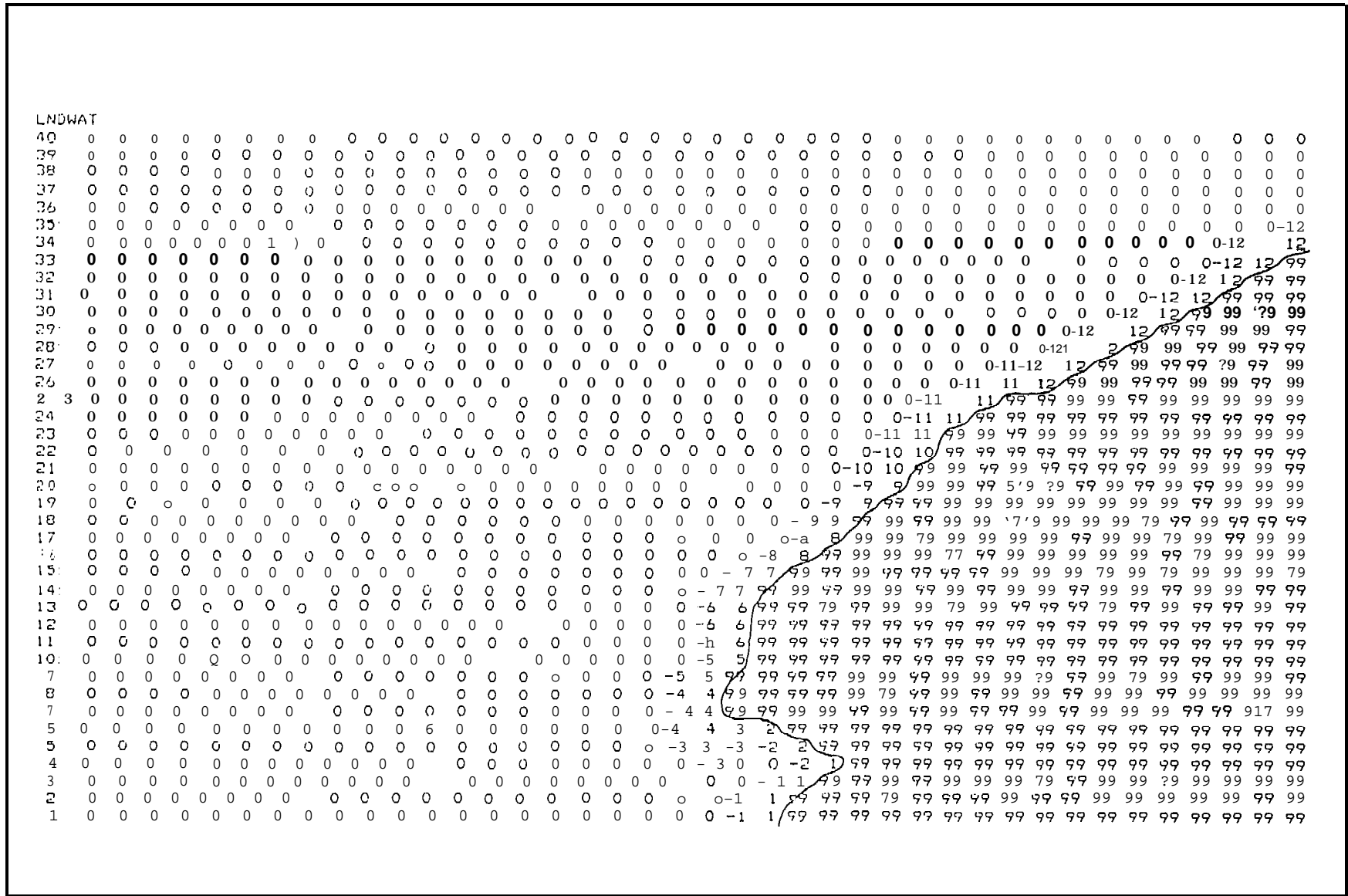


FIGURE 5.2. Digital land/water grid ('O' indicates water: '99' indicates land). The MLW line occurs at the boundary between positive (coastal/dry) and negative (coastal/wet) cells. Sequential numbers near "shoreline" refer to compartments.

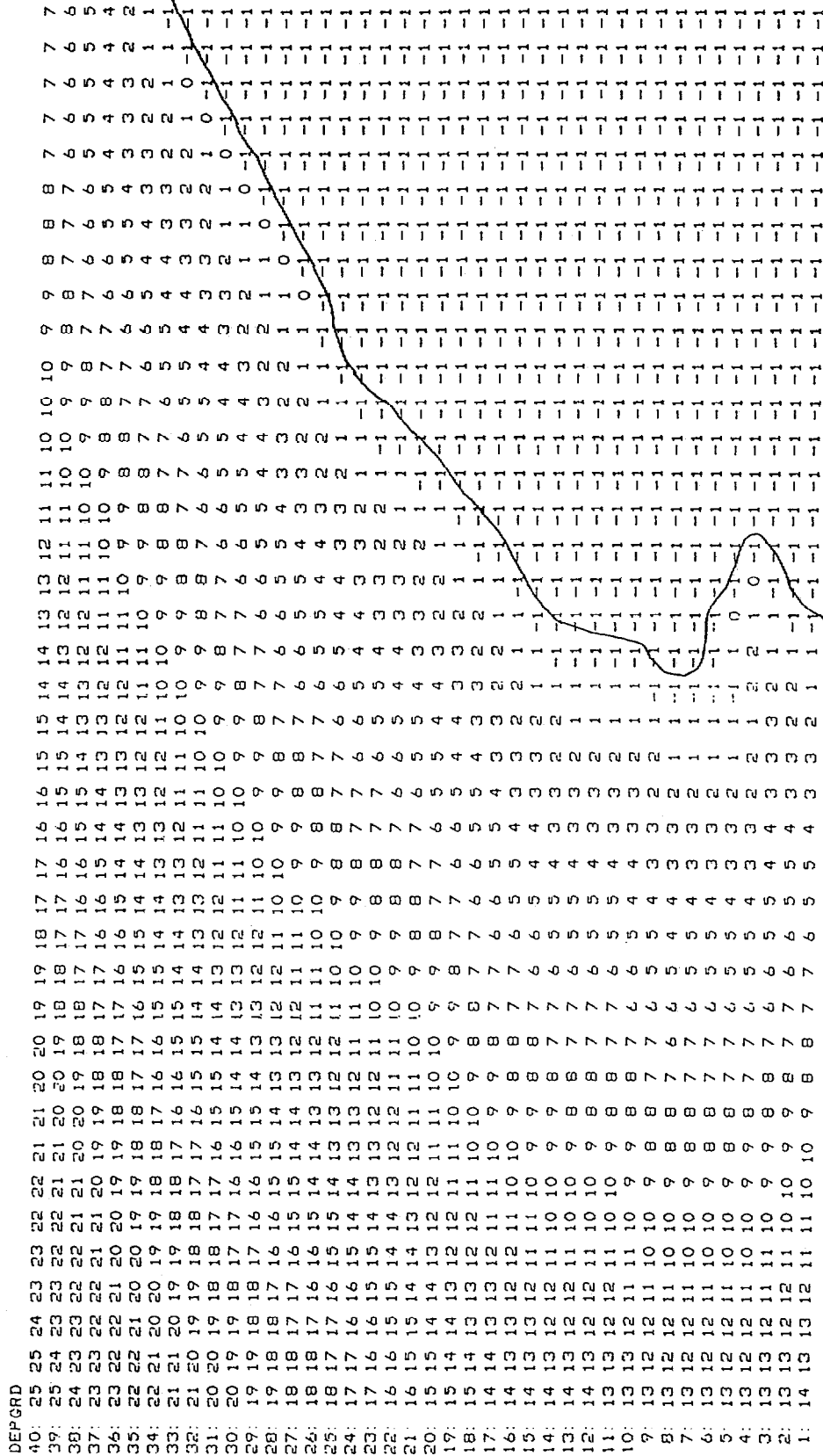


FIGURE 5.3. Digital depth grid. Depths shown are rounded to meters below MLW ('-1' indicates land cells).

TABLE 5.2. Comparison of modeled and observed breaking-wave heights and angles for case 1 (September 6-10, 1986). [Model output from reach 10]

*Estimated value.
**waves breaking more than one grid cell (260 m) offshore. Onshore wave heights are 0.2-0.4 meters.

Date	Time	Model Input			Tidal Height (m)	Model Output		Observations	
		Hs (m)	T _s (s)	β ("T)		' b (m)	' b (")	' b (m)	' b (°)
Sept 6	1500	0.82	8.0	80	2.2	0.9	10	0.6	18
	2100	0.85	8.0*	110	1.2	1.1	-3	0.7	14
Sept 7	0300	0.82	7.2	140	1.2	1.1	-6	1.3	0
	0900	1.01	6.8	120	1.2	0.9	0	1.8	0
Sept 8	0900	2.19	6.0	120	0.3	0.8**	-8	1.2	0
Sept 9	0900	1.28	6.0	110	0.0	0.8**	-3	1.1	0
Sept 10	0900	1.55	6.9	100	-0.3	0.8**	0	1.0	0

TABLE 5.3. Comparison of modeled and observed breaking wave heights and angles for test case 2 (August 22-29, 1986).

● Estimated value.
** Waves breaking more than one grid cell (260 m) offshore. Onshore wave heights are 0.4-0.4 meters.

Date	Time	Model Input			Tidal Height (m)	Model Output		Observations	
		Hs (m)	T _s (s)	β (*T)		' b (m)	' b (°)	' b (m)	' b (")
Aug 22	1600	5.6	11.0*	90	0.6	1.1**	8	1.0	10
Aug 23	1210	5.0*	11.0	90	1.2	1.3**	10	1.5	15
Aug 24	1400	1.8	7.0	70	1.8	1.8	13	1.3	15*
Aug 25	1400	1.8	8.0	70	0.6	0.6	5	0.5	0
Aug 26	1445	1.0	9.0	70	0.6	1.1**	5	0.9	3
	1915	1.0	7.0	90	2.8	1.0	10	0.5	8
Aug 27	1530	2.1	6.0	90	0.3	1.0**	3	0.75	3
Aug 28	1930	1.6	6.5	80	2.3	1.6	13	1.0	5
Aug 29	1330	1.1	5.0	70	0.3	0.4	10	0.2	3

TABLE 5.4. Comparison of modeled and observed breaking wave heights and angles for test case 3 (August 12-20, 1986).

*Estimated value.

**Waves breaking more than one grid cell (260 m) offshore. Onshore wave heights are 0.1-0.9 meters.

Date	Time	Model Input			Tidal Height (m)	Model Output		Observations	
		H _s (m)	T _s (s)	β ("T)		' b (m)	^a (°)	' b (m)	R (°)
Aug 12	1500	1.4	5.3	70	0.8	1.3**	10	1.4	25
Aug 13	1400	1.6	5.5	80	0.0	1.5	6	0.8	10
Aug 14	1300	1.9	7.0	80	-0.8	1.4**	9	1.2	10
	2100	2.2	7.5	80	3.8	2.1	16	2.3	15
Aug 15	1430	0.9	8.0	125	-0.9	1.1**	1	1.1	0*
Aug 16	2100	1.7	8.0	85	2.5	1.8	10	1.0	-5
Aug 17	1600	1.3	5.8	110	-1.2	0.6**	2	0.5	0
Aug 18	1750	0.8	5.0	110	-0.6	0.7**	1	0.4	0
Aug 19	2000	0.9	7.0	115	-0.8	1.1**	2	1.2	0
Aug 20	2030	1.1	5.5	120	0.0	1.2**	-6	1.3	-5

Tables 5.5 and 5.6 give statistical summaries of the comparisons between observed breaker heights and angles and those computed by the model. Case I shows a consistent bias between the observed and modeled wave angles, with the modeled angles being an average of 6° more southerly than those observed. Since no such systematic errors occur in the other two cases, we infer that the problem is associated with the hindcast methodology. The average error over all three cases is about 1° to the south. The standard deviation around the mean is 6.6°. To the extent that we can rely on the hindcast waves as inputs, we can expect the model to be within 6.6° of the observations 68 percent of the time.

Summary statistical comparisons of wave height are shown in Table 5.6. The overall mean error is 10 cm. Although one could infer that the model tends to overpredict wave heights, 10 cm is probably well within the uncertainty limits of the wave hindcast results and the observational accuracy.

TABLE 5.5. Statistical summary of model test results for wave angle.

Case	Number of Comparisons	Mean Absolute Error (*)	Mean Error (°)	σ_{n-1}
1	7	6.0	-6.0	5.9
2	9	3.7	1.7	4.4
3	10	4.3	-0.01	7.3
OVERALL	26	4.6	-1.0	6.6

$$\text{Absolute Sum of Errors} = \sum_{i=1}^n |x_{i,\text{mod}} - x_{i,\text{obs}}|$$

$$\text{Mean Absolute Error} = 1/n \sum_{i=1}^n |x_{i,\text{mod}} - x_{i,\text{obs}}|$$

$$\text{Mean Error} = 1/n \sum_{i=1}^n [x_{i,\text{mod}} - x_{i,\text{obs}}]$$

TABLE 5.6. Statistical summary of model test results for wave height.

Case	Number of Comparisons	Mean Absolute Error (°)	Mean Error (°)	σ_{n-1}
1	7	0.2	-0.2	0.4
2	9	0.3	0.3	0.3
3	10	0.3	0.2	0.3
OVERALL	26	0.3	0.1	0.3

There is also uncertainty as to where in the model grid one should compare model output with the observations. when wave breaking occurs in several offshore grid cells. As an example, Figure 5.4 shows the model wave breaking matrix for the input conditions of September 8, 0900 (case 1, Table 5.2). In Figure 5.4, 'O*' indicates no breaking; '11' indicates breaking; and '99' is a land cell. The heavy line indicates MLW along reach 10, where the observations were recorded. Wave breaking is initiated in four grid cells. or over a kilometer offshore. Figure 5.5. which gives wave height as a function of grid cell, shows waves shoaling up to 2.3-2.4 m before breaking for the first time at a depth of about 3 m. Subsequent breaking events reduce wave heights at the beach to about 0.5 m. Observations were made about 100 m into the surf zone, but very local topographic variabilities (e.g., presence of an offshore bar) were not reflected in the model: bathymetry can also bias the results.

The mean wave height for the three cases is about 1 m. The standard deviation overall of 0.3 m can be interpreted to mean that 68 percent of the time-modeled wave heights will fall within 30 percent of actual values.

5.2 SENSITIVITY ANALYSIS

5.2.1 Spreading in the Surf Zone

An equation for spreading/compression of oil slicks in the surf zone was developed as part of this project (section 2, equation 2.40). The equation balances wind stress normal to the shoreline against the gravity/viscous force to determine the rate of change of the onshore/offshore (minor) axis of the slick as a function of time. The longshore (major) axis increases according to the same rate equation used offshore. The dynamic behavior of the minor axis of a 100 m³ oil slick under the influence of various onshore wind speeds is shown in Figure 5.6 (a, b). For these test cases, the slick was initiated with a thickness of 1 cm and a radius of about 56 m. A minor axis length of 1 m was also specified. At a wind speed of 1 m/sec, the time for the onshore/offshore axis to reach this limit is about an hour, versus about 15 minutes at 4 m/sec (Fig. 5.6a). At 15 m/sec, the time to reach a 1 m minor axis length is about 4 minutes. It should be noted that these tests are independent of any other processes in the model. The surf-zone wave field associated with 15 or 20 m/sec winds, for example, would rapidly entrain surface oil into the water column, so that consideration of foreshortening rates at these higher wind speeds becomes somewhat irrelevant.

5.2.2 Penetration Rates

Penetration of oil into various sediment types is computed via Darcy's law (equation 2.43) and an equation for intrinsic permeability as a function of grain size (section 2, equation 2.44). Model tests were performed to demonstrate penetration rates as a function of sediment type and oil viscosity. Note that the penetration equations are being solved in these tests for an infinite sediment, neglecting the presence of groundwater, which is accounted for in the model. Figure 5.7a shows penetration depth as a function of time for a light diesel fuel in five sediment types. For comparison, data from a laboratory test of an equivalent viscosity oil in Canadian borrow pit sands (Holoboff and Foster, 1987) is shown. The penetration rate for sand matches the data quite well. The rates for other sediments is qualitatively as expected relative to the rate for sand.

Figure 5.7b shows the penetration depths versus time for Prudhoe Bay crude, with a viscosity about three times that of light diesel. After 12 hours, the Prudhoe Bay crude has penetrated to a depth of 1 m, versus about 3 m for the light diesel of

Figure 5.7a. Weathered Prudhoe Bay crude, with a viscosity of 350 cp, or ten times the viscosity of the fresh crude, reaches a depth of about 0.1 m after 12 hours (Fig. 5.7c). These proportionalities are consistent with the fact that the penetration rate is inversely proportional to the viscosity.

5.2.3 Retention of Oil in Groundwater System

The retention of petroleum in the beach groundwater system is governed by equations (2.51) to (2.53) described in section 2. The partitioning coefficient, K_p , is an unknown parameter in this formulation. A series of simulations was therefore performed to allow selection of the value for K_p , which results in retentive behavior of the model as shown in Figure 5.8 (a-c). The observations (Vandermeulen and Gordon, 1976; Harper et al., 1985; McLaren, 1985) suggest that oil in beach groundwater systems remains detectable for several years after introduction. We estimate from a qualitative evaluation of the information cited above that a half life for oil in a sandy or gravel beach is about six months, or three years in a mudflat. From Figure 5.8 (a-c), we therefore have adopted a value for K_p of 1,000 which the user can adjust.

The governing partitioning equation (2.52) shows that the removal rate will be equally sensitive to the fraction of the beach sediment which is composed of organic matter. This sensitivity is demonstrated for a cobble beach in Figure 5.8 (d-f). The coefficients F_c for various beach types are taken from Trask (1939), but again the user has the option to alter these default values.

5.2.4 Whole-Model Sensitivity Tests

A series of model runs was performed to demonstrate overall model behavior for various types of coastal reaches. In each case, a single uniform straight stretch of coastline 5 km in length is simulated. One thousand barrels (141 mt) of Prudhoe Bay crude oil are released in 24 spinets over 48 hours. The release point is 1 km offshore and about midway along the reach. The wind is constant at 5 m/sec, and is 10° away from being directly onshore. Other parameters for the specification of these tests are given in Tables 5.7 and 5.8. Only the reach type is changed from one test to the next.

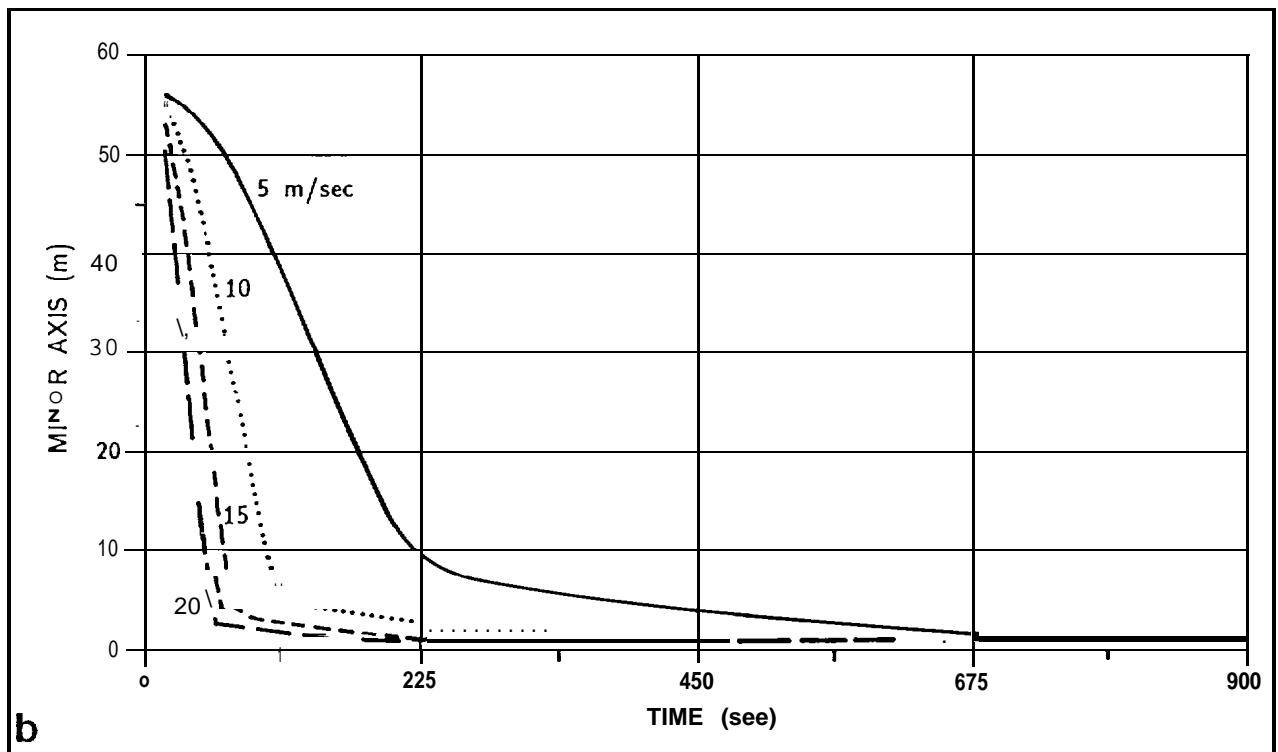
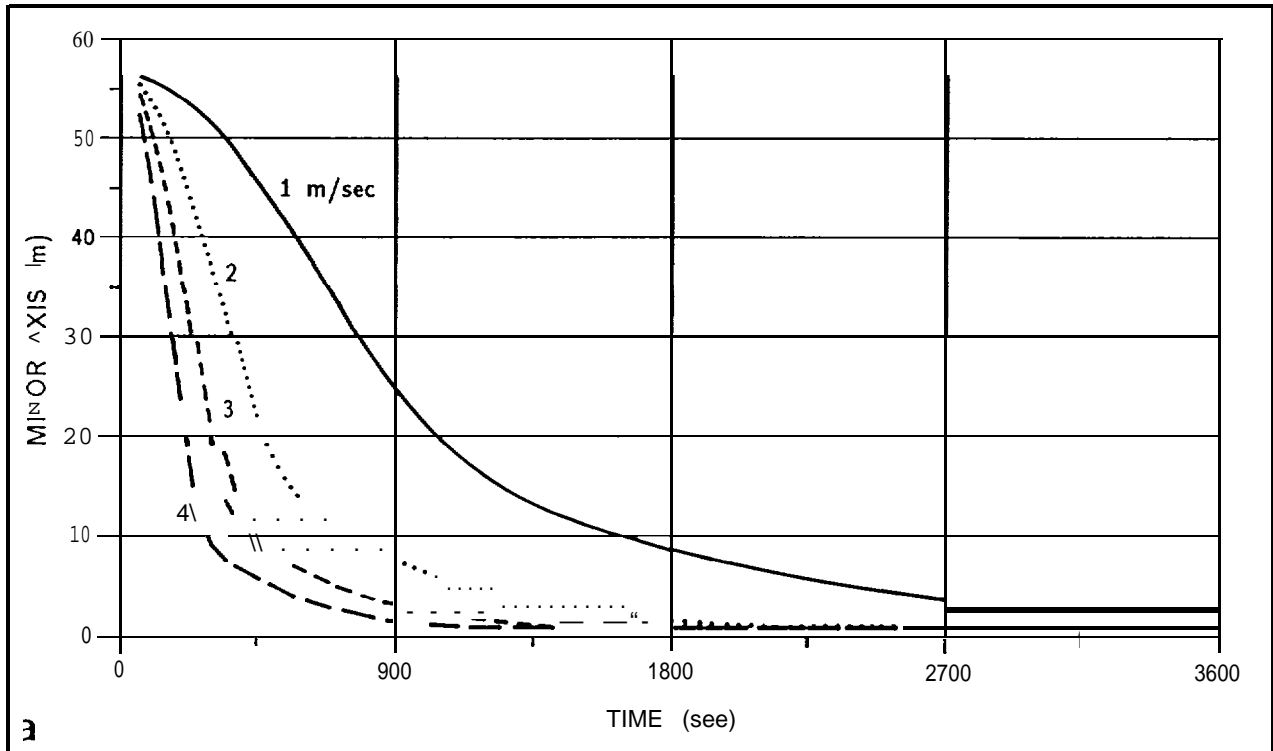


FIGURE 5.6. The dynamic behavior of the minor axis of a 100-m³ oil slick for a range of wind speeds at (a) 1-4 m/s and (b) 5-20 m/s.

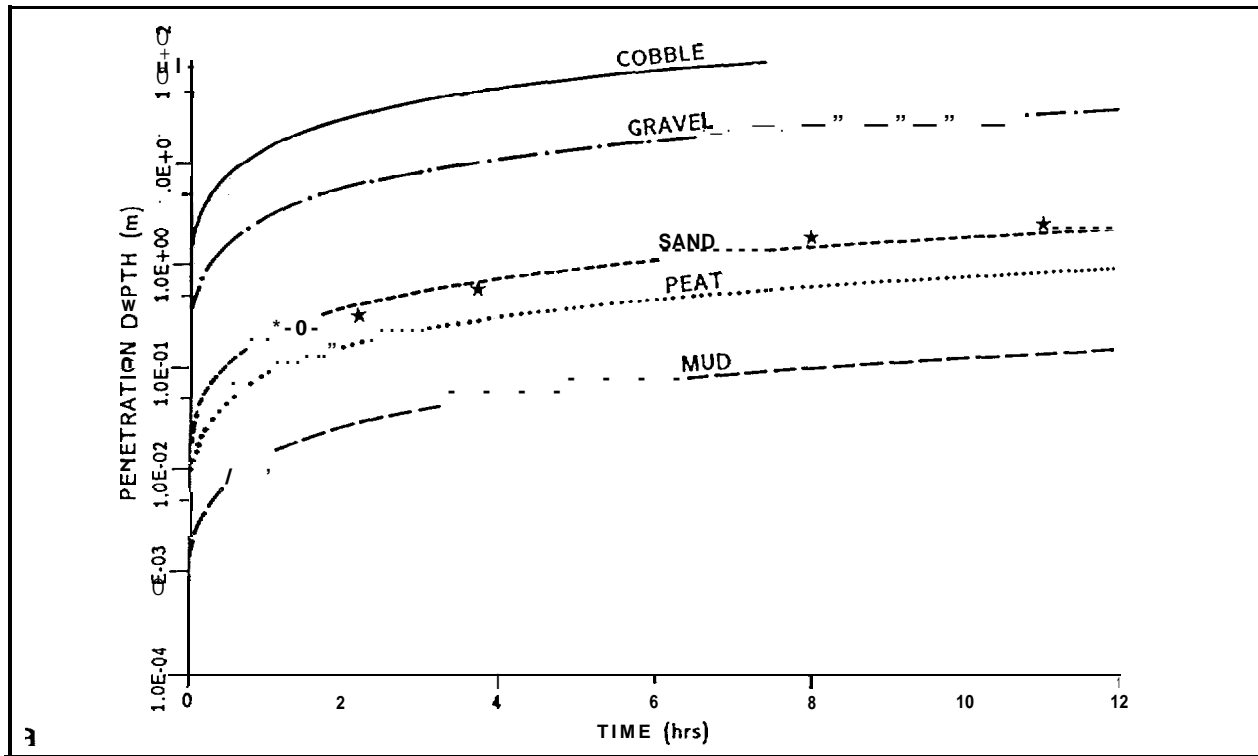


FIGURE 5.7a. Penetration depth as a function of time for diesel fuel (viscosity = 11 cp) on various sediment types. Asterisks show data from laboratory tests by Holoboff and Foster (1987).

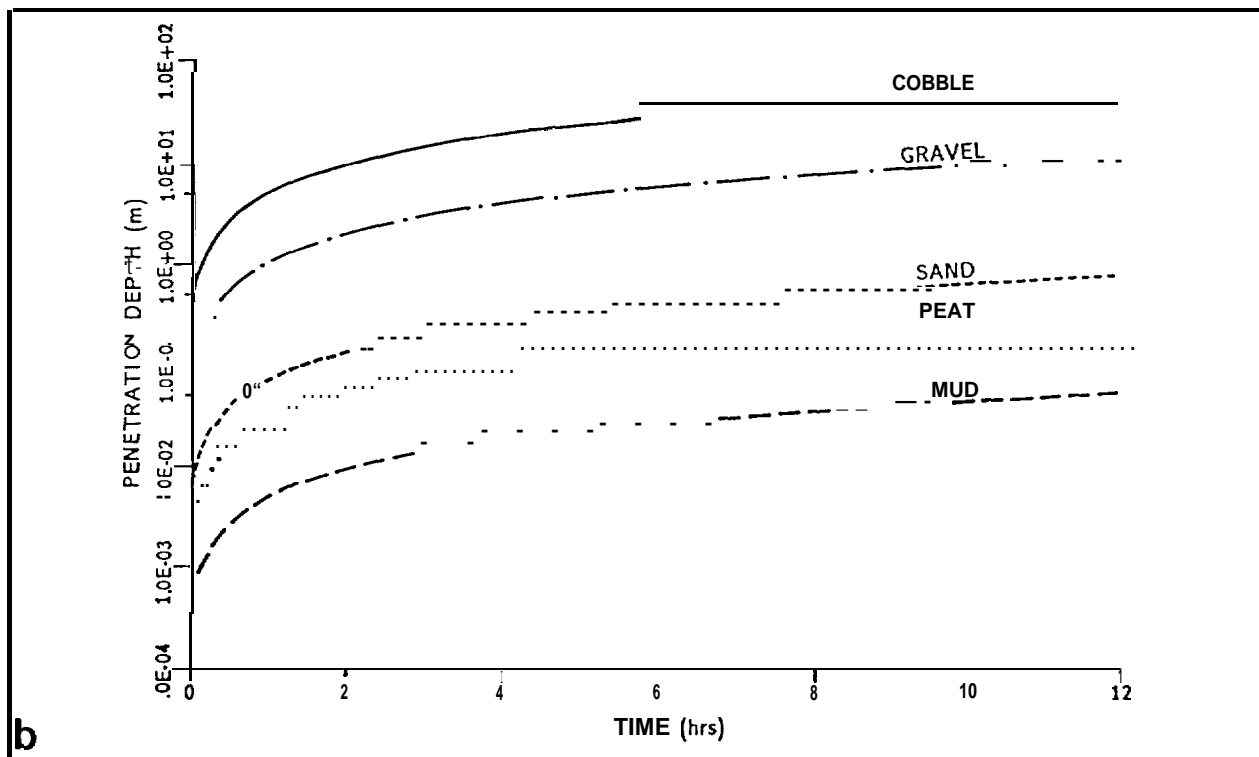


FIGURE 5.7b. Penetration depth as a function of time for fresh Prudhoe Bay oil (viscosity = 35 cp) on various sediment types.

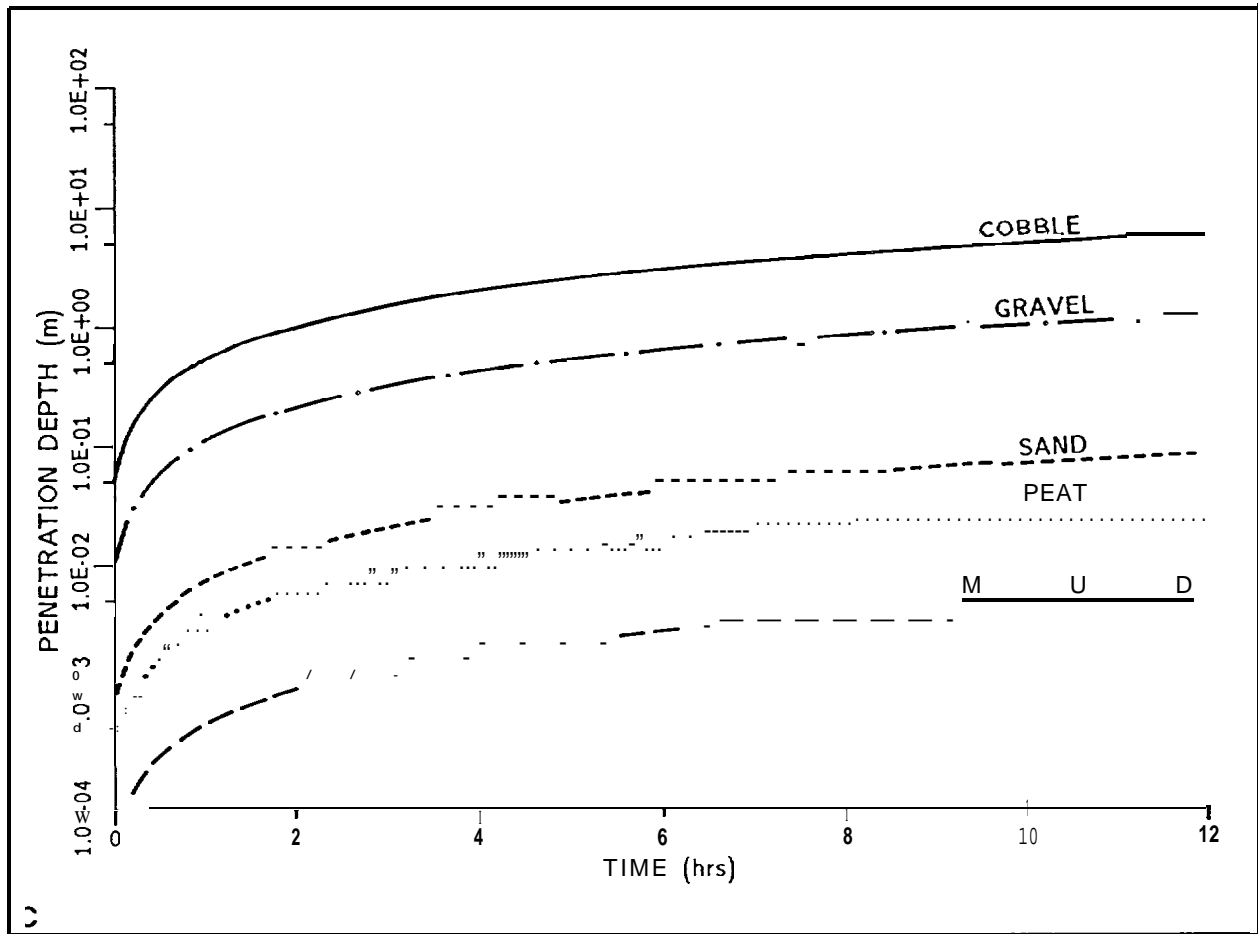


FIGURE 5.7c. Penetration depth as a function of time for weathered Prudhoe Bay crude oil (viscosity = 350 cp) on various sediment types.

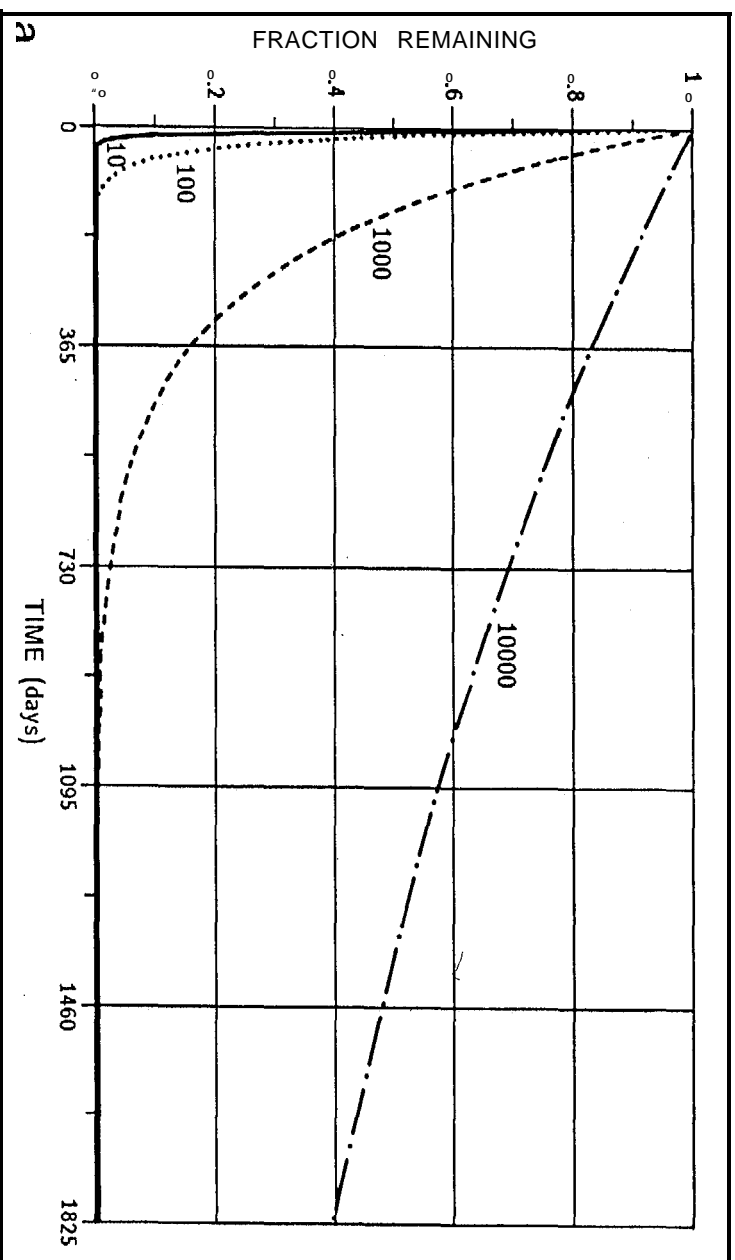


FIGURE 5.8a. Retention of oil in a sand beach for various values of the partition coefficient K_p .

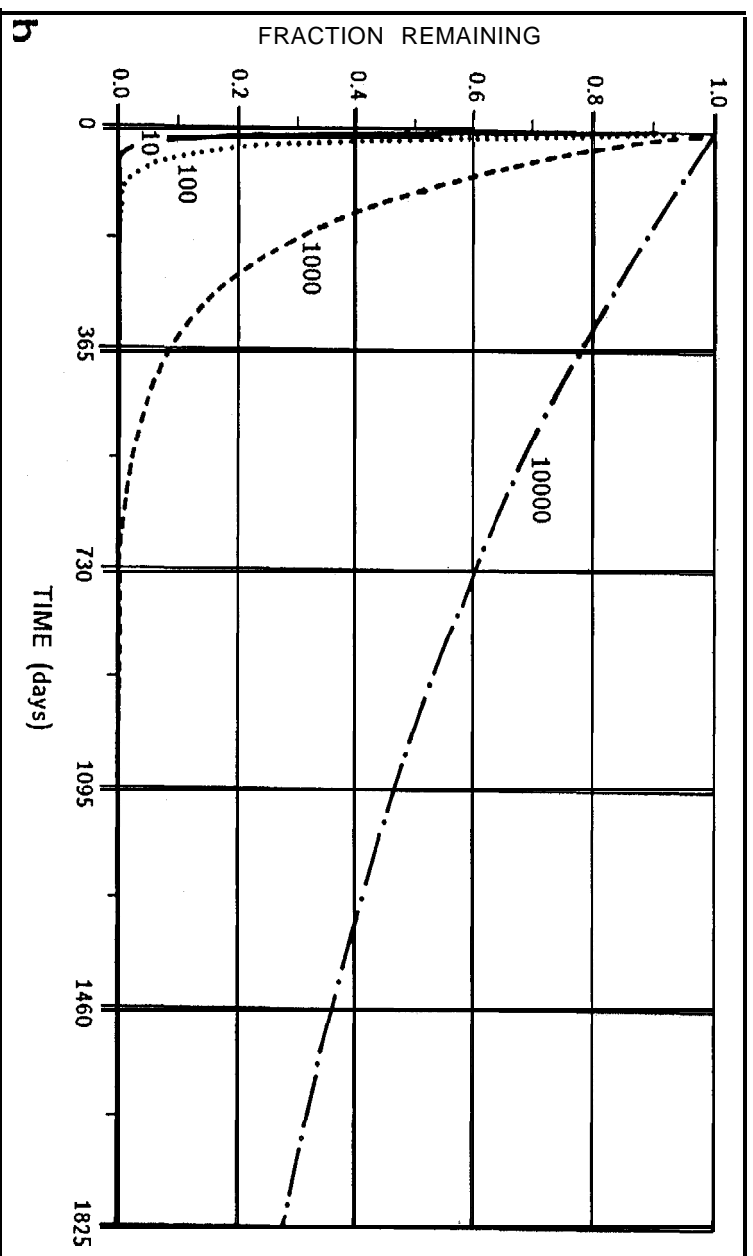


FIGURE 5.8b. Retention of oil in a gravel beach for various values of the partition coefficient K_p .

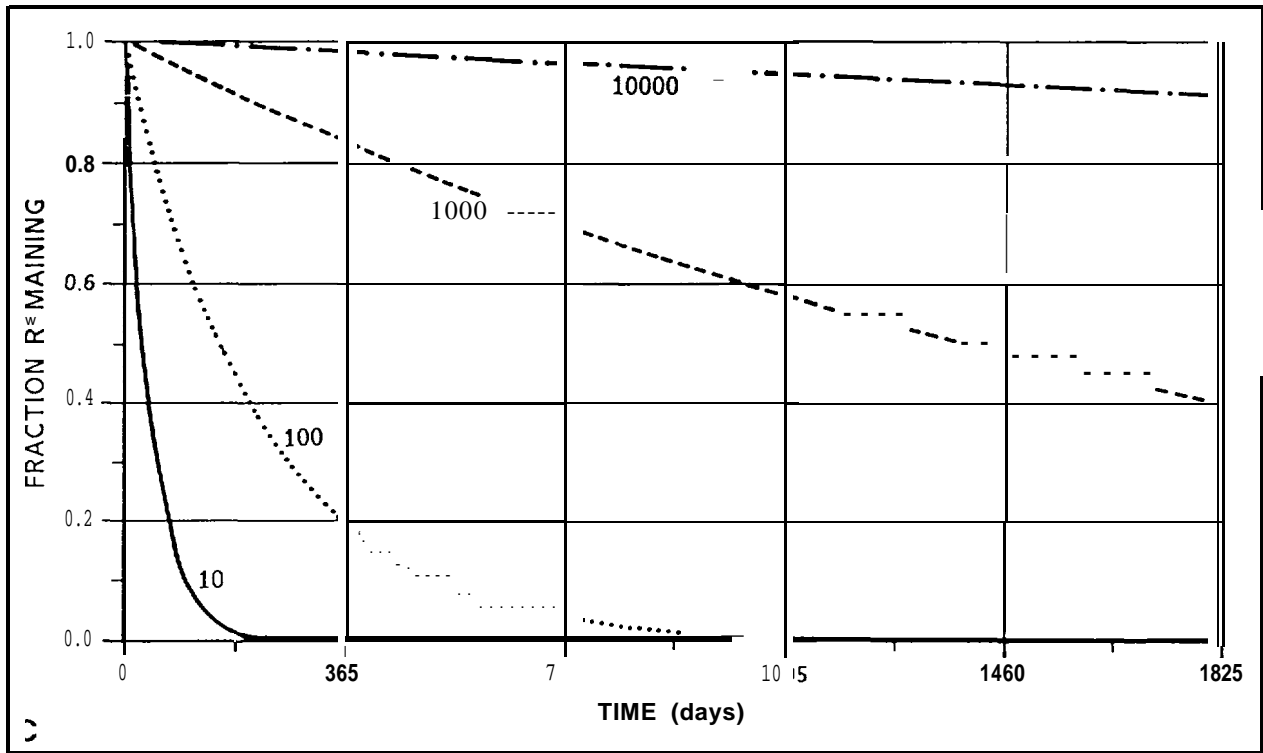


FIGURE 5.8c. Retention of oil in a tidal mud flat for various values of the partition coefficient K_p .

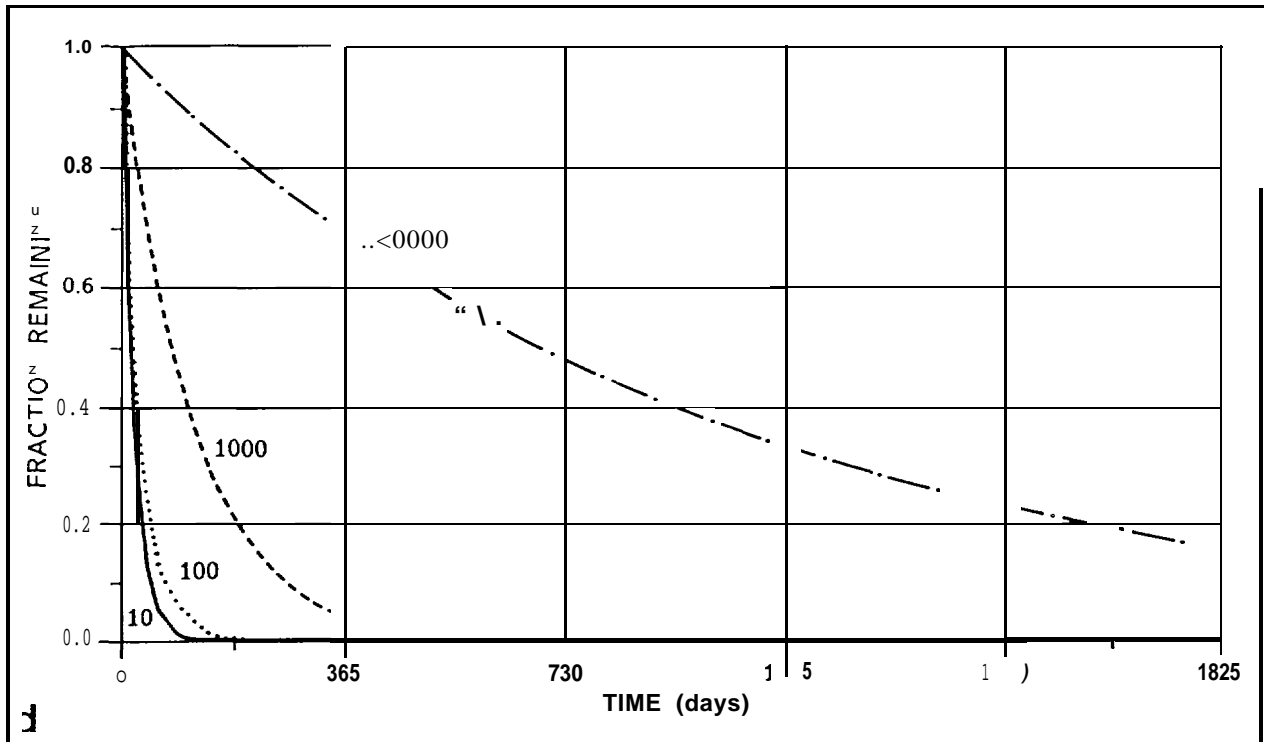


FIGURE 5.8d. Retention of oil in a cobble beach for various values of the partition coefficient K_p . The carbon fraction of the sediments is 0.005.

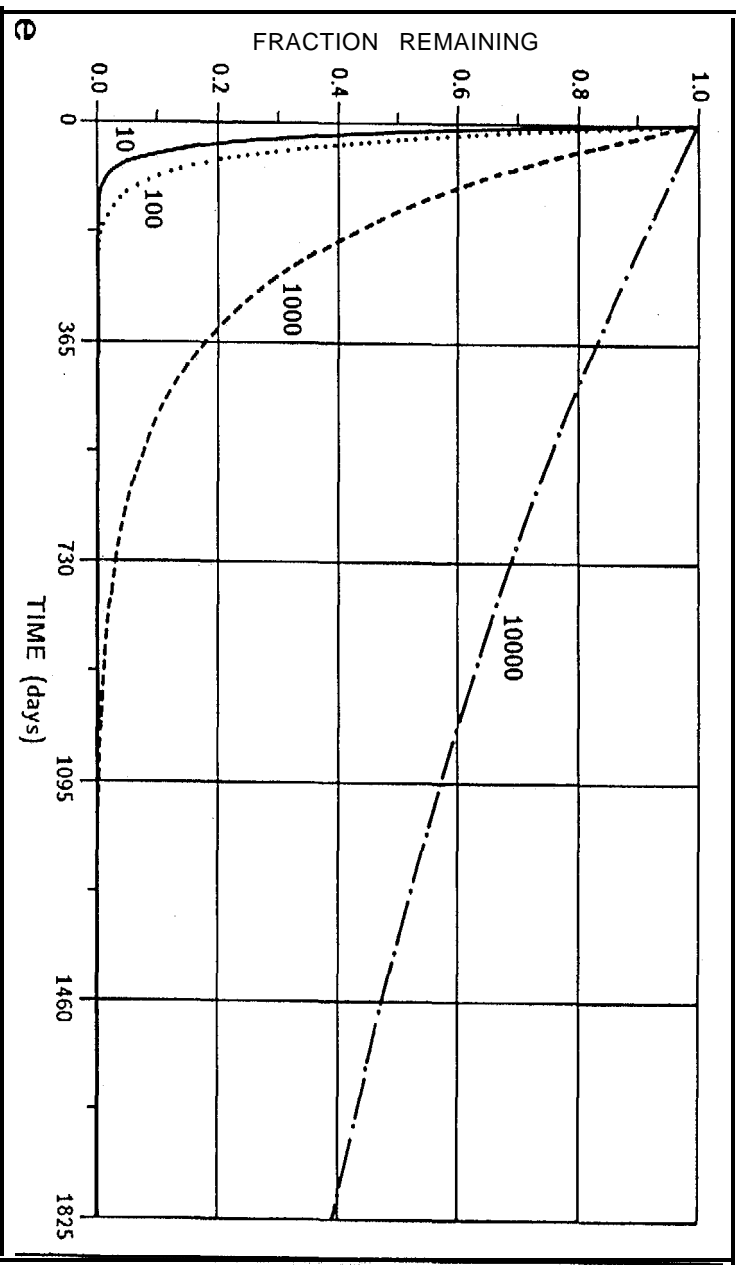


FIGURE 5.8e. Retention of oil in a cobble beach for various values of the partition coefficient K_p . The carbon fraction of the sediments is 0.01.

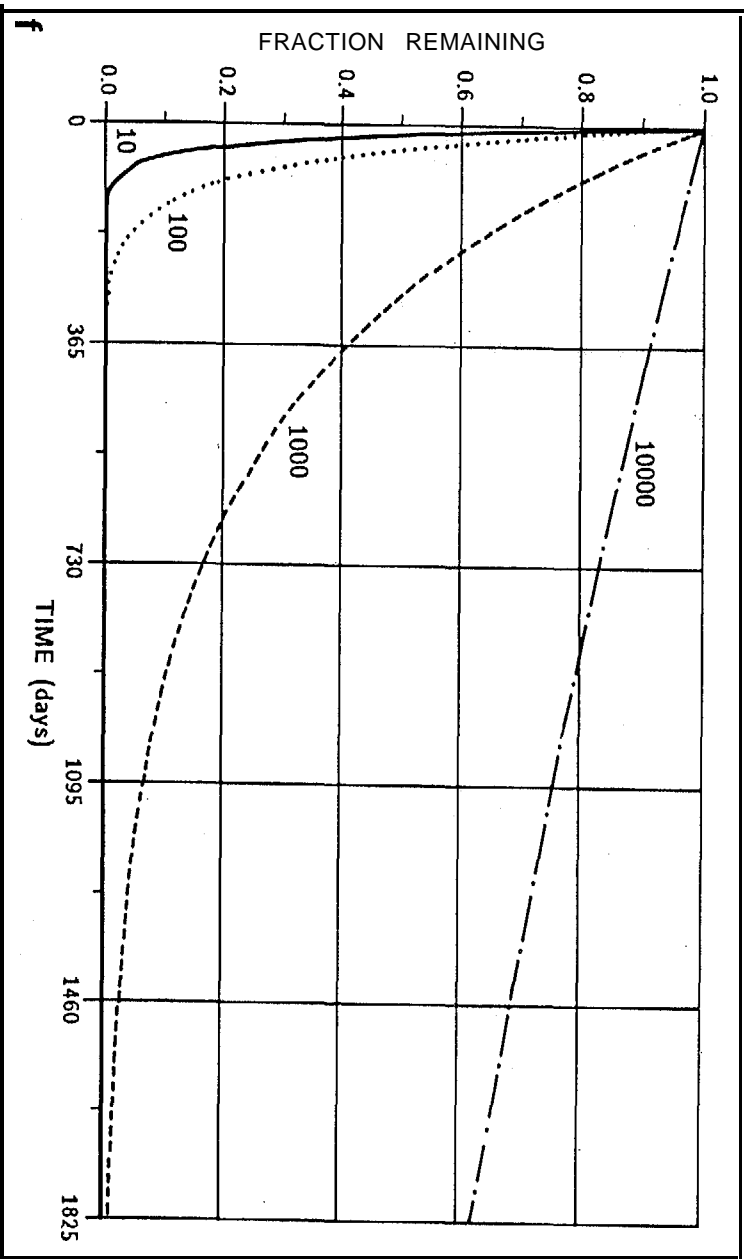


FIGURE 5.8f. Retention of oil in a cobble beach for various values of the partition coefficient K_p . The carbon fraction of the sediments is 0.02.

TABLE 5.7. COZOIL model input parameters for the single reach test cases.

a	! v = verbose: a = abbreviated output
1	! 1 - 7 for oil type
15	! # tbp cuts
87,4,15,10	! yr, m, d, hr of spill
60	! air temp degrees f
90	! # days to simulate
21600	! seconds between outputs to screen for first 24 hours
86400	! " " " " thereafter
1000	! spill size in barrels
24	! # spinets
1	! 1 = Audunson/Spaulding: 2 = Mackay entrainment
N	! no change to PARTGND, PARTSPL
N	! no change to SPECYLD, POROSTY, FCARB, KSUBP
1	! 1 = stand-alone: 2 = run with offshore model
2	! Hours between release of subsequent spinets
Y	! reach definition from predefine file (reach definition file) "
	! blank to continue 'after display of reaches
n	! no corrections
N	! not output to new reach file
2	! 2 = access old wind file (wind onshore at 5 m/sec)
Y	! make new tidal data set (tide file)
10	! max longshore tidal current (cm/sec)
12.4	! tidal period
4.0	! meters of tidal range (low to high)
0.0	! hours after mean low water for simulation start
Y	! create a new wind-driven vel data set from the wind record (wind file name)
Y	! Y = compute waves from the wind record: N = input from user
N	! N = not include wave diffraction computations
0.1, 2.0	! x, y of spinet start (km)
N	! no change in frac water-in-oil max
N	! no change in mousse de-watering e-folding time

TABLE 5.8. Reach specification parameters for single reach COZOIL model test.

Parameter	Value
Reach Length	5000 m
Backshore Width	100 m
Foreshore Width	100 m
Offshore distance	1000 m
Backshore Slope	0.01
Foreshore Slope	0.05
Offshore Depth	10 m
Orientation	0" True N

The mass balance as a function of time for oil coming ashore on a sand beach is shown in Figure 5.9 (a-d). Since the travel time from the oil release point 1 km offshore is about two hours, the release of spinets subsequent to the first is approximately balanced by previous spinets arriving at the sandy shoreline (Fig. 5.9a). This oil is compressed against the shoreline by the wind, which reduces surface area and slows evaporation rates. Oil deposited on the shore does not spread further and is also absorbed into the beach face. These factors combine to reduce the net amount of mass which will evaporate relative to the 20 percent expected for this oil in an offshore simulation. The tidal signal is clearly discernible in the trace of oil mass on the water surface; the rising tide corresponding to the increase in oil mass on the surface. The longshore currents for this test case are about 6 cm/sec due to waves, plus 2 cm/sec at the surface due to wind. The travel time from the reach midpoint to the boundary, 2.5 km, is therefore about 9 hours for oil at the surface and 12 hours for oil entrained in the surf-zone water column.

During the first 60 hours of the simulation, surface oil leaving the model domain a longshore represents the primary contribution to oil which is "outside" (Fig. 5.9a). In the longer term (e.g., 90 days, as shown in Fig. 5.9 b), the lower-level contribution from the surf zone becomes the dominant mechanism for oil removal from the study area. Figure 5.9c shows a detailed mass balance for the oil on the shore. The top trace, "Total Ashore," corresponds to the trace labeled "Ashore" in Figure 5.9a. As oil comes ashore, it rapidly penetrates the foreshore surface sediments and, thereafter, begins to enter the beach groundwater system. The "Foreshore Surface" trace in Figure 5.9c is 180° out of phase with the oil on the water surface (Fig. 5.9a), since deposition of the beach surface is the opposite of refloitation. The modeled half life of oil in the foreshore surface sediments agrees well with the 3-5 days estimated by CSE/ASA/BAT (1986). Figure 5.9d shows the same trace as Figure 5.9c, but carried out for a period of 90 days. After about 20 days, virtually all remaining oil is associated with the beach groundwater system from which removal is relatively slow, flushing to the surf zone.

Figure 5.10 shows the overall mass balance for an eroding peat scarp. Here, the oil removal rate from the groundwater system is relatively slower than that for sand (Fig. 5.9 b), since the organic content of the sediments is generally higher. The mass balance for a mudflat is shown in Figure 5.11. Here, relatively little oil is initially retained in the sediments, but release is much slower than for either sand or

peat scarp sediments. This difference is due not only to increased organic content, but also to relatively low specific yield of mud sediments during ebb tides. That oil which does penetrate these fine-grained sediments is therefore flushed out much more slowly as well. The removal rate from the gravel beach (Fig. 5.12) is higher than that for sand, due to lower organic content and more rapid flushing. The removal rate from the cobble beach (Fig. 5.13) is even faster, for the same reasons. The case for oil coming ashore on relatively smooth rock outcropping or seawalls is shown in Figure 5.14. Here, no location deposition is expected to occur, the ground water system being essentially nonexistent. In general, a COZOIL simulation will consist of multiple reaches of various lengths and types. In such cases, the model computes and retains complete, detailed mass-balance information for each reach, as shown in Figure 5.9 (a-d) for the sandy beach. Although the information is written to a set of output files, subsequent display and analysis depend on user needs and available hardware. The creation of appropriate plotting software is therefore left as an exercise for the user.

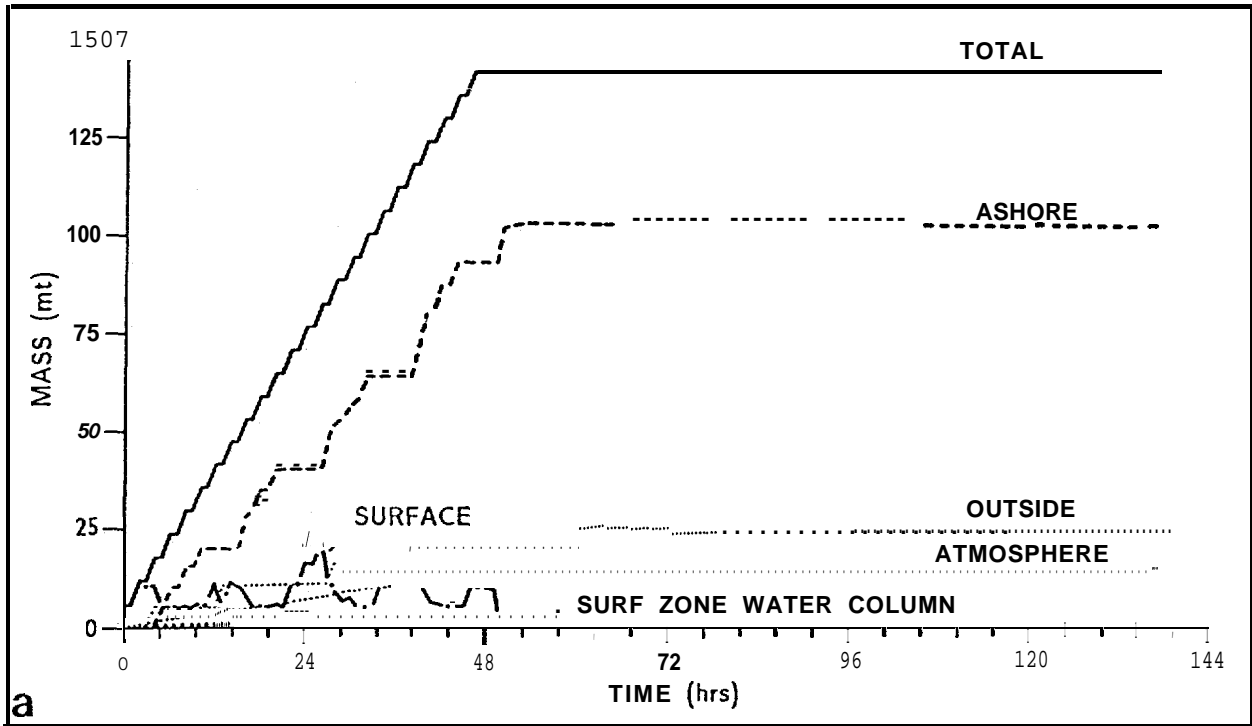


FIGURE 5.9a. Overall mass balance for Prudhoe Bay crude oil coming ashore on a sand beach (first 6 days).

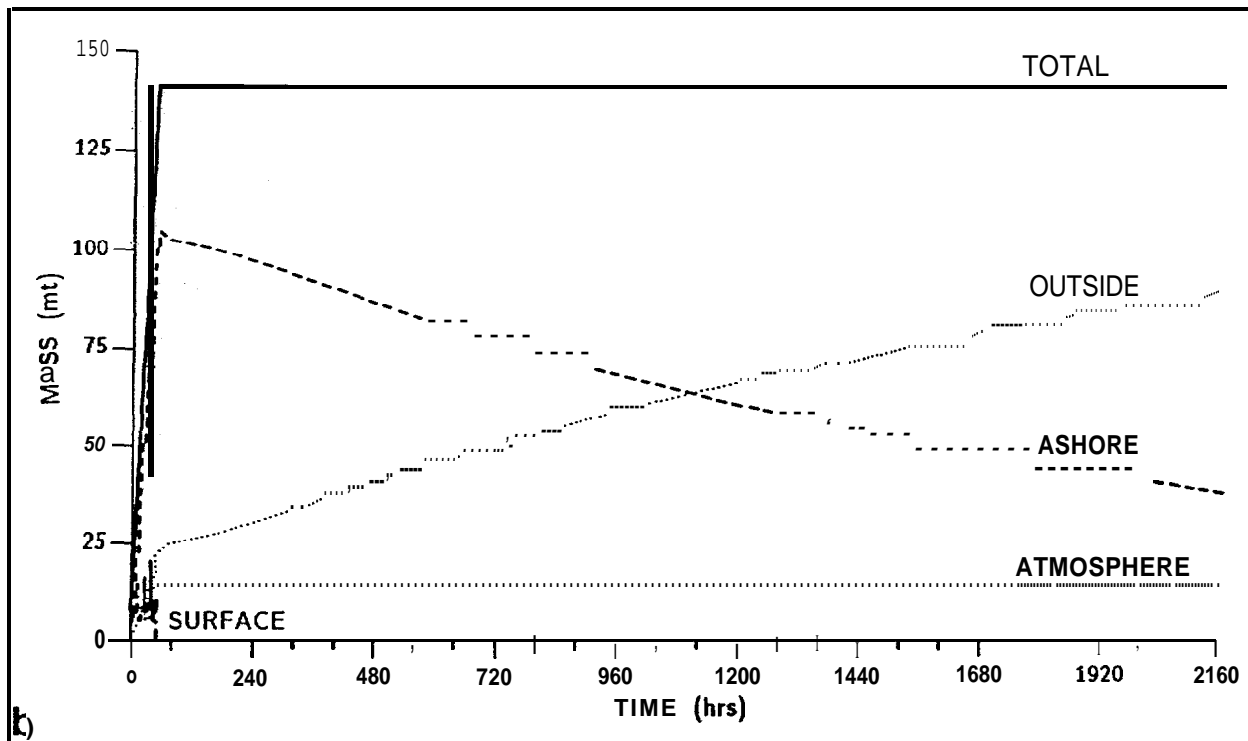


FIGURE 5.9b. Overall mass balance for Prudhoe Bay crude oil coming ashore on a sand beach (first 90 days).

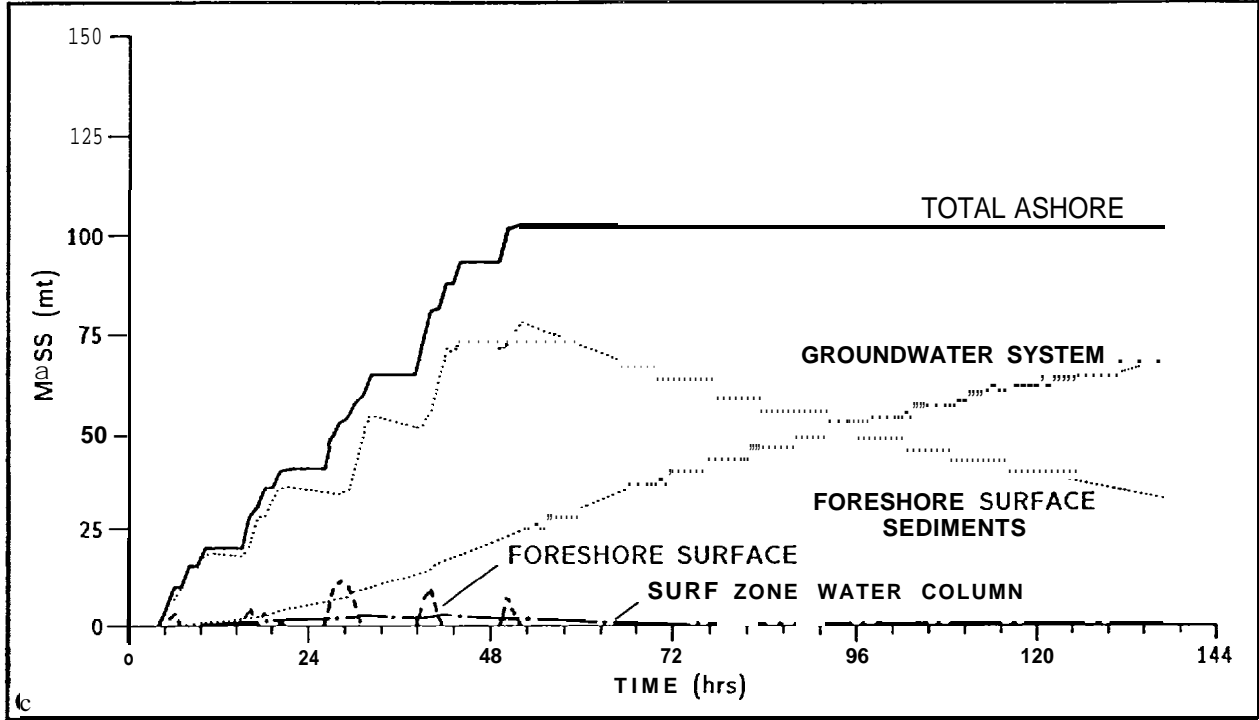


FIGURE 5.9c. Mass balance for oil associated with the coastline in Figure 5.9a.

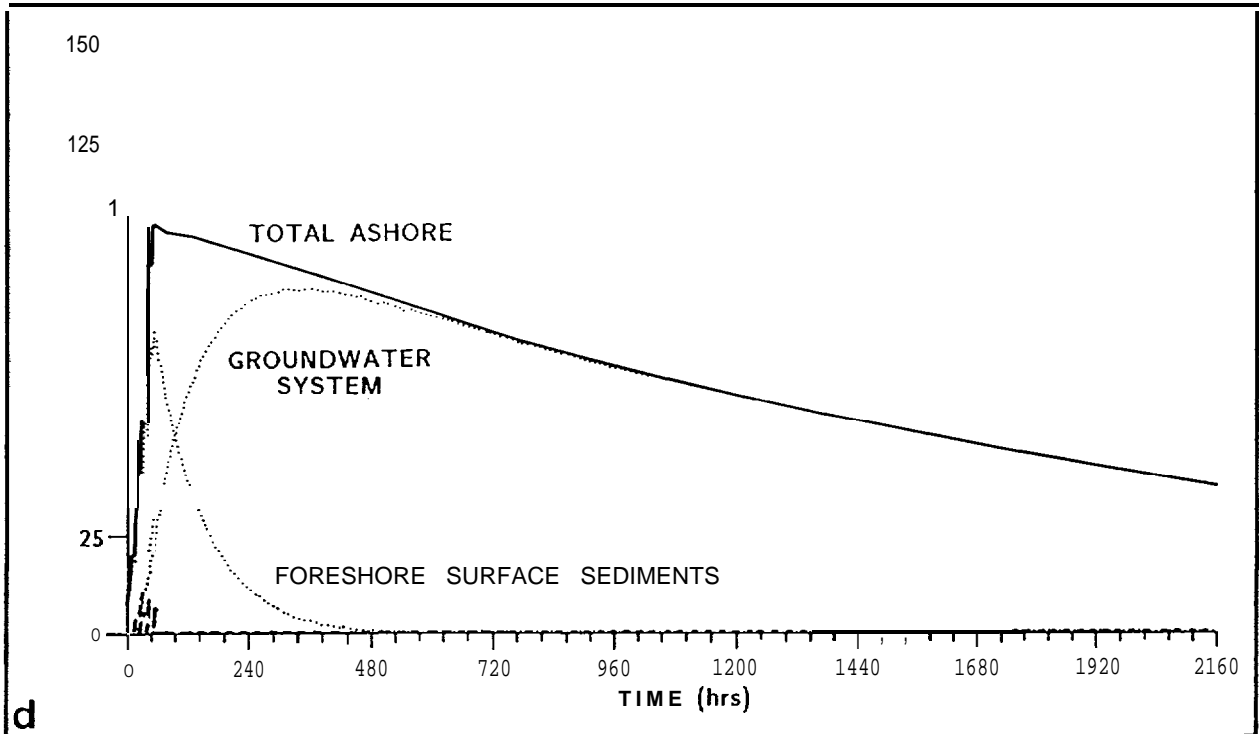


FIGURE 5.9d. Mass balance for oil associated with the coastline in Figure 5.9b.

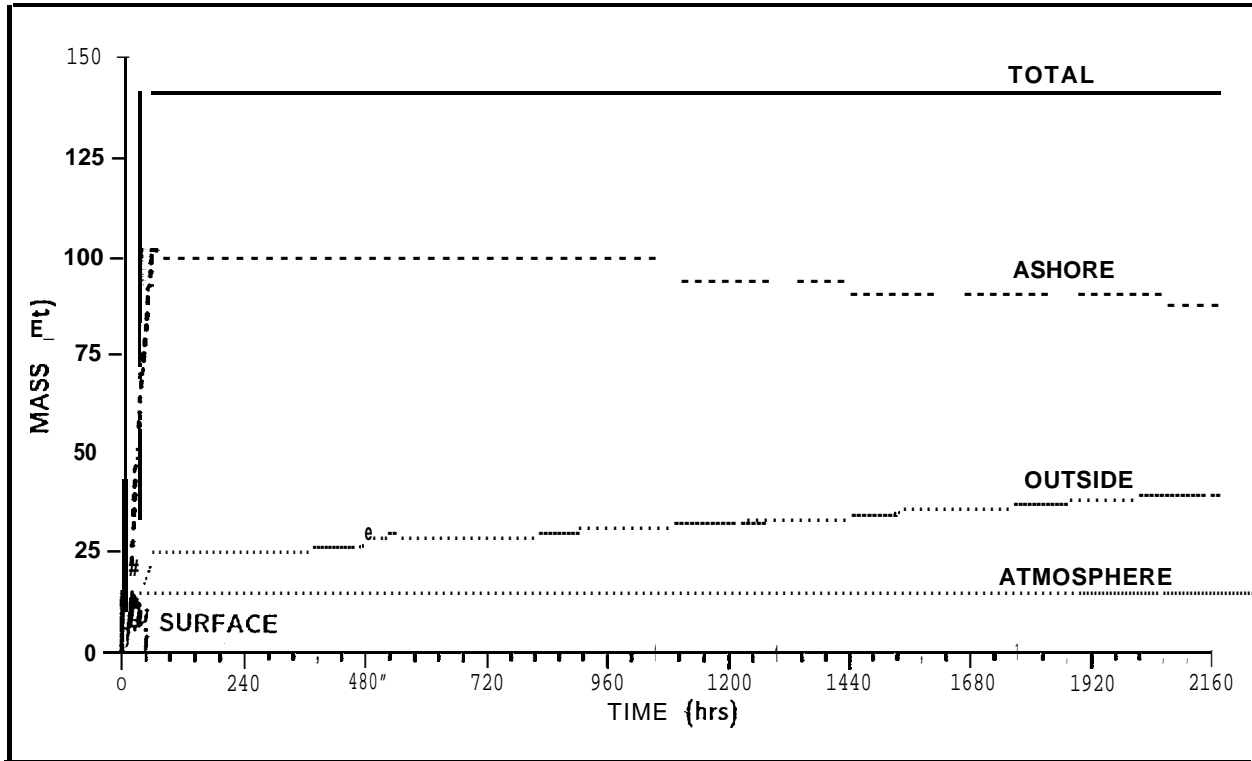


FIGURE 5.10. Overall mass balance for Prudhoe Bay crude oil coming ashore on an eroding peat scarp.

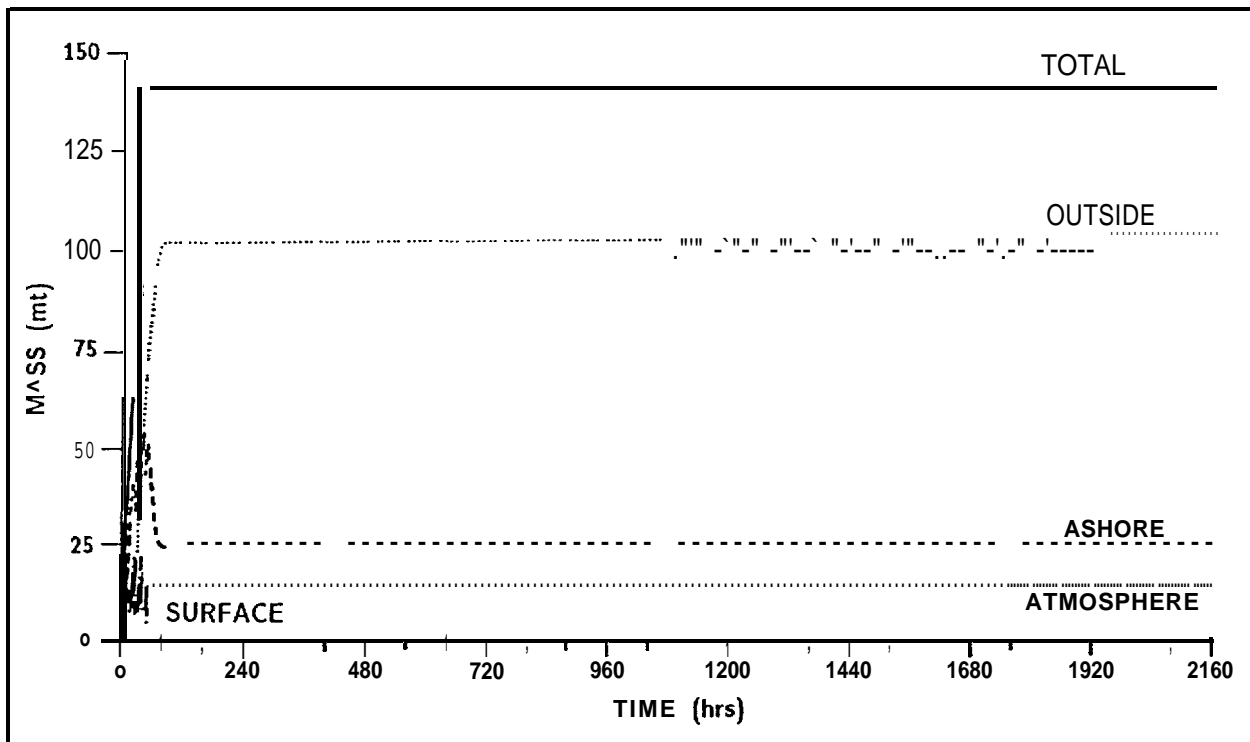


FIGURE 5.11. Overall mass balance for Prudhoe Bay crude oil coming ashore on a tidal mud flat.

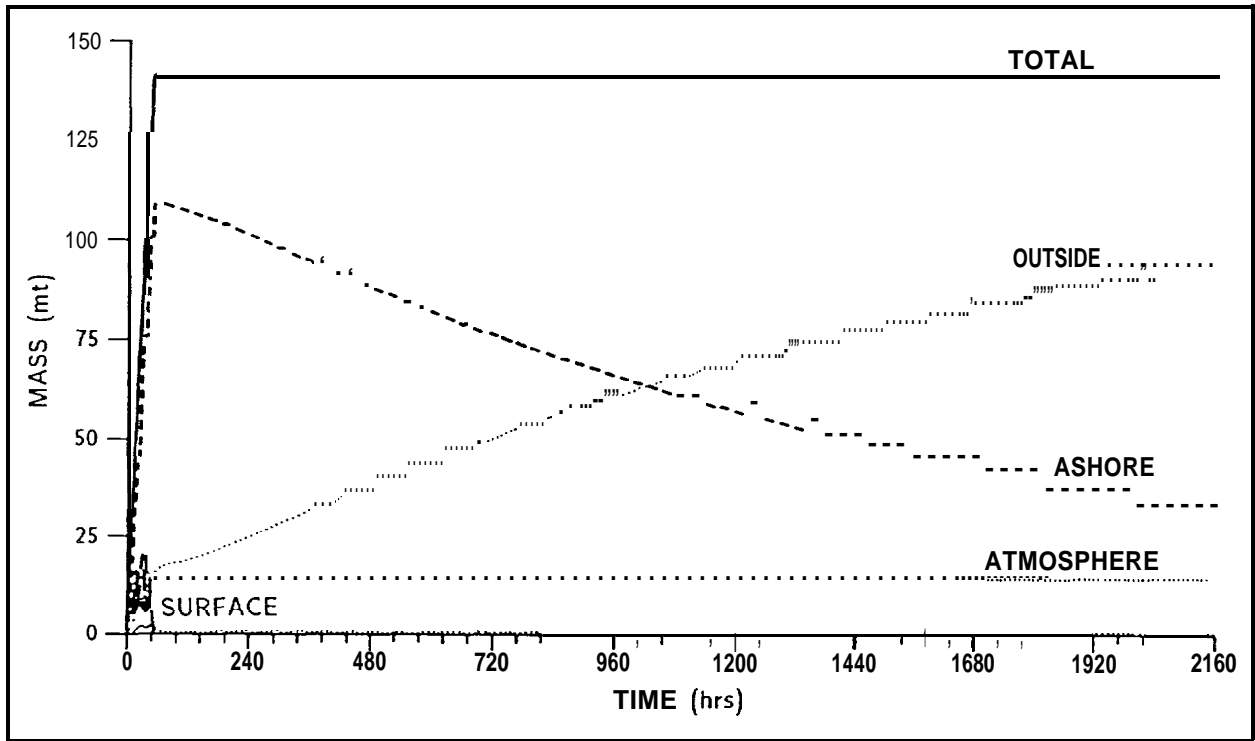


FIGURE 5.12. Overall mass balance for Prudhoe Bay crude oil coming ashore on a gravel beach.

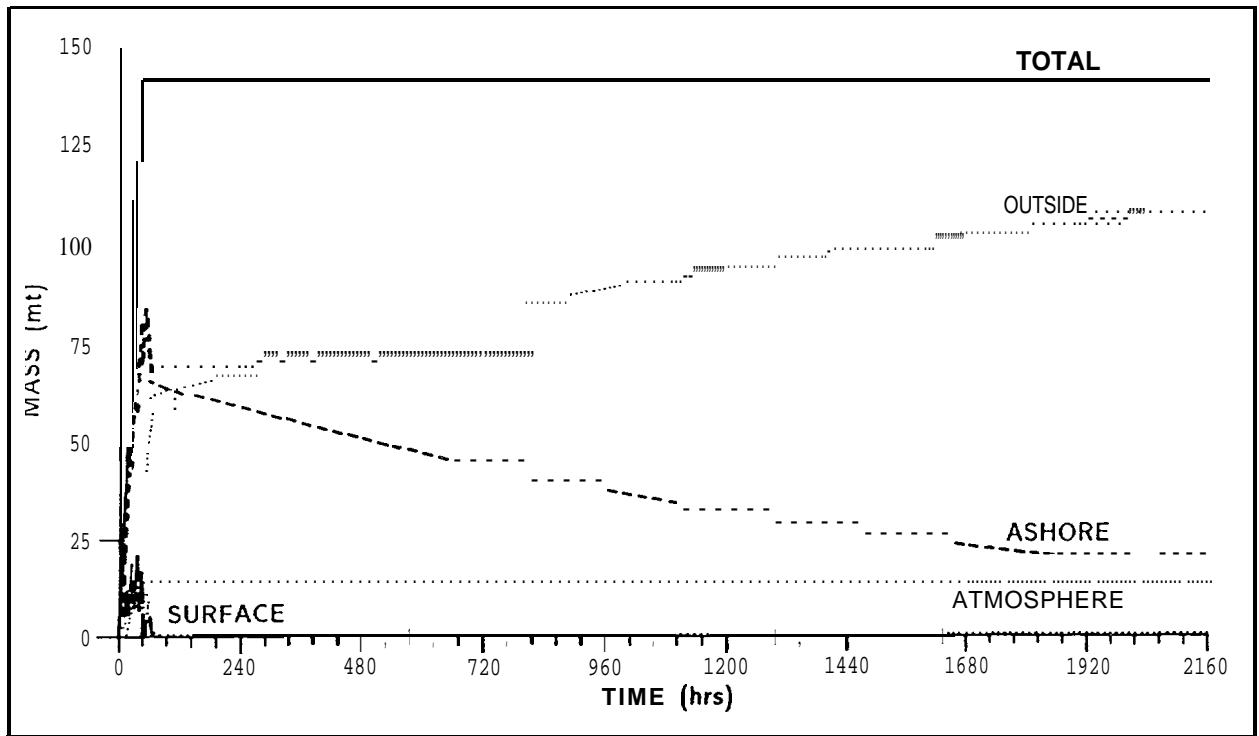


FIGURE 5.13. Overall mass balance for Prudhoe Bay crude oil coming ashore on a cobble beach.

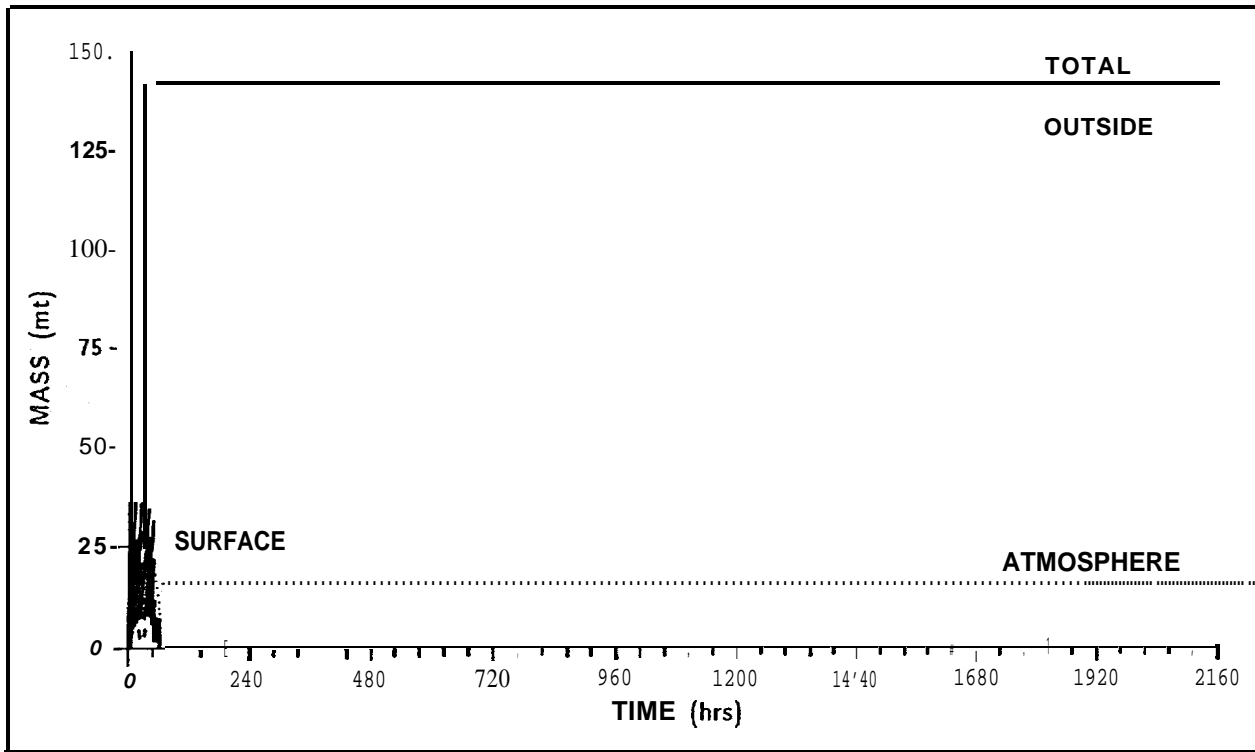


FIGURE 5.14. overall mass balance for Prudhoe Bay crude oil coming ashore on smooth rock or seawall.

6.0 AMOCO CADIZ H IN DCAST

6.1 INTRODUCTION

The most severe test of any model is a hindcast of a real event having a strong observational data base. The Amoco *Cadiz* spill offers the most complete data set of any coastal oil spill to date and therefore was selected to test the coastal zone oil spill (COZOIL) model developed for the U.S. Department of Interior, Minerals Management Service. Principal summary references on the spill are Hess (1978), CNEXO (1981), and NOAA/CNEXO (1982).

The sequence of events to be hindcast begins at 0600 on 17 March 1978 when the supertanker began to break apart 2.4 km off the Brittany (France) coastline after grounding during storm conditions (Hess, 1978). A location map of the site is provided in Figure 6.1. The ship's cargo consisted of about 220,000 metric tons (ret) of light Middle Eastern crude oil and a small amount of bunker oil, all of which was lost over the next two weeks (Fig. 6.2) (Hess, 1978). The oil rapidly emulsified in the high waves around the vessel, incorporating up to 90 percent water (Harm et al., 1978). After initial oil transport to the south, strong winds spread the oil toward the east for the first ten days. A shift in wind direction to the northeast then carried oil offshore, with a reversal toward the southwest after six days (Hess, 1978). Oil was ultimately spread over more than 300 km of coastline and a large area of offshore waters (Fig. 6.1).

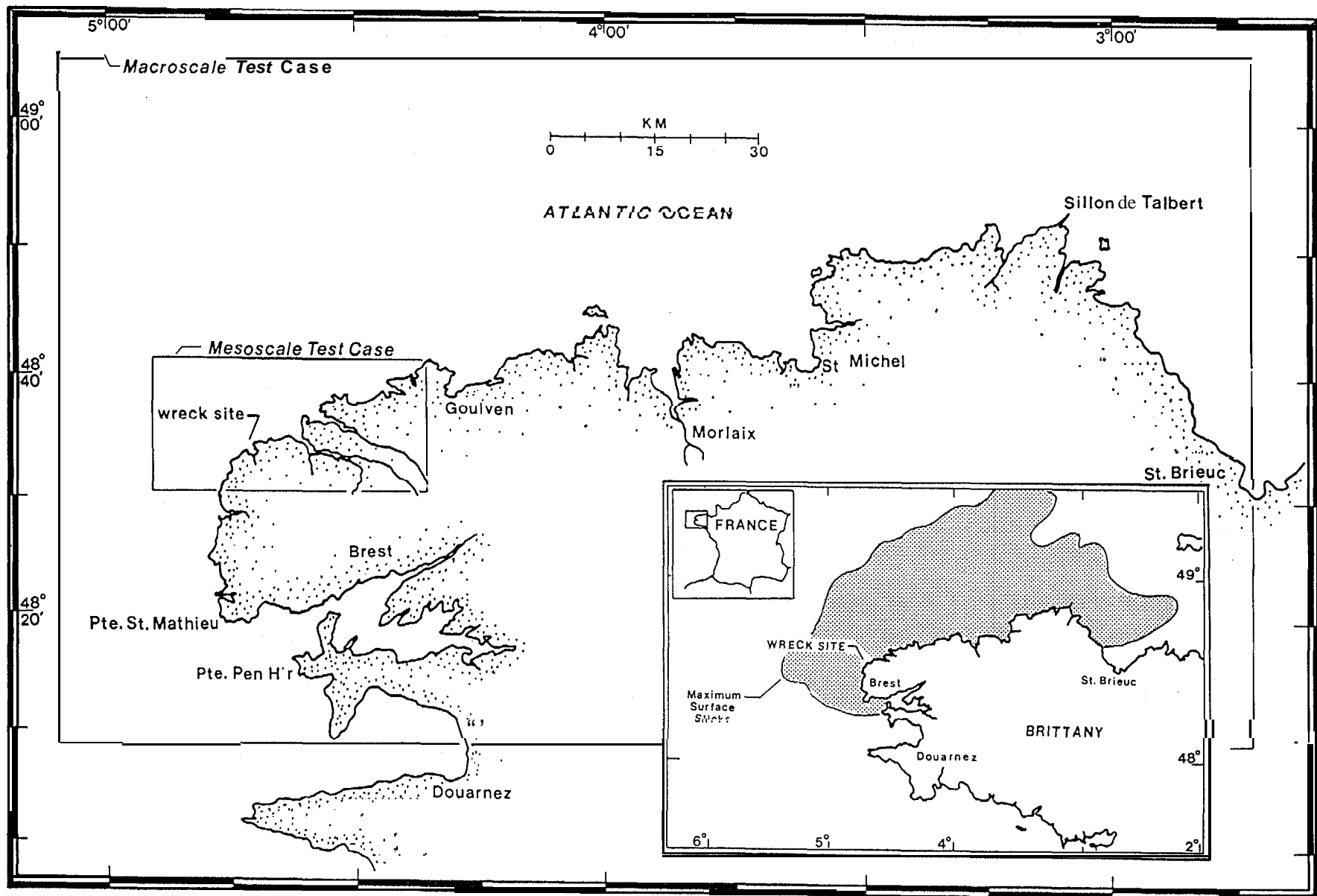


FIGURE 6.1. Study area map for the *Amoco Cadiz* hindcast showing coastal areas impacted by oil and borders of the mesoscale and macroscale test cases.

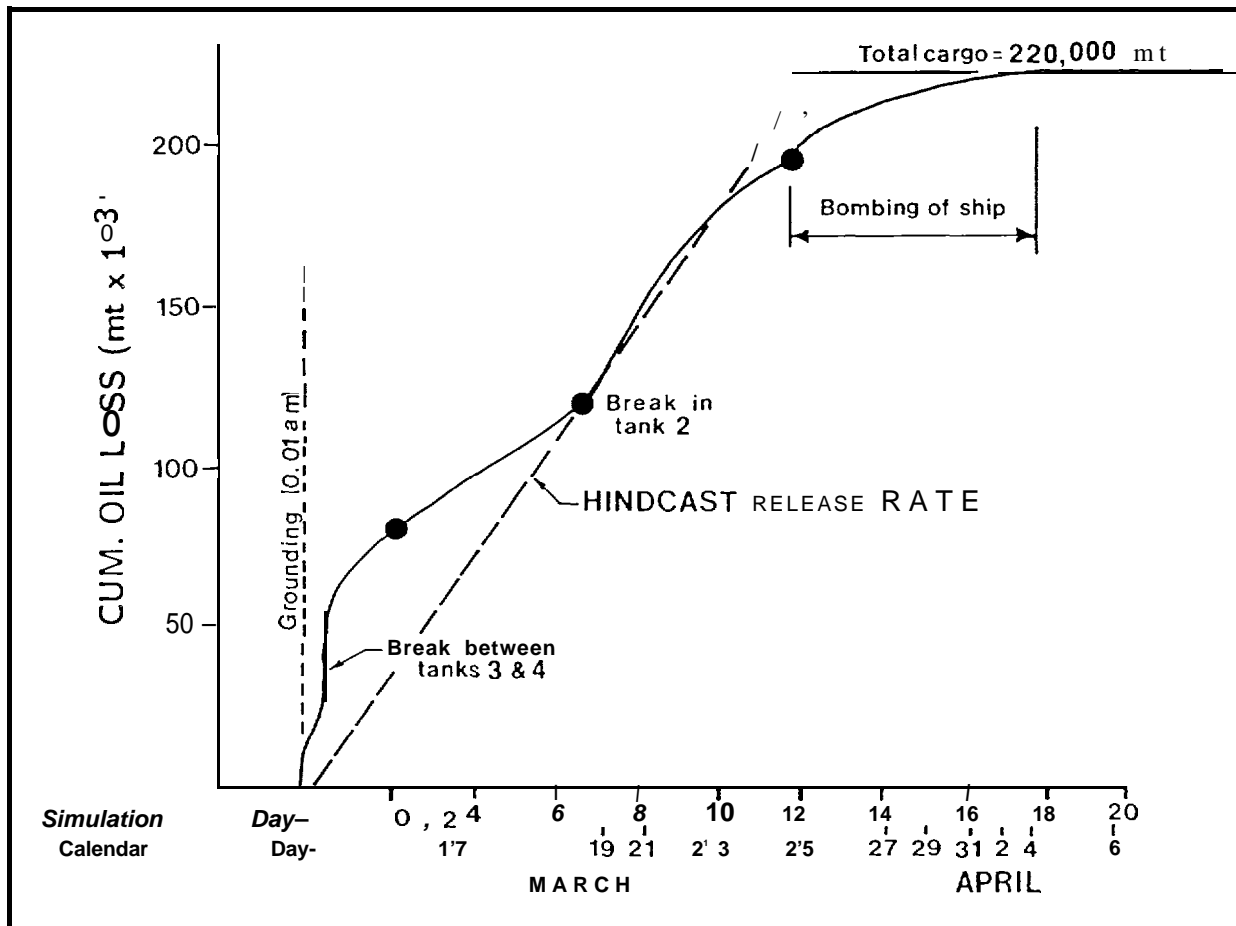


FIGURE 6.2, Estimated cumulative release of oil from the *Amoco Cadiz*. The solid line is from Harm et al. (1978). The dashed line is the release rate used in the model hindcast.

6.2 MODEL INPUT DATA

COZOIL can operate in either a stochastic or deterministic mode, the latter being appropriate for hindcasting purposes. The fundamental inputs necessary to perform a deterministic simulation of a specific scenario, and the inputs used for the *Amoco Cadiz* test cases are presented in Table 6.1. Other inputs, such as simulation duration and time intervals between subsequent output to the monitor or data files are also required, but do not materially affect the computations.

The COZOIL model contains a library with seven crude oils and petroleum products. Of these, Murban Abu Dhabi appears to closely approximate the oil carried by the *Amoco Cadiz* (Anonymous, 1973; NOAA/CNEXO, 1982). The basic characteristics of the Murban crude oil are given in Table 6.2.

Air temperature for March and April 1978, as measured at the Brest airport, averaged about 7.5°C (Fig. 6.3). The wind time series used in the hindcast (Fig. 6.3) is also from Brest airport. Although this location is approximately 25 km inland, it is the closest to the spill site from which we were able to obtain a continuous record for the period of interest. This time series compares well with two others obtained at the time of the incident (Gait, 1978; Gundlach and Hayes, 1978).

Figure 6.2 indicates an estimate of tank ruptures after grounding (Harm et al., 1978) and the release rate used in the model hindcast. One "pool" or "spinet" of oil is released in the simulation every other hour for 12 days, for a total of 144 separate spinets of about 1528 mt each.

The tidal range of the spill site increases from a mean of 6 m in the west to over 8 m in the east, with a spring-neap variability of 2 m or more (SHOM, 1973, 1978). A 6.5-m tide range is used in the model. The tidal current amplitude used is 1.46 meters per second (m/sec) (SHOM, 1973).

Hindcasts of the fate of the spilled oil were performed on mesoscale and macroscale (Fig. 6.1) to reflect localized oiling within the convoluted coastline adjacent to the grounding site and to cover oil distribution over the entire spill-affected area. The Brittany shoreline being represented in the COZOIL model is complex and diverse, containing a closely spaced mixture of bedrock-dominated shores, mixed sand and gravel beaches, sand beaches backed by dunes or riprap, and estuaries with large mud flats. Because of the large tidal range, sand flats extending up to several kilometers from shore are exposed at low tide.

TABLE 6.1. COZOIL input parameters for deterministic simulation and values used for the *Amoco Cadiz* hindcasts.

Input Parameters	Value	Comments
Oil type	Murban crude	Primarily light Arabian crudes (Hess, 1978)
Spill size	220,000 mt	1,613,000 bbl (Hess, 1978)
Number of spinets	144	Conforms to Harm et al. (1978), Figure 6.2
Interval between sequential releases	1 every 2 hours	Conforms to Harm et al. (1978), Figure 6.2
Coastal reach parameters	Tables 6.3-6.5	Some field measurements, Figure 6.4
Air temperature	7.5°C	Brest airport. Figure 6.3
Wind time series	Figure 6.3	Brest airport
Tidal period	12.4 hour	SHOM (1973, 1978)
Range	6.5 m	SHOM (1973, 1978)
Tidal current amplitude	1.46 m/sec	SHOM (1973, 1978)
Time after mean low tide for simulation start	6 hr	SHOM (1978)

TABLE 6.2. Summary of boiling point characteristics of Murban. Abu Dhabi crude oil. [Overall characteristics: API gravity 40.5: viscosity @ 20° C 35.9 cp]

cut #	Boiling Point (°F)	API Gravity (API Units)	Specific Gravity (ret/m ³)	Mass Fraction (%)	Molecular Weight (gin/mole)	Viscosity (cp)
1	151.	90.0	0.628	3.548	89.	0.4
2	212.	70.6	0.688	4.142	105.	0.5
3	257.	62.3	0.718	5.289	117.	0.6
4	302.	55.7	0.743	6.205	131.	0.7
5	347.	51.6	0.760	6.064	147.	0.9
6	392.	48.5	0.773	5.410	164.	1.2
7	437.	45.6	0.785	5.402	183.	1.5
8	392.	43.0	0.797	5.874	203.	2.0
9	527.	40.0	0.811	4.881	222.	2.6
10	580.	35.8	0.831	5.820	248.	3.7
11	638.	34.0	0.840	5.780	287.	4.8
12	685.	30.0	0.861	6.876	312.	8.4
13	738.	28.4	0.870	6.410	353.	16.2
14	790.	26.6	0.880	6.051	395.	34.2
15	850.	16.7	0.939	22.247	600.	134.7

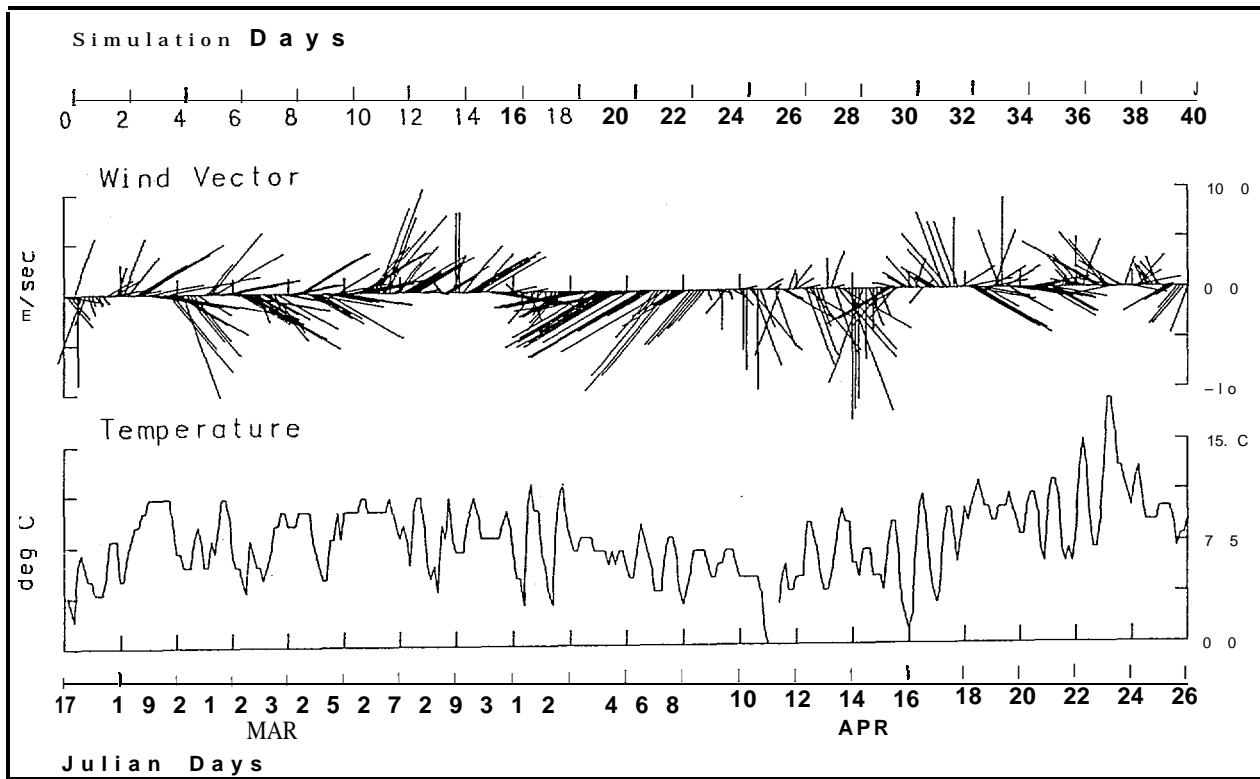


FIGURE 6.3. Temperature ($^{\circ}\text{C}$) and wind velocity (m/sec) from Brest airport (France) for the major portion of the Amoco *Cadiz* spill duration (17 March - 26 April 1978).

The parameters defining the coastline for all hindcasts are given in Tables 6.3-6.5. Shoreline classification is based on Berne (1982), modified to conform with shoreline types defined by the COZOIL model. Shoreline slopes are based on the measurement of topographic profiles across sand, coarse sand with fine gravel, and gravel beaches in Brittany at the time of the spill. Examples from the *AmocoCadiz* site are provided in Figure 6.4. Values for adjacent beaches were estimated using these measurements as a basis and from repeated observations of the shoreline by Gundlach. The foreshore slope, as defined by model requirements, is the slope of a straight line between the berm or high-water mark and the low-tide line. The backshore is the area above the berm or high watermark. The position of the line dividing the foreshore and backshore can vary substantially in Brittany depending on the tidal phase. A value of 20 m is used as representative of the narrow back shores common in Brittany.

The resulting coastlines for the three hindcasts are shown in Figure 6.5. In the mesoscale case, lengths of individual shoreline segments or reaches vary from about 1.7 to 5 km. At this scale, the model is capable of resolving individual estuaries and embayments along the coast. For example, the Abers Benoit and Vrach (Fig. 6.5, upper) are clearly represented. For the macroscale test case (Fig. 6.5, middle), the reach lengths range from 20 to 46 km, a much coarser representation in which 11 reaches cover over 600 km of actual coastline. The third hindcast (Fig. 6.5, lower) evaluates model sensitivity to coastline resolution by having the central portion of the macroscale coastline (i. e., that portion nearest and to the east of the spill source) replaced with a set of shorter, finer resolution reaches (Table 6.5).

TABLE 6.3. Coastal reach parameters for mesoscale test case.*

*Field profile data were used for reach 3 [station AMC1, AMC2], 5 (AMC4), 6 (AMC5), 10 (AMC11) and 14 (AMC12) (Gundlach and Hayes, 1978; see Fig. 6.4).

**Shoreline types are (1) cliffs or seawalls, (2) cobble/boulder beaches, (3) eroding Peat scarps, (4) sand beaches, (5) gravel beaches, (6) tidal flats, and (7) marshes.

Coastal Reach Number	Shoreline Type**	Length (m)	Backshore		Foreshore		Orientation ("N)
			Width (m)	Slope (%)	Width (m)	Slope (%)	
1	2	4000.	20.	0.098	66.	0.098	25.
2	2	3400.	20.	0.098	66.	0.098	45.
3	4	1806.	20.	0.094	296.	0.020	136.
4	4	2000.	20.	0.094	170.	0.038	0.
5	5	1731.	20.	0.145	110.	0.055	82.
6	4	4030.	20.	0.082	292.	0.022	78.
7	5	3000.	20.	0.249	100.	0.065	113.
8	5	2500.	20.	0.249	100.	0.065	321.
9	4	2800.	20.	0.167	680.	0.009	29.
10	2	1981.	20.	0.167	610.	0.010	163.
11	4	1915.	20.	0.167	680.	0.009	75.
12	6	2700.	20.	0.249	100.	0.065	93.
13	6	2400.	20.	0.145	100.	0.065	294.
14	4	2201.	20.	0.156	545.	0.012	341.
15	7	1830.	20.	0.156	190.	0.032	91.
16	4	1770.	4.	1.000	165.	0.036	341.
17	2	2630.	20.	0.250	40.	0.163	99.
18	2	1770.	20.	0.250	280.	0.021	147.
19	2	2300.	20.	0.250	95.	0.068	74.
20	4	2550.	20.	0.082	250.	0.024	48.
21	4	2990.	20.	0.082	290.	0.021	98.
22	4	2594.	20.	0.082	115.	0.057	290.
23	4	1700.	20.	0.115	343.	0.019	31.
24	4	3000.	20.	0.167	45.	0.144	82.
25	4	3000.	20.	0.167	90.	0.072	54.

TABLE 6.4. Coastal reach parameters for macroscale test case.

*Shoreline types are (1) cliffs or seawalls, (2) cobble/boulder beaches, (3) eroding peat scarps, (4) sand beaches, (5) gravel beaches, (6) tidal flats, and (7) marshes.

Coastal Reach Number	Shoreline Type*	Length (m)	Backshore		Foreshore		Orientation ("N)
			Width (m)	Slope (%)	Width (m)	Slope (%)	
1	1	20000.	20.	0.800	20.	0.325	9.
2	5	24000.	20.	0.110	60.	0.108	110.
3	5	20000.	20.	0.160	200.	0.033	0.
4	5	40000.	20.	0.160	200.	0.033	250.
5	2	24000.	20.	0.110	60.	0.108	2.
6	5	34000.	20.	0.160	200.	0.033	63.
7	4	26600.	20.	0.130	100.	0.065	78.
8	5	31000.	20.	0.160	200.	0.033	101.
9	5	17000.	20.	0.160	200.	0.033	4.
10	5	35000.	20.	0.160	200.	0.033	80.
11	5	46000.	20.	0.160	200.	0.033	144.

TABLE 6.5. Coastal reach parameters for macroscale test case having additional detail near the spill site.

*Field profile data were used for reach 7 (AMC5), 8 (AMC12), 10 (AMC13), 11 (AMC4), 14 (AM C16), 15 (AM C16), 17 (AMC10), and 18 (AMC9) (Gundlach and Hayes, 1978: see Fig. 6.4).

\$* Shoreline types are (1) cliffs or seawalls, (2) cobble/boulder beaches, (3) eroding peat scarps, (4) sand beaches, (5) gravel beaches, (6) tidal flats, and (7) marshes.

Coastal Reach Number	Shoreline Type**	Length (m)	Backshore		Foreshore		Orientation (*N)
			Width (m)	Slope (%)	Width (m)	Slope (%)	
1	1	20000.	20.	0.800	20.	0.325	9.
2	5	24000.	20.	0.110	60.	0.108	110.
3	5	20000.	20.	0.160	200.	0.033	0.
4	5	40000.	20.	0.160	200.	0.033	250.
5	2	24000.	20.	0.110	60.	0.108	2.
6	2	6000.	20.	0.200	75.	0.087	53.
7	4	6400.	20.	0.080	350.	0.019	87.
8	5	7900.	20.	0.160	545.	0.012	27.
9	2	6900.	20.	0.200	75.	0.087	103.
10	4	10700.	20.	0.120	345.	0.019	56.
11	4	4400.	20.	0.170	205.	0.032	115.
12	4	4000.	20.	0.080	780.	0.008	211.
13	4	8100.	20.	0.080	825.	0.008	70.
14	5	4400.	20.	0.250	150.	0.043	34.
15	4	4900.	20.	0.250	140.	0.046	78.
16	2	4500.	20.	0.250	70.	0.093	120.
17	4	3900.	20.	0.060	470.	0.014	18.
18	4	5400.	20.	0.130	105.	0.062	65.
19	5	31000.	20.	0.160	200.	0.033	101.
20	5	17000.	20.	0.160	200.	0.033	4.
21	5	35000.	20.	0.160	200.	0.033	80.

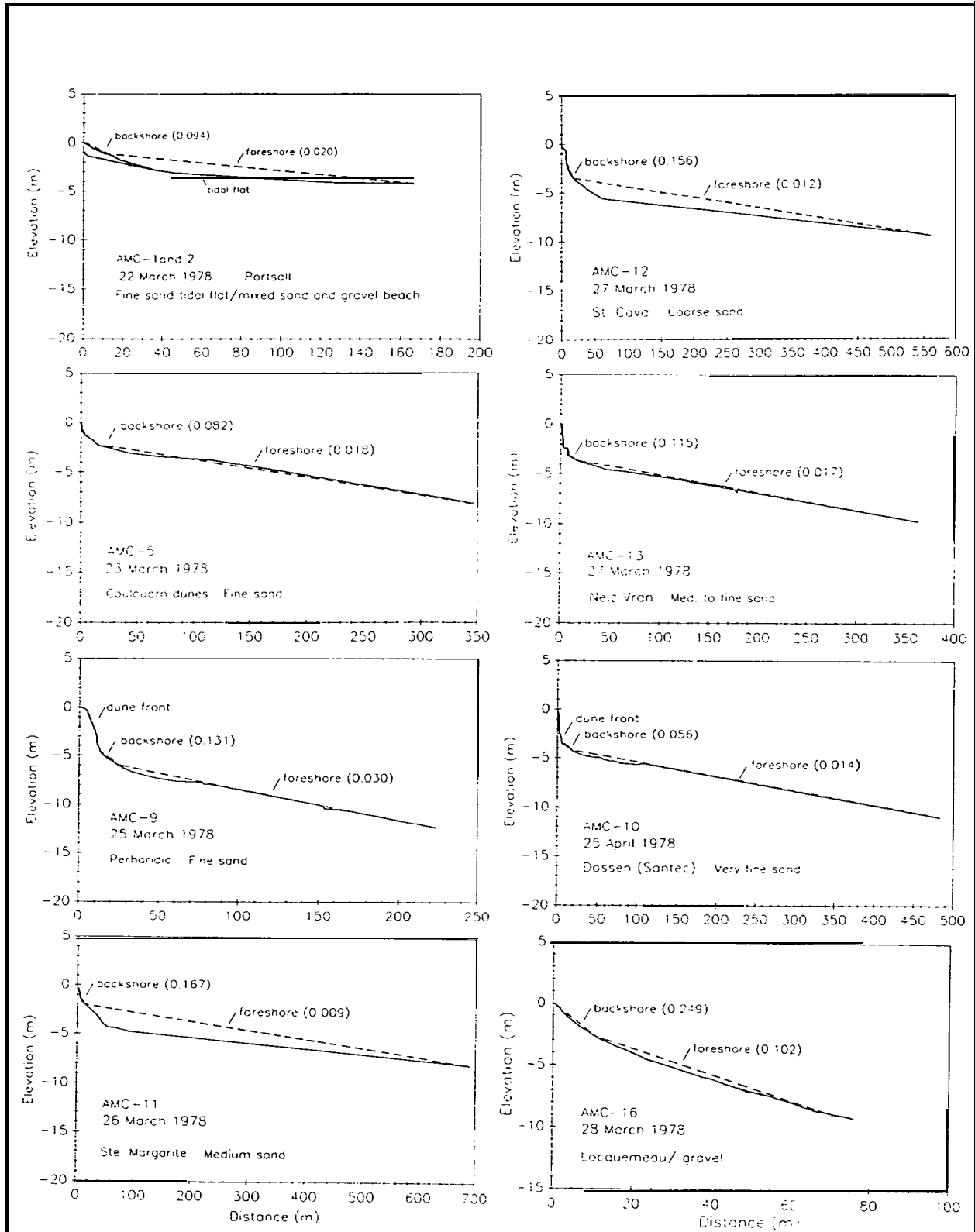


FIGURE 6.4. Profiles for various beaches in the spill site which served as a basis for backshore and foreshore slopes used in the three test cases. Station locations are provided in Gundlach and Hayes (1978).

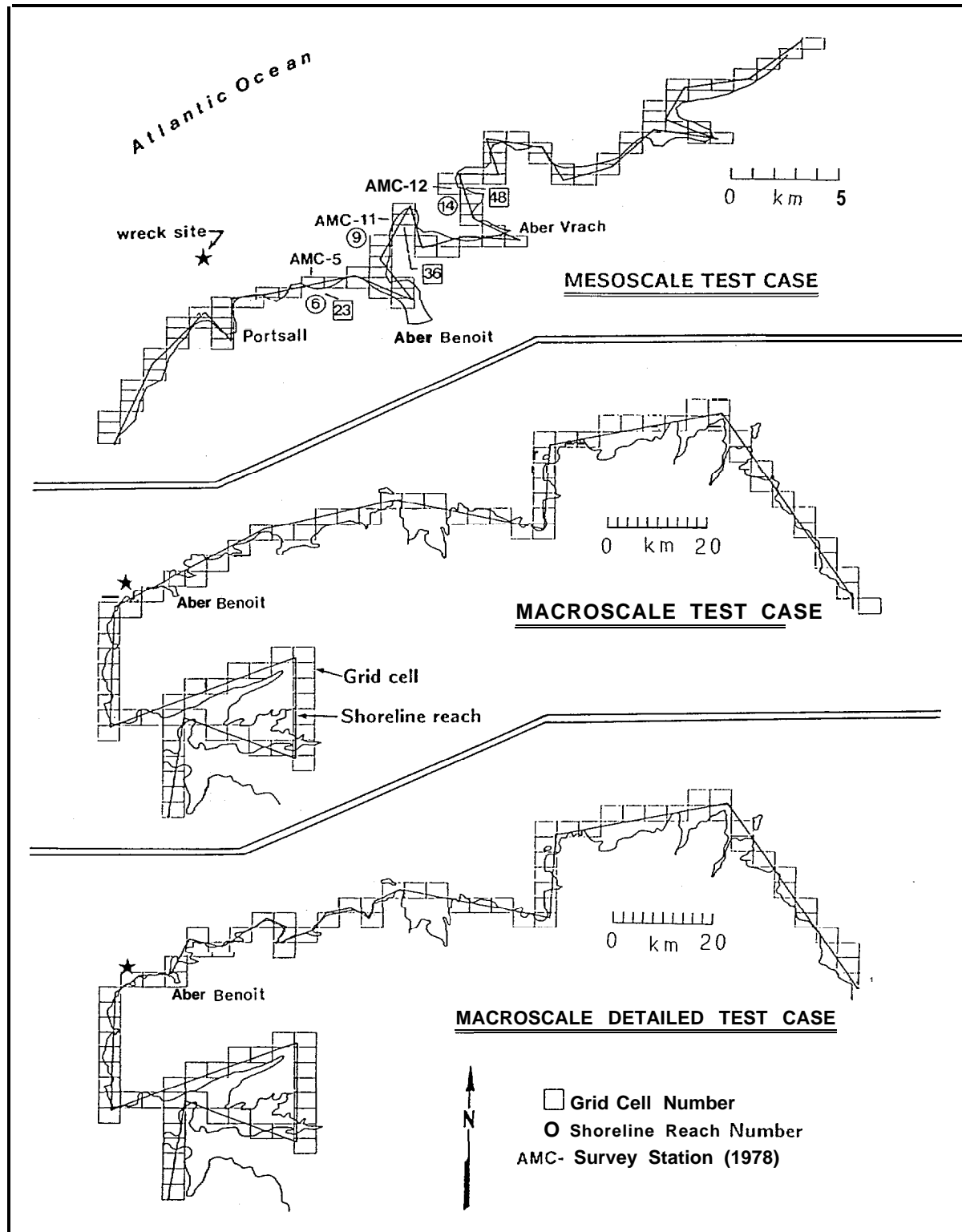


FIGURE 6.5. Modeled coastline for all three test cases. Grid cells and shoreline reaches are indicated for each. The locations of field stations AMC-5, 11, and 12. are indicated in the upper diagram.

6.3 SUMMARY OF OIL DISTRIBUTION DATA

The distribution and quantity of oil along the shoreline during the *Amoco Cadiz* spill was based on surveys conducted by a combined French-American field team. Measurements during the spill included oil thickness, surface coverage, burial, and alongshore distribution at 20 stations along the coast, augmented by approximately 150 additional ground observation stations and an extensive set of oblique and vertical aerial photographs. Results, published in Gundlach and Hayes (1978), D'Ozouville et al. (1978), and Finkelstein and Gundlach (1981), indicate that approximately 62,000 mt of oil were onshore during the period of 17 March to 2 April, and that from 20-28 April slightly less than 10,000 mt was onshore.

For these simulations, original data were analyzed and recalculated to determine more exact dates with respect to onshore oiling, to differentiate between surface and buried oil, and to calculate 95 percent confidence intervals for each time period. The field data set is presented in Table 6.6 indicating the sampling date and quantity of oil (ret/km shoreline). Stations within the mesoscale shoreline section were surveyed most often and provide oil quantities for three time periods--8.5, 15, and 36 days after the beginning of the spill (Table 6.7). Summary data for the macroscale shoreline are presented in Table 6.8. For this data set, shoreline oil was calculated for 9 and 38.5 days after the initial release of oil. In all cases, the extent of shoreline oiling (in km) was taken from Finkelstein and Gundlach (1981) and D'Ozouville et al. (1978). Only oiling of the mainland was considered as offshore islands and rocks are not represented in these model test cases.

TABLE 6.6. Quantity of oil measured at stations within the *Amoco Cadiz* spill site. Dash indicates that the amount of subsurface oil is included in the surface oil value. Station locations are in Gundlach and Hayes (1978).

Station	Date	Time (hrs)	Length (km)	Buried (ret)	Surface (ret)	Total (ret)	Oil/km (ret)
AMC-1	22 Mar	1400	0.18	0	50.2	50.2	280.5
	31 Mar	1425		0	28.2	28.2	156.6
	22 Apr	0935			7.3	7.3	40.5
AM C-2	22 Mar	1330	0.22	0	1.8	1.8	8.2
	31 Mar	1640		0	0.2	0.2	0.9
	22 Apr	1200		0	5.5	5.5	24.9
AM C-3	23 Mar	1045	0.5	0	44.6	44.6	89.2
	31 Mar	1320		0	76.2	76.2	152.4
	22 Apr	1140		0	5.5	5.5	11.0
AMC-4	23 Mar	1150	0.35	118.7	284.1	402.8	1150.9
	31 Mar	1600		8.9	36.9	45.8	130.9
	22 Apr	1400			2.5	2.5	7.1
AMC-5	23 Mar	1250	1.25	105.0	1036.9	1146.9	917.5
	31 Mar	1700		0	1.7	1.7	1.4
	22 Apr	1430		0	2.5	2.5	2.0
AMC-6	24 Mar	1200	0.15	8.5	51.8	60.2	401.9
	01 Apr	1650		0	0.3	0.3	1.8
	26 Apr	1800		0	1.0	1.0	6.6
AMC-7	24 Mar	1430	0.55	4.0	102.5	106.5	193.6
	01 Apr	1550		3.7	2.5	6.2	11.4
	26 Apr	1725			1.7	1.7	3.1
AMC-8	25 Mar	1250	0.2	25.5	9.6	35.1	175.4
	01 Apr	1800		0.1	10.2	10.3	51.3
	26 Apr	1630		0	0.4	0.4	2.0
AMC-9	25 Mar	1230	2.0	65.5	973.9	1039.4	519.7
	01 Apr	1830		34.0	95.8	126.6	63.3
	26 Apr	1600			10.6	10.6	5.3
AMC-10	25 Mar	1500	1.35	36.1	46.4	82.5	61.1
	26 Apr	1300			6.0	6.0	4.4
AMC-11	26 Mar	1630	0.50	8.5	175.2	183.7	367.4
	01 Apr	0830		17.0	13.8	30.8	61.7
AMC-12	27 Mar	1300	0.45	3.8	357.7	361.5	803.4
	23 Apr	1000		23.0	6.3	29.6	65.8
AMC-13	27 Mar	1630	0.55	0	248.3	248.3	449.6
	23 Apr	1330		14.0	0.6	14.6	26.5
AMC-15	28 Mar	1600	0.45	0	83.3	83.3	185.1
	25 Apr	1800			1.6	1.6	3.5
AMC-16	28 Mar	1800	0.20	20.2	61.0	81.2	406.0
	24 Apr	1800		66.3	0.0	66.3	331.5
AMC-17	29 Mar	1300	1.05	0	545.6	545.6	519.6
	24 Apr	1130		0	1.6	1.6	1.5
AMC-18	29 Mar	1200	area				7400
	25 Apr	1200	area				2760

TABLE 6.7. Summary of oil measured in the mesoscale test case. Sections II and III refer to shoreline divisions from Gundlach and Hayes (1978). Station locations are provided in the same reference. The length of shoreline oiled in each section is indicated.

	March						April				
	22 Q 1400 hrs	23 Q 1200 hrs	24 Q 1300 hrs	25 Q 1400 hrs	26 Q 1630 hrs	27 Q 1300 hrs	31 Q 1600 hrs	01 Q 1700 hrs	22 Q 1200 hrs	23 Q 1000 hrs	26 Q 1700 hrs
Section II											
AMC-1	3091						1727		533		
AMC-2	88						11		325		
AMC-3		979					1672		143		
AMC-4		12660					1441		91		
AMC-5		10098					11		26		
	Day 6.0 (mt oil/n km)			Day 14.7 (mt oil/n km)			Day 35 [mt oil/13 km]				
Total Oil:											
-95%CI	394						197		44		
Average	5166						972		224		
+95%CI	9938						1747		404		
Section III											
AMC-11				5872			992		442		
AMC-12					12848					1452	
				Day 10.0 (mt oil/16 km)		Day 15.7 (mt oil/16 km)		Day 36.0 (mt oil/22 km)			
Total Oil:											
-95%CI				2524					-621		
Average				9360		992			748		
+95%CI				16196					2127		
Sections II + III (combined)											
	Day 8.5 (mt oil/27 km)			Day 15 (mt oil/27 km)			Day 36.0 (mt oil/35 km)				
AMC-1	7587			4239			1435				
AMC-2	216			27			875				
AMC-3	2403			4104			385				
AMC-4	31080			3537			245				
AMC-5	24773			27			70				
AMC-11	9909			1674			70				
AMC-12	21680						2310				
Total Oil:											
-95%CI	5138			698			148				
Average	13950			2268			770				
+95%CI	22762			3838			1392				

TABLE 6.8. Summary of oil (ret/km) for the entire *Amoco Cad/z* spill site. The shoreline during the 20-28 April 1978 field survey is divided into light (l) and heavily (h) oiled shorelines based on Finkelstein and Gundlach (1981) and D'Ozouville et al. (1978). Oiling of offshore rocks and islands is not included. Data from all stations, except AMC-18, are averaged and extrapolated over the entire length of oiled shoreline to yield a total quantity of oil on days 9.0 and 38.5. AMC-18 is separately added to the determined average because it represents an anomalously large concentration of oil in one particular environment (7,400 mt within only a few kilometers of shoreline).

Site	March										April					
	22	23	24	25	26	27	28	29	31	01	22	23	24	24	26	
AM C-1	281								157		41(h)					
AMC-2	8								1		25(h)					
AMC-3		89							152		11(l)					
AM C-4		1151							131		7(l)					
AMC-5		918							1		2(1)					
AMC-6			402							2					7(1)	
AM C-7			194							11					3(1)	
AMC-8				175						51					2(1)	
AM C-9				520						63					5(1)	
AMC-10				61											4(l)	
AMC-11					367					62	2(1)					
AMC-12						803						66(h)				
AMC-13						450						27(h)				
AMC-15							185								4(1)	
AMC-16							406						332(h)			
AMC-17								520					2(1)			
AMC-18*									7400						760	

Km oiled:					Day 9.0							Day 38,5				
					51							55 heavy, 213 light				
-95%CI					24200							2375				
Average					36250							9062				
+95%CI					48300							15757				

6.4 RESULTS

The first simulation discussed is the mesoscale test case, with 25 coastal reaches extending about 30 km from the spill site. The second is an order of magnitude more extensive spatially, with only 11 reaches representing over 600 km of actual coastline. The third covers the same geographical area as the second, but achieves more detail near the spill site with a total of 21 reaches.

6.4.1 Mesoscale Test Case

For this test case, shoreline reaches vary from 1.7 km to 5 km in length adjacent to the wreck site. The offshore model boundary is located 15 km or less from the shoreline (see Fig. 6.1).

Offshore and onshore distribution

The distribution of oil on the water surface and on the shoreline for the mesoscale test case is presented for four time periods in Figure 6.6. At 5 days, oil has already been distributed over the entire study area (onshore and offshore), conforming well with the distribution reported by study of aerial photographs (CNEXO et al., 1978). This rapid distribution is the result of strong tidal currents and winds, plus longshore transport inside the surf zone. At day 5, the model shows the highest surface oil concentration in Aber Benoit, an area that was heavily impacted by the spill and contained traces of oil at least until 1987. By day 10, oil quantity within Aber Benoit has decreased while oil in the nearshore area remains fairly evenly distributed alongshore but with less occurring along the eastern edge. Between days 10 and 20, most of the oil on the water surface has been transported out the northern model boundary due to strong offshore winds. A subsequent wind to the southwest, beginning about day 18, carries most of the remaining surface oil out the western model boundary. The overall sequence of oil distribution conforms very well to observations except that the actual spill contained no artificial boundaries so that re-oiling of the shoreline and offshore waters to the southwest occurred after transport offshore.

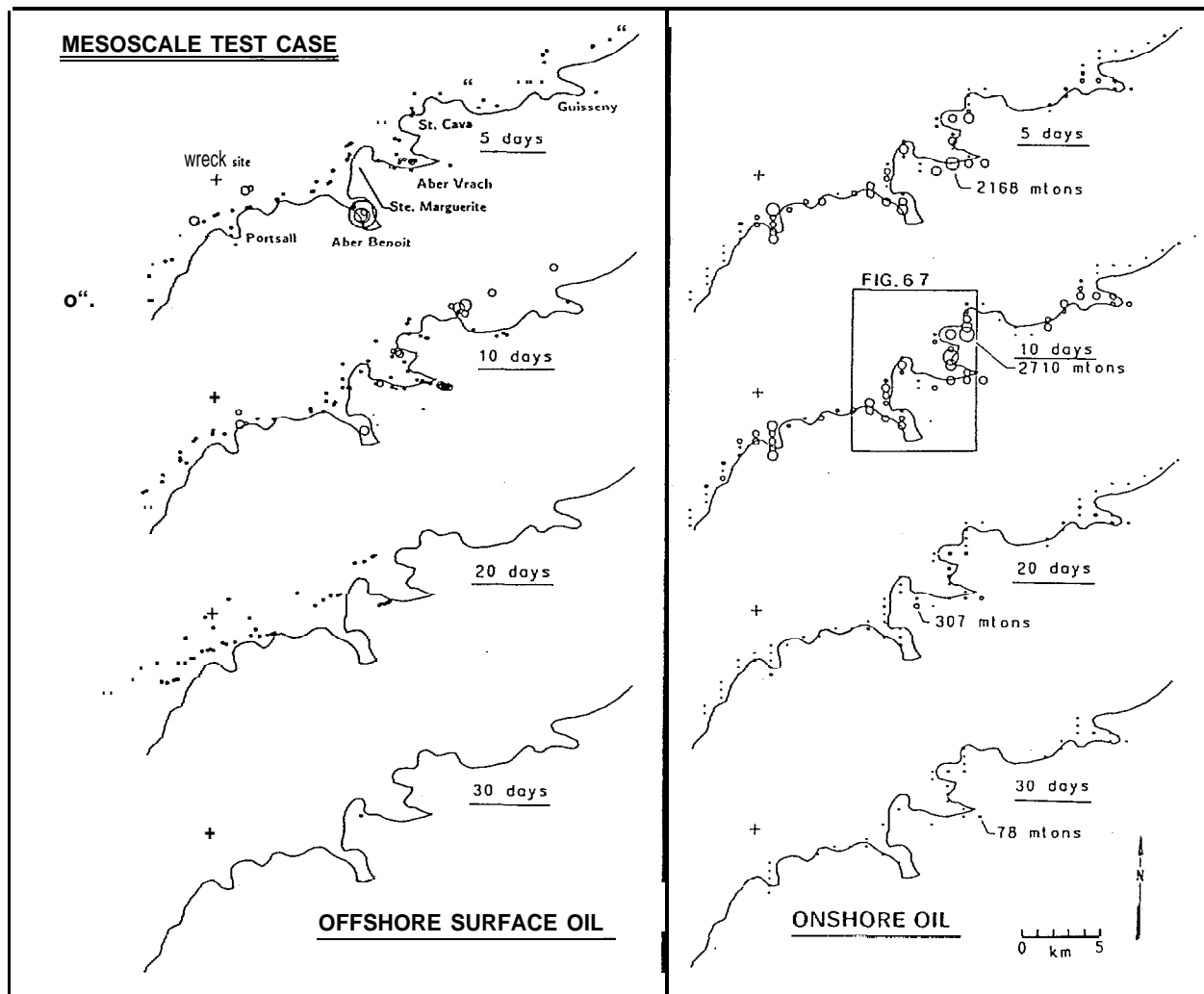


FIGURE 6.6. Distribution of offshore surface oil and onshore oil [foreshore, surface, and backshore] for the mesoscale test case. Offshore circles indicate computed "a real" coverage of thick oil. The areas of onshore circles are proportional to the oil mass associated with each grid cell. The maximum value for each time plot is given.

The onshore distribution of oil (Fig. 6.6) is represented by circles proportional to the total mass of oil found on the foreshore surface of the beach and the backshore of each grid cell. On day 5, shoreline oil is concentrated in Portsall harbor adjacent to the wreck site, in Abers Benoit and Vrach, and on the two north-trending headlands (Presqu'île Ste. Marguerite and St. Cava) which form a barrier to the easterly drifting oil. This conforms very well with observations made at the time of the spill (Fig. 6.7).

At day 10, the model indicates substantial oiling of the embayment at Guisseny as did occur: however, the model may overestimate oiling at this location because of the lack of shoreline detail. In this case, a large spit protecting the embayment is not adequately represented (see Fig. 6.5, upper). At days 20 and 30, oil is found along most of the coast in continually decreasing quantities.

The maximum amount of oil within any one cell equals 2,710 mt and occurs at day 10, corresponding to about 2 mt of oil per linear meter of coastline. This maximum occurs on reach number 14, a sand beach, at a tidal height of 4.5 m. If the oil is evenly distributed over the exposed foreshore and backshore then the reach parameters (Table 6.3) indicate an areal coverage of about 15 kilograms per square meter (kg/m^2), or about 1.7 cm thick, considering that the oil has a density of approximately 0.9 g/cm^3 . This is the maximum oil holding capacity the model will allow for a sand beach (Gundlach and Reed, 1986; Gundlach, 1987). Thus oil arriving subsequently along this coastal cell on the water surface will be precluded from deposition until the tide drops exposing more beach face, or oil on the beach surface is removed to the surf zone or penetrates into surface sediments.

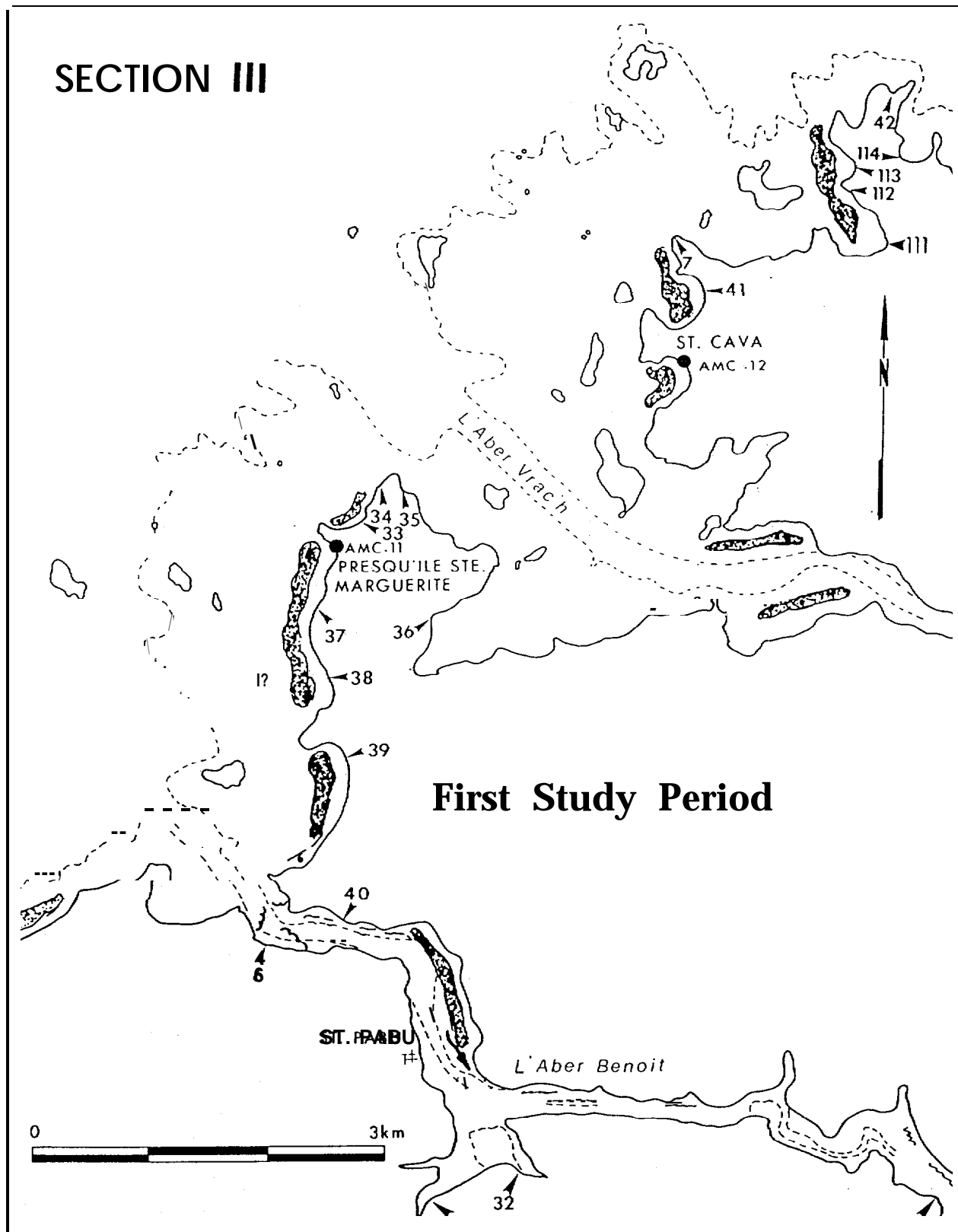


FIGURE 6.7. Diagram indicating the observed distribution of Amoco *Cadiz* oil during late March from west of Aber Benoit to north of St. Cava. Compare to Figure 6.6. onshore oil distribution at ten days. Arrowheads and dots indicate 1978 field stations (from Gundlach and Hayes, 1978).

Dynamic mass balances of oil quantity

The dynamic mass balance of oil for 40 days of simulation time is shown in Figure 6.8 for the mesoscale study area. The lower diagram shows the overall mass balance of oil divided into five major spill components--ashore, water surface, atmosphere, water column, and outside the simulation area. The curve labeled "Ashore" corresponds to the curve labeled "Total Ashore" of the middle diagram, which is composed of four subdivisions--foreshore, backshore, ground water, and surf zone. The upper diagram of Figure 6.8 represents the total oil on the beach, composed of surface and backshore oil but excluding oil in the ground water. This represents the quantity of oil that would be measured on the beaches at the time of the spill. Estimated amounts of oil along this section of shoreline during the spill, compiled for 8.5, 15, and 36 days after the spill, are superimposed on this plot.

Figure 6.8 illustrates that the proximity of the release point to shore, combined with the onshore winds (see Fig. 6.2) result in a steadily increasing amount of oil deposited onshore during the first ten days. The removal and deposition of oil in conjunction with the rising and falling of the tide is clearly reflected in the interchange of oil between the ashore and water surface components (lower diagram). From days 10 to 15, the abrupt increase in oil mass leaving the study area (shown by the curve labeled "outside") is due to strong offshore winds. Note the simultaneous decrease in oil on the water surface (Fig. 6.8, lower).

In comparing the observed versus simulated total quantity of oil ashore (Fig. 6.8, upper), simulation values exceed observed values on both days 8.5 and 15, but compare well with those from day 36. Observations in the field were always made within low- to mid-tide levels, which conform to the higher values of total oil on the beach surface. The high oil quantities simulated on the shoreline could be due in part to removal rates which are too slow in the model and/or the absence of storm surge events in the hindcast. Two such events were recorded during the first two weeks following the start of the spill (Hess, 1978) and resulted in the rapid removal and transport of oil from several segments of the shoreline. The model, however, clearly shows dynamic variability both from low to high tide and from one tidal cycle to the next, which is entirely consistent with the field observations (Gundlach and Hayes, 1978).

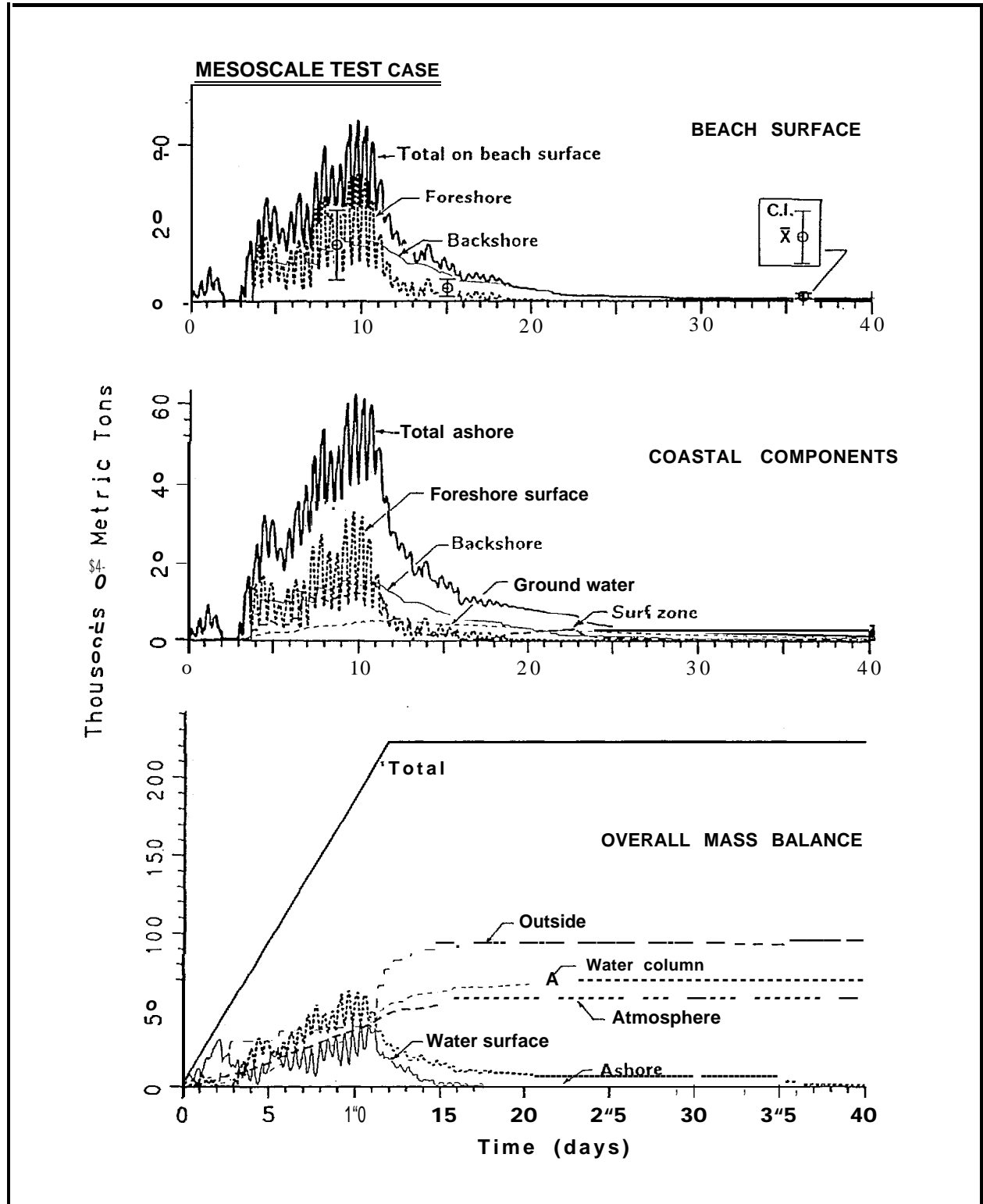


FIGURE 6.8. Dynamic mass balances (overall, coastal components, and beach surface) for oil associated with the mesoscale test case. Observed values of oil quantity on the shoreline and 95-percent confidence intervals are indicated in the upper diagram.

Additional potential sources of error lie in the hydrodynamics incorporated into the model. As indicated in Figure 6.6, much of the onshore oil in the mesoscale hindcast is associated with estuaries and embayments (Portsall, Aber Benoit, Aber Vrach, and Guisseny). Although most were indeed heavily polluted, the natural cleansing of these areas by tides is not represented in the simple hydrodynamics incorporated in the model. Thus a better hydrodynamics data set, compatible with the detail of the coastline, would improve model performance. Finally, the hindcast does not include oil removed during cleanup, but this is thought to account for less than 20 percent of the oil ashore and did not reach maximum operation until two weeks into the spill (Harm et al., 1978).

Grid cell analysis

To view model predictions in further detail, oil distribution within three grid cells and their respective beach segments were analyzed with respect to field site information. The locations of the shoreline reach, grid cells, and field stations, are presented in Figure 6.5 (upper). Plots of simulated and observed oil quantity in ret/km for each of the three areas are presented in Figure 6.9. The individual grid cells, in particular, show large fluctuations in the amount of oil onshore, reflecting oil impacts followed by removal and transport to adjacent cells. Substantially less variability is evidenced when shoreline reaches (composed of 4 to 5 grid cells) are considered. This again corresponds to observations at the *Amoco Cadiz* spill site where it was common during the first two weeks to have very large oil concentrations at one beach while the adjacent beach escaped oiling entirely. The large increases in oil within the shoreline grid cell, as for stations AMC-11 (at days 5 and 10) and AMC-12 (at days 9 and 12) correspond to these large impacts. In these plots, the field value of oil quantity at AM C-5 is higher than that simulated, but comes close to the quantity observed less than two days later. The other two stations, AMC-11 and AMC-12, have observed oil quantities that are lower than simulation values for the shoreline reach, but are similar to those for the single grid cell.

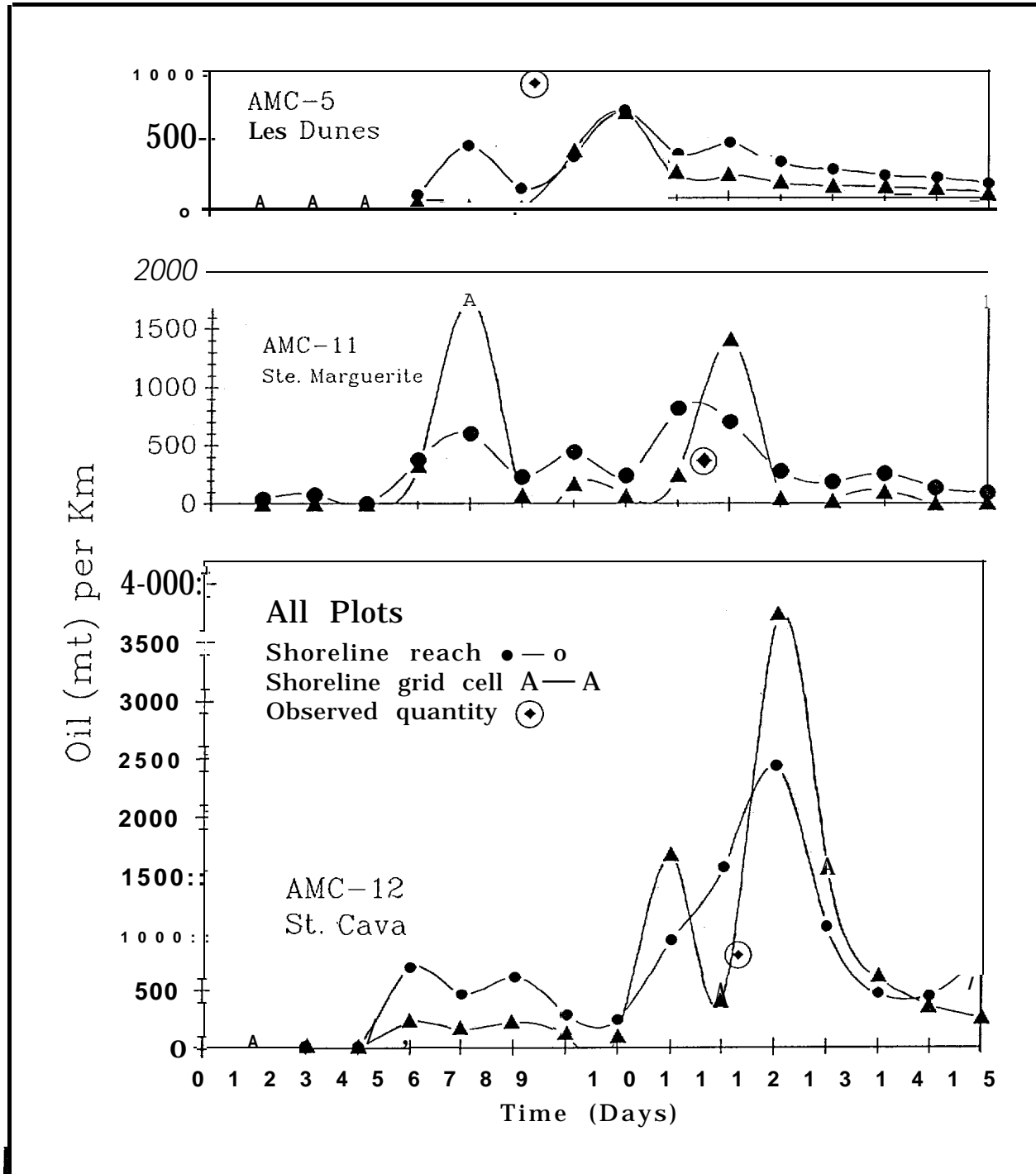


FIGURE 6.9. Comparison of simulated oil quantity within individual grid cells and for the associated shoreline reach (composed of 4 to 5 grid cells) during the first 15 days of the oil spill. Values measured at field stations within the grid cell are indicated.

6.4.2 Macroscale Test Case

This case encompasses the entire northwestern Brittany region and contains only 11 coastal segments ranging in length from 20 to 46 km in contrast to the previous case having a maximum length of 5 km (see Fig. 6.5). At this scale, only coastline trends and very large embayments, as at Brest, can be resolved.

Offshore and onshore distribution

Results of the macroscale simulation of the distribution of the oil is indicated in Figure 6.10. The distribution of offshore surface oil after 5 days compares extremely well with that observed after 4.5 days using vertical aerial photographs taken by the French government (CNEXO et al., 1978) during the spill (Fig. 6.10, upper left). The onshore distribution at this time also conforms very well with that reported. Note the oiling at St. Michel, the site of a large kill of intertidal organisms (Hess, 1978). The consistent distribution for both the onshore and offshore cases continues through 10 days. Note particularly the oil along the shoreline from St. Michel to Ile Grande. Ile Grande was the site of extremely heavy concentrations within a marsh environment (Hess, 1978).

Between days 10 and 20, much of the onshore and nearshore oil is transported offshore because of the wind shift, and at day 20 the oil is returning from its northern excursion and poised to come onshore again. At day 30, this oil is transported to the southwest, oiling the shoreline south of the wreck site. This sequence of offshore transport with very late oiling of the shoreline to the south of the wreck site was well documented at the time of the spill (Gundlach and Hayes, 1978). The southernmost extent of shoreline oiling is essentially correct, ending at Pointe de St. Mathieu. The model, however, inadequately depicts the true eastward transport of oil to Sillon de Talbert (Fig. 6.10), perhaps due to underestimation of tidal currents for this portion of the study area.

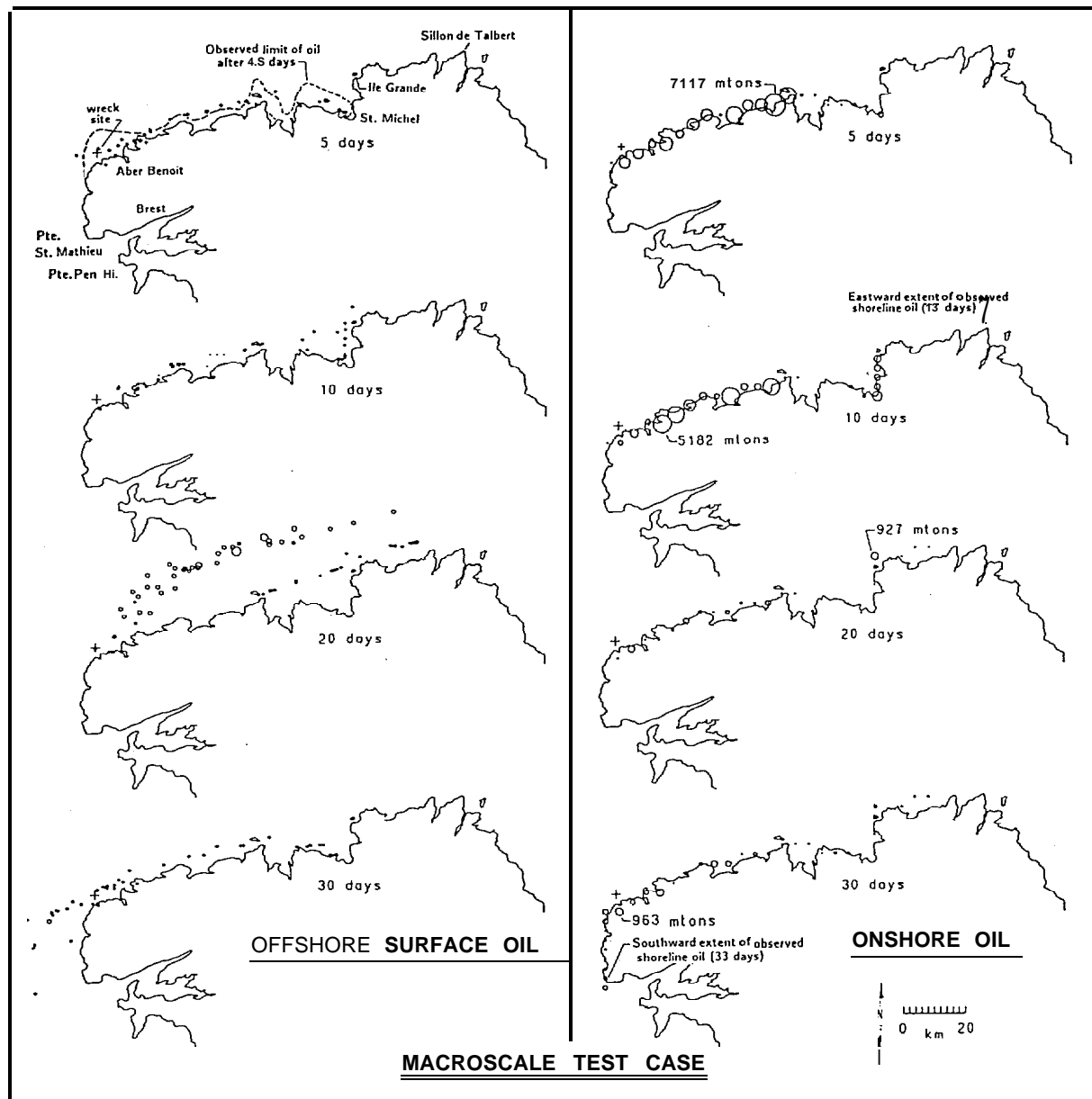


FIGURE 6.10. Distribution of offshore surface oil and onshore oil (foreshore, surface, and backshore) for the macroscale test case. Offshore circles indicate computed areal coverage of thick oil. Onshore circles are proportional to the oil mass associated with each grid cell. The maximum value for each time plot is given.

Dynamic mass balances of oil quantity

The various mass balances for the macroscale hindcast are shown in Figure 6.11. The effect of the extended boundary is immediately apparent when comparing this overall mass balance to that from the mesoscale analysis (see Fig. 6.8). The total lost out the model boundaries reduces from 30 percent after 15 days in the mesoscale study to about 15 percent after 30 days in the macroscale test. Oil is transported north during the southerly wind event from days 10 to 15, but remains within the model boundaries. When the wind shifts back toward the southwest between days 16 and 21, some of the surface oil which was transported offshore comes ashore between days 22 and 29. Note the increase in the oil ashore at this time, particularly in plots of the coastal components and beach surface.

The total oil ashore is approximately the same (62,000-64,000 mt) for the macroscale and mesoscale test cases for the first 20 days. This is because the wind is almost continuously onshore for the first 10 days, then offshore for 5 days, and onshore again. The amount of oil on the beach surface, however, now agrees reasonably well with the field values after 9 days and 38.5 days. This result further supports the hypothesis that the mesoscale test retains too much oil in coastal irregularities, due perhaps to inadequate hydrodynamic resolution.

6.4.3 Macroscale Test Case with Additional Detail

This model test includes a series of more detailed shoreline reaches within the macroscale shoreline previously discussed. The number of shoreline components increases from 11 to 21, with a minimal resolution of 3.9 km instead of 17 km (Table 6.5).

Offshore and onshore distribution

Figure 6.12 provides the distribution of oil for this third hindcast test. Comparison with results from the simpler macroscale test case (see Fig. 6.10). show some significant differences. The increased geomorphic complexity of the coastline results in more trapping of the oil and notably less transport of water surface oil to the east by day 5. The comparison to the observed limit of oil after day 4.5 is not nearly as good as under the previous. macroscale test case. By day 10, however, distributions of offshore oil between the two macroscale cases are again similar and remain so thereafter.

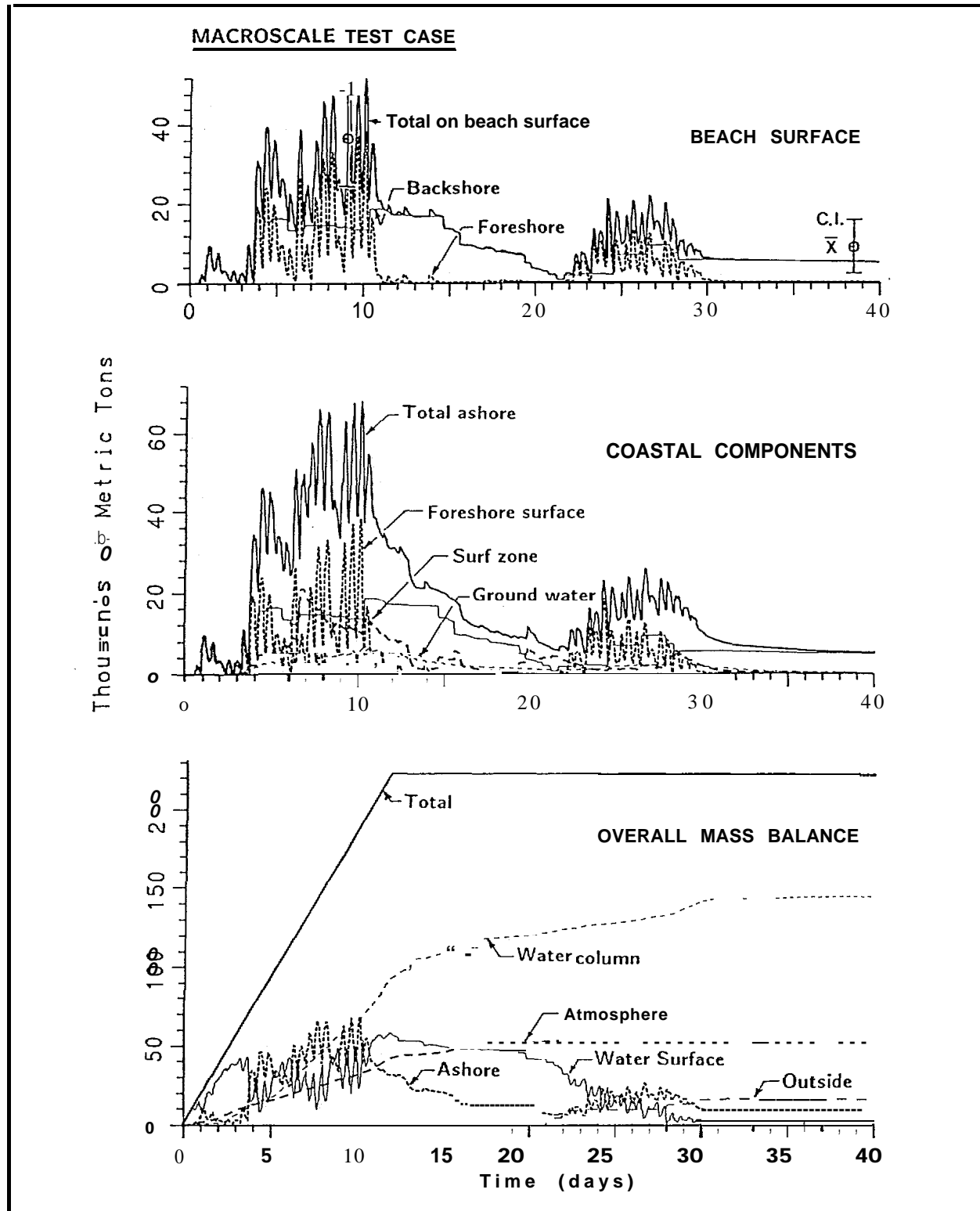


FIGURE 6.11. Dynamic mass balances (overall, coastal components, and beach surface) for oil associated with the macroscale test case. A second heavy oiling of the shoreline, reflected in the observations but not in the mesoscale test results, is visible between days 23 and 28. Observed values of oil quantity on the shoreline and 95 percent confidence intervals are indicated in the upper diagram.

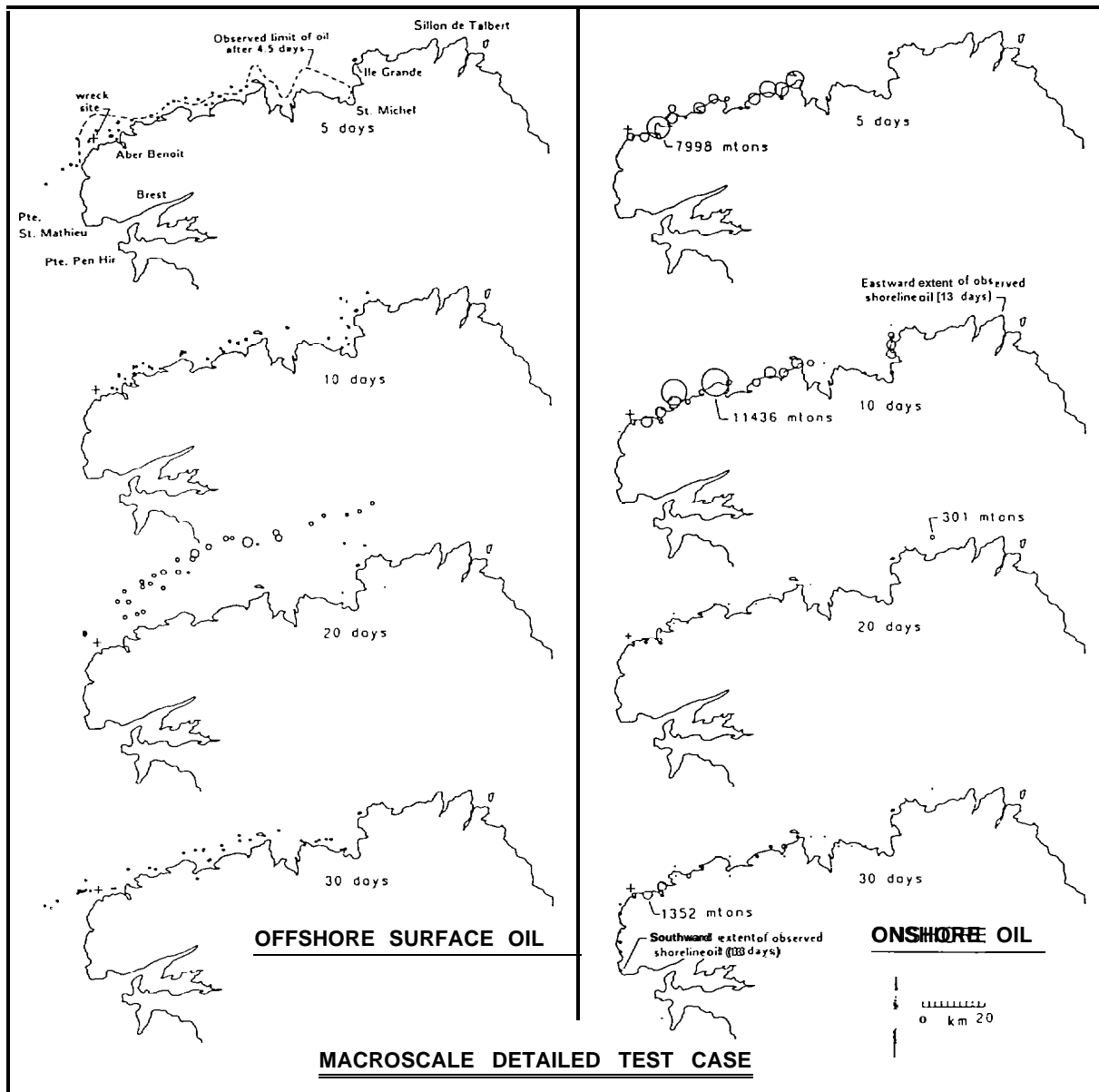


FIGURE 6.12. Distribution of offshore surface oil and onshore oil (foreshore, surface, and backshore) for the macroscale detailed test case. Offshore, circles indicate computed areal coverage of thick oil. Onshore, circles are proportional to the oil mass associated with each grid cell. The maximum value for each time plot is given.

Comparison of the two modeled distributions of onshore oil (Figs. 6.10 and 6.12) reflect some of the same differences as those seen in the comparison of oil on the water surface. The more detailed shoreline case (Fig. 6.12) shows more oil near the spill site at 5 days, and none reaching even close to the St. Michel area to the east. At 10 days, concentrations of oil near the source are about twice as large in the more complex case as in the simpler macroscale case (11,436 mt versus 5,182 mt; Figs. 6.12 and 6.10, respectively). At day 20, however, the situation is reversed, with the simple case showing a higher maximum value. At day 30, the distributions are nearly comparable, although the more detailed case again shows a higher maximum value.

The overall extent of oiled shoreline in both directions from the wreck site is similar for the two macroscale test cases (Figs. 6.10 and 6.12). The southernmost limit of both cases are in agreement with observations, although at 30 days some shoreline impacts are evident at Pointe de Pen Hir, south of Brest. To the east, both cases fail to show the easternmost impacts observed at Sillon de Talbert, being about 30 km short. Again, insufficient hydrodynamics are probably the cause.

Dynamic mass balances of oil quantity

The third model test, with more coastal detail near the spill site, resulted in mass balances similar to those for the simpler macroscale test (Figs. 6.13 and 6.11). A slightly higher amount of total oil ashore is retained in the macroscale detailed case (79,000 versus 68,000 ret). Likewise, the total on the beach surface is also somewhat higher (approximately 57,000 mt versus 50,000 mt) for the macroscale detailed case, but still conforms to estimated oil quantities at the time of the spill. None of these global mass-balance figures indicates any substantial change in model performance due to the added complexity in the coastal representation.

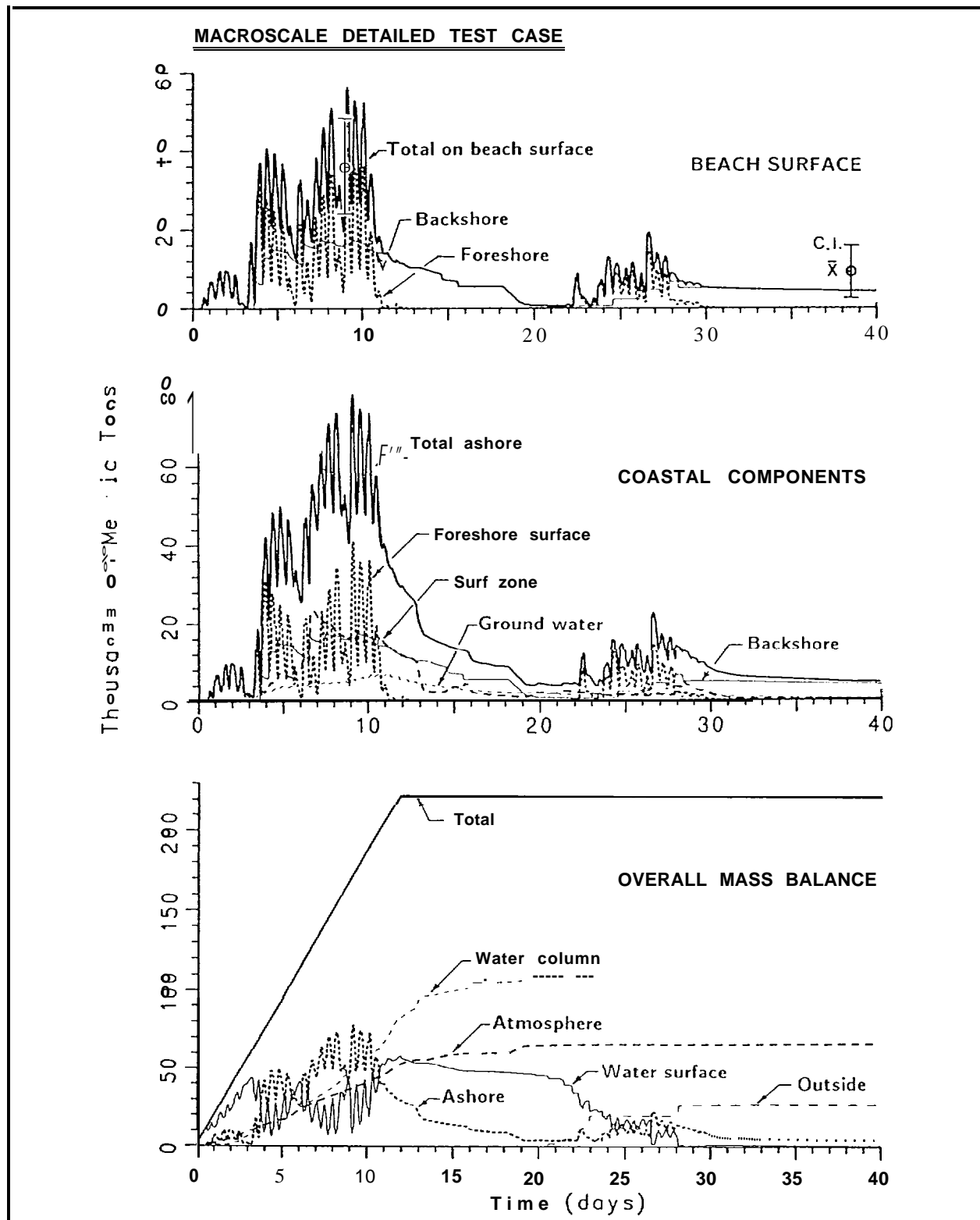


FIGURE 6.13. Dynamic mass balances (overall, coastal components, and beach surface) for oil associated with the macroscale detailed test case. Observed values of oil quantity on the shoreline and 95 percent confidence intervals are indicated in the upper diagram.

6.5 CONCLUSIONS

Three test cases of the COZOIL model against the *Amoco Cadiz* data set have been performed. In general, the model has effectively reproduced the offshore and onshore distribution of the *Amoco Cadiz* oil spill and realistically predicted mass-balance distributions, considered from a variety of viewpoints. All three test cases reflect the lifting of oil off the intertidal beach surface and its redeposition on a falling tide under appropriate wind conditions. Differences between the model test cases are discussed below.

The mesoscale test case, with relatively detailed resolution of the coastline adjacent to the site appropriately illustrated onshore and offshore surface oil distributions, but generally placed too much oil onshore, probably due to a lack of correct hydrodynamics at a similar spatial scale. The limited boundaries also inhibited the model from effectively reproducing the subsequent redeposition of oil after being transported offshore by winds. On a very fine scale of 0.5 km, the model reproduced the general variance noted in the *Amoco Cadiz* spill incident, and came relatively close to observed values at three particular stations. Variations in oil quantities onshore within specific grid cells can be lessened by grouping together oil within the grid cells composing the same shoreline reach.

The macroscale test case, using only 11 shoreline segments over the entire area, generally portrayed the overall distribution of offshore and onshore oil quite well, although falling about 30 km short in the eastern migration of the oil, probably due to inaccurate hydrodynamics. The mass balance of onshore oil quite realistically depicts the actual spill case and compares well with observations.

The macroscale detailed case, containing additional coastal segments within the macroscale shoreline model, shows slightly less accuracy in overall spill distributions because oil tends to remain within the indentations of the coast, probably due to the lack of accurate hydrodynamics at the same operational scale. Once oil is eventually freed from these sites, few differences between the two macroscale cases are observed. Offshore and onshore distributions are similar in range, although quantities of oil within particular grid cells vary substantially between tests. The total quantity of oil on the beach surface and ashore achieves slightly higher maxima under the macroscale detailed case, although still comparing well to observational data.

In terms of COZOIL model formulation, these test cases indicate that the proper selection of shoreline scale is particularly important. As discussed further in the COZOIL user's manual, hydrodynamics must also be accurate to the same scale as coastal resolution. Irregularities in the coastline appropriately trap oil, but if hydrodynamic conditions are not resolved to the same scale or are inadequate for the area (e.g., inaccurate or nonexistent estuarine flushing), then the release rate of oil from these localities may be artificially slow.

7.0 COMPATIBILITY OF COZOIL WITH RELATED MMS TRANSPORT MODELS

COZOIL has been programmed to be as flexible as possible in regard to linkages with other models used by MMS for oil spill transport. Specifically, COZOIL will accept as input hydrodynamic data created by any two- or three-dimensional model. If the hydrodynamic model grid does not overlay that of the COZOIL application, then an interpolation procedure must be supplied by the user.

COZOIL will also accept oil spill initialization data from any offshore oil spill model which represents surface oil in discrete batches or spinets and an array of mass/boiling point fractions. The prototype for the oil representation is that described in Paine et al. (1984) and incorporated into the weather/hydrodynamics/sea ice/oil spill mass-transport model system developed and applied by Spaulding et al. (1986, 1988a, b). In addition, each spinet must have associated with it a geographical location. In general, the user must supply an intermediate processing program which converts offshore model coordinates to the COZOIL application coordinates and which creates an input file compatible with the format anticipated by COZOIL in subroutine NEWOILIN_OFFSHORE.

8.0 SUMMARY AND RECOMMENDATIONS

A coastal zone oil spill model (COZOIL) has been designed, coded, and tested. The model incorporates a relatively detailed set of interacting oil fates and environmental processes in the coastal zone. Results of a hindcast of the *Amoco Cadiz* oil spill using this model bear a remarkable degree of similitude with observations from the actual event.

The model includes capabilities for developing deterministic, zeroth, and first-order Markov process winds. Waves are computed from the wind record, or input by the user. Wave computations include refraction, diffraction, breaking, phase transformations, runup, and setup. Capabilities are also included which allow the user to create tidal and wind-driven hydrodynamic data sets. Thus the model is really an expert system, allowing a user to simulate a complete oil spill scenario, in either stochastic or deterministic mode. No auxiliary software or models are necessary, although COZOIL allows for coupling to exterior hydrodynamic models.

Oil-fates processes simulated offshore include spreading, evaporation, entrainment, emulsification, and advection of both surface and subsurface oil. Spreading of oil inside the surf zone is modified to allow compression of the slick transverse to the shoreline. The waves contribute to longshore transport in the surf zone based on radiation stress concepts. Oil-fates processes simulated onshore include deposition on the beach foreshore or backshore surface, depending on tide height. Oil deposited on the backshore is subject to continued evaporation and may be returned to the surf zone during subsequent high-water events. Oil on the foreshore surface may also penetrate into the sediments, eventually reaching the beach ground water system. Removal from the groundwater is generally the slowest process simulated and occurs during ebb tides. All of these control processes are computed up and down the modeled coastline, as long as oil is present.

The model outputs include boiling-point cut information, overall mass balance, and line plots showing the location of surface and a longshore oil distributions. Other physical parameters such as the depth and shoreline grids and wave and current fields can be displayed. COZOIL is inherently deterministic with respect to results from any single simulation. Stochastic oil-distribution estimates are produced by combining the results of multiple simulations under a statistical analysis subroutine.

COZOIL was tested against prototype data for wave predictions using Bristol Bay field data obtained by the study team in August-September 1986. Results indicate the

model produces realistic approximations of wave height, wave period, and approach angle from a local or offshore wind field.

Three hindcast tests were also performed against data from the 1978 *Amoco Cadiz* oil spill off Brittany, France. Tests were conducted at two scales or levels of grid resolution:

- 1) A mesoscale area (20x40 km) near the wreck site.
- 2) A macroscale area (1 OOX175 km) encompassing virtually the entire shoreline impact area.

A third test was performed which combined fine resolution near the spill site with coarse resolution farther away. The mesoscale test case overestimated the quantity of oil onshore but reproduced the general variance and distribution of oil. Model and prototype differences are considered to be due to the complexity of the shoreline in question and limitations of the hydrodynamic algorithms at these spatial scales. The macroscale test cases provided less resolution because of grid-cell size, but reproduced the overall distribution of offshore and onshore oil quite well. The mass balance of onshore oil realistically depicts the actual spill case and compares well with observations.

Our work with the model has highlighted several areas in which future improvements should be made. First, the model requires as input a set of nine parameters for each coastal reach or segment used to define the coastline during a simulation. Manual entry of these parameters for a complex coastline is an error-prone process, and requires time consuming proofreading for each application. A graphic mapping program to allow visual comparison of input coastlines with the original coast would greatly facilitate error-checking.

The oil spill hindcast tests also revealed that model performance, as measured by the degree of similitude between model results and observations, can be degraded by either over- or under-resolving the coastline. Proper resolution must be determined by the variability of the coastal geomorphology and the resolution of the hydrodynamic input to the model. The determination of a proper resolution level for a particular application is therefore an iterative process requiring the creation of several coastal reach parameter files for model tests. A significant improvement to COZOIL would therefore consist of an auxiliary set of software which would allow facile setup of underlying databases to assist in applications.

COZOIL is not presently capable of simulating oil spill behavior in the presence of ice. This is potentially a significant shortcoming vis-a-vis application in Alaskan coastal waters. Sufficient knowledge exists to include oil/ice interactions in the model, should this be desired in the future.

The coastal zone oil spill model described here is a composite of concepts and algorithms drawn from a variety of disciplines. Some of these numerical representations are well established in the relevant literature; others are relatively new and hypothetical. Where established algorithms have been used, as for example in the computation of oil penetration rates into beach sediments, tests of the code have been performed to assure that the implementation produces results which are comparable with available observations. Where new algorithms have been developed or concepts have been applied in new ways, tests against empirical data are even more important. Unfortunately, such data have not always been available: future experimental work may be indicated in such cases.

COZOIL incorporates a modification to the radial spreading equation of Fay (1971) and Hoult (1972) as recast by Mackey et al. (1980). This modification allows a circular slick which contacts the shoreline to become elliptical, with the dynamics of the minor axis being governed by a force balance between the onshore component of the wind stress and the spreading force. The rate of onshore/offshore foreshortening is proportional to a drag coefficient. As no data have been identified in the literature to establish foreshortening rate as a function of wind speed, the drag coefficient has been set equal to an established value for wind on water. The resulting behavior of the algorithms has been reported and appears reasonable, but empirical support would strengthen this aspect of the model. The onshore/offshore foreshortening and a longshore spreading of oil spinets affect the evaporation rate through the surface area, the entrainment rate through the thickness, and the deposition rate on the coastline through both the longshore and transverse dimensions of the slick.

All of the algorithms for deposition of oil from a surface slick onto a shoreline are new. Results of model tests compare well with overall mass-deposition estimates. It would be useful to plan and prepare a study to observe and record dynamic deposition rates through several tidal cycles during spills of opportunity. In cases for which coastal cleanup is not subsequently undertaken, studies of penetration rates, long-term retention rates, and detailed observations of oil behavior within the beach groundwater system would also strengthen the model.

The wind-driven hydrodynamic component presently incorporated into COZOIL could be improved by the inclusion of a surface slope term in the governing equations. For interactive use, only a one-dimensional model such as that developed by Hubertz (1987) is computationally reasonable. This means that conservation of water mass will not be assured between the offshore areas associated with adjoining reaches. The wind-driven hydrodynamic model component has the most marked effect on the transport of subsurface entrained hydrocarbons outside the surf zone. Since the physical location of these hydrocarbons is essentially irrelevant to the distribution of oil along the coastline, an update of this aspect of COZOIL would seem to carry a relatively low priority.

An empirical mass-transfer equation is incorporated into the model to reflect the observation that wave exposure is an important parameter in determining removal rates for oil on the foreshore surface (Owens, et al., 1983, 1987; McLaren, 1984). This equation was originally designed for less turbulent regimes than are typical in the marine surf zone. An adjustment in the proportionality constant was made here to reproduce more accurately the observational data on removal rates which are available (CSE/ASA/BAT, 1986). As part of the previously suggested studies using spills of opportunity, some carefully quantified measures of removal rates as a function of beach and wave parameters would be useful.

REFERENCES

- Andersen, J. W., et al. 1984. Recommended methods for testing the fate and effects of dispersed oil in marine sediments. In T.E. Allen (cd.), *Oil Spill Chemical Dispersants: Research, Experience, and Recommendation*, STP 840, ASTM, Philadelphia.
- Anonymous. 1973. Evaluation of the world's important crudes. The Petroleum Publ. Co., Tulsa, Okla., 77 pp.
- Audunson, T. 1979. Fate of oil spills on the Norwegian continental shelf. In Proc. 1979 Oil Spill Conf., API Publ. No. 4308. American Petroleum Inst., Wash., D.C.
- Basin, N. J., and T. Ichiye. 1977. Flocculation behavior of suspended sediment and oil emulsions. *Jour. Seal. Petrol.* Vol. 47(2), pp. 473-484.
- Battjes, J.A. 1974. Surf similarity. In Proc. 14th Conf. Coastal Eng., ASCE, New York, N. Y., pp. 466-480.
- Berne, S. 1982. Vielle ecologique vulnerability morpho-sedimentaire du littoral aux pollutions par hydrocarbures de la Pointe Saint-Mathieu au Sillon du Talbert, 47 pp.
- Berridge, S. A., R. Dean, R. Fallows, and A. Fish. 1968a. The properties of persistent oils at sea. In P. Heggge (cd.), *Symp. on Scientific Aspects of Pollution of the Sea by Oil*, pp. 2-11.
- Berridge, S. A., M. Thew, and A. Loriston-Clarke. 1968b. The formation and stability of emulsions of water in crude petroleum. *Jour. Inst. Petrol.*, Vol. 54, pp. 333-357.
- Berkhoff, J.C.W. 1972. Computation of combined refraction- diffraction. In Proc. 13th Intl. Conf. on Coastal Engineering, ASCE, Vol. 1, pp. 471-490.
- Berkhoff, J. C., N. Booy, and A. Radder. 1982. Verification of numerical wave propagation models for simple harmonic linear water waves. *Coastal Eng.* Vol. 6, pp. 255-279.
- Brenninkmeyer, B.M. 1974. Sediment concentration changes in the surf zone. *Mem. Inst. Geol. Bassin Aquitaine*, No. 7. pp. 115-118.
- Brenninkmeyer, B.M. 1976. Sand fountains in the surf zone. In R.A. Davis, Jr., and R. Ethington (eds.), *Beach and Nearshore Sedimentation*, SEPM Spec. Publ. 24, pp. 69-91.
- Buist, I.A. 1987. A preliminary feasibility study of in-situ burning of spreading oil slicks. In Proc. 1987 Oil Spill Conference, Amer. Petrol. Inst., Wash., D. C., pp. 359-367.
- Buist, I. A., and E.M. Twardus. 1984. In-situ burning of uncontained oil slicks. In Proc. Seventh Annual Arctic Marine Oil Spill Program, pp. 127-154.
- Calder, J., J. Lake, J. Laseter. 1978. Chemical composition of selected environmental and petroleum samples from the Amoco *Cadiz* oil spill. In W. Hess (cd.), *The Amoco Cadiz Oil Spill*, NOAA/EPA Special Report, U.S. Govt. Printing Office, Wash., D. C., pp. 21-84.
- CERC. 1984. Shore protection manual. Vol. 1, U.S. Army Corps of Engineers, Coastal Engineering Research Center, Ft. Belvoir, Vir.
- CNEXO. 1981. *Amoco Cadiz*, Fates and Effects of the Oil Spill. Centre National pour l'Exploitation des Ocans. Brest, France. 881 p.
- CNEXO, IFP, and IGN. 1978. *Amoco Cadiz*, teledetection des pollutions par hydrocarbures, rapport preliminaire, Centre National pour l'Exploitation des Oceans, Paris, 9 maps.
- Convery, M.P. 1971. The behavior and movement of petroleum products in unconsolidated surficial sediments. *Natl. Wild. Fed. and Amer. Petrol. Inst.* 212 pp. + appendices.

- Csanady, G .T. 1973. Turbulent diffusion in the environment. D. Reidel Publ. CO.. Boston. Mass.. 248 pp.
- CSE/ASA/BAT. 1986. Development of a coastal oil spill SMEAR model: Phase 1. Analysis of available and proposed models. Report to U.S. Dept. Interior, MMS: Coastal Science & Engineering, Inc., Applied Science Associates, Inc., and Battelle New England Marine Research Laboratory, Contract 14-12-0001-30130, 121 pp.
- Dally, W.R. 1980. A numerical model for beach profile evaluation. Master's Thesis, University of Delaware, Newark, Del.
- Dally, W. R., R.G. Dean, and R.A. Dalrymple. 1984. Modeling wave transformation in the surf zone. Misc. Paper CERC-84-8, U.S. Army Engineer Waterways Experiment Station, Vicksburg, Miss.
- D'Ozouville, L., E.R. Gundlach, and M.O. Hayes. 1978. Effect of coastal processes on the distribution and persistence of oil spilled by the *Amoco Cadiz*--preliminary conclusions. Actes de Colloques, No. 6. COB-CNEXO, Brest, France, pp. 69-96.
- Ebersole, B. A., M.A. Cialone, and M.D. Prater. 1986. Regional coastal processes numerical modeling system. Report 1. RCPWAVE - A Linear Wave Propagation Model for Engineering Use. Dept. of the Army, Waterways Experiment Station, Vicksburg, Miss., 71 pp. + appendices.
- Economic Analysis and Applied Science Associates. 1987. Measuring damages to coastal and marine natural resources: concepts and data relevant for CERCLA Type A. Damage Assessments. Report to CERCLA 301 Project, U.S. Department of Interior. Washington, D. C., 2 vols. + 4 floppy disks.
- Emery, K. O., and J.F. Foster. 1948. Water table in marine beaches. Jour. Marine Res., Vol. 7, pp. 644-654.
- Fay, J.A. 1971. Physical processes in the spread of oil on a water surface. In Proc. 1971 Oil Spill Conf., Amer. Petrol. Inst., Wash., D. C., pp. 463-467.
- Finkelstein, K., and E.R. Gundlach. 1981. Method of estimating spilled oil quantity on the shoreline. Environ. Sci. & Technol., Vol. 15, pp. 545-549.
- Ford, R.G. 1983. Oil slick sizes and length of coastline affected: a literature survey and statistical analysis. Final Report to U.S. Dept. Interior, MMS Contract No. 14-12-0001-30226, 34 pp.
- Gait, J., 1978. Investigations of physical processes. In W. Hess (cd.), *The Amoco Cadiz Oil Spill*, NOAA/EPA Special Report, U.S. Govt. Printing Office, Wash., D.C., pp. 7-20.
- Galvin, C. J., Jr. 1968. Breaker type classification on three laboratory beaches. Jour. Geophys. Res., Vol. 73(12), pp. 3651-3659.
- Gundlach, E.R. 1982. Ecological study of the *Amoco Cadiz* oil spill, part 1. Report of the N OAA/CNEXO Joint Scientific Commission, U.S. Dept. Commerce. 478 pp.
- Gundlach, E.R. 1987. Oil holding capacities and removal coefficients for different shoreline types to computer simulate spills in coastal waters. In Proc. 1987 Oil Spill Conference. Amer. Petrol. inst., Wash., D.C., pp. 451-457.
- Gundlach, E. R., and M.O. Hayes. 1978. Investigations of beach processes. In W. Hess [cd.], *The Amoco Cadiz Oil Spill*. NOAA/EPA Special Report. U.S. Govt. Printing Office, Wash.. D. C., pp. 85-196.
- Gundlach, E. R.. and M. Reed. 1986. Quantification of oil deposition and removal rates for a shoreline/oil spill interaction model. In Proc. Ninth Arctic Marine Oil Spill Conf., Edmonton, Alberta, pp. 65-76.

- Gundlach, E. R., P.D. Boehm, M. Marchand, R.M. Atlas, D.M. Ward, and D.A. Wolfe. 1983. The fate of *Amoco Cadiz* oil. *Science*, Vol. 221, pp. 122-129.
- Harm, R., L. Rice, M. Trujillo, and H. Young. 1978. Oil spill cleanup activities. In W.N. Hess (cd.), *The Amoco Cadiz Oil Spill*. pp. 229-276.
- Harper, J. R., G.A. Miskulin, D.R. Green, D. Hope, J. Vandermeulen. 1985. Experiments on the fate of oil in low energy marine environments. In *Proc. Eighth AMOP Conference*, pp. 383-399.
- Harris, T. F. W., J.M. Jordan, W.R. McMurray, C.J. Vervey, and F.P. Anderson. 1962. Mixing in the surf zone. In *Proc. Intl. Conf. on Water Pollution Res.*, London.
- Hayes, M.O. 1972. Forms of sediment accumulation in the beach zone. In R. Meyer (cd.), *Waves on Beaches and Resulting Forms of Sediment Accumulation*, Academic Press, New York, pp. 297-356.
- Hayes, M. O., E.H. Owens, D.K. Hubbard, and R.W. Abele. 1973. Investigations of form and processes in the coastal zone. In D.R. Coates (Ed.), *Coastal Geomorphology*, Proc. 3rd Annual Geomorphology Symposia Series, Binghamton, New York. pp 11-41.
- Hess, W.N. (cd.). 1978. *The Amoco Cadiz oil spill*. NOAA/EPA Special Report, U.S. Govt. Printing Office, Wash., D. C.. 281 pp. + 66 plates.
- Holoboff, A. and R. Foster. 1987. Saturation/penetration of Norman Wells crude oil into Ukalerk borrow pit sand. In *Proc. 10th AMOP Seminar*, pp. 63-78.
- Horikawa, K., and C. Kuo. 1966. A study of wave transformation inside the surf zone. In *Proc. 10th Intl. Conf. on Coastal Eng.*, ASCE, pp. 217-233.
- Horikawa, K. 1978. *Coastal engineering — an introduction to ocean engineering*. Univ. Tokyo Press. Japan, 402 pp.
- Hoult, D.P. 1972. Oil spreading on the sea. *Ann. Rev. Fluid Mech.*, pp. 341-368.
- Hubertz, J.M. 1987. A wind- and wave-driven nearshore current model: the one-dimensional model. Dept. of the Army, Coastal Engineering Research Center, Vicksburg, Miss., NTIS AD-A178 751, 24 PP.
- Isumiya, T. 1984. A study of wave and wave-induced nearshore currents in the surf zone. Ph.D. Dissertation, Univ. Tokyo, Japan.
- Iwata, K., and T. Sawaragi. 1982. Wave deformation in the surf zone. *Memoirs of the Faculty of Engineering*, Vol. 34 (2), Nagoya University, Nagoya, Japan, pp. 239-283.
- Jassman, G., and W. Gunkel. 1983. Long term investigations on chemical and microbial changes of a slightly oil polluted beach. In *Proc. 1983 Oil Spill Conf.*, Amer. Petrol. Inst., Wash., D. C., p. 479-483.
- Kana, T.W. 1976. A new apparatus for collecting simultaneous water samples in the surf zone. *Jour. Seal. Petrol.*, Vol. 46, pp. 1031-1034.
- Kana, T.W. 1977. Suspended sediment transport at Price Inlet, South Carolina. In *Proc. Coastal Sediments '77 Conf.* (Charleston, S.C.), ASCE, New York, N. Y., pp 366-382.
- Kana, T.W. 1979. Suspended sediment in breaking waves. Tech. Rept. No. 18-CRD, Coastal Res. Div., Dept. Geol., USC, Columbia, 153 pp.
- Kozo, T.L. 1985. Wave hindcast statistics for the Hope Basin, North Chukchi and South Chukchi areas. Annual Report to MMS (Contr. No. NA84-ABC-00174), Occidental College, Los Angeles, CA, 78 pp.

- Krumbein, W. D., and G.D. Munk. 1943. Permeability as a function of size parameters of unconsolidated sands. *Trans. AIME*, Vol. 151, pp. 153-163.
- Kullenberg, G. (cd.). 1982. Pollutant transfer and transport in the sea. Vol. I. CRC Press, Boca Raton, Fla., 227 pp.
- Liss, P., and P. Slater. 1974. Flux of gases across the air-sea interface. *Nature*, Vol. 247, pp. 181-184.
- Liu, H., and J. Lin. 1979. Effects of an oil slick on wind waves. In *Proc. 1979 Oil Spill Conf.*, API Publ. No. 4308, American Petroleum Inst., Wash., D. C., pp. 665-674.
- Longuet-Higgins, M.S. 1970. Longshore currents generated by obliquely incident sea waves. *Jour. of Geophysical Res.*, Vol. 75(33), pp. 6778-6801.
- Lyman, W. J., W.F. Reehl, and D.H. Rosenblatt. 1982. Handbook of chemical property estimation methods. McGraw-Hill Book Co., N. Y., 900 pp.
- Mackay, D., and R.S. Matsugu. 1973. Evaporation rates of liquid hydrocarbon spills on land and water. *Can. Jour. Chem. Eng.*, Vol. 51, pp. 434-439.
- Mackay, D., I. Buist, R. Mascaraenas, and S. Paterson. 1980. Oil spill processes and models. Report EE-8 to Environment Protection Service, Ottawa: Univ. Toronto, Ontario, Canada.
- Mackay, D., W.Y. Shiu, K. Hossain, W. Stiver, D. McCurdy, S. Paterson, and P. Tebeau. 1982. Development and calibration of an oil spill behavior model. U.S. Coast Guard Research and Development Center. Contr. No. DT CG-39-81-C-80294, Rept. No. CG-D-27-83, 83 pp.
- McLaren, P. 1984. The Whytecliff oil spill, British Columbia: sediment trends and oil movement on a beach. *Spill Tech. Newsletter* 9(2), pp. 11-19.
- McLaren, P. 1985. Behavior of diesel fuel on a high energy beach. *Mar. Poll. Bull.*, Vol. 16(5), pp. 191-196.
- Michel, J., D.D. Domeracki, L.C. Thebeau, C.D. Getter, and M.O. Hayes. 1982. Sensitivity of environments and wildlife to spilled oil of the Bristol Bay area of the Bering Sea, Alaska. 117 pp. + 64 maps.
- Miller, R.L. 1976. Role of vortices in surf-zone prediction: sedimentation and wave forces. In R.A. Davis, Jr., and R. Ethington (eds.), *Beach and Nearshore Sedimentation*, SEPM Spec. Publ. 24, pp. 92-114.
- Mooney, M. 1951. The viscosity of a concentrated suspension of spherical particles. *Jour. Colloidal Science*, Vol. 10, pp. 162-170.
- NOAA/CNEXO. 1982. Ecological study of the *Amoco Cadiz* oil spill: Part 1. E. Gundlach (cd.), Report of the NOAA/CNEXO Joint Scientific Commission., U.S. Dept. Commerce, 478 pp.
- Nummedal, D., and M.F. Stephen. 1976. Coastal dynamics and sediment transportation, northeast Gulf of Alaska. Tech. Rept. 9-CRD, Dept. Geol., Univ. South Carolina, Columbia, 148 pp.
- Okubo, A. 1971. Oceanic diffusion diagrams. *Deep Sea Research*, Vol. 8, pp. 789-802.
- O'Sullivan, A.J. 1978. The *Amoco Cadiz* oil spill. *Mar. Poll. Bull.*, Vol. 9, pp. 123-128.
- Owens, E., J. Harper, C. Foget, and W. Robson. 1983. Shoreline experiments and the persistence of oil on arctic beaches. In *Proc. 1983 Oil Spill Conference*, Amer. Petrol. Inst., Wash., D. C., pp. 261-268.

- Owens, E. H., W. Robson, B. Humphrey, D. Hope, and J. Harper. 1987. The fate of stranded oil four years after an experimental spill on sheltered gravel beach. In Proc. 1987 Oil Spill Conference.. Amer. Petrol. Inst., Wash., D. C., pp. 473-478.
- Payne, J. R., B.E.Kirstein, G.D.McNabb, J. Lanbach, R. Redding, R. Jordan, W. Horn, C. Deoliveira, G.S. Smith, D.M. Baxter, and R. Gragel. 1984a. Multivariate analysis of petroleum weathering in the marine environment-subarctic. In Environmental Assessment of the Alaska Continental Shelf: Final Report of Principal Investigators, Vol. 22, U.S. Dept. Commerce. NOAA/ NO S/OAD; U.S. Dept. Interior, MMS. Vol. II. appendices.
- Payne, J. R., B.E.Kirstein, G.D.McNabb, J. Lanbach, R. Redding, R. Jordan, W. Horn, C. Deoliveira, G.S. Smith, D.M. Baxter, and R. Gragel. 1984b. Multivariate analysis of petroleum in the marine environment-subarctic. U.S. Dept. Commerce, Vol. 21 of OCSEAP Final Reports, Juneau, Alaska.
- Payne, J. R., and C.R. Phillips. 1985. Petroleum spills in the marine environment: the chemistry and formation of water-in-oil emulsions and tar balls. Lewis Publishers, Inc., 148 pp.
- Perry, R. H., and C. Chilton. 1973. Chemical Engineering Handbook. 5th Edition, McGraw-Hill Book Co., New York, N.Y.
- Pollock, L. W., and W.D.Hummon. 1971. Cyclic change in interstitial water content, atmospheric exposure, and temperature in a marine beach. Limnol. and Oceanogr., Vol. 16, pp. 522-535.
- Reed, M., D. French, and S. Feng. 1988. The chemical data base for the CERCLA type A natural resource damage assessment model. Oil and Chemical Pollution Special Issue, in review.
- Reed, M., M.L. Spaulding, and P.C. Cornillon. 1980. An oil spill--fishery interfactional model: development and applications. Dept. Ocean Engineering, Univ. Rhode Island, 180 pp.
- Reed, M., M.L. Spaulding, E.R. Gundlach, T.W. Kana. 1986. Formulation of a shoreline/oil spill interaction model. In Proc. Ninth Arctic Marine Oil Spill Conf., Edmonton, Alberta, pp. 77-100.
- Seip, K. L., K.A.Brekke, K. Kveseth, and H. Ibrekk. 1986. Models for calculating oil spill damages to shores. Oil and Chemical Pollution, Vol. 3. pp. 69-81.
- Schneider, C. 1981. The littoral environment observation (LEO) data collection program. CETA Rept. 81-5, Coastal Engineering Research Center, U.S. Army Corps of Eng., Ft. Belvoir, Vir.
- Short, A.D. 1979. Wave power and beach stages: a global model. In Proc. 16th Intl. Conf. Coastal Eng., ASCE, New York, N. Y., pp. 1145-1162.
- SHOM. 1973. Courante de Maree de Dunkerque a Brest. Service Hydrographique et Oceanographique de la Marine. Brest, France. 20 pp.
- SHOM. 1978. Maree de Brest. Service Hydrographique et Oceanographique de la Marine, Brest, France, 6 pp.
- Smith, R. and T. Sprinks. 1975. Scattering of surface waves by a conical island. Jour. Fluid Mechanics, Vol. 72(2), pp. 373-384.
- Spaulding, M. L., K. Jayko, and E. Anderson. 1982a. Hindcast of the Argo *Merchant* spill using the URI oil spill fates model. Jour. Ocean Engineering, Vol. 9(5), pp. 455-482.
- Spaulding, M. L., T. Isaji, K. Jayko, and C. Turner. 1988a. Ocean circulation and oil spill trajectory simulations for Alaskan waters: spill trajectory simulations for Navarin Basin oil and gas lease sale number 107. Report to NOAA/OCSEAP, Anchorage, Alaska, 113 pp.
- Spaulding, M. L., T. Isaji, K. Jayko, and C. Turner, and D. Mendelssohn. 1988b. Ocean circulation and oil spill trajectory simulations for Alaskan waters: spill trajectory simulations for St. George Basin oil and gas lease sale number 101. Report to NOAA/OCSEAP, Anchorage, Alaska, 100+ pp.

- Spaulding, M. L., T. Isaji, E. Anderson, C. Turner, K. Jayko, and M. Reed. 1986. Oil spill trajectory and fates modeling for Shumagin Basin, Alaska. Report to NOAA/OCSEAP.
- Spaulding, M. L., S.B.Saila, M. Reed, C. Swanson, T. Isaji, E. Anderson, E. Lorda, V. Pigoga, K. Marti, J. Hoenig, H. Walker, F. White, R. Glazman, and K. Jayko. 1982b. Assessing the impact of oil spills on a commercial fishery. Final Report to MMS, Contr. No. AA851-CTO-75, NTIS No. PB83-149104.
- Stewart, R.J. 1976. The interaction of waves and oil spills. MIT Sea Grant Report No. MITSG75-22, NTIS No. PB262 458, 192 pp.
- Stive, M., and H. Wind. 1982. A study of radiation stress and setup in the nearshore region. Coastal Eng., Vol. 6, pp. 1-25.
- Stive, M. and H. Wind. 1986. Cross-shore mean flow in the surf zone. Coastal Eng., Vol. 10, pp. 325-340.
- Sunamura, T. and K. Horikawa. 1974. Two-dimensional beach transformation due to waves. In Proc. 14th Coastal Engineering Conf., ASCE, New York, N. Y., pp. 920-938.
- Sveum, P. 1987. Fate and effects of dispersed and non-dispersed oil on arctic mud flats. In Proc. 10th AMOP Seminar, pp. 149-167.
- Thibodeaux, L.J. 1977. Mechanisms and idealized dissolution modes for high density immiscible chemicals spilled in flowing aqueous environments. AI Che., Vol. 23(5), pp. 553-555.
- Thibodeaux, L.J. 1979. Chemodynamics. John Wiley and Sons, N. Y., 501 pp.
- Thornton, E. B., and R.T.Guza. 1982. Energy saturation and phase speeds measured on a natural beach. Jour. Geophysical Research, Vol 87(C12), pp. 9499-9508.
- Todd, D.K. 1959. Ground water hydrology. John Wiley & Sons, Inc., N. Y., 336 pp.
- Trask, P.D. 1939. Organic content of recent marine sediments. In P.D. Trask (cd.), Recent Marine Sediments, A Symposium; Dover Publications, N.Y. pp. 428-453.
- USDC. 1976. Tidal current tables: Pacific Coast of North American and Asia. U.S. Dept. Commerce, Nat'l Ocean Serv., Rockville, Md.. 255 pp.
- USDC. 1986. Tide tables: West Coast of North and South America. U.S. Dept. Commerce, Nat'l. Ocean Serv., Rockville, Md., 231 pp.
- Urish, D.W. 1987. Coastal groundwater outflow: solution to a dynamic problem. In Proc. Coastal Zone '87, ASCE, New York. N. Y., pp. 1837-1847.
- Vandermeulen, J. H., and J.H. Gordon, Jr. 1976. Reentry of 5-year old stranded bunker c fuel oil from a low-energy beach into the water, sediments, and biota of Chadabucto Bay, Nova Scotia. Jour. Fisheries Research Board Canada, Vol. 55(542), pp. 2002-2010.
- Weggel, J.R. 1972. Maximum breaker height. Jour. Waterways, Harbors, and Coastal Engineering Division, Vol. 78(WW4), pp. 529-548.
- Wright, L. D., and A.D. Short. 1983. Morphodynamics of beaches and surf zones in Australia. In P.D. Komar (cd.), Handbook of Coastal Processes and Erosion, CRC Press, pp. 35-64.

APPENDIX I
User's Manual
Model Documentation
(under separate cover)

APPENDIX II-A
Beach Profiles for 20 Beach Monitoring Stations
at Port Heiden, Alaska

Original surveys were in English units because survey instrumentation was set up for stadia measurements using English calibration. Graphics have been converted to metric units.

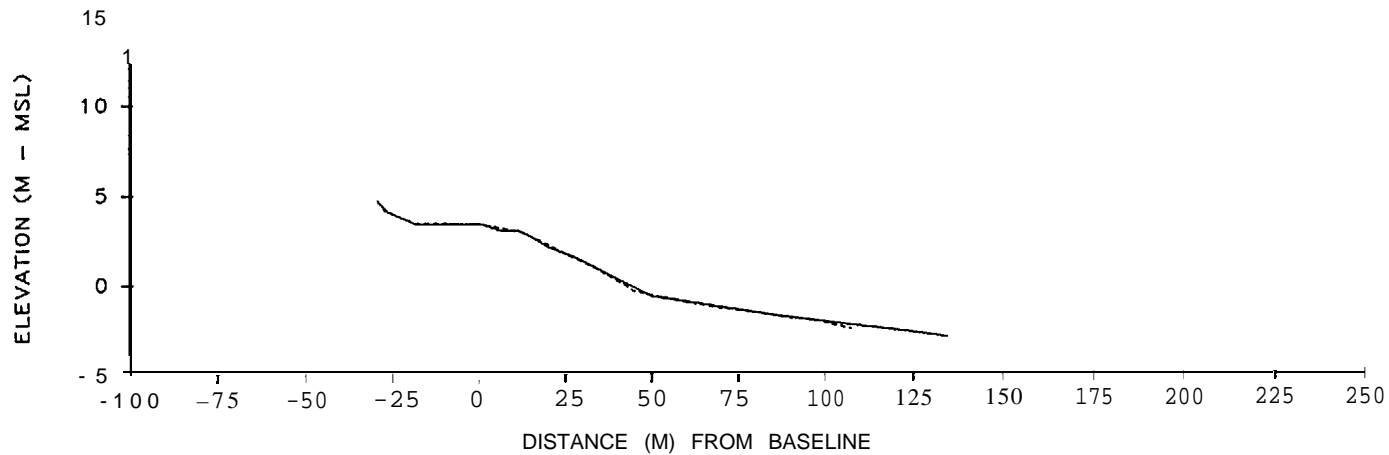
STATION 1 - NEAR FUEL TANKS

PH-1 21 AUG 86

.....

PH-1 10 SEP 86

————



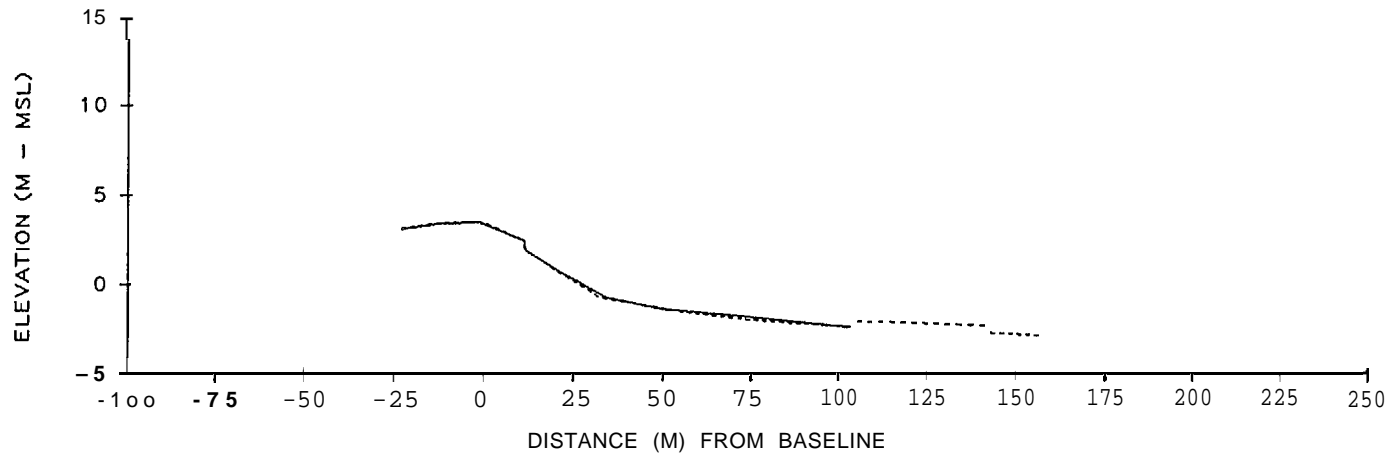
STATION 2 - IN COVE BEHIND SPIT

PH-2 21 AUG 86

.....

PH-2 10 SEP 86

————



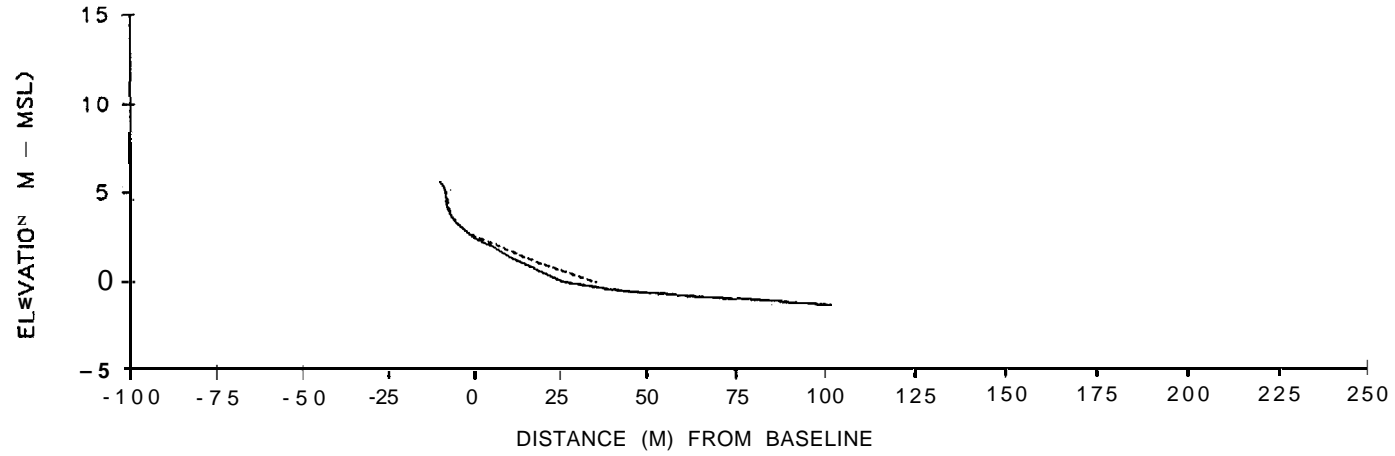
STATION 3 - {N COVE BEHIND SPIT

PH-3 21 AUG 86

.....

PH-3 10 SEP 86

————



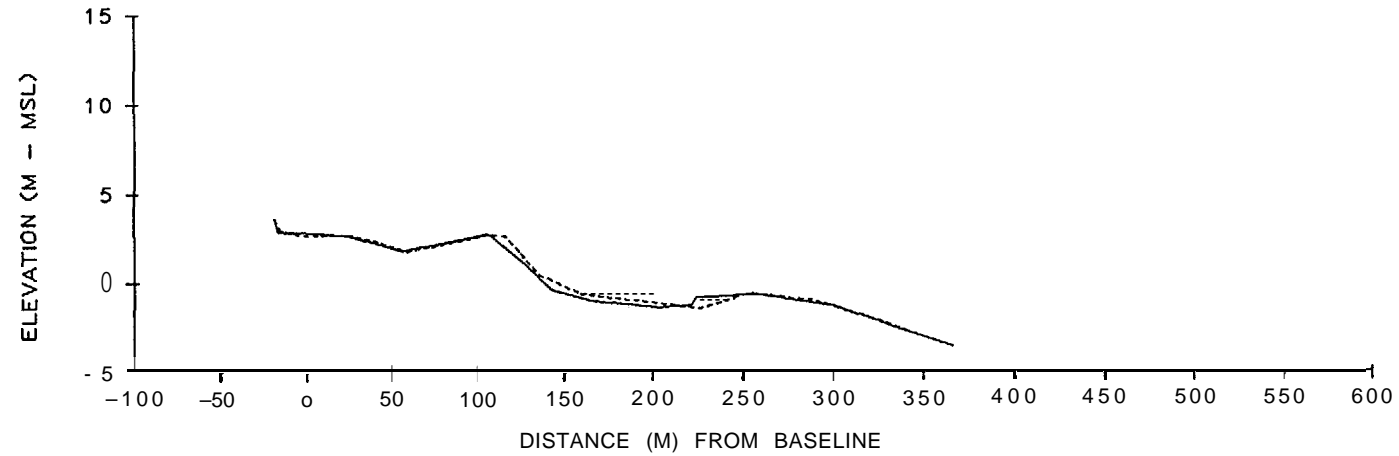
STATION 4 - ON RECURVED SPIT

PH-4 21 AUG 86

.....

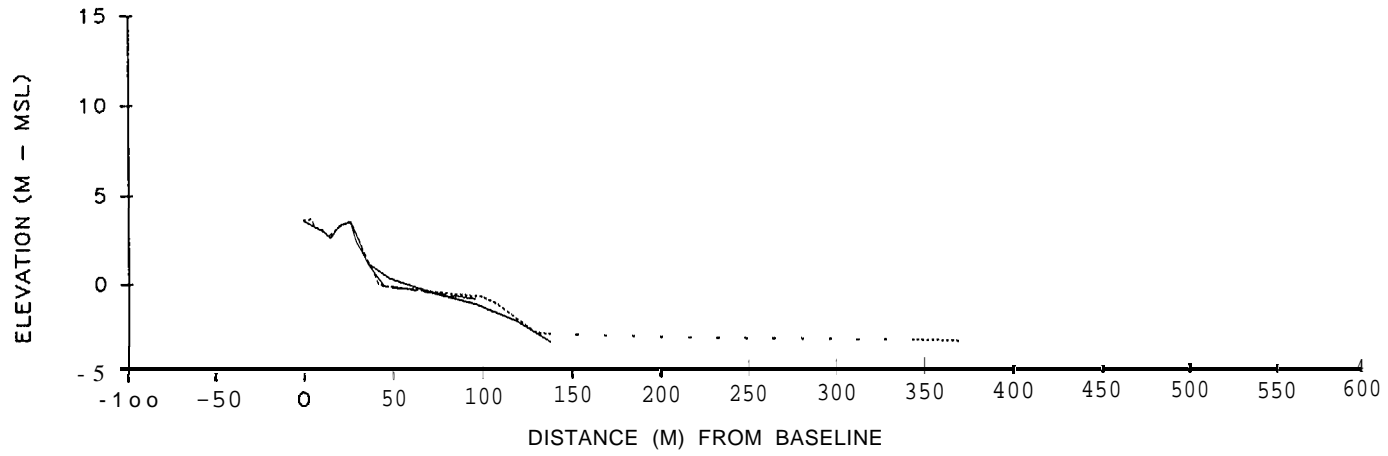
PH-4 10 SEP 86

————



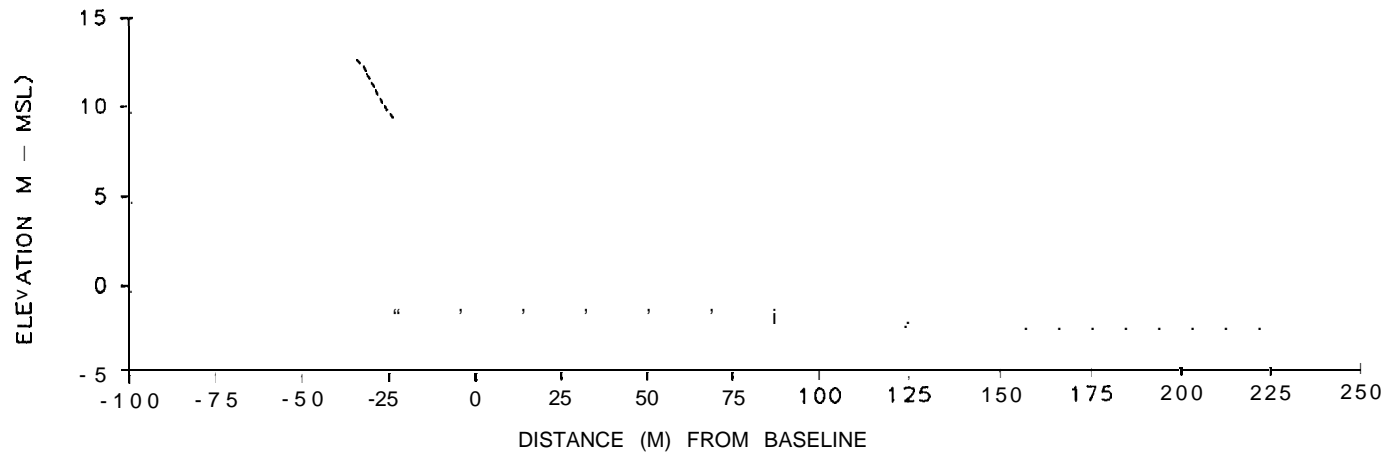
STATION 5 - NORTH OF SPIT

PH-5	19 AUG 86
PH-5	25 AUG 86	-----
PH-5	10 SEP 86	—————



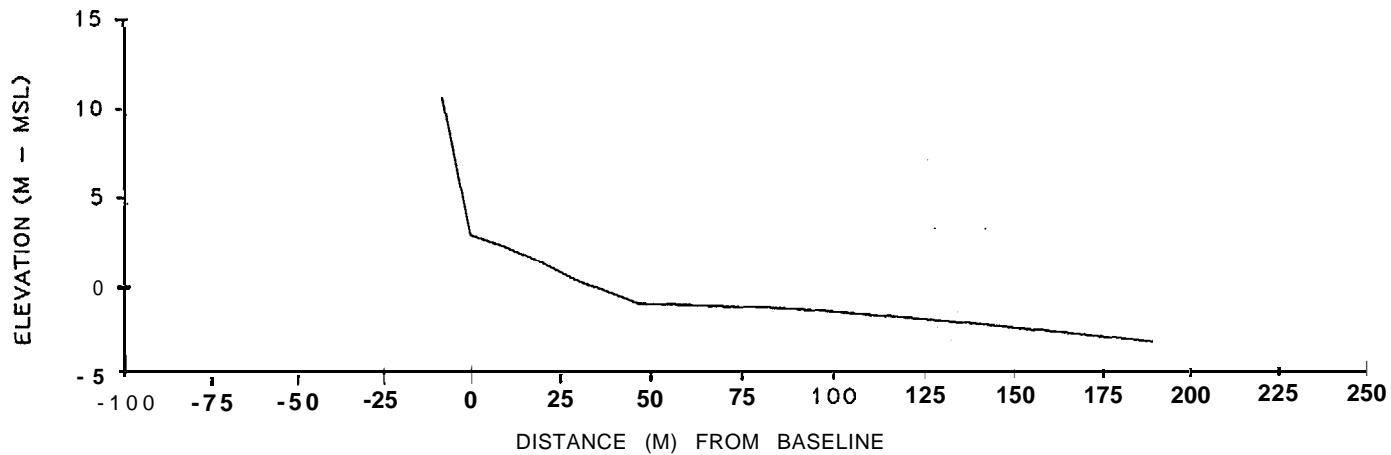
STATION 6 - MODERATE SLOPING BEACH

PH-6	21 AUG 86
PH-6	10 SEP 86	—————



STATION 7 - ERODING BLUFF

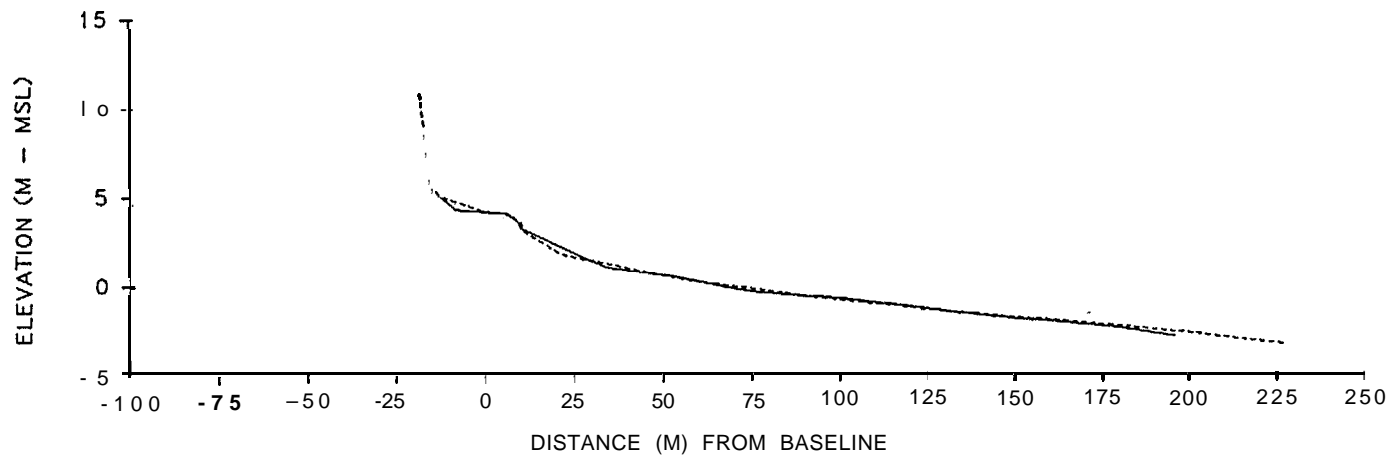
PH-7 21 AUG 86



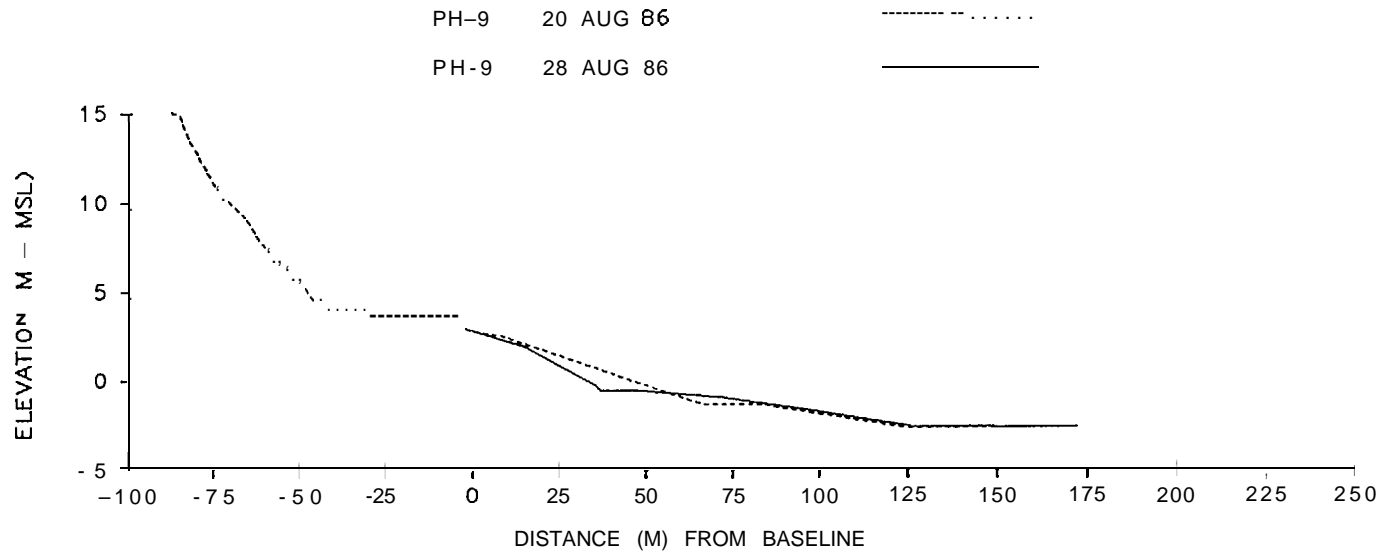
STATION 8 - ERODING BLUFF

PH-8 21 AUG 86

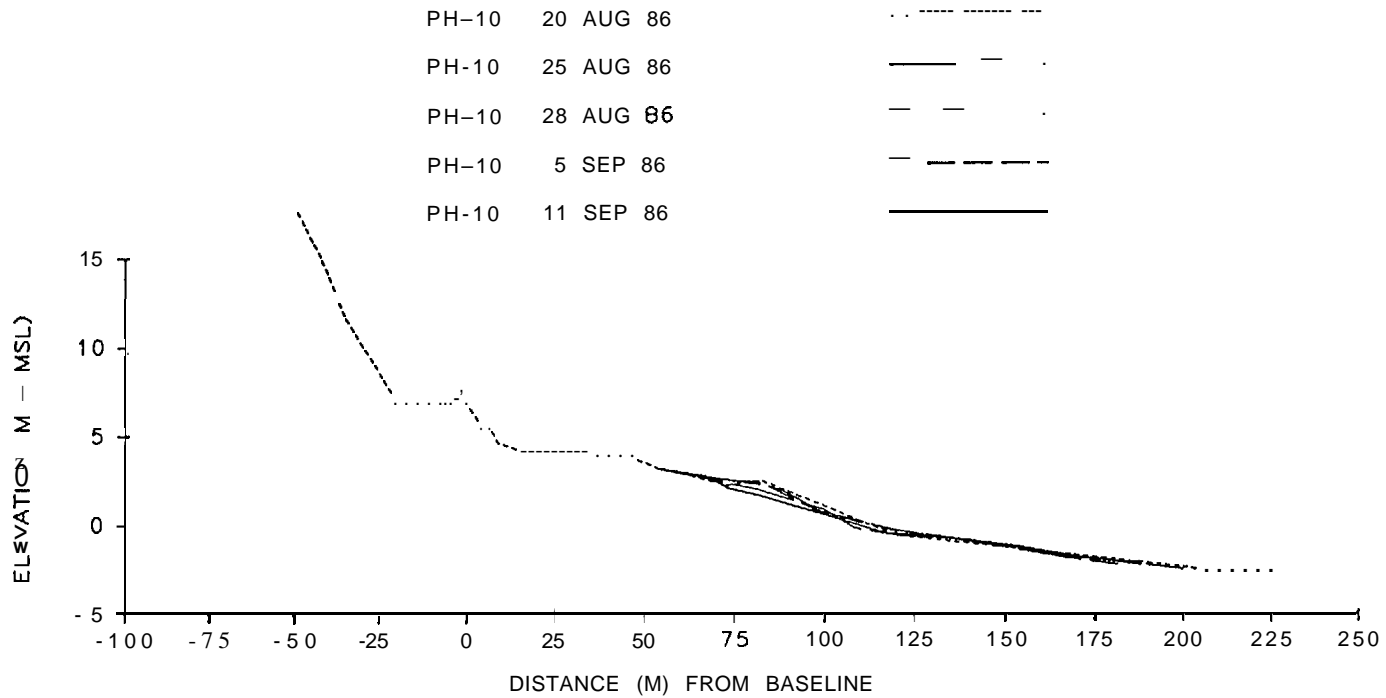
PH-8 11 SEP 86



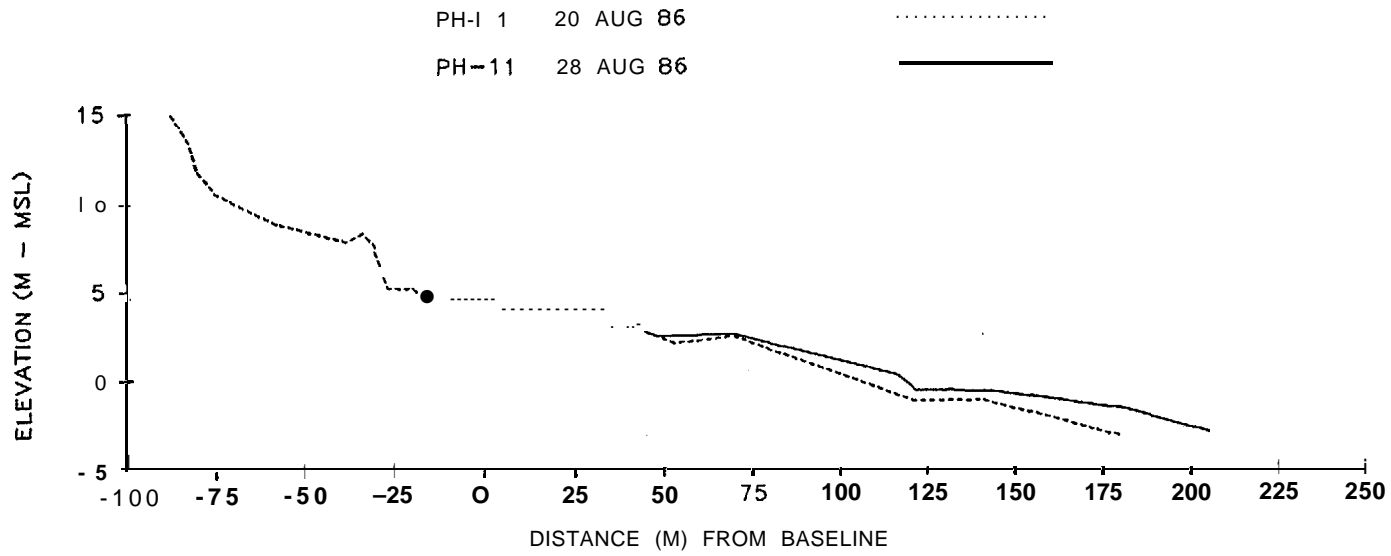
STATION 9 – 100 M SOUTH OF STATION 10



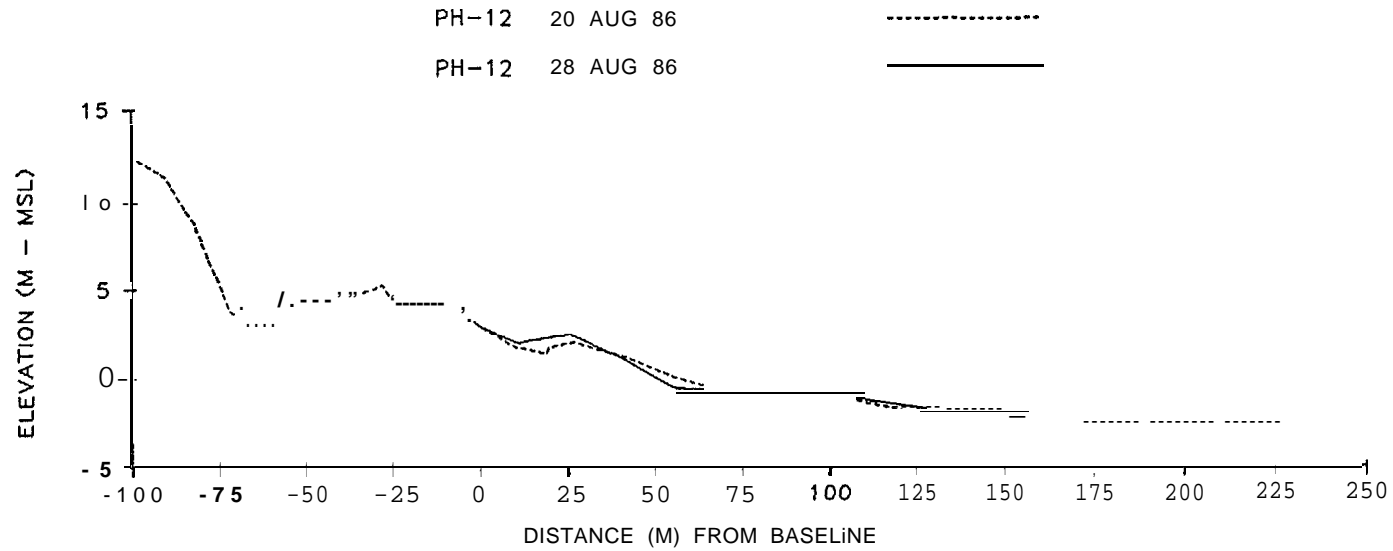
STATION 10 – PRIMARY BEACH STATION



STATION 11 - 100 M NORTH OF STATION 10



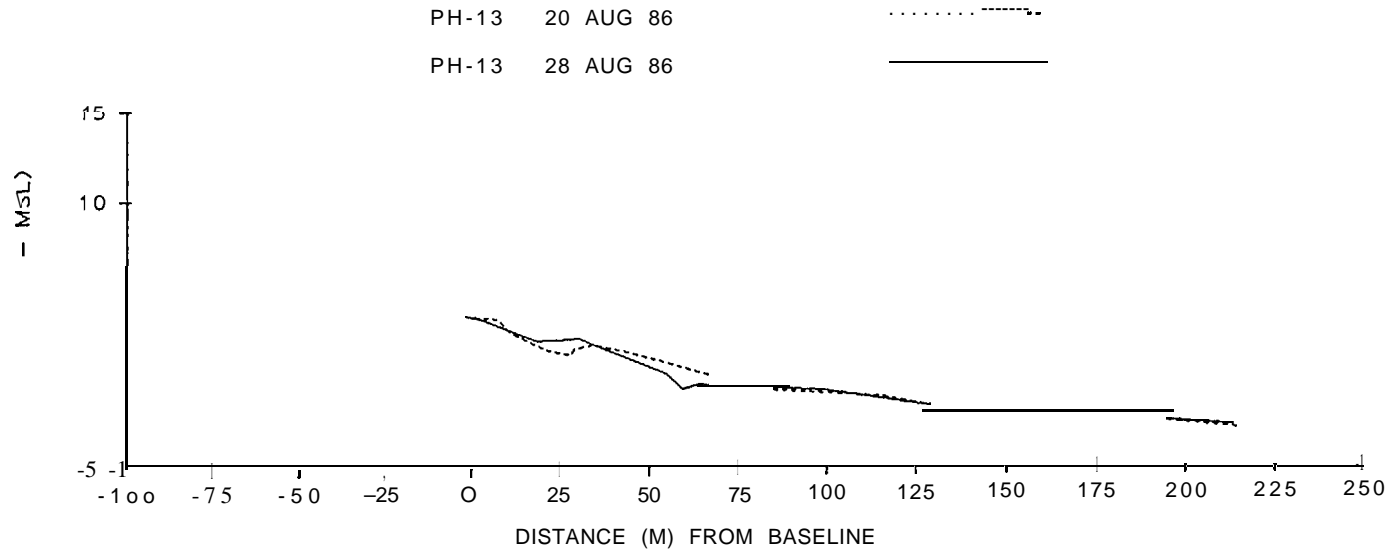
STATION 12 - 200 M NORTH OF STATION 10



STATION 13 – 300 M NORTH OF STATION 10

PH-13 20 AUG 86

PH-13 28 AUG 86

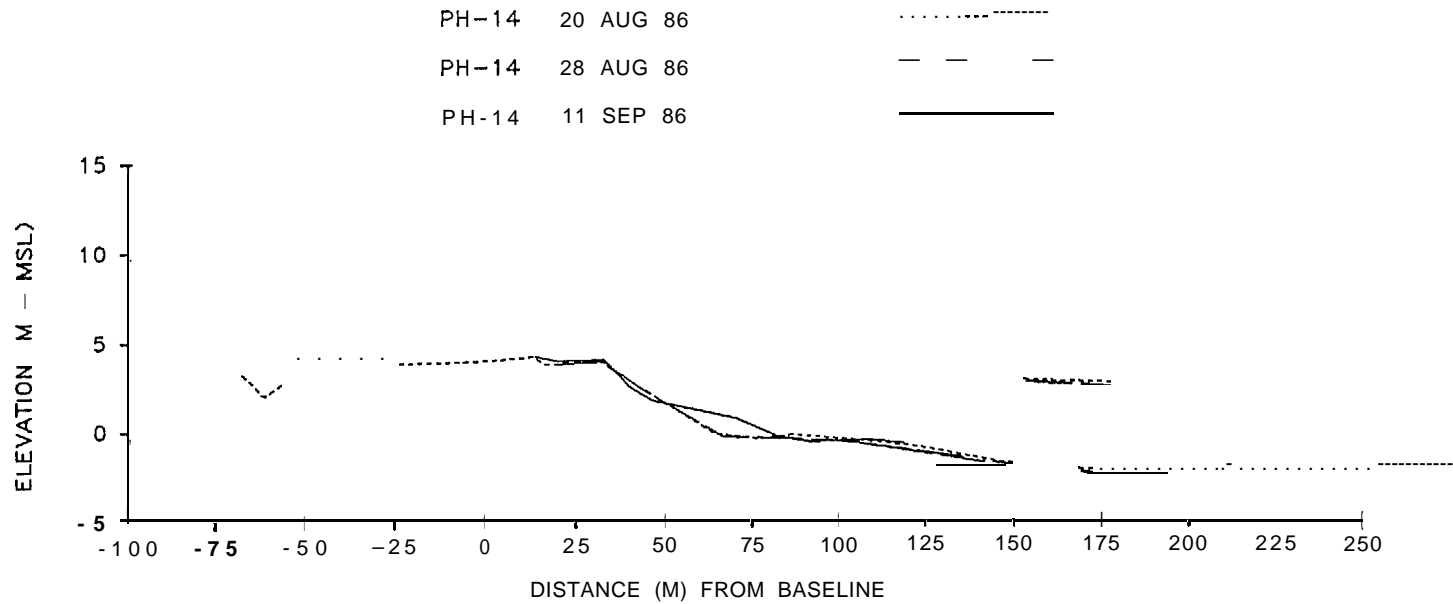


STATION 14 – 500 M NORTH OF STATION 10

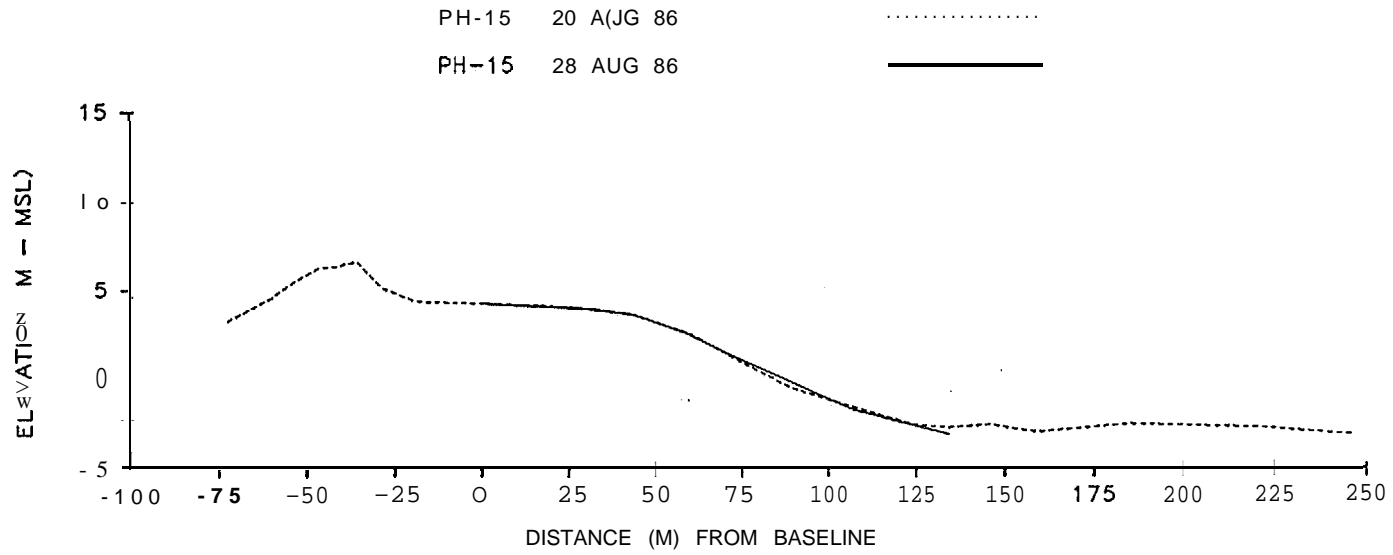
PH-14 20 AUG 86

PH-14 28 AUG 86

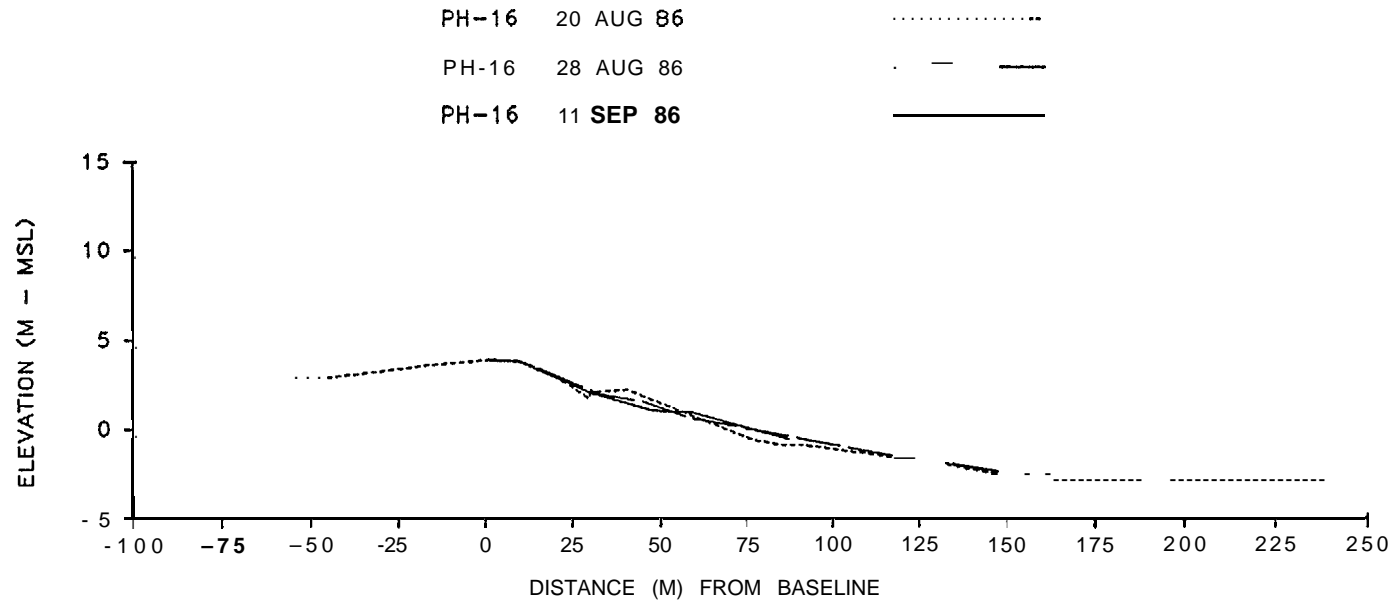
PH-14 11 SEP 86



STATION 15 - 800 M NORTH OF STATION 10

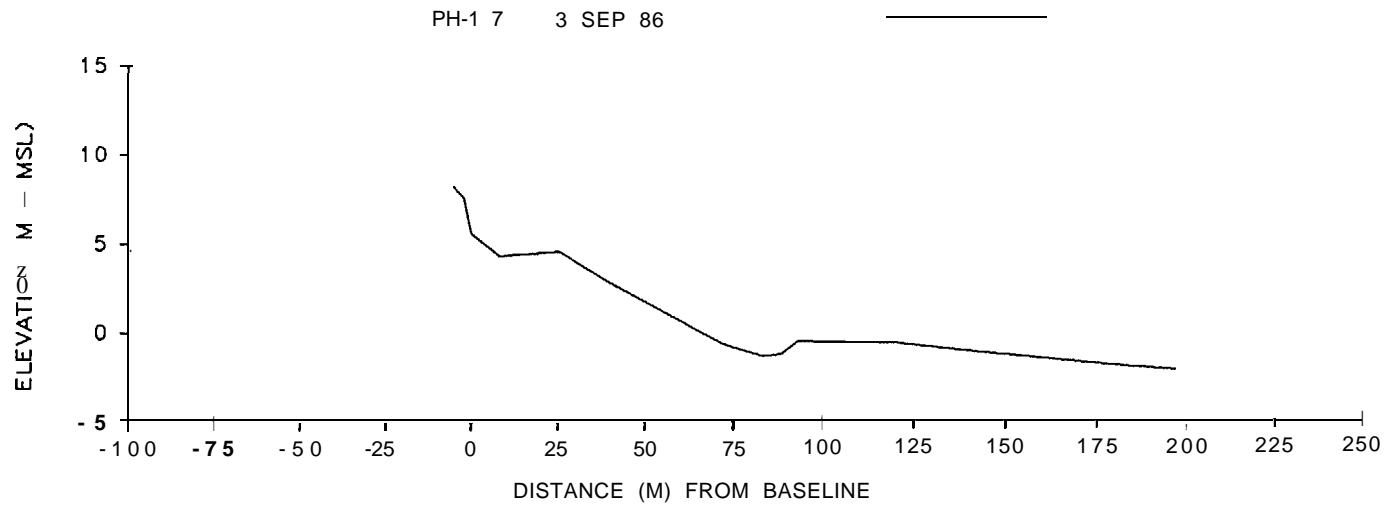


STATION 16 - 1000 M NORTH OF STATION 10



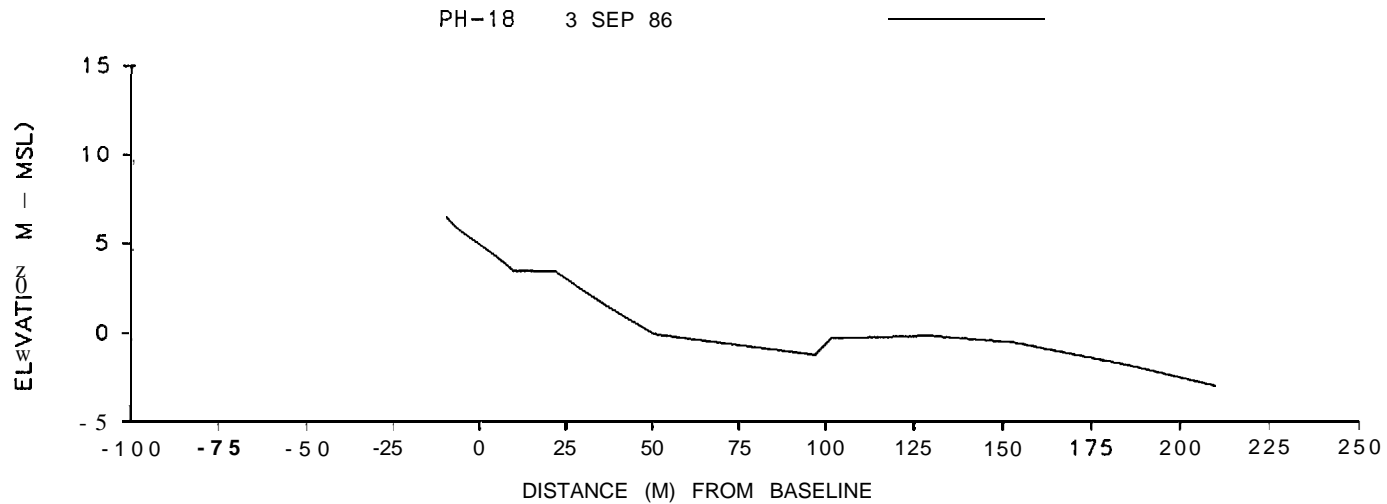
STATION 17 – 1 KM NORTH OF NORTH RIVER

PH-1 7 3 SEP 86



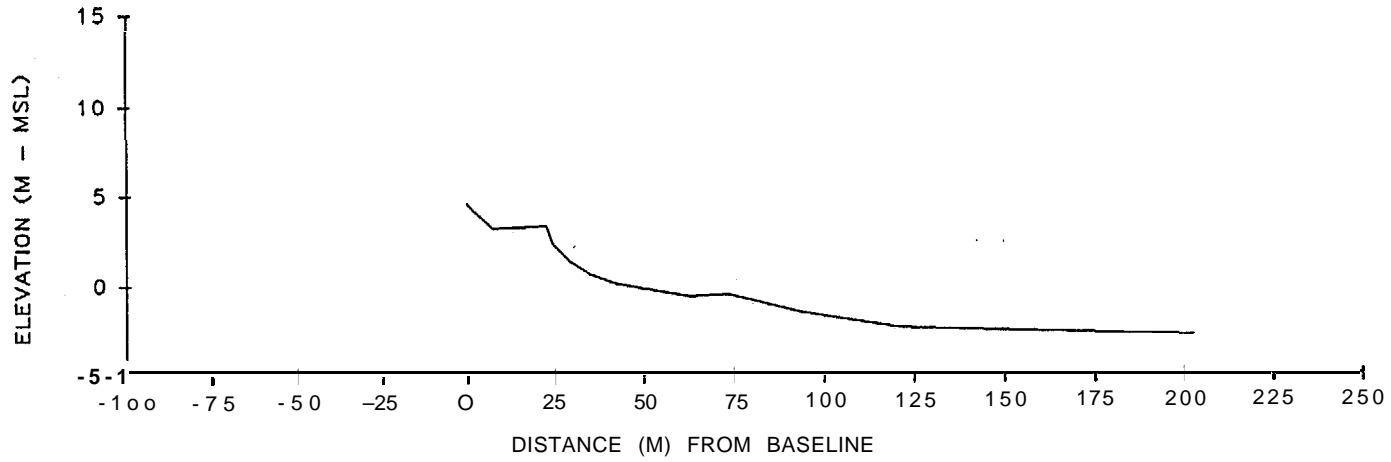
STATION 18 – EXPOSED SANDY BEACH

PH-18 3 SEP 86



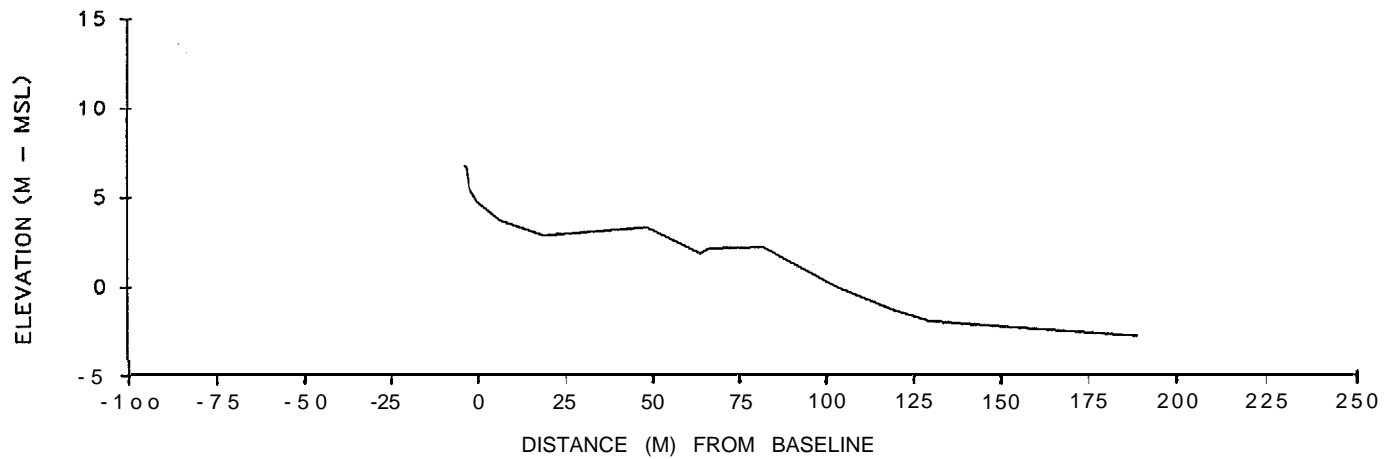
STATION 19 – EXPOSED SANDY BEACH

PH-19 9 SEP 86



STATION 20 – EXPOSED SANDY BEACH

PH-20 4 SEP 86



APPENDIX II-B

Contour movement summaries for 20 beach monitoring stations.
Key contours are as follows:

- +3.0 m MSL– spring berm crest
- 0 m MSL– mean water level
- 0.9 m MSL– toe of lower beach face
- 2.4 m MSL– maximum wading depth of profile

For subsequent profiles at each station, an absolute change and an annualized rate of change are computed. Also, the beach slope between contours is determined for each survey date. The width of beach is computed for the beach face (+3 m to -0.9 m) and the low-tide terrace (-0.9 m to -2.4 m).

CONTOUR MOVEMENT SUMMARY FOR PORT HEIDEN

RANGE PH-1 NEAR FUEL TANKS

DISTANCE TO CONTOUR ISOPLETH (M)

DATE	+3.0	+0.0	-0.9	-2.4
21 AUG 1986	8.8	41.4	58.1	106.0
10 SEP 1986	5.1	42.9	58.0	115.0

CONTOUR MOVEMENT BETWEEN SURVEYS (M)

TIME PERIOD	NO. DAYS	+3.0	+0.0	-0.9	-2.4
21 AUG 1986 - 10 SEP 1986	20	-3.7	1.5	-0.1	9.0

NET CHANGE

TIME PERIOD	NO. DAYS	+3.0	+0.0	-0.9	-2.4
21 AUG 1986 - 10 SEP 1986	20	-3.7	1.5	-0.1	9.0

ANNUALIZED CONTOUR CHANGES (M/YR)

TIME PERIOD	NO. DAYS	+3.0	+0.0	-0.9	-2.4
21 AUG 1986 - 10 SEP 1986	20	-66.9	27.9	-1.1	163.6

AVERAGE **ANNUALIZED** CHANGE

TIME PERIOD	NO. DAYS	+3.0	+0.0	-0.9	-2.4
21 AUG 1986 - 10 SEP 1986	20	-66.9	27.9	-1.1	163.6

BEACH SLOPES BETWEEN CONTOURS

DATE	+3.0 TO +0.0	+0.0 TO -0.9	-0.9 TO -2.4
21 AUG 1986	-0.0935	-0.0547	-0.0319
10 SEP 1986	-0.0806	-0.0604	-0.0269

WIDTH OF BEACH (M)

DATE	+3.0 TO -0.9	-0.9 TO -2.4
21 AUG 1986	49.3	47.9
10 SEP 1986	62.9	57.0

CONTOUR MOVEMENT SUMMARY FOR PORT HEIDEN

RANGE PH-2 IN COVE BEHIND SPIT

DISTANCETO CONTOUR ISOPLETH (M)

DATE	+3.0	+0.0	-0.9	-2.4
21 AUG 1986	5.9	29.6	40.9	112.5
10 SEP 1986	5.2	31.0	42.2	*****

CONTOUR MOVEMENT BETWEEN SURVEYS (M)

TIME PERIOD	NO. DAYS	+3.0	+0.0	-0.9	-2.4
21 AUG 1986 - 10 SEP 1986	20	-0.7	1.4	1.3	*****

NET CHANGE

TIME PERIOD	NO. DAYS	+3.0	+0.0	-0.9	-2.4
21 AUG 1986 - 10 SEP 1986	20	-0.7	1.4	1.3	*****

ANNUALIZED CONTOUR CHANGES (M/YR)

TIME PERIOD	NO. DAYS	+3.0	+0.0	-0.9	-2.4
21 AUG 1986 - 10 SEP 1986	20	-13.2	24.9	23.3	*****

AVERAGE ANNUALIZED CHANGE

TIME PERIOD	NO. DAYS	+3.0	+0.0	-0.9	-2.4
21 AUG 1986 - 10 SEP 1986	20	-13.2	24.9	23.3	*****

BEACH SLOPES BETWEEN CONTOURS

DATE	+3.0 TO +0.0	+0.0 TO -0.9	-0.9 TO -2.4
21 AUG 1986	-0.1287	-0.0808	-4.0213
10 SEP 1986	-0.1183	-0.0814	*****

WIDTH OF BEACH (M)

DATE	+3.0 TO -0.9	-0.9 TO -2.4
21 AUG 1986	35.0	71.7
10 SEP 1986	37.0	*****



CONTOUR MOVEMENT SUMMARY FOR PORT HEIDEN

RANGE PH-3 IN COVE BEHIND SPIT

DISTANCE TO CONTOUR ISOPLETH (M)

DATE	+3.0	+0.0	-0.9	-2.4
21 AUG 1986	-3.7	34.8	*****	*****
10 SEP 1986	-3.6	26.0	67.2	*****

CONTOUR MOVEMENT BETWEEN SURVEYS (M)

TIME PERIOD	NO. DAYS	+3.0	+0.0	-0.9	-2.4
21 AUG 1986 - 10 SEP 1986	20	0.0	-8.9	*****	*****

NET CHANGE

TIME PERIOD	NO. DAYS	+3.0	+0.0	-0.9	-2.4
21 AUG 1986 - 10 SEP 1986	20	0.0	-8.9	*****	*****

ANNUALIZED CONTOUR CHANGES (M/YR)

TIME PERIOD	NO. DAYS	+3.0	+0.0	-0.9	-2.4
21 AUG 1986 - 10 SEP 1986	20	0.8	-161.9	*****	*****

AVERAGE ANNUALIZED CHANGE

TIME PERIOD	NO. DAYS	+3.0	+0.0	-0.9	-2.4
21 AUG 1986 - 10 SEP 1986	20	0.8	-161.9	*****	*****

BEACH SLOPES BETWEEN CONTOURS

DATE	+3.0 TO +0.0	+0.0 TO -0.9	-0.9 TO -2.4
21 AUG 1986	-0.0792	*****	*****
10 SEP 1986	-0.1030	-0.0221	*****

WIDTH OF BEACH (M)

DATE	+3.0 TO -0.9	-0.9 TO -2.4
21 AUG 1986	*****	*****
10 SEP 1986	70.8	*****

CONTOUR MOVEMENT SUMMARY FOR PORT HEIDEN

RANGE PH-4 ON RECURVED SPIT

DISTANCE TO CONTOUR ISOPLETH (M)

DATE	+3.0	+0.0	-0.9	-2.4
21 AUG 1986	-14.8	147.3	287.4	336.9
10 SEP 1986	-16.1	139.6	277.7	334.7

CONTOUR MOVEMENT BETWEEN SURVEYS (M)

TIME PERIOD	NO. DAYS	+3.0	+0.0	-0.9	-2.4
21 AUG 1886 - 10 SEP 1986	20	-1.4	-7.6	-9.7	-2.1

NET CHANGE

TIME PERIOD	NO. DAYS	+3.0	+0.0	-0.9	-2.4
21 AUG 1988 - 10 SEP 1986	20	-1.4	-7.6	-9.7	-2.1

ANNUALIZED CONTOUR CHANGES (M/YR)

TIME PERIOD	NO. DAYS	+3.0	+0.0	-0.9	-2.4
21 AUG 1986 - 10 SEP 1986	20	-24.8	-139.5	-177.0	-38.9

AVERAGE **ANNUALIZED** CHANGE

TIME PERIOD	NO. DAYS	+3.0	+0.0	-0.9	-2.4
21 AUG 1986 - 10 SEP 1986	20	-24.8	-139.5	-177.0	-38.9

BEACH SLOPES BETWEEN CONTOURS

DATE	+3.0 TO +0.0	+0.0 TO -0.9	-0.9 TO -2.4
21 AUG 1986	-0.0188	-0.0065	-0.0310
10 SEP 1986	-0.0196	-0.0066	-0.0268

WIDTH OF BEACH (M)

DATE	+3.0 TO -0.9	-0.9 TO -2.4
21 AUG 1986	302.2	49.4
10 SEP 1986	293.9	57.0



CONTOUR MOVEMENT SUMMARY FOR PORT HEIDEN

RANGE PH-6 NORTH OF SPIT

DISTANCE TO CONTOUR ISOPLETH (M)

DATE	+3.0	+0.0	-0.9	-2.4
19 AUG 1986	62.6	77.6	177.4	228.2
25 AUG 1986	52.0	80.9	169.4	*****
10 SEP 1986	60.6	99.1	148.9	226.2

CONTOUR MOVEMENT BETWEEN SURVEYS (M)

TIME PERIOD	NO. DAYS	+3.0	+0.0	-0.9	-2.4
19 AUG 1986 - 26 AUG 1986	6	-0.6	3.3	-18.0	*****
26 AUG 1986 - 10 SEP 1986	16	-1.4	18.3	-10.6	*****

NET CHANGE

TIME PERIOD	NO. DAYS	+3.0	+0.0	-0.9	-2.4
19 AUG 1986 - 10 SEP 1986	22	-2.0	21.6	-28.6	-3.0

ANNUALIZED CONTOUR CHANGES (M/YR)

TIME PERIOD	NO. DAYS	+3.0	+0.0	-0.9	-2.4
19 AUG 1986 - 25 AUG 1986	6	-34.4	198.5	-1094.2	*****
26 AUG 1986 - 10 SEP 1986	16	-32.5	417.2	-241.3	*****

AVERAGE ANNUALIZED CHANGE

TIME PERIOD	NO. DAYS	+3.0	+0.0	-0.9	-2.4
19 AUG 1986 - 10 SEP 1986	22	-33.4	307.9	-867.8	*****

BEACH SLOPES BETWEEN CONTOURS

DATE	+3.0 TO +0.0	+0.0 TO -0.9	-0.9 TO -2.4
19 AUG 1986	-0.1220	-0.0091	-0.0301
25 AUG 1986	-0.1068	-0.0116	*****
10 SEP 1986	-0.0628	-0.0183	-0.0200

WIDTH OF BEACH (M)

DATE	+3.0 TO -0.9	-0.9 TO -2.4
19 AUG 1986	124.8	60.8
25 AUG 1986	107.4	*****
10 SEP 1986	98.2	76.3

CONTOUR MOVEMENT SUMMARY FOR PORT HEIDEN

RANGE PH-6 MODERATE SLOPING BEACH

DISTANCE TO CONTOUR ISOPLETH (M)

DATE	+3.0	+0.0	-0.9	-2.4
21 AUG 1986	5.3	58.2	87.8	177.4
10 SEP 1986	5.2	62.1	90.7	*****

CONTOUR MOVEMENT BETWEEN SURVEYS (M)

TIME PERIOD	NO. DAYS	+3.0	+0.0	-0.9	-2.4
21 AUG 1986 - 10 SEP 1986	20	-0.1	3.9	2.9	*****

NET CHANGE

TIME PERIOD	NO. DAYS	+3.0	+0.0	-0.9	-2.4
21 AUG 1986 - 10 SEP 1986	20	-0.1	3.9	2.9	*****

ANNUALIZED CONTOUR CHANGES (M/YR)

TIME PERIOD	NO. DAYS	+3.0	+0.0	-0.9	-2.4
21 AUG 1986 - 10 SEP 1986	20	-2.4	70.6	53.5	*****

AVERAGE ANNUALIZED CHANGE

TIME PERIOD	NO. DAYS	+3.0	+0.0	-0.9	-2.4
21 AUG 1986 - 10 SEP 1986	20	-2.4	70.6	53.5	*****

BEACH SLOPES BETWEEN CONTOURS

DATE	+3.0 TO +0.0	+0.0 TO -0.9	-0.9 TO -2.4
21 AUG 1986	-0.0576	-0.0308	-0.0171
10 SEP 1986	-0.0536	-0.0318	*****

WIDTH OF BEACH (M)

DATE	+3.0 TO -0.9	-0.9 TO -2.4
21 AUG 1986	82.5	89.6
10 SEP 1986	85.5	*****

CONTOUR MOVEMENT SUMMARY FOR PORT HEIDEN

RANGE PH-7 ERODING BLUFF

DISTANCE TO CONTOUR ISOPLETH (M)

DATE	+3.0	+0.0	-0.9	-2.4
21 AUG 1986	-0.2	33.0	44.4	142.9

CONTOUR MOVEMENT BETWEEN SURVEYS (M)

TIME PERIOD	NO. DAYS	+3.0	+0.0	-0.9	-2.4
-------------	----------	------	------	------	------

NET CHANGE

TIME PERIOD	NO. DAYS	+3.0	+0.0	-0.9	-2.4
21 AUG 1986 - 21 AUG 1986	0	0.0	0.0	0.0	0.0

ANNUALIZED CONTOUR CHANGES (M/YR)

TIME PERIOD	NO. DAYS	+3.0	+0.0	-0.9	-2.4
-------------	----------	------	------	------	------

AVERAGE ANNUALIZED CHANGE

TIME PERIOD	NO. DAYS	+3.0	+0.0	-0.9	-2.4
21 AUG 1986 - 21 AUG 1986	0	*****	*****	*****	*****

BEACH SLOPES BETWEEN CONTOURS

DATE	+3.0 TO +0.0	+0.0 TO -0.9	-0.9 TO -2.4
21 AUG 1986	-0.0919	-0.0798	-0.0155

WIDTH OF BEACH (M)

DATE	+3.0 TO -0.9	-0.9 TO -2.4
21 AUG 1986	44.6	98.6

CONTOUR MOVEMENT SUMMARY FOR PORT HEIDEN

RANGE PH-8 ERODING BLUFF

DISTANCE TO CONTOUR **ISOPLETH (M)**

DATE	+3.0	+0.0	-0.9	-2.4
21 AUG 1986	10.7	64.7	100.1	187.0
11 SEP 1986	10.7	63.8	1134.9	180.8

CONTOUR MOVEMENT BETWEEN SURVEYS (M)

TIME PERIOD	NO. DAYS	+3.0	+0.0	-0.9	-2.4
21 AUG 1986 - 11 SEP 1986	21	-0.1	-0.9	4.8	-6.2

NET CHANGE

TIME PERIOD	NO. DAYS	+3.0	+0.0	-0.9	-2.4
21 AUG 1986 - 11 SEP 1986	21	-0.1	-0.9	4.8	-6.2

ANNUALIZED CONTOUR CHANGES (M/YR)

TIME PERIOD	NO. DAYS	+3.0	+0.0	-0.9	-2.4
21 AUG 1986 - 11 SEP 1986	21	-1.3	-15.9	82.7	-107.9

AVERAGE ANNUALIZE CHANGE

TIME PERIOD	NO. DAYS	+3.0	+0.0	-0.9	-2.4
21 AUG 1986 - 11 SEP 1986	21	-1.3	-15.9	82.7	-107.9

BEACH SLOPES BETWEEN CONTOURS

DATE	+3.0 TO +0.0	+0.0 TO -0.9	-0.9 TO -2.4
21 AUG 1986	-0.0565	-0.0267	-0.0176
11 SEP 1986	-0.0573	-0.0222	-0.0202

WIDTH OF BEACH (M)

DATE	+3.0 TO -0.9	-0.9 TO -2.4
21 AUG 1986	89.4	86.8
11 SEP 1986	94.2	75.9



CONTOUR MOVEMENT SUMMARY FOR PORT HEIDEN

RANGE PH-9 100 M SOUTH OF STATION 10

DISTANCE TO CONTOUR ISOPLETH (M)

DATE	+3.0	+0.0	-0.9	-2.4
20 AUG 1986	-4.3	46.0	59.8	117.4
28 AUG 1986	***III**	33.0	69.2	121.6

CONTOUR MOVEMENT BETWEEN SURVEYS (M)

TIME PERIOD	NO. DAYS	+3.0	+0.0	-4.9	-2.4
20 AUG 1986 - 28 AUG 1986	8	*****	-13.0	9.6	4.2

NET CHANGE

TIME PERIOD	NO. DAYS	+3.0	+0.0	-0.9	-2.4
20 AUG 1986 - 28 AUG 1986	8	*****	-13.0	9.6	4.2

ANNUALIZED CONTOUR CHANGES (M/YR)

TIME PERIOD	NO. DAYS	+3.0	+0.0	-0.9	-2.4
20 AUG 1986 - 28 AUG 1986	8	*****	-591.5	436.6	191.3

AVERAGE ANNUALIZED CHANGE

TIME PERIOD	NO. DAYS	+3.0	+0.0	-0.9	-2.4
20 AUG 1986 - 28 AUG 1986	8	*****	-591.5	436.6	191.3

BEACH SLOPES BETWEEN CONTOURS

DATE	+3.0 TO +0.0	+0.0 TO -0.9	-0.9 TO -2.4
20 AUG 1986	-0.0606	-0.0667	-0.0265
28 AUG 1986	*****	-0.0252	-0.0292

WIDTH OF BEACH (M)

DATE	+3.0 TO -0.9	-0.9 TO -2.4
20 AUG 1986	64.0	57.7
28 AUG 1986	*****	62.3

CONTOUR MOVEMENT SUMMARY FOR PORT HEIDEN

RANGE **PH-10** PRIMARY BEACH STATION

DISTANCETO CONTOUR ISOPLETH (M)

DATE	+3.0	+0.0	-0.9	-2.4
20 AUG 1986	56.9	112.6	133.1	201.1
25 AUG 1986	57.0	106.9	138.9	*****
28 AUG 1986	57.2	113.6	140.5	196.4
5 SEP 1986	57.7	112.7	139.3	*****
11 SEP 1986	56.6	109.2	141.6	*****

CONTOUR MOVEMENT BETWEEN SURVEYS (M)

TIME PERIOD	NO. DAYS	+3.0	+0.0	-0.9	-2.4
20 AUG 1986 - 25 AUG 1986	5	0.1	-5.7	5.8	*****
25 AUG 1986 - 28 AUG 1986	3	0.2	6.7	1.6	*****
28 AUG 1986 - 5 SEP 1986	8	0.4	-0.9	-1.2	*****
5 SEP 1986 - 11 SEP 1986	6	-1.0	-3.5	2.2	*****

NET CHANGE

TIME PERIOD	NO. DAYS	+3.0	+0.0	-0.9	-2.4
20 AUG 1986 - 11 SEP 1986	22	-0.3	-3.5	8.5	*****

ANNUALIZED CONTOUR CHANGES (M/YR)

TIME PERIOD	NO. DAYS	+3.0	+0.0	-0.9	-2.4
20 AUG 1986 - 25 AUG 1986	5	7.5	-417.5	424.8	*****
25 AUG 1986 - 28 AUG 1986	3	28.4	816.4	196.3	*****
28 AUG 1986 - 5 SEP 1986	8	19.9	-41.8	-54.1	*****
5 SEP 1986 - 11 SEP 1986	6	-63.2	-214.4	13s.7	*****

AVERAGE ANNUALIZED CHANGE

TIME PERIOD	NO. DAYS	+3.0	+0.0	-0.9	-2.4
20 AUG 1986 - 11 SEP 1986	22	-1.9	35.7	175.7	*****

BEACH SLOPES BETWEEN CONTOURS

DATE	+3.0 TO +0.0	+0.0 TO -0.9	-0.9 TO -2.4
20 AUG 1986	-0.0547	-0.0445	-0.0225
26 AUG 1986	-0.0611	-0.0286	*****
28 AUG 1986	-0.0541	-0.0338	-0.0274
6 SEP 1986	-0.0554	-0.0342	*****
11 SEP 1988	-0.0580	-0.0281	*****

WIDTH OF BEACH (M)

DATE	+3.0 TO -0.9	-0.9 TO -2.4
20 AUG 1986	76.2	68.0
25 AUG 1986	81.9	*****
28 AUG 1986	83.3	66.8
5 SEP 1986	81.7	*****
11 SEP 1986	85.0	*****

CONTOUR MOVEMENT SUMMARY FOR PORT HEIDEN

RANGE PH-11 100 M NORTH OF STATION 10

DISTANCE TO CONTOUR ISOPLETH (M)

DATE	+3.0	+0.0	-0.9	-2.4
20 AUG 1986	36.8	102.7	115.8	164.3
28 AUG 1986	*****	117.6	148.9	194.7

CONTOUR MOVEMENT BETWEEN SURVEYS (M)

TIME PERIOD	NO. DAYS	+3.0	+0.0	-0.9	-2.4
20 AUG 1986 - 28 AUG 1986	8	*****	14.9	33.1	30.4

NET CHANGE

TIME PERIOD	NO. DAYS	+3.0	+0.0	-0.9	-2.4
20 AUG 1986 - 28 AUG 1986	8	*****	14.9	33.1	30.4

ANNUALIZED CONTOUR CHANGES (M/YR)

TIME PERIOD	NO. DAYS	+3.0	+0.0	-0.9	-2.4
20 AUG 1986 - 28 AUG 1986	8	*****	678.2	1509.5	1385.6

AVERAGE ANNUALIZED CHANGE

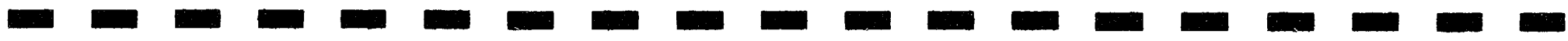
TIME PERIOD	NO. DAYS	+3.0	+0.0	-0.9	-2.4
20 AUG 1986 - 28 AUG 1986	8	*****	678.2	1509.5	1385.6

BEACH SLOPES BETWEEN CONTOURS

DATE	+3.0 TO +0.0	+0.0 TO -0.9	-0.9 TO -2.4
20 AUG 1986	-0.0462	-0.0695	-0.6315
28 AUG 1986	*****	-0.0291	-0.0334

WIDTH OF BEACH (M)

DATE	+3.0 TO -0.9	-0.9 TO -2.4
20 AUG 1986	79.1	48.5
28 AUG 1986	*****	45.8



CONTOUR MOVEMENT SUMMARY FOR PORT HEIOEN

RANGE PH-12 200 M NORTH OF STATION 10

DISTANCE TO CONTOUR ISOPLETH (M)

DATE	+3.0	+0.0	-0.9	-2.4
20 AUG 1986	-1.0	56.9	95.5	164.1
28 AUG 1986	*****	51.1	96.2	167.5

CONTOUR MOVEMENT BETWEEN SURVEYS (M)

TIME PERIOD	NO. DAYS	+3.0	+0.0	-0.9	-2.4
20 AUG 1986 - 28 AUG 1986	8	*****	-5.8	-0.4	3.4

NET CHANGE

TIME PERIOD	NO. DAYS	+3.0	+0.0	-0.9	-2.4
20 AUG 1986 - 28 AUG 1986	8	*****	-5.8	-0.4	3.4

ANNUALIZED CONTOUR CHANGES (M/YR)

TIME PERIOD	NO. DAYS	+3.0	+0.0	-0.9	-2.4
20 AUG 1986 - 28 AUG 1986	8	*****	-262.5	-16.1	155.7

AVERAGE ANNUALIZED CHANGE

TIME PERIOD	NO. DAYS	+3.0	+0.0	-0.9	-2.4
20 AUG 1986 - 28 AUG 1986	8	*****	-262.6	-16.1	155.7

BEACH SLOPES BETWEEN CONTOURS

DATE	+3.0 TO +0.0	+0.0 TO -0.9	-0.9 TO -2.4
20 AUG 1986	-0.0527	-0.0236	-0.0223
28 AUG 1986	*****	-0.0207	-0.0211

WIDTH OF BEACH (M)

DATE	+3.0 TO -0.9	-0.9 TO -2.4
20 AUG 1986	96.5	68.6
28 AUG 1986	*****	72.4

CONTOUR MOVEMENT SUMMARY FOR PORT HEIDEN

RANGE PH-13 300 M NORTH OF STATION 10

DISTANCE TO CONTOUR ISOPLETH (M)

DATE	+3.0	+0.0	-0.9	-2.4
20 AUG 1986	9.4	70.3	106.6	191.8
28 AUG 1986	7.3	56.3	107.5	192.9

CONTOUR MOVEMENT BETWEEN SURVEYS (M)

TIME PERIOD	NO. DAYS	+3.0	+0.0	-0.9	-2.4
20 AUG 1986 - 28 AUG 1986	8	-2.1	-14.0	0.9	1.0

NET CHANGE

TIME PERIOD	NO. DAYS	+3.0	+0.0	-0.9	-2.4
20 AUG 1986 - 28 AUG 1986	8	-2.1	-14.0	0.9	1.0

ANNUALIZED CONTOUR CHANGES (M/YR)

TIME PERIOD	NO. DAYS	+3.0	+0.0	-0.9	-2.4
20 AUG 1986 - 28 AUG 1986	8	-95.5	-637.9	42.4	46.5

AVERAGE ANNUALIZED CHANGE

TIME PERIOD	NO. DAYS	+3.0	+0.0	-0.9	-2.4
20 AUG 1986 - 28 AUG 1986	8	-95.5	-637.9	42.4	46.5

BEACH SLOPES BETWEEN CONTOURS

DATE	+3.0 TO +0.0	+0.0 TO -0.9	-0.9 TO -2.4
20 AUG 1986	-0.0601	-0.0251	-0.0180
28 AUG 1986	-0.0623	-0.0178	-0.0179

WIDTH OF BEACH (M)

DATE	+3.0 TO -0.9	-0.9 TO -2.4
20 AUG 1986	97.2	85.2
28 AUG 1986	100.2	85.3

CONTOUR MOVEMENT SUMMARY FOR PORT HEIDEN

RANGE PH-14 500 M NORTH OF STATION 10

DISTANCE TO CONTOUR ISOPLETH (M)

DATE	+3.0	+0.0	-0.9	-2.4
20 AUG 1986	17.9	42.2	102.4	211.0
28 AUG 1986	18.2	43.2	92.2	180.3
11 SEP 1986	16.8	57.8	*****	*****

CONTOUR MOVEMENT BETWEEN SURVEYS (M)

TIME PERIOD	NO. DAYS	+3.0	+0.0	-0.9	-2.4
20 AUG 1986 - 28 AUG 1986	8	0.3	0.9	-10.2	-30.8
28 AUG 1986 - 11 SEP 1986	14	-1.3	14.6	*****	*****

NET CHANGE

TIME PERIOD	NO. DAYS	+3.0	+0.0	-0.9	-2.4
20 AUG 1986 - 11 SEP 1986	22	-1.0	15.6	*****	*****

ANNUALIZED CONTOUR CHANGES (M/YR)

TIME PERIOD	NO. DAYS	+3.0	+0.0	-0.9	-2.4
20 AUG 1986 - 28 AUG 1986	8	12.6	42.9	-464.7	-1404.0
28 AUG 1986 - 11 SEP 1986	14	-34.5	381.2	*****	*****

AVERAGE ANNUALIZED CHANGE

TIME PERIOD	NO. DAYS	+3.0	+0.0	-0.9	-2.4
20 AUG 1986 - 11 SEP 1986	22	-11.0	212.1	-464.7	-1404.0

BEACH SLOPES BETWEEN CONTOURS

DATE	+3.0 TO +0.0	+0.0 TO -0.9	-0.9 TO -2.4
20 AUG 1986	-0.1252	-0.0151	-0.0141
28 AUG 1986	-0.1218	-0.0186	-0.0174
11 SEP 1986	-0.0744	*****	*****

WIDTH OF BEACH (M)

DATE	+3.0 TO -0.9	-0.9 TO -2.4
20 AUG 1986	84.5	108.7
28 AUG 1986	74.0	88.1
11 SEP 1986	*****	*****

CONTOUR MOVEMENT SUMMARY FOR PORT HEIDEN

RANGEPH-15 800 M NORTH OF STATION 10

DISTANCETO CONTOUR ISOPLETH (M)

DATE	+3.0	+0.0	-0.9	-2.4
20 AUG 1986	52.5	84.7	96.9	123.8
28 AUG 1986	52.2	88.0	98.6	123.0

CONTOUR MOVEMENT **BETWEEN SURVEYS (M)**

TIME PERIOD	NO. DAYS	+3.0	+0.0	-0.9	-2.4
20 AUG 1986 - 28 AUG 1986	8	-0.3	3.2	1.7	-0.8

NET CHANGE

TIME PERIOD	NO. DAYS	+3.0	+0.0	-0.9	-2.4
20 AUG 1988 - 28 AUG 1986	8	-0.3	3.2	1.7	-0.8

ANNUALIZED CONTOUR CHANGES (M/YR)

TIME PERIOD	NO. DAYS	+3.0	+0.0	-0.9	-2.4
20 AUG 1986 - 28 AUG 1986	8	-13.0	147.6	76.3	-38.3

AVERAGE ANNUALIZED CHANGE

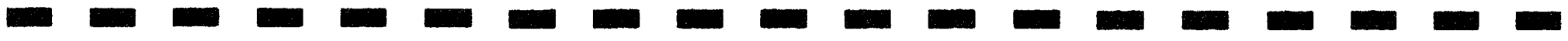
TIME PERIOD	NO. DAYS	+3.0	+0.0	-0.9	-2.4
20 AUG 1986 - 28 AUG 1986	8	-13.0	147.6	76.3	-38.3

BEACH SLOPES BETWEEN CONTOURS

DATE	+3.0 TO +0.0	+0.0 TO -0.9	-0.9 TO -2.4
20 AUG 1986	-0.0947	-0.0747	-0.0569
28 AUG 1986	-0.0854	-0.0859	-0.0627

WIDTH OF BEACH (M)

DATE	+3.0 TO -0.9	-0.9 TO -2.4
20 AUG 1986	44.4	26.9
28 AUG 1986	46.3	24.4



CNTOUR EMEN FOR EN
 RANGE PH-16 M NCR H OF STATION 10

DISTANCE TO CONTOUR ISOPLETH (M)

DATE	+3.0	+0.0	-0.9	-2.4
20 AUG 1986	17.5	69.1	94.2	146.9
28 AUG 1986	18.4	76.7	102.3	154.1
11 SEP 1986	16.9	76.8	*****	*****

CONTOUR MOVEMENT BETWEEN SURVEYS (M)

TIME PERIOD	NO. DAYS	+3.0	+0.0	-0.9	-2.4
20 AUG 1986 - 28 AUG 1986	8	0.9	7.6	8.1	7.1
28 AUG 1986 - 11 SEP 1986	14	-1.5	0.1	*****	*****

NET CHANGE

TIME PERIOD	NO. DAYS	+3.0	+0.0	-0.9	-2.4
20 AUG 1986 - 11 SEP 1986	22	-0.6	7.7	*****	*****

ANNUALIZED CONTOUR AN (M/YR)

TIME PERIOD	NO. DAYS	+3.0	+0.0	-0.9	-2.4
20 AUG 1986 - 28 AUG 1986	8	40.0	345.1	369.1	324.9
28 AUG 1986 - 11 SEP 1986	14	-38.7	3.4	*****	*****

AVERAGE ANNUALIZED CHANGE

TIME PERIOD	NO. DAYS	+3.0	+0.0	-0.9	-2.4
20 AUG 1986 - 11 SEP 1986	22	0.7	174.3	369.1	324.9

BEACH SLOPES BETWEEN CONTOURS

DATE	+3.0 TO	+0.0	+0.0 TO	-0.9	-0.9 TO	-2.4
20 AUG 1986	-0.0591	-0.0363	-0.0290	-0.0290		
28 AUG 1986	-0.0523	-0.0356	-0.0296	-0.0296		
11 SEP 1986	-0.0509	*****	*****	*****		

WIDTH OF BEACH (M)

DATE	+3.0 TO	-0.9	-0.9 TO	-2.4
20 AUG 1986	76.7	52.7		
28 AUG 1986	83.9	51.8		
11 SEP 1986	*****	*****		

CONTOUR MOVEMENT SUMMARY FOR PORT HEIDEN

RANGE PH-17 1 KM NORTH OF NORTH RIVER

DISTANCE TO CONTOUR ISOPLETH (M)

DATE	+3.0	+0.0	-0.9	-2.4
3 SEP 1986	38.0	66.1	132.8	*****

CONTOUR MOVEMENT BETWEEN SURVEYS (M)

TIME PERIOD	NO. DAYS	+3.0	+0.0	-0.9	-2.4
-------------	----------	------	------	------	------

NET CHANGE

TIME PERIOD	NO. DAYS	+3.0	+0.0	-0.9	-2.4
3 SEP 1986 - 3 SEP 1986	0	0.0	0.0	0.0	*****

ANNUALIZED CONTOUR CHANGES (M/YR)

TIME PERIOD	NO. DAYS	+3.0	+0.0	-0.9	-2.4
-------------	----------	------	------	------	------

AVERAGE ANNUALIZED CHANGE

TIME PERIOD	NO. DAYS	+3.0	+0.0	-0.9	-2.4
3 SEP 1986 - 3 SEP 1986	0	*****	*****	*****	*****

BEACH SLOPES BETWEEN CONTOURS

DATE	+3.0 TO +0.0	+0.0 TO -0.9	-0.9 TO -2.4
3 SEP 1986	-0.1089	-0.4136	*****

WIDTH OF BEACH (M)

DATE	+3.0 TO -0.9	-0.9 TO -2.4
3 SEP 1986	94.8	*****



CONTOUR MOVEMENT SUMMARY FOR PORT HEIDEN

RANGE PH-18 EXPOSED SANDY BEACH

DISTANCE TO CONTOUR ISOPLETH (M)

DATE	+3.0	+0.0	-0.9	-2.4
3 SEP 1986	24.6	49.8	182.8	198.8

CONTOUR MOVEMENT BETWEEN SURVEYS (M)

TIME PERIOD	NO. DAYS	+3.0	+0.0	-0.9	-2.4
-------------	----------	------	------	------	------

NET CHANGE

TIME PERIOD	NO. DAYS	+3.0	+0.0	-0.9	-2.4
3 SEP 1986 - 3 SEP 1986	0	0.0	0.0	0.0	0.0

ANNUALIZED CONTOUR CHANGES (M/YR)

TIME PERIOD	NO. DAYS	+3.0	+0.0	-0.9	-2.4
-------------	----------	------	------	------	------

AVERAGE ANNUALIZED CHANGE

TIME PERIOD	NO. DAYS	+3.0	+0.0	-0.9	-2.4
3 SEP 1986 - 3 SEP 1986	0	*****	*****	*****	*****

BEACH SLOPES BETWEEN CONTOURS

DATE	+3.0 TO +0.0	+0.0 TO -0.9	-0.9 TO -2.4
3 SEP 1986	-0.1209	-0.0081	-0.0425

WIDTH OF BEACH (M)

DATE	+3.0 TO -0.9	-0.9 TO -2.4
3 SEP 1986	138.2	36.0

CONTOUR MOVEMENT SUMMARY FOR PORT HEIDEN

RANGE PH-19 EXPOSED SANDY BEACH

DISTANCE TO CONTOUR ISOPLETH (M)

DATE	+3.0	+0.0	-0.9	-2.4
9 SEP 1986	23.2	47.7	83.9	156.9

CONTOUR MOVEMENT BETWEEN SURVEYS (M)

TIME PERIOD	NO. DAYS	+3.0	+0.0	-0.9	-2.4
-------------	----------	------	------	------	------

NET CHANGE

TIME PERIOD	NO. DAYS	+3.0	+0.0	-0.9	-2.4
9 SEP 1986 - 9 SEP 1986	0	0.0	0.0	0.0	0.0

ANNUALIZED CONTOUR CHANGES (M/YR)

TIME PERIOD	NO. DAYS	+3.0	+0.0	-0.9	-2.4
-------------	----------	------	------	------	------

AVERAGE ANNUALIZED CHANGE

TIME PERIOD	NO. DAYS	+3.0	+0.0	-0.9	-2.4
9 SEP 1986 - 9 SEP 1986	0	*****	*****	*****	*****

BEACH SLOPES BETWEEN CONTOURS

DATE	+3.0 TO +0.0	+0.0 TO -0.9	-0.9 TO -2.4
9 SEP 1986	-0.1244	-0.0252	-0.0209

WIDTH OF BEACH (M)

DATE	+3.0 TO -0.9	-0.9 TO -2.4
9 SW 1986	60.7	73.0



CONTOUR MOVEMENT SUMMARY FOR PORT HEIOEN

RANGE PH-20 EXPOSED SANDY BEACH

DISTANCE TO CONTOUR ISOPLETH (M)

DATE	+3.0	+0.0	-0.9	-2.4
4 SEP 1986	52.6	105.1	117.0	183.7

CONTOUR MOVEMENT BETWEEN SURVEYS (M)

TIME PERIOD	NO. DAYS	+3.0	+0.0	-0.9	-2.4
-------------	----------	------	------	------	------

NET CHANGE

TIME PERIOD	NO. DAYS	+3.0	+0.0	-0.9	-2.4
4 SEP 1986 - 4 SEP 1986	0	0.0	0.0	0.0	0.0

ANNUALIZED CONTOUR CHANGES (M/YR)

TIME PERIOD	NO. DAYS	+3.0	+0.0	-0.9	-2.4
-------------	----------	------	------	------	------

AVERAGE ANNUALIZED CHANGE

TIME PERIOD	NO. DAYS	+3.0	+0.0	-0.9	-2.4
4 SEP 1986 - 4 SEP 1986	0	*****	*****	*****	*****

BEACH SLOPES BETWEEN CONTOURS

DATE	+3.0 TO +0.0	+0.0 TO -0.9	-0.9 TO -2.4
4 SEP 1986	-0.0680	-0.0770	-0.0229

WIDTH OF BEACH (M)

DATE	+3.0 TO -0.9	-0.9 TO -2.4
4 SEP 1986	64.4	66.8

APPENDIX II-C

Volumetric changes at each of the beach monitoring stations. Lenses used are as follows:

Lens 1	top of profile to +3.0 m	– supratidal beach
Lens 2	+3.0 m to 0 m	— upper beach face
Lens 3	0 m to -0.9 m	- lower beach face
Lens 4	-0.9 m to -2.4 m	– low-tide terrace

[In order to account for different profiles starting at benchmarks located at different points along the profiles, volume calculations were started at the +3.0 m MSL contour. This forces Lens 1 volumes to be calculated as zero, which is purely a consequence of the analysis scheme used.

For subsequent profiles, absolute volume changes and annualized rates of change are determined.

Following the volumetric summaries for each station, a table is given which summarizes the initial survey volumes and the change in volume from the first to last survey for Lenses 2-4.

Volumetric summaries for all beach stations, showing initial survey volume and change between first and last surveys. Units are m³/m.

Station	Lens 2		Lens 3		Lens 4		Total	
	Initial	Change	Initial	Change	Initial	Change	Initial	Change
1	65.8	0.5	39.3	0.5	118.5	3.3	223.5	4.3
2	38.3	0.8	26.3	1.5	97.5	4.3	162.0	6.5
3	53.3	-11.5	41.8	0.3	97.5	97.3	192.5	86.0
4	60.3	-12.3	56.5	-7.8	299.8	-4.3	416.5	-24.3
5	43.5	3.8	60.0	6.0	239.8	-26.5	342.8	-16.8
6	67.0	-6.3	60.5	3.5	188.0	7.5	315.5	4.8
7	50.5	---	35.5	---	147.3	---	233.3	---
8	59.5	2.3	65.0	-1.3	199.0	-2.0	323.5	-1.0
9	82.3	-17.5	52.3	-7.5	143.0	11.3	277.5	-13.8
10	103.3	-20.3	57.5	0.3	168.3	-0.8	329.0	-20.8
11	113.5	24.5	66.3	13.8	163.5	47.8	343.3	86.0
12	88.8	7.8	65.5	-5.3	187.5	12.0	341.8	14.5
13	90.8	-4.0	67.5	-3.3	206.0	-1.8	364.3	-9.0
14	40.0	12.5	52.5	2.5	178.5	11.3	271.3	26.3
15	53.5	2.5	34.5	3.0	88.0	-1.5	176.0	4.0
16	85.0	-5.3	54.8	8.0	160.8	-20.3	300.5	-17.5
17	43.0	---	41.5	---	198.3	---	282.8	---
18	38.3	---	72.8	---	236.3	---	347.3	---
19	22.5	---	39.8	---	125.3	---	187.5	---
20	96.3	---	53.5	---	131.8	---	281.5	---

END AREAS OF DESIGNATED LENSES IN CUBIC METERS/METER

PORT HEIDEN

LENS 1 TOP TO 3.0 METERS
 LENS 2 3.0 TO 0.0
 LENS 3 0.0 TO -0.9
 LENS 4 -0.9 TO -2.4

() =THE NUMBER OF DAYS BETWEEN THE INDICATED SURVEY AND THE PREVIOUS

CALCULATIONS START AT 4.9

BY S&I INC

RANGE PH-1

	LENS 1	2	3	4
(0) 21AUG86	0.3	65.9	39.2	118.8
		66.2	105.4	224.2
CUMULATIVE				
(20) 10SEP86	0.0	66.4	39.7	122.1
		66.4	106.2	228.3
CUMULATIVE				

AREA CHANGES AT DESIGNATED RANGES IN CUBIC METERS/METER PORT HEIDEN

RANGE PH-1

LENS 1 TOP TO 3.0 METERS
 LENS 2 3.0 TO 0.0
 LENS 3 0.0 TO -0.9
 LENS 4 -0.9 TO -2.4

(0) 21AUG86

	LENS 1	2	3	4
AREA CHANGE	-0.3	0.5	0.5	3.3
AREA CHANGE CUMULATIVE		0.2	0.7	4.0

ANNUALIZED CHANGE
 (CUBIC M/M/YR)
 ANNUALIZED CHANGE CUMULATIVE
 (CUBIC M/M/YR)

(20) 10SEP86

	-5.0	9.2	9.4	60.3
	4.2	4.2	13.6	73.9

END AREAS OF DESIGNATED LENSES IN CUBIC METERS/METER

PORT HEIDEN

LENS 1 TOP TO 3.0 METERS
 LENS 2 3.0 TO 0.0
 LENS 3 0.0 TO -0.9
 LENS 4 -0.9 TO -2.4

() =THENUMBER OF DAYS BETWEEN THE INDICATED SURVEY AND THE PREVIOUS SURVEY

CALCULATIONS START AT 5.2 METERS FROM BASELINE

RANGE PH-2

	LENS	1	2	3	4
(0) 21AUG86		0.0	38.3	26.2	97.7
	CUMULATIVE		38.3	64.5	182.2
(20) 10SEP86		0.0	39.0	27.8	102.0
	CUMULATIVE		39.0	66.8	168.9

AREA CHANGES AT DESIGNATED RANGES IN CUBIC METERS/METER PORT HEIDEN

LENS 1 TOP TO 3.0 METERS
 LENS 2 3.0 TO 0.0
 LENS 3 0.0 TO -0.9
 LENS 4 -0.9 TO -2.4

RANGE PH-2

	LENS	1	2	3	4
(0) 21AUG86					
AREA CHANGE		0.0	0.7	1.6	4.4
AREA CHANGE CUMULATIVE			0.7	2.3	6.6
ANNUALIZED CHANGE (CUBIC M/M/YR)		-0.4	13.5	28.7	79.6
ANNUALIZED CHANGE CUMULATIVE (CUBIC M/M/YR)			13.0	41.7	121.4
(20) 10SEP86					

END AREAS OF DESIGNATED LENSES IN CUBIC METERS/METER

PORT HEIDEN

LENS 1 TOP TO 3.0 METERS
 LENS 2 **3.0** TO 0.0
 LENS 3 **0.0** TO -0.9
 LENS 4 -0.9 TO -2.4

() = THE NUMBER OF DAYS BETWEEN THE INDICATED SURVEY AND THE PREVIOUS SURVEY

CALCULATIONS START AT -4.0 METERS FROM BASELINE

RANGE PH-3

	LENS	1	2	3	4
(0) 21AUG86		0.0	63.3	41.8	97.7
	CUMULATIVE		53.3	95.1	192.7
(20) 10SEP86		0.0	41.8	42.0	195.1
	CUMULATIVE		41.8	83.8	278.9

AREA CHANGES AT DESIGNATED RANGES IN CUBIC METERS/METER PORT HEIDEN

LENS 1 TOP TO 3.0 METERS
 LENS 2 3.0 TO 0.0
 LENS 3 0.0 TO **-0.9**
 LENS 4 -0.9 TO -2.4

RANGE PH-3

	LENS	1	2	3	4
(0) 21AUG86					
AREA CHANGE		0.0	-11.5	0.3	97.5
AREA CHANGE CUMULATIVE			-11.5	-11.3	86.2
ANNUALIZED CHANGE (CUBIC M/M/YR)		0.0	-210.7	5.0	1779.0
ANNUALIZED CHANGE CUMULATIVE (CUBIC M/M/YR)			-210.7	-205.7	1573.3
(20) 10SEP86					

END AREAS OF DESIGNATED LENSES IN CUBIC METERS/METER

PORT HEIDEN

LENS 1 TOP TO 3.0 METERS
 LENS 2 3.0 TO 0.0
 LENS 3 0.0 TO -0.9
 LENS 4 -0.9 TO -2.4

() = THE NUMBER OF DAYS BETWEEN THE INDICATED SURVEY AND THE PREVIOUS SURVEY

CALCULATIONS START AT 106.7 METERS FROM BASELINE

RANGE PH-4

	LENS 1	2	3	4
(0) 21AUG86	0.0	60.3	56.7	300.6
CUMULATIVE		60.3	117.1	417.6
(20) 10SEP86	0.0	47.9	49.0	296.2
CUMULATIVE		47.9	96.9	393.1

AREA CHANGES AT DESIGNATED RANGES IN CUBIC METERS/METER PORT HEIDEN

LENS 1 TOP TO 3.0 METERS
 LENS 2 3.0 TO 0.0
 LENS 3 0.0 TO -0.9
 LENS 4 -0.9 TO -2.4

RANGE PH-4

	LENS 1	2	3	4
(0) 21AUG86				
AREA CHANGE	0.0	-12.4	-7.7	-4.3
AREA CHANGE CUMULATIVE		-12.4	-20.1	-24.4
ANNUALIZED CHANGE (CUBIC M/M/YR)	0.0	-226.2	-141.1	-78.4
ANNUALIZED CHANGE CUMULATIVE (CUBIC M/M/YR)		-226.2	-367.3	-446.6
(20) 10SEP86				

END AREAS OF DESIGNATED LENSES IN CUBIC METERS/METER

LENS 1 TOP TO 3.0 METERS
 LENS 2 3.0 TO 0.0
 LENS 3 0.0 TO -0.9
 LENS 4 -0.9 TO -2.4

() =THE NUMBER OF DAYS BETWEEN THE INDICATED SURVEY AND THE PREVIOUS SURVEY

CALCULATIONS START AT 50.6 METERS FROM BASELINE

RANGE PH-5

	LENS 1	2	3	4
(0) 19AUG86	0.3	43.5	60.1	239.9
CUMULATIVE		43.8	103.9	343.8
(6) 25AUG86	0.1	42.4	66.9	283.9
CUMULATIVE		42.6	99.4	383.2
(16) 10SEP86	0.0	47.3	66.3	213.2
CUMULATIVE		47.3	113.6	326.8

AREA CHANGES AT DESIGNATED RANGES IN CUBIC METERS/METER PORT HEIDEN

LENS 1 TOP TO 3.0 METERS
 LENS 2 3.0 TO 0.0
 LENS 3 0.0 TO -0.9
 LENS 4 -0.9 TO -2.4

RANGE PH-5

	LENS 1	2	3	4
(0) 19AUG86				
AREA CHANGE	-0.1	-1.1	-3.3	44.0
AREA CHANGE CUMULATIVE		-1.3	-4.5	39.6
ANNUALIZED CHANGE (CUBIC M/M/YR)	-8.2	-68.1	-199.8	2676.9
ANNUALIZED CHANGE CUMULATIVE (CUBIC M/M/YR)		-76.2	-276.0	2400.8
(6) 25AUG86				
AREA CHANGE	-0.1	4.9	9.4	-70.6
AREA CHANGE CUMULATIVE		4.8	14.2	-56.4
ANNUALIZED CHANGE (CUBIC M/M/YR)	-3.2	112.6	214.8	-1611.6
ANNUALIZED CHANGE CUMULATIVE (CUBIC M/M/YR)		109.4	324.2	-1287.4
(16) 10SEP86				
*** NET AREA CHANGE BETWEEN 19 AUG 1986 AND 10 SEP 1986				22 DAYS ***
NET AREA CHANGE	-0.3	3.8	6.1	-26.6
NET AREA CHANGE CUMULATIVE		3.5	9.7	-17.0
NET ANNUALIZED CHANGE (CUBIC M/M/YR)	-4.6	63.3	101.7	-442.0
NET ANNUALIZED CHANGE CUMULATIVE (CUBIC M/M/YR)		68.8	160.5	-281.5

END AREAS OF DESIGNATED LENSES IN CUBIC METERS/METER

PORT HEIDEN

LENS 1 TOP TO 3.0 METERS
 LENS 2 3.0 TO 4.0
 LENS 3 0.0 TO -0.9
 LENS 4 -0.9 TO -2.4

() =THE NUMBER OF DAYS BETWEEN THE INDICATED SURVEY AND THE PREVIOUS SURVEY

CALCULATIONS START AT 5.2 METERS FROM BASELINE

RANGE PH-6

	LENS	1	2	3	4
(0) 21AUG86		0.0	67.1	60.7	188.4
	CUMULATIVE		67.1	127.8	316.2
(20) 10SEP86		0.0	64.8	64.2	195.9
	CUMULATIVE		60.8	124.9	320.9

AREA CHANGES AT DESIGNATED RANGES IN CUBIC METERS/METER PORT HEIDEN

LENS 1 TOP TO 3.0 METERS
 LENS 2 3.0 TO 0.0
 LENS 3 0.0 TO -0.9
 LENS 4 -0.9 TO -2.4

RANGE PH-6

	LENS	1	2	3	4
(0) 21AUG86					
AREA CHANGE		0.0	-6.3	3.5	7.5
AREA CHANGE CUMULATIVE			-6.3	-2.8	4.7
ANNUALIZED CHANGE (CUBIC M/M/YR)		0.0	-115.4	63.8	136.9
ANNUALIZED CHANGE CUMULATIVE (CUBIC M/M/YR)			-116.4	-51.6	85.3
(20) 10SEP86					

END AREAS OF DESIGNATED LENSES IN CUBIC METERS/METER

PORT HEIDEN

LENS 1 TOP TO 3.0 METERS
LENS 2 3.0 TO 0.0
LENS 3 0.0 TO -0.9
LENS 4 -0.9 TO -2.4

() =THE NUMBER OF DAYS BETWEEN THE **INDICATED** SURVEY AND THE PREVIOUS SURVEY

CALCULATIONS START AT -0.3 METERS FROM BASELINE

RANGE PH-7

	LENS	1	2	3	4
(Ø) 21AUG86		0.0	60.6	35.6	147.6
	CUMULATIVE		50.5	86.2	233.8

END AREAS OF DESIGNATED LENSES IN CUBIC METERS/METER

PORT HEIDEN

LENS 1 TOP TO 3.0 METERS
 LENS 2 3.0 TO 0.0
 LENS 3 0.0 TO -0.9
 LENS 4 -0.9 TO -2.4

() =THE NUMBER OF DAYS BETWEEN THE INDICATED SURVEY AND THE PREVIOUS SURVEY

CALCULATIONS START AT 10.7 METERS FROM BASELINE

RANGE PH-8

	LENS	1	2	3	4
(0) 21AUG86		0.0	59.6	65.2	199.4
	CUMULATIVE		59.6	124.8	324.3
(21) 11SEP86		0.0	61.8	64.1	197.4
	CUMULATIVE		61.8	125.9	323.3

AREA CHANGES AT DESIGNATED RANGES IN CUBIC METERS/METER

PORT HEIDEN

LENS 1 TOP TO 3.0 METERS
 LENS 2 3.0 TO 0.0
 LENS 3 0.0 TO -0.9
 LENS 4 -0.9 TO -2.4

RANGE PH-8

	LENS	1	2	3	4
(0) 21AUG86					
AREA CHANGE		0.0	2.2	-1.2	-2.1
AREA CHANGE CUMULATIVE			2.2	1.0	-1.0
ANNUALIZED CHANGE (CUBIC M/M/YR)		0.0	38.7	-20.4	-35.7
ANNUALIZED CHANGE CUMULATIVE (CUBIC M/M/YR)			38.6	18.2	-17.5
(21) 11SEP86					

END AREAS OF DESIGNATED LENSES IN CUBIC METERS/METER

PORT HEIDEN

LENS 1 TOP TO 3.0 METERS
 LENS 2 3.0 TO 0.0
 LENS 3 0.0 TO -0.9
 LENS 4 -0.9 TO -2.4

() =THE NUMBER OF DAYS BETWEEN THE INDICATED SURVEY AND THE PREVIOUS SURVEY

CALCULATIONS START AT -4.8 METERS FROM BASELINE

RANGE PH-9

	LENS	1	2	3	4
(0) 20AUG86		0.0	82.5	62.6	143.3
	CUMULATIVE		82.5	134.9	278.2
(8) 28AUG86		0.0	64.9	45.0	154.6
	CUMULATIVE		64.9	110.0	264.6

AREA CHANGES AT DESIGNATED RANGES IN CUBIC METERS/METER PORT HEIDEN

LENS 1 TOP TO 3.0 METERS
 LENS 2 3.0 TO 0.0
 LENS 3 0.0 TO -0.9
 LENS 4 -0.9 TO -2.4

RANGE PH-9

	LENS	1	2	3	4
(0) 20AUG86					
AREA CHANGE		0.0	-17.5	-7.4	11.3
AREA CHANGE CUMULATIVE			-17.5	-25.0	-13.7
ANNUALIZED CHANGE (CUBIC M/M/YR)		-0.1	-799.5	-339.7	516.1
ANNUALIZED CHANGE CUMULATIVE (CUBIC M/M/YR)			-799.6	-1139.3	-623.3
(8) 28AUG86					

END AREAS OF DESIGNATED LENSES IN CUBIC METERS/METER

PORT HEIDEN

LENS 1 TOP TO 3.0 METERS
 LENS 2 3.1d TO 0.0
 LENS 3 0.0 TO -0.9
 LENS 4 -0.9 TO -2.4

() =THE NUMBER OF DAYS BETWEEN THE INDICATED SURVEY AND THE PREVIOUS SURVEY

CALCULATIONS START AT 56.7 METERS FROM BASELINE

RANGE PH-10

	LENS	1	2	3	4
(0) 20AUG86		0.0	103.5	67.5	188.6
	CUMULATIVE		103.5	161.0	329.6
(5) 25AUG86		0.0	92.0	57.3	160.1
	CUMULATIVE		92.0	149.2	309.4
(3) 28AUG86		0.0	100.3	62.7	167.6
	CUMULATIVE		100.3	163.0	330.7
(8) 5SEP86		0.0	98.7	61.8	168.7
	CUMULATIVE		98.7	160.5	329.2
(6) 11SEP86		0.0	83.5	57.8	167.9
	CUMULATIVE		83.5	141.3	309.3

AREA CHANGES AT DESIGNATED RANGES IN CUBIC METERS/METER PORT HEIDEN

LENS 1 TOP TO 3.0 METERS
 LENS 2 3.0 TO 0.0
 LENS 3 0.0 TO -0.9
 LENS 4 -0.9 TO -2.4

RANGE PH-10

	LENS	1	2	3	4
(0) 20AUG86					
AREA CHANGE		0.0	-11.5	-0.3	-8.4
AREA CHANGE CUMULATIVE			-11.6	-11.8	-20.3
ANNUALIZED CHANGE (CUBIC M/M/YR)		0.1	-842.0	-21.1	-616.7
ANNUALIZED CHANGE CUMULATIVE (CUBIC M/M/YR)			-841.9	-863.0	-1479.7
(5) 25AUG86					
AREA CHANGE		0.0	8.3	5.5	7.5
AREA CHANGE CUMULATIVE			8.3	13.8	21.3
ANNUALIZED CHANGE (CUBIC M/M/YR)		0.4	1009.6	666.9	912.1
ANNUALIZED CHANGE CUMULATIVE (CUBIC M/M/YR)			1010.1	1677.0	2589.1
(3) 28AUG86					
AREA CHANGE		0.0	-1.6	-0.9	1.1
AREA CHANGE CUMULATIVE			-1.6	-2.5	-1.4
ANNUALIZED CHANGE (CUBIC M/M/YR)		0.5	-72.9	-41.6	48.4
ANNUALIZED CHANGE CUMULATIVE (CUBIC M/M/YR)			-72.4	-114.0	-65.7
(8) 5SEP86					
AREA CHANGE		0.0	-16.2	-4.0	-0.8
AREA CHANGE CUMULATIVE			-15.2	-19.2	-20.0
ANNUALIZED CHANGE (CUBIC M/M/YR)		-0.9	-922.6	-243.1	-47.1
ANNUALIZED CHANGE cumulative (CUBIC M/M/YR)			-923.5	-1166.7	-1213.7
(6) 11SEP86					
*** NET AREA CHANGE BETWEEN 20 AUG 1986 AND 11 SEP 1986					22 DAYS ***
NET AREA CHANGE		0.0	-20.0	0.3	-0.7
NET AREA CHANGE CUMULATIVE			-20.0	-19.7	-20.4
NET ANNUALIZED CHANGE (CUBIC M/M/YR)		0.0	-331.8	4.7	-11.0
NET ANNUALIZED CHANGE CUMULATIVE (CUBIC M/M/YR)			-331.8	-327.1	-338.1

END AREAS OF DESIGNATED LENSES IN CUBIC METERS/METER

PORT HEIDEN

LENS 1 TOP TO 3.0 METERS
 LENS 2 3.0 TO 0.0
 LENS 3 0.0 TO -0.9
 LENS 4 -0.9 TO -2.4

() =THE NUMBER OF DAYS BETWEEN THE INDICATED SURVEY AND THE PREVIOUS SURVEY

CALCULATIONS START AT 36.6 METERS FROM BASELINE

RANGE PH-11

	LENS	1	2	3	4
(0) 20AUG86		0.0	113.8	66.6	164.0
	CUMULATIVE		113.8	180.3	344.3
(8) 28AUG86		0.0	138.3	80.3	212.0
	CUMULATIVE		138.3	218.7	430.7

AREA CHANGES AT DESIGNATED RANGES IN CUBIC METERS/METER PORT HEIDEN

LENS 1 TOP TO 3.0 METERS
 LENS 2 3.0 TO 0.0
 LENS 3 0.0 TO -0.9
 LENS 4 -0.9 TO -2.4

RANGE PH-11

	LENS	1	2	3	4
(0) 20AUG86					
AREA CHANGE		0.0	24.5	13.9	48.0
AREA CHANGE CUMULATIVE			24.5	38.4	86.4
ANNUALIZED CHANGE (CUBIC M/M/YR)		-0.1	1117.9	633.4	2189.0
ANNUALIZED CHANGE CUMULATIVE (CUBIC M/M/YR)			1117.8	1751.2	3940.2
(8) 28AUG86					

END AREAS OF DESIGNATED LENSES IN CUBIC METERS/METER

PORT HEIDEN

LENS 1 TOP TO 3.0 METERS
 LENS 2 3.0 TO 0.0
 LENS 3 0.0 TO -0.9
 LENS 4 -0.9 TO -2.4

() =THE NUMBER OF DAYS BETWEEN THE INDICATED SURVEY AND THE PREVIOUS SURVEY

CALCULATIONS START AT -1.2 METERS FROM BASELINE

RANGE PH-12

	LENS 1	2	3	4
(0) 20AUG86	0.0	88.9	65.8	188.0
CUMULATIVE		88.9	154.7	342.7
(8) 28AUG86	0.0	96.6	60.5	200.1
CUMULATIVE		96.6	157.1	357.2

AREA CHANGES AT DESIGNATED RANGES IN CUBIC METERS/METER PORT HEIDEN

LENS 1 TOP TO 3.0 METERS
 LENS 2 3.0 TO 0.0
 LENS 3 0.0 TO -0.9
 LENS 4 -0.9 TO -2.4

RANGE PH-12

	LENS 1	2	3	4
(0) 20AUG86				
AREA CHANGE	0.0	7.7	-5.2	12.1
AREA CHANGE CUMULATIVE		7.7	2.4	14.6
ANNUALIZED CHANGE (CUBIC M/M/YR)	-0.2	349.8	-238.9	552.6
ANNUALIZED CHANGE CUMULATIVE (CUBIC M/M/YR)		349.6	110.8	663.3
(8) 28AUG86				

END AREAS OF DESIGNATED LENS IN CUBIC METERS/METER

PORT HEIDEN

LENS 1 TOP TO 3.0 METERS
 LENS 2 3.0 TO 0.0
 LENS 3 0.0 TO -0.9
 LENS 4 -0.9 TO -2.4

() = THE NUMBER OF DAYS BETWEEN THE INDICATED SURVEY AND THE PREVIOUS SURVEY

CALCULATIONS START AT 7.3 METERS FROM BASELINE

RANGE PH-13

	LENS 1	2	3	4
(0) 20AUG86	0.5	91.0	67.7	206.4
		91.5	159.2	365.6
(8) 28AUG86	0.0	86.9	64.4	204.6
		86.9	151.3	355.9

AREA CHANGES AT DESIGNATED RANGES IN CUBIC METERS/METER PORT HEIDEN

LENS 1 TOP TO 3.0 METERS
 LENS 2 3.0 TO 0.0
 LENS 3 0.0 TO -0.9
 LENS 4 -0.9 TO -2.4

RANGE PH-13

	LENS 1	2	3	4
(0) 20AUG86				
AREA CHANGE	-0.5	-4.1	-3.3	-1.8
AREA CHANGE CUMULATIVE		-4.6	-7.9	-9.7
ANNUALIZED CHANGE (CUBIC M/M/YR)	-20.7	-188.3	-151.2	-84.3
ANNUALIZED CHANGE CUMULATIVE (CUBIC M/M/YR)		-209.0	-360.2	-444.5

(8) 28AUG86

END AREAS OF DESIGNATED LENSES IN CUBIC METERS/METER

PORT HEIDEN

LENS 1 TOP TO 3.0 METERS
 LENS 2 3.0 TO 0.0
 LENS 3 0.0 TO -0.9
 LENS 4 -0.9 TO -2.4

() =THE NUMBER OF DAYS BETWEEN THE INDICATED SURVEY ANO THE PREVIOUS SURVEY

CALCULATIONS START AT 16.8 METERS FROM BASELINE

RANGE PH-14

	LENS	1	2	3	4
(0) 20AUG86		0.1	40.2	62.7	178.9
CUMULATIVE			40.3	92.9	271.8
(8) 28AUG86		0.1	40.8	57.1	323.2
CUMULATIVE			40.9	98.0	421.2
(14) 11SEP86		0.0	52.7	65.2	190.1
CUMULATIVE			52.7	107.9	298.0

AREA CHANGES AT DESIGNATED RANGES IN CUBIC METERS/METER PORT HEIDEN

LENS 1 TOP TO 3.0 METERS
 LENS 2 3.0 TO 0.0
 LENS 3 0.0 TO -0.9
 LENS 4 -0.9 TO -2.4

	LENS	1	2	3	4
(0) 20AUG86					
AREA CHANGE		0.1	0.6	4.5	144.2
AREA CHANGE CUMULATIVE			0.6	5.1	149.3
ANNUALIZED CHANGE (CUBIC M/M/YR)		2.5	26.5	203.3	6681.3
ANNUALIZED CHANGE CUMULATIVE (CUBIC M/M/YR)			29.1	232.4	6813.7
(8) 28AUG86					
AREA CHANGE		-0.1	11.9	-1.9	-133.0
AREA CHANGE CUMULATIVE			11.6	9.9	-123.2
ANNUALIZED CHANGE (CUBIC M/M/YR)		-3.5	310.6	-50.1	-3467.8
ANNUALIZED CHANGE CUMULATIVE (CUBIC M/M/YR)			307.1	257.0	-3210.8
(14) 11SEP86					
*** NET AREA CHANGE BETWEEN 20 AUG 1986 ANO 11 SEP 1986					2 2 DAYS ***
NET AREA CHANGE		-0.1	12.5	2.5	11.2
NET AREA CHANGE CUMULATIVE			12.4	15.0	26.2
NET ANNUALIZED CHANGE (CUBIC M/M/YR)		-1.3	207.3	42.1	186.4
NET ANNUALIZE CHANGE CUMULATIVE (CUBIC M/M/YR)			206.0	248.0	434.5

END AREAS OF DESIGNATED LENSES IN CUBIC METERS/METER

PORT HEIDEN

LENS 1 TOP TO 3.0 METERS
 LENS 2 3.0 TO 0.0
 LENS 3 0.0 TO -0.9
 LENS 4 -0.9 TO -2.4

() =THE NUMBER OF DAYS BETWEEN THE INDICATED SURVEY AND THE PREVIOUS SURVEY

CALCULATIONS START AT 52.1 METERS FROM BASELINE

RANGE PH-15

	LENS 1	2	3	4
(0) 20AUG86	0.0	53.5	34.7	88.3
CUMULATIVE		53.5	88.2	176.6
(8) 28AUG86	0.0	56.1	37.6	86.9
CUMULATIVE		56.1	93.7	180.5

AREA CHANGES AT DESIGNATED RANGES IN CUBIC METERS/METER PORT HEIDEN

LENS 1 TOP TO 3.0 METERS
 LENS 2 3.0 TO 0.0
 LENS 3 0.0 TO -0.9
 LENS 4 -0.9 TO -2.4

RANGE PH-15

	LENS 1	2	3	4
(0) 20AUG86				
AREA CHANGE	0.0	2.6	2.9	-1.5
AREA CHANGE CUMULATIVE		2.6	5.5	4.0
ANNUALIZED CHANGE (CUBIC M/M/YR)	-0.3	116.6	132.6	-67.0
ANNUALIZED CHANGE CUMULATIVE (CUBIC M/M/YR)		116.4	248.9	181.9
(8) 28AUG86				

END AREAS OF DESIGNATED LENSES IN CUBIC METERS/METER

PORT HEIDEN

LENS 1 TOP TO 3.0 METERS
 LENS 2 3.0 TO 0.0
 LENS 3 0.0 TO -0.9
 LENS 4 -0.9 TO -2.4

() =THE NUMBER OF DAYS BETWEEN THE INDICATED SURVEY AND THE PREVIOUS SURVEY

CALCULATIONS START AT 16.8 METERS FROM BASELINE

RANGE PH-16

	LENS 1	2	3	4
(0) 20AUG86	0.0	85.2	64.9	161.2
CUMULATIVE		85.2	140.1	301.3
(8) 28AUG86	0.1	82.3	66.5	156.3
CUMULATIVE		82.4	148.9	316.1
(14) 11 SEP86	0.0	80.0	63.0	140.9
CUMULATIVE		80.0	143.0	283.9

AREA CHANGES AT DESIGNATED RANGES IN CUBIC METERS/METER PORT HEIDEN

LENS 1 TOP TO 3.0 METERS
 LENS 2 3.0 TO 0.0
 LENS 3 0.0 TO -0.9
 LENS 4 -0.9 TO -2.4

RANGE PH-16

	LENS 1	2	3	4
(0) 20AUG86				
AREA CHANGE	0.1	-2.9	11.6	5.1
AREA CHANGE CUMULATIVE		-2.8	8.8	13.8
ANNUALIZED CHANGE (CUBIC M/M/YR)	3.4	-132.6	530.3	23% .5
ANNUALIZED CHANGE CUMULATIVE (CUBIC M/M/YR)		-129.2	401.0	631.5
(8) 28AUG86				
AREA CHANGE	-0.1	-2.2	-3.5	-25.4
AREA CHANGE CUMULATIVE		-2.3	-6.9	-31.2
ANNUALIZED CHANGE (CUBIC M/M/YR)	-2.8	-68.4	-92.6	-661.0
ANNUALIZED CHANGE CUMULATIVE (CUBIC M/M/YR)		-61.2	-153.7	-814.7
(14) 11SEP86				

*** NET AREA CHANGE BETWEEN 20 AUG 1986 AND 11 SEP 1986 22 DAYS ***

NET AREA CHANGE	0.0	-5.1	8.1	-20.3
NET AREA CHANGE CUMULATIVE		-5.2	2.9	-17.4
NET ANNUALIZED CHANGE (CUBIC M/M/YR)	-0.5	-85.4	133.9	-336.8
NET ANNUALIZED CHANGE CUMULATIVE (CUBIC M/M/YR)		-85.9	48.0	-288.8

END AREAS OF DESIGNATED LENSES IN CUBIC METERS/METER

PORT HEIDEN

LENS 1 TOP, TO 3.0 METERS
LENS 2 **3.0** TO 0.0
LENS 3 0.0 TO **-0.9**
LENS 4 -0.9 TO -2.4

() =THE NUMBER OF DAYS BETWEEN THE **INDICATED** SURVEY AND THE PREVIOUS SURVEY

CALCULATIONS START AT 37.8 METERS FROM BASELINE

RANGE **PH-17**

	LENS	1	2	3	4
(0) 3SEP86		0.0	43.1	41.6	198.6
	CUMULATIVE		43.1	84.7	283.3

END AREAS OF DESIGNATED LENSES IN CUBIC METERS/METER

PORT HEIDEN

LENS 1 TOP TO 3.0 METERS
LENS 2 3.0 TO 0.0
LENS 3 0.0 TO -0.9
LENS 4 -0.9 TO -2.4

() THE NUMBER OF DAYS BETWEEN THE INDICATED SURVEY AND THE PREVIOUS SURVEY

CALCULATIONS START AT 24.4 METERS FROM BASELINE

RANGE PH-18

	LENS	1	2	3	4
(0) 3SEP86		0.0	38.3	73.0	236.8
	CUMULATIVE		38.3	111.2	348.0

END AREAS OF DESIGNATED LENSES IN CUBIC METERS/METER

PORT HEIDEN

LENS 1 TOP TO 3.0 METERS
LENS 2 3.0 TO 0.0
LENS 3 0.0 TO -0.9
LENS 4 -0.9 TO -2.4

() =THE NUMBER OF DAYS BETWEEN THE INDICATED SURVEY AND THE PREVIOUS SURVEY

CALCULATIONS START AT 23.2 METERS FROM BASELINE

RANGE **PH-19**

	LENS	1	2	3	4
(0) 9SEP86		0,0	22.5	39.9	125.5
	CUMULATIVE		22.5	62,4	187.9

END AREAS OF DESIGNATED LENSES IN CUBIC METERS/METER

PORT HEIDEN

LENS 1 TOP TO 3.0 METERS
LENS 2 3.0 TO 0.0
LENS 3 0.0 TO -0.9
LENS 4 -0.9 TO -2.4

() =THE NUMBER OF DAYS BETWEEN THE INDICATED SURVEY AND THE PREVIOUS SURVEY

CALCULATIONS START AT 52.4 METERS FROM BASELINE

RANGE PH-20

	LENS	1	2	3	4
(0) 4SEP88		0.0	96.5	53.6	132.1
	CUMULATIVE		96.5	150.1	282.1

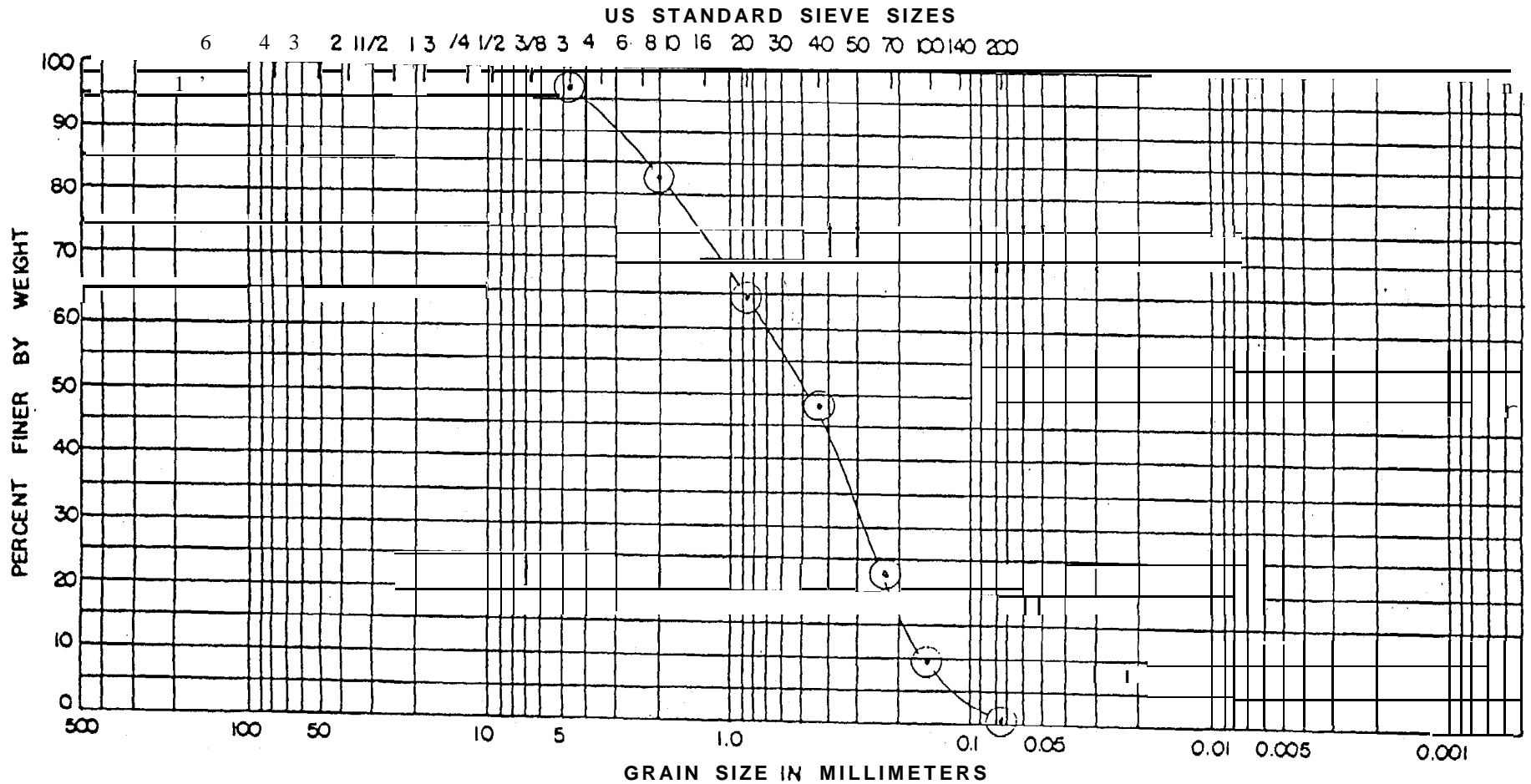
APPENDIX II-D

Beach Sand Sieving Analysis Graphs

Port Heiden, Alaska

Sand samples were taken at Stations 1-7, 10, 16, and 19. At each of these stations, samples were taken from five geomorphological features: dune, berm, berm trough, beach face, and low-tide terrace. For analysis of each individual station, a physical composite sample was made up from the five geomorphological feature samples for that station. Then, for analysis of each geomorphological feature, a physical composite sample was made up from the corresponding feature samples from five stations, as follows:

Feature	Station									
	1	2	3	4	5	6	1	6	1	9
Dune	x			x		x	x			x
Berm	x	x			x	x				x
Berm trough	x	x			x	x			x	
Beach face			x		x	x			x	x
Low-tide terrace	x	x			x			x		x



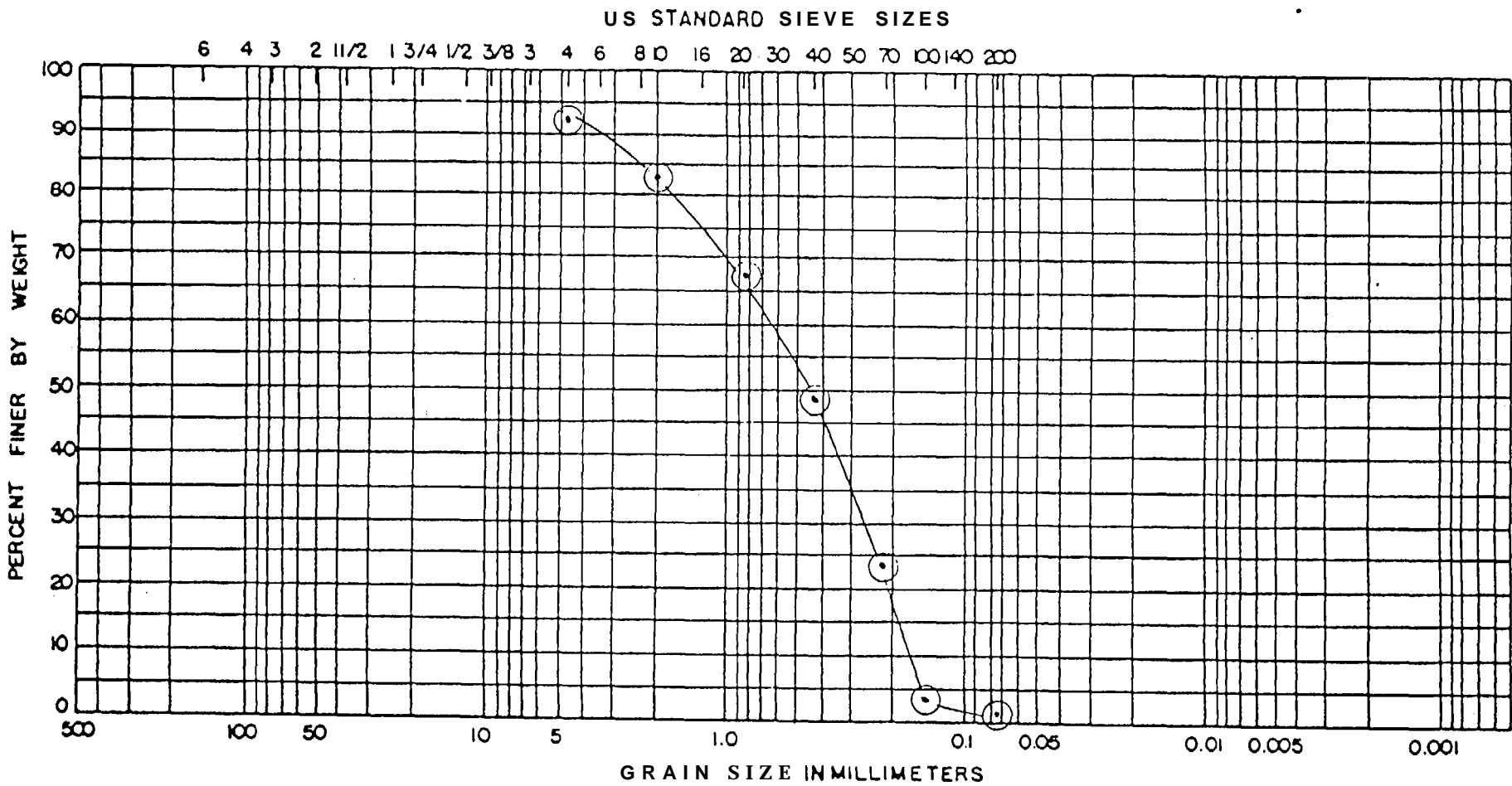
BOUL DERS	COBBLES	GRAVEL		SAND			FINES		
		COARSE	FINE	COARSE	MEDIUM	FINE	SILT	SIZES	CLAY-SIZES

BORING NO.	ELEV. OR DEPTH	NAT WC	LL	PL	PI	CLASSIFICATION
						PORT HEIDEN - STATION 2

GRAIN SIZE DISTRIBUTION

JOB NO. _____

SOIL a MATERIAL ENGINEERS, INC.



BOULDERS	COBBLES	GRAVEL		SAND			FINES		
		COARSE	FINE	COARSE	MEDIUM	FINE	SILT SIZES	CLAY SIZES	

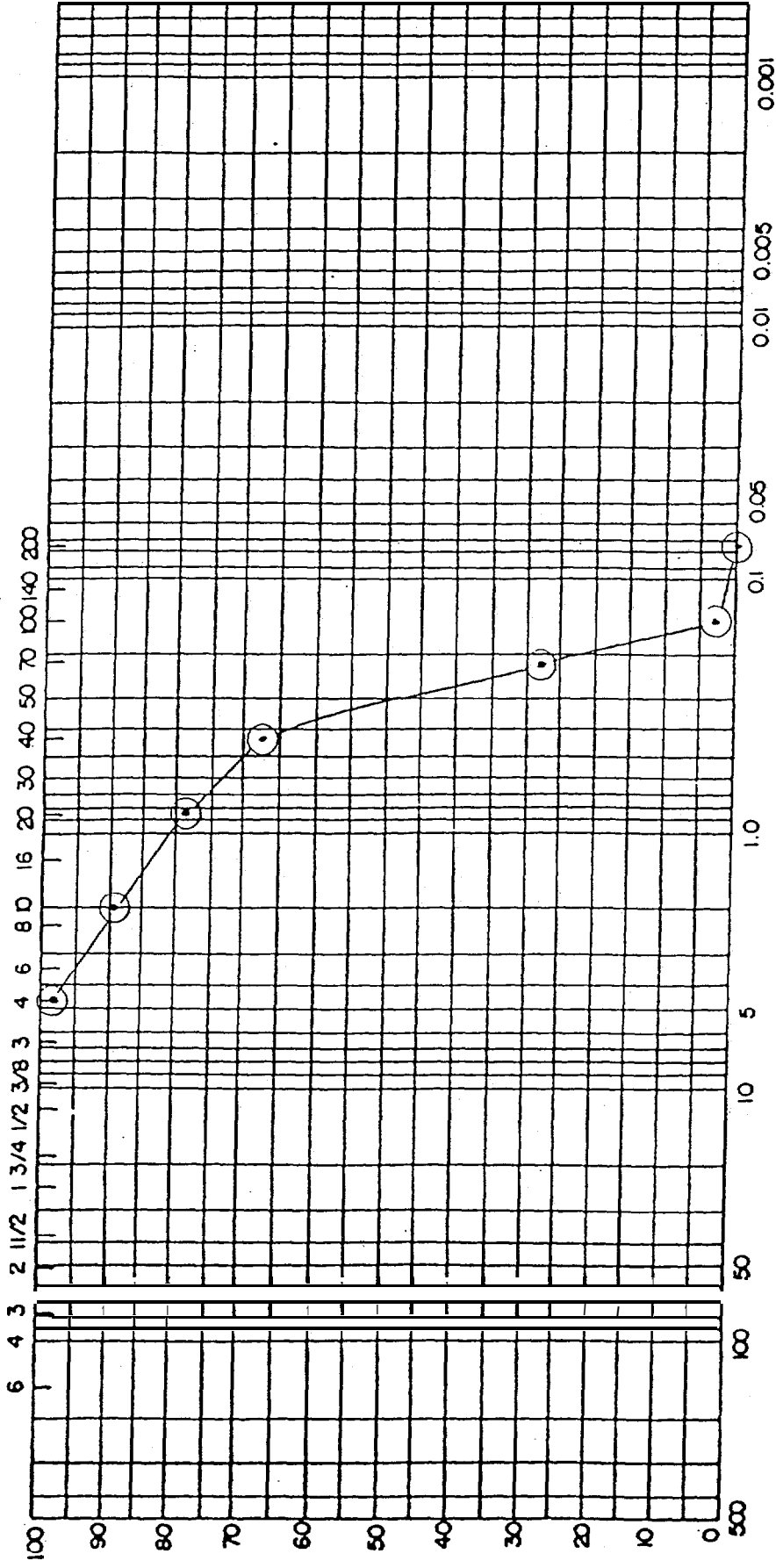
BORING NO.	ELEV. OR DEPTH	NAT WC	LL	PL	P _s	CLASSIFICATION
						PORT HEIDEN - STATION 3

GRAIN SIZE DISTRIBUTION

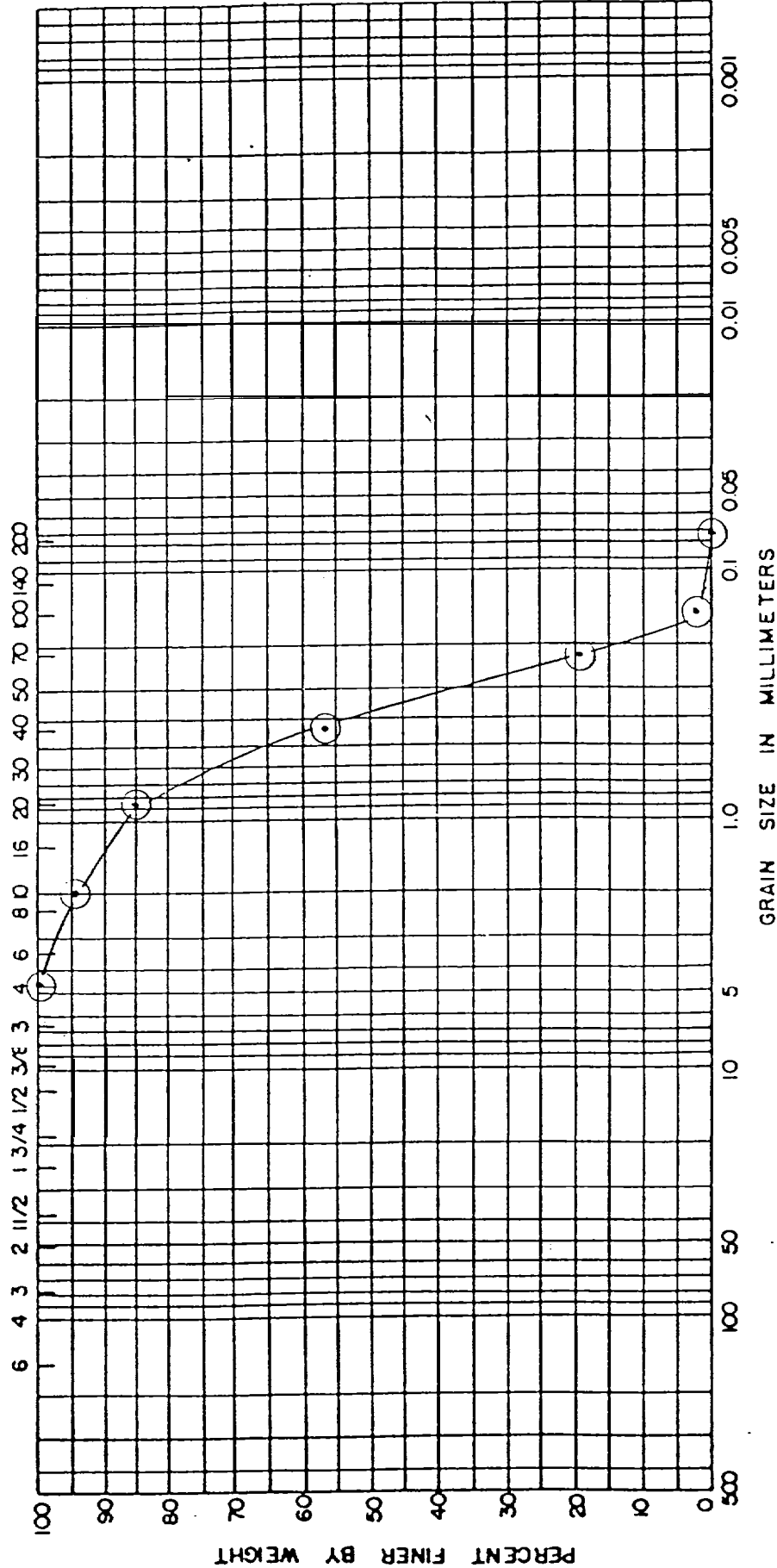
JOB NO, _____

SOIL & MATERIAL ENGINEERS, INC.

US STANDARD SIEVE SIZES

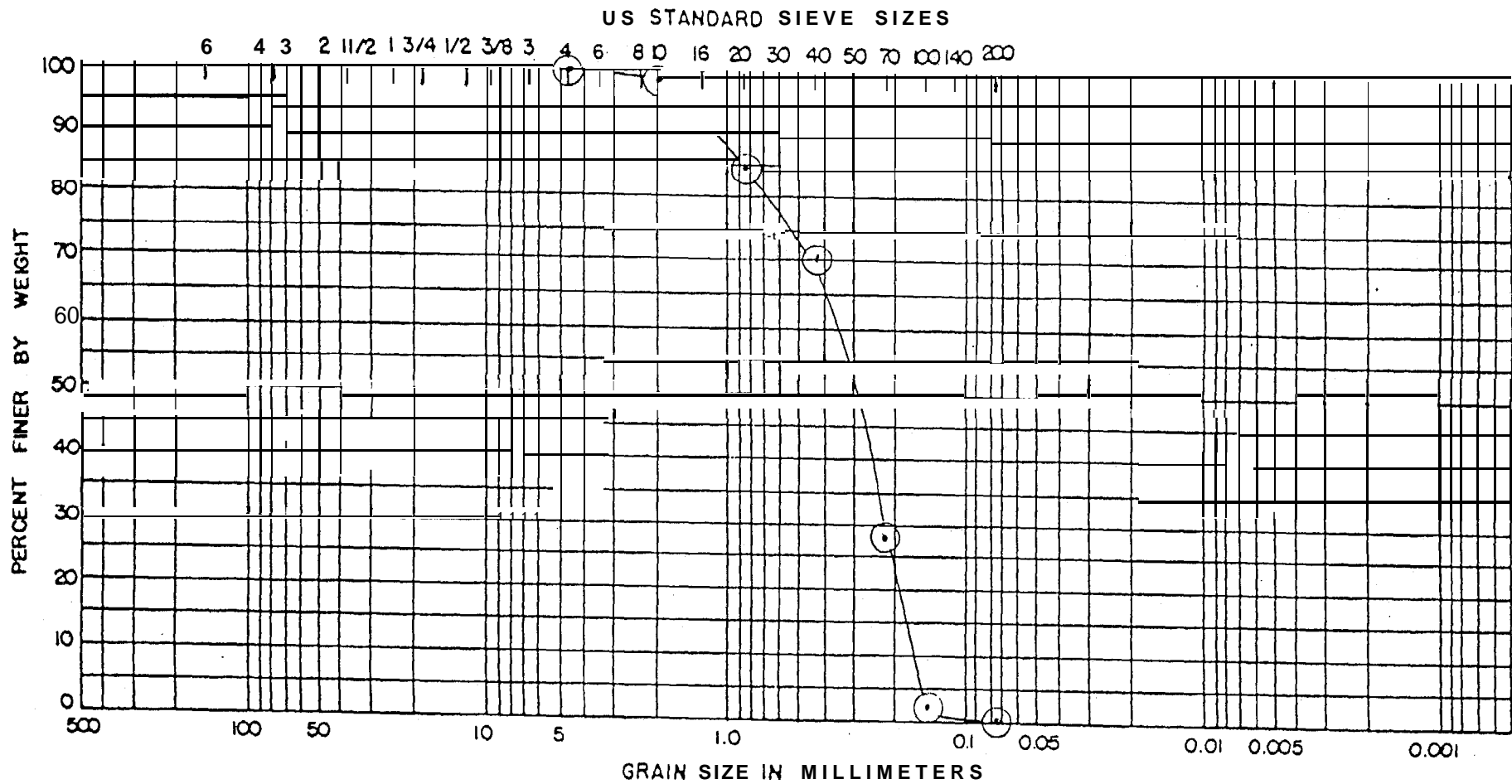


US STANDARD SIEVE SIZES



SOIL DEFS	GRAVEL		SAND		FINES	
	COARSE	FINE	COARSE	MEDIUM	FINE	CLAY SIZES

BORING NO.	ELEV. OR DEPTH	NAT	WC	LL	PL	PI	CLASSIFICATION	GRAIN SIZE DISTRIBUTION	JOB NO. _____	SOIL & MATERIAL ENGINEER INC.



BOULDERS	COBBLES	GRAVEL		SAND			FINES		
		COARSE	FINE	COARSE	MEDIUM	FINE	SILT SIZES	CLAY SIZES	

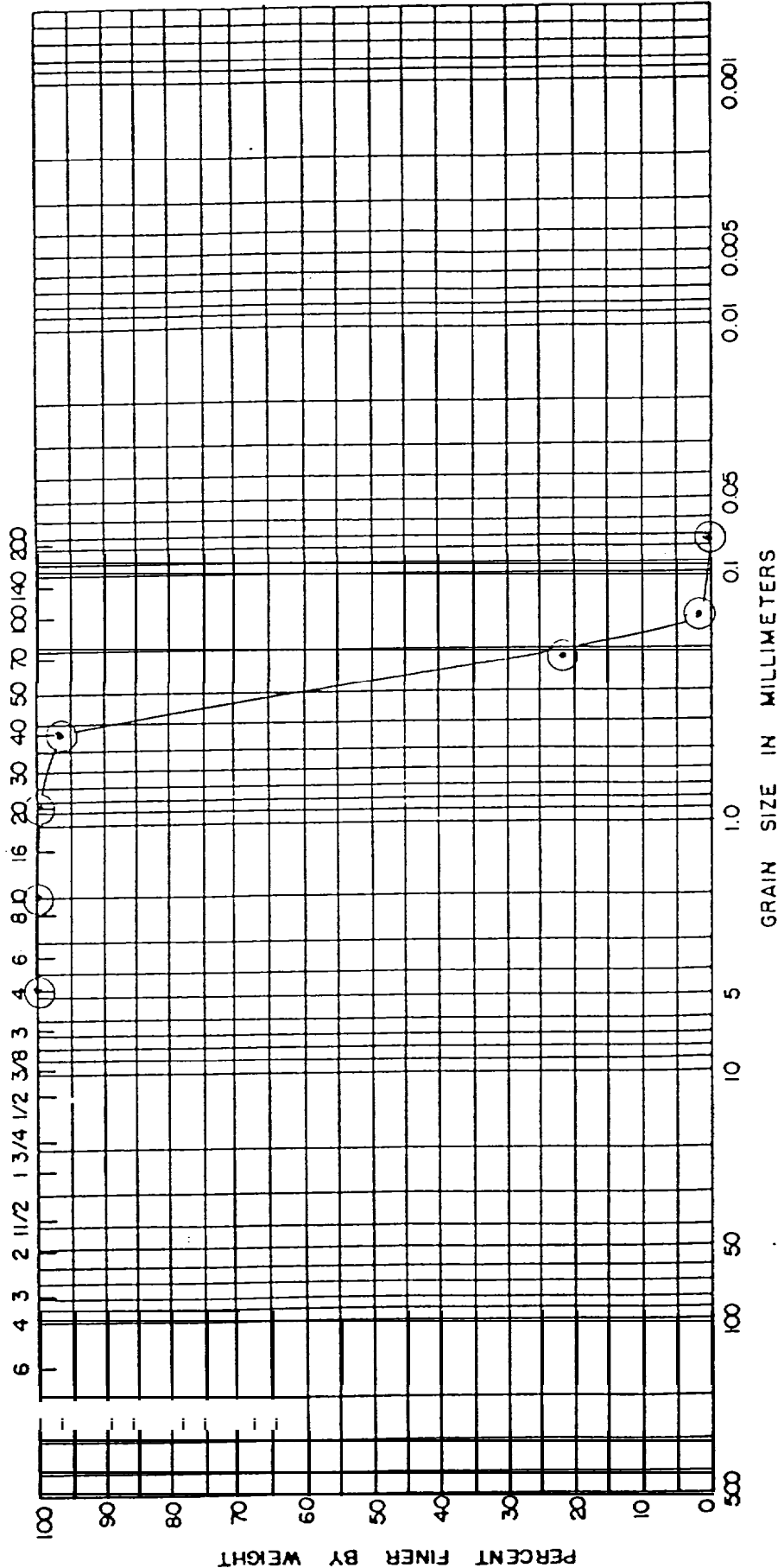
BORING No.	ELEV. OR DEPTH	NAT WC	LL	PL	PI	CLASSIFICATION
						PORT HEIDEN - STATION 6

GRAIN SIZE DISTRIBUTION

JOB N O

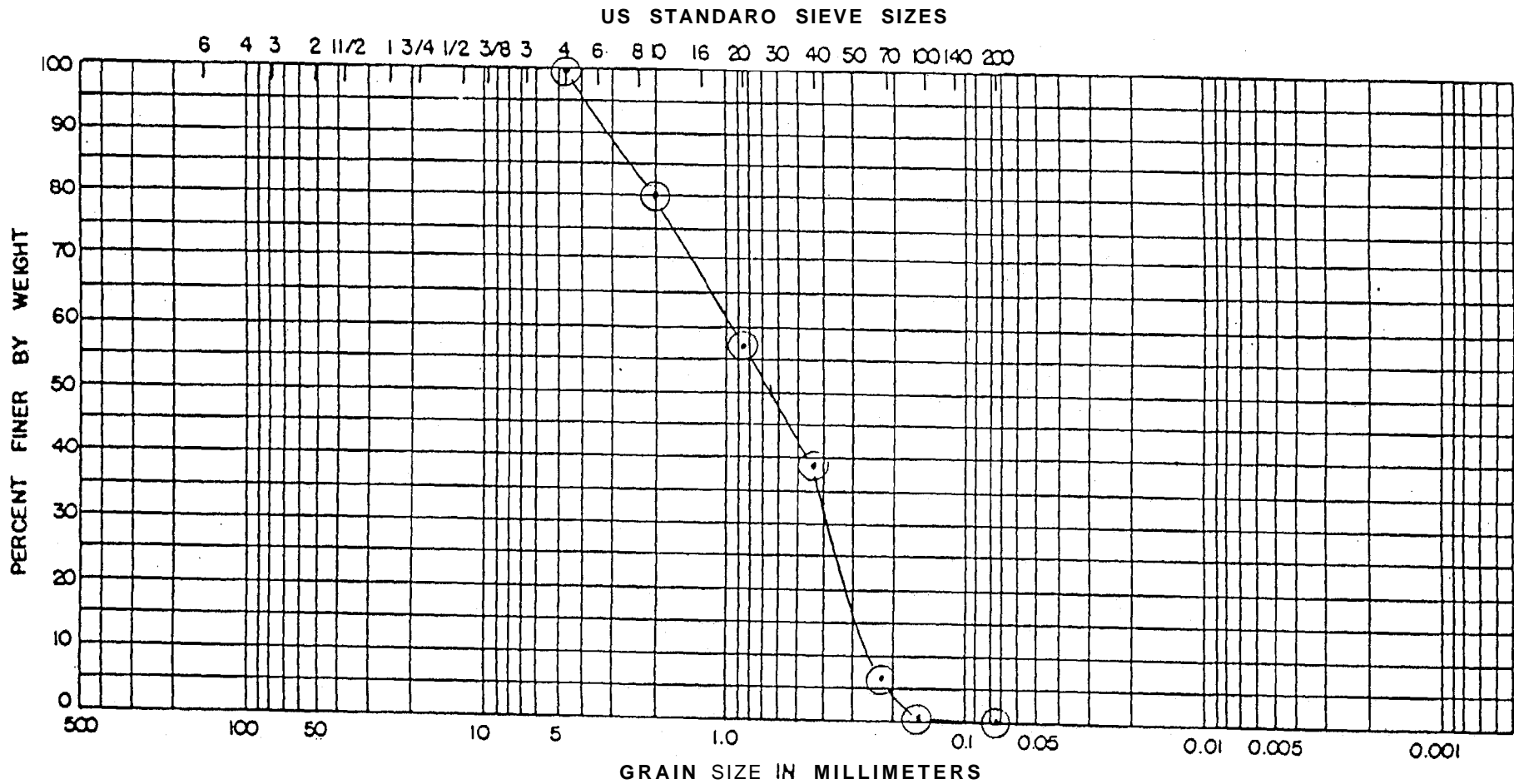
SOIL & MATERIAL ENGINEERS, INC.

US STANDARD SIEVE SIZES



BOUL DERS	GRAVEL		SAND			FINES	
	COARSE	FINE	COARSE	MEDIUM	FINE	SILT SIZES	CLAY SIZES

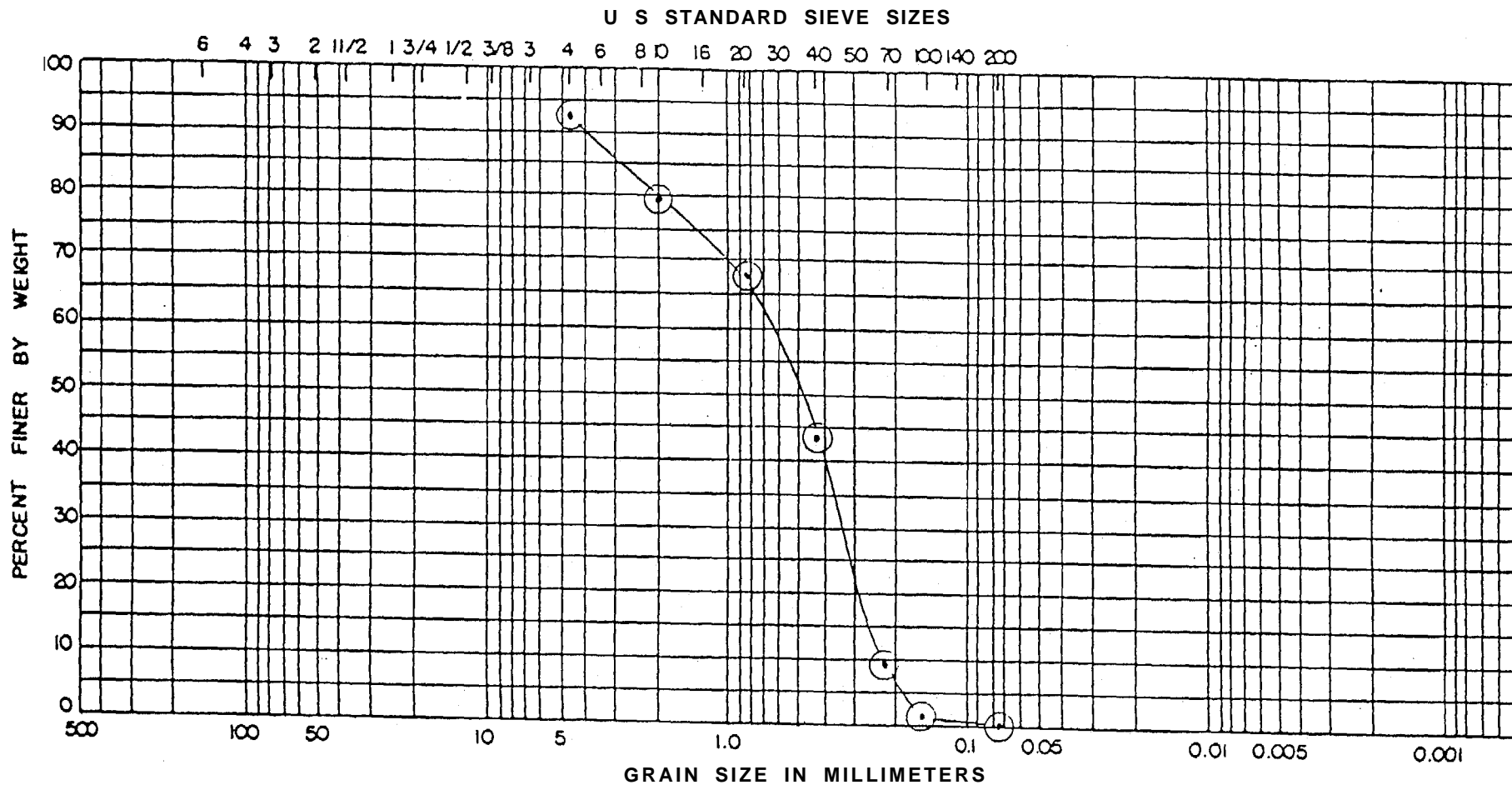
BORING NO.	ELEV. OR DEPTH	NAT WC	LL	PL	PI	CLASSIFICATION	GRAIN SIZE DISTRIBUTION	JOB NO. _____	SOIL & MATERIAL ENGINEERS, INC.



BOULDERS	COBBLES	GRAVEL		SAND			FINES	
		COARSE	FINE	COARSE	MEDIUM	FINE	SILT SIZES	CLAY-SIZES

BORING NO.	ELEV. CR. DEPTH	NAT. WC	LL	PL	PI	CLASSIFICATION
						PORT HEIDEN - STATION 10

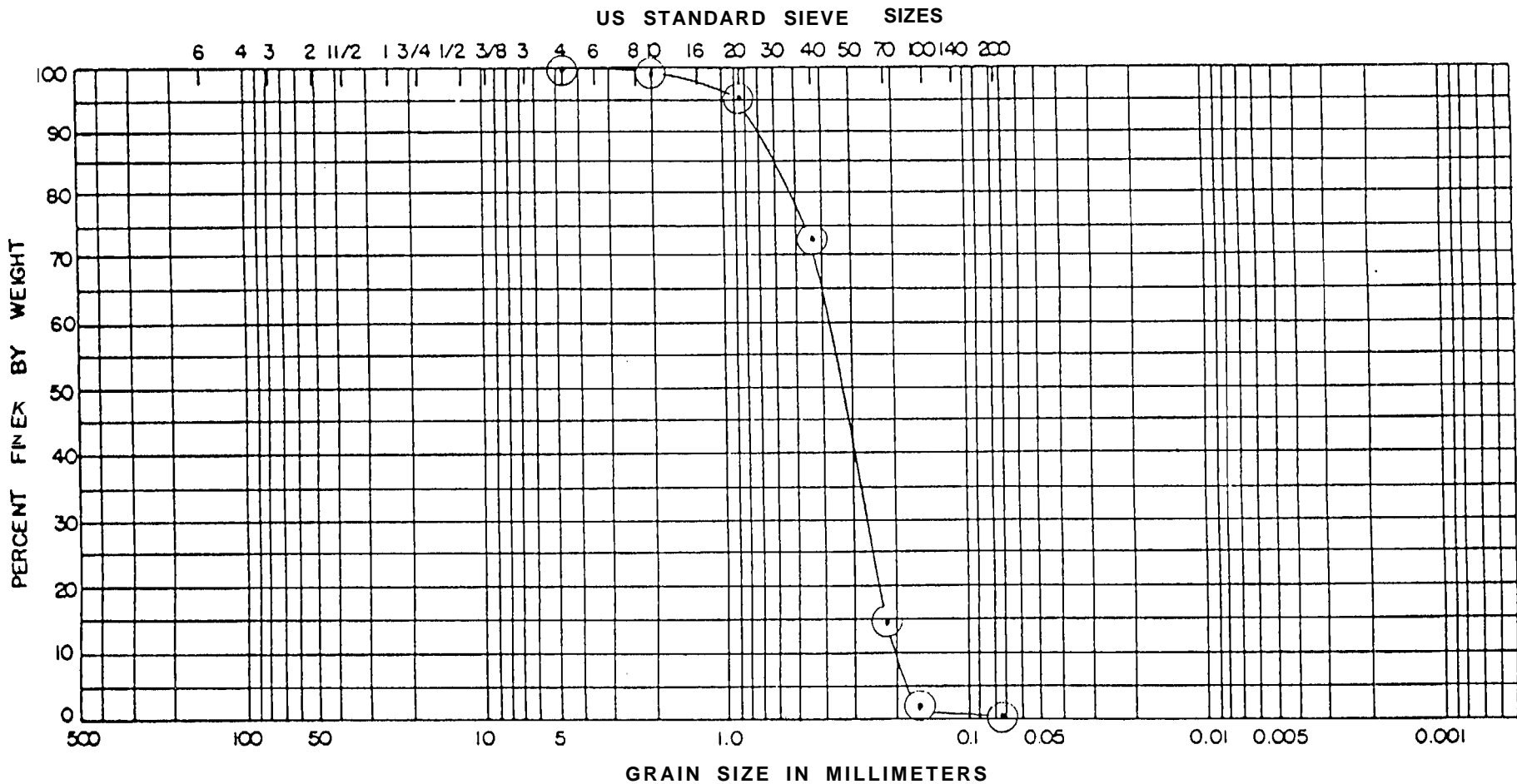
GRAIN SIZE DISTRIBUTION
 JOB N O
 SOIL MATERIAL ENGINEERS, INC.



SOIL CLASSIFICATION	GRAVEL		SAND			FINES		
	COBBLES	COARSE	FINE	COARSE	MEDIUM	FINE	SILT SIZES	CLAY SIZES

BORING NO.	ELEV. OR DEPTH	NAT WC	LL	PL	PI	CLASSIFICATION
						PORT HEIDEN - STATION 19

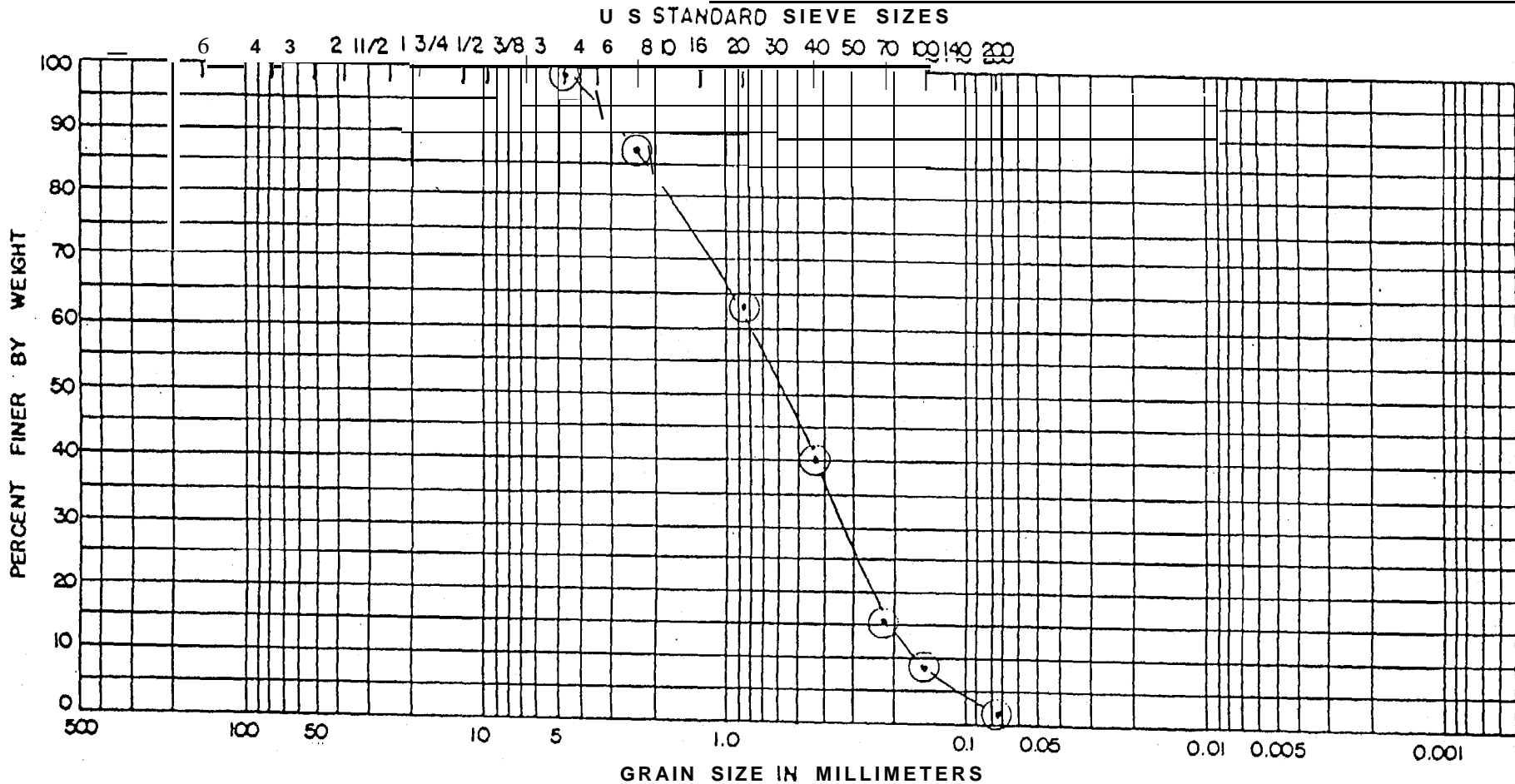
GRAIN SIZE DISTRIBUTION
 JOB NO, _____
 SOIL & MATERIAL ENGINEERS, INC.



BOUL DERS	COBBLES	GRAVEL		SAND			FINES		
		COARSE	FINE	COARSE	MEDIUM	FINE	SILT SIZES	CLAY SIZES	

BORING NO.	ELEV OR DEPTH	NAT WC	LL	PL	PI	CLASSIFICATION
						PORT HEIDEN - DUNE

GRAIN SIZE DISTRIBUTION
 JOB NO. _____
 SOIL MATERIAL ENGINEERS, INC.



BOULDERS	COBBLES	GRAVEL		SAND			FINES	
		COARSE	FINE	COARSE	MEDIUM	FINE	SILT SIZES	CLAY-SIZES

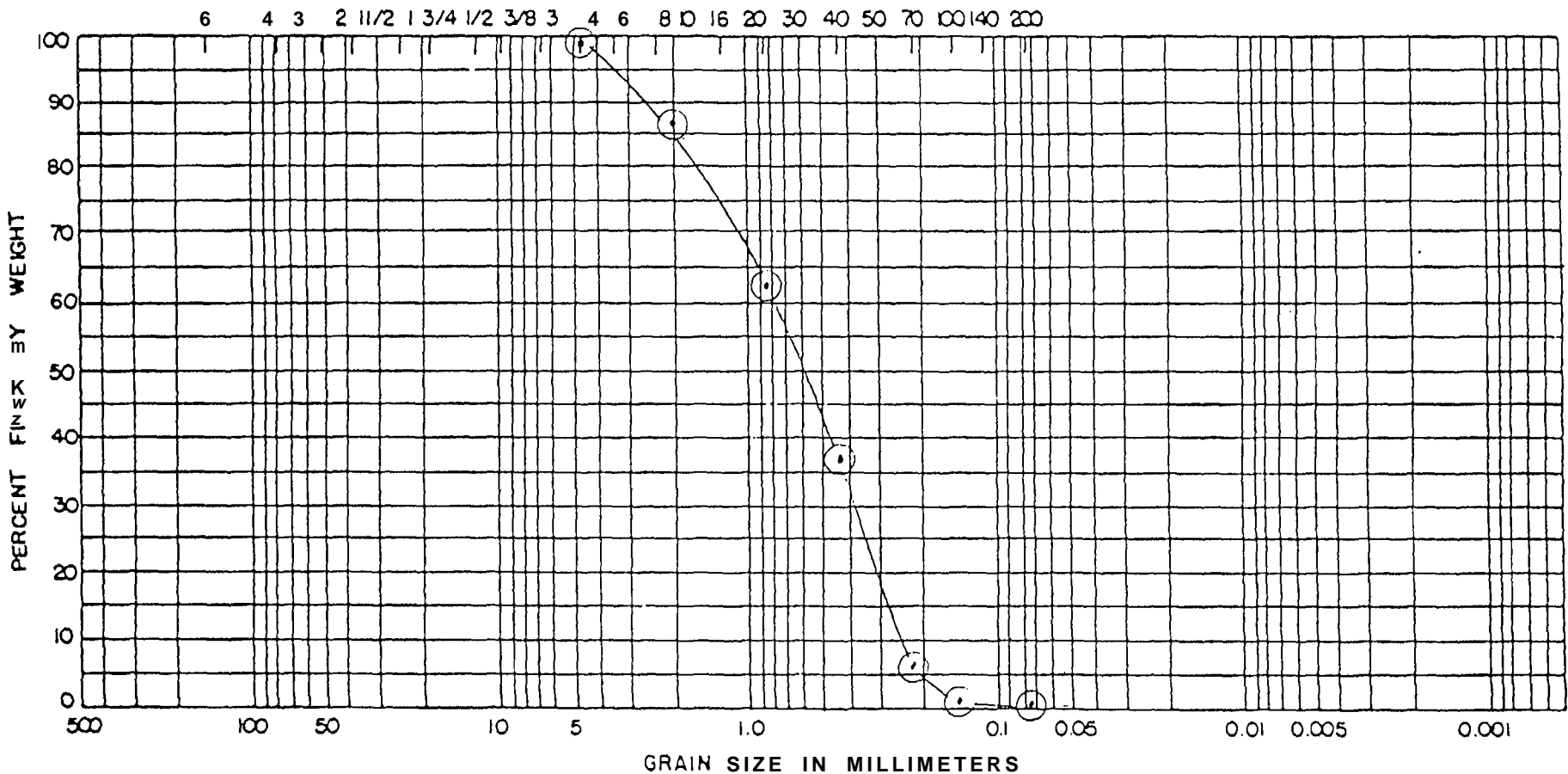
BORING NO.	ELEV. OR DEPTH	NAT WC	LL	PL	PI	CLASSIFICATION
						PORT HEIDEN - BERM

GRAIN SIZE DISTRIBUTION

JOB NO. _____

SOIL & MATERIAL ENGINEERS, INC.

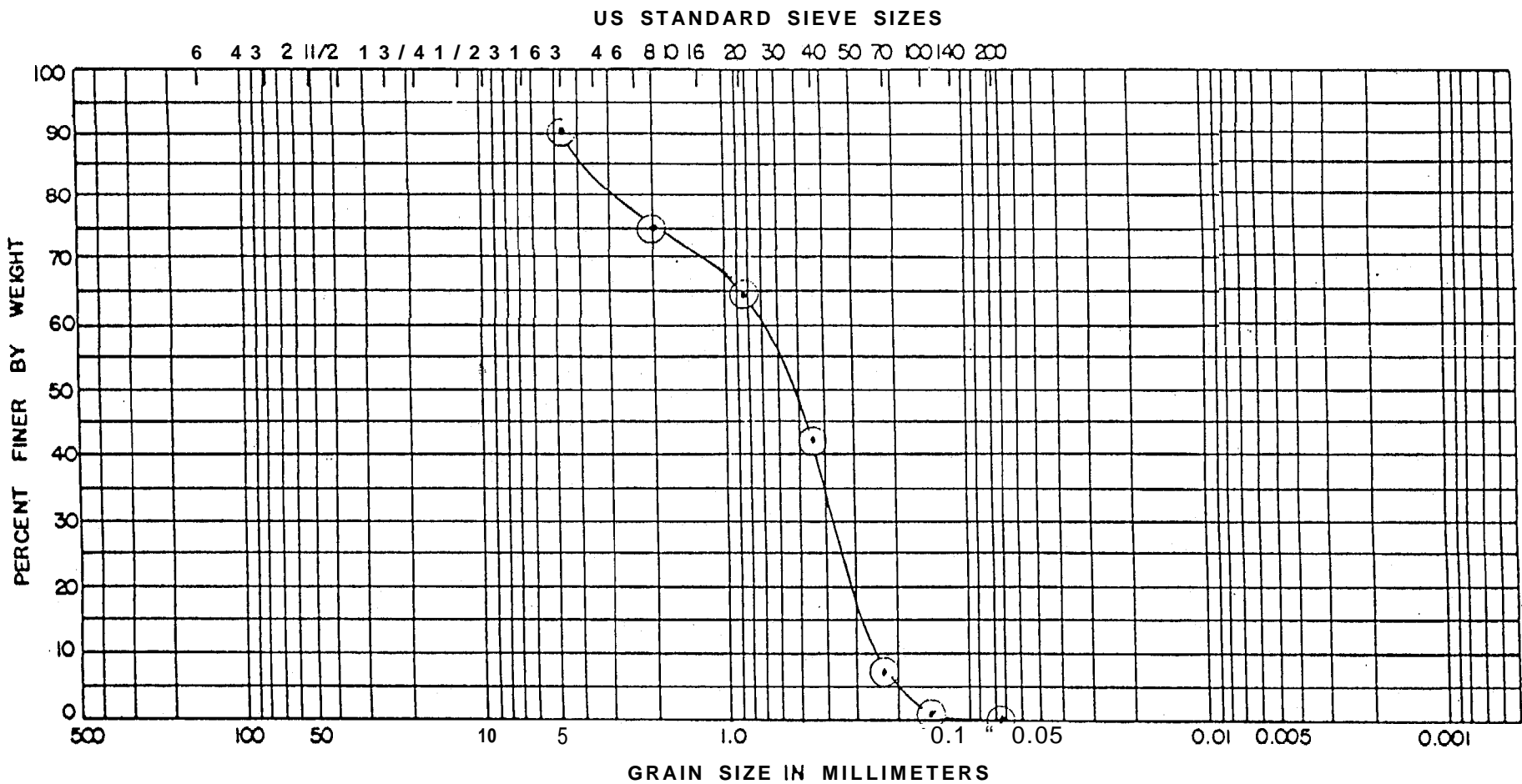
U S STANDARD SIEVE SIZES



BOUL DERS	COBBLES	GRAVEL		SAND			FINES		
		COARSE	FINE	COARSE	MEDIUM	FINE	SILT SIZES	CLAY SIZES	

BORING NO	ELEV OR DEPTH	NAT WC	LL	PL	PI	CLASSIFICATION
						PORT HEIDEN - BERM TROUGH

GRAIN SIZE DISTRIBUTION
 JOB NO. _____
 SOIL MATERIAL ENGINEERS, INC.



BOUL DERS	COBBLES	GRAVEL		SAND			FINES		
		COARSE	FINE	COARSE	MEDIUM	FINE	SILT SIZES	CLAY SIZES	

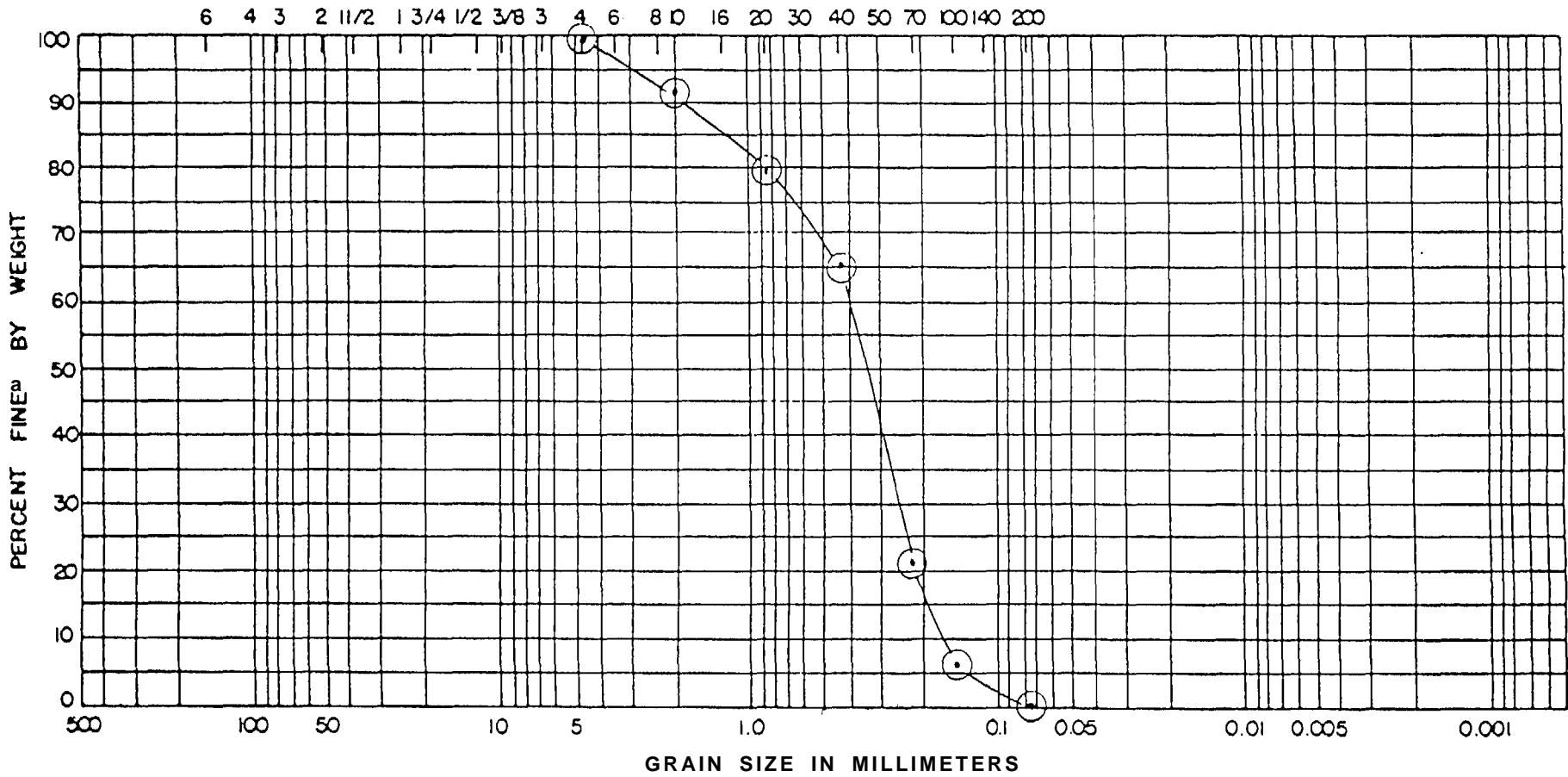
BORING NO.	ELEV. OR DEPTH	NAT WC	LL	PL	PI	CLASSIFICATION
						PORT HEIDEN - BEACH FACE

GRAIN SIZE DISTRIBUTION

JOB NO. _____

SOIL & MATERIAL ENGINEERS, INC.

US STANDARD SIEVE SIZES



BOULDERS	COBBLES	GRAVEL		SAND			FINES		
		COARSE	FINE	COARSE	MEDIUM	FINE	SILT SIZES	CLAY SIZES	

BORING NO.	ELEV. OR DEPTH	NAT WC	LL	PL	PI	CLASSIFICATION
						PORT HEIDEN - LOW TIDE TERRACE

GRAIN SIZE DISTRIBUTION

JOEI NO. _____

SOIL & MATERIAL ENGINEERS, INC.

APPENDIX II-E

Table of corrected wind speed and direction for the CSE beach tower near station 10 and the NOAA-Port Heiden (Alaska) air station about 3 km inland.

PORT HEIDEN WINDS, 16 AUG - 11 SEP 1986

[Speed: m/see]

[Dir: "True]

Month	Day	Time	Beach Speed	Beach Direction	Airstrip Speed	Airstrip Direction	Speed Difference	Direction Difference
8	16	005	1.34	300				
8	16	150	2.68	285				
8	16	250	0.89	180				
8	16	350	3.13	180				
8	16	450	3.13	180				
8	16	550	3.58	180	2.57	170	-1.01	-10
8	16	650	3.58	180	2.57	180	-1.01	0
8	16	750	2.68	180				
8	16	850	2.23	180	3.08	170	0.85	-10
8	16	950	2.23	180	2.06	200	-0.18	20
8	16	1050	2.23	240	1.03	290	-1.21	50
8	16	1150	1.34	270	2.06	290	0.72	20
8	16	1250	1.79	270	2.57	290	0.78	20
8	16	1350	2.23	300				
8	16	1450	2.23	300				
8	16	1550	2.68	300				
8	16	1650	2.23	300				
8	16	1750	2.23	285				
8	16	1850	2.23	300	2.06	270	-0.18	-30
8	16	1950	2.23	285				
8	16	2050	2.23	300				
8	16	2150	2.23	300				
8	16	2250	1.34	270				
8	16	2350	0.45	225				
8	17	050	1.34	160				
8	17	150	3.13	215				
8	17	250	2.68	210				
8	17	350	2.23	195				
8	17	450	4.47	255				
8	17	550	4.47	240				
8	17	650	3.58	230				
8	17	750	3.13	220				
8	17	850	3.13	220	2.57	210	-0.56	-10
8	17	950	3.58	240				
8	17	1050	4.47	230				
8	17	1150	3.58	250				
8	17	1250	3.13	270				
8	17	1350	4.02	300				
8	17	1450	3.58	300				
8	17	1550	4.02	300	3.60	300	-0.42	0
8	17	1650	3.58	290				
8	17	1750	4.47	300				
8	17	1850	4.92	290	3.08	280	-1.83	-10
8	17	1950	4.92	280				
8	17	2050	5.36	285				
8	17	2150	4.02	250				
8	17	2250	3.58	220				
8	17	2350	6.70	230				
8	18	050	4.47	230				
8	18	150	6.70	240				
8	18	250	7.60	270				
8	18	350	7.60	270				
8	18	450	6.70	280	4.11	270	-2.59	-10

PORT HEIDEN WINDS, 16 AUG - 11 SEP 1986

[Speed: m/sec]

[Dir: "True"]

Month	Day	Time	Beach Speed	Beach Direction	Airstrip Speed	Airstrip Direction	Speed Difference	Direction Difference
8	18	550	7.60	270	4.63	270	-2.97	0
8	18	650	7.60	285	5.14	280	-2.46	-5
8	18	750	7.15	290	4.11	280	-3.04	-10
8	18	850	5.81	285	6.17	280	0.36	-5
8	18	950	7.15	290	5.65	280	-1.50	-10
8	18	1050	6.70	290	4.63	280	-2.08	-10
8	18	1150	5.81	300	4.63	280	-1.18	-20
8	18	1250	5.36	300	4.63	280	-0.74	-20
8	18	1350	4.92	300				
8	18	1450	4.02	300	3.08	280	-0.94	-20
8	18	1550	2.68	300	3.08	310	0.40	10
8	18	1650	2.23	310	4.11	320	1.88	10
8	18	1750	3.58	320	3.60	310	0.02	-10
8	18	1850	3.58	310	2.57	310	-1.01	0
8	18	1950	3.13	320				
8	18	2050	1.79	300				
8	18	2150	1.34	250				
8	18	2250	1.34	195				
8	18	2350	3.13	255				
8	19	050	3.13	255				
8	19	150	4.02	280				
8	19	250	3.13	270				
8	19	350	3.13	255				
8	19	450	3.13	280				
8	19	550	3.13	270	2.06	270	-1.07	0
8	19	650	2.23	300	1.03	300	-1.21	0
8	19	750	0.00	285	1.54	270	1.54	-15
8	19	850	2.23	270				
8	19	950	2.23	220				
8	19	1050	2.68	250				
8	19	1150	2.23	270				
8	19	1250	2.23	300	2.06	250	-0.18	-50
8	19	1350	2.68	310				
8	19	1450	2.68	310				
8	19	1550	3.13	320	2.57	320	-0.56	0
8	19	1650	2.68	330				
8	19	1750	2.23	350				
8	19	1850	4.02	360	2.06	340	-1.97	-20
8	19	1950	1.34	360				
8	19	2050	1.79	330				
8	19	2150	1.34	330				
8	19	2250	0.00	315				
8	19	2350	3.13	300				
8	20	050	1.79	270				
8	20	150	2.68	280				
8	20	250	2.23	290				
8	20	350	3.13	290				
8	20	450	2.23	330	0.51	110	-1.72	-220
8	20	550	2.23	290	1.54	110	-0.69	-180
8	20	650	2.68	150	1.03	150	-1.65	0
8	20	750	2.23	210	0.00	140	-2.23	-70
8	20	850	0.45	210	0.51	130	0.07	-80
8	20	950	1.34	270	1.03	240	-0.31	-30

PORT HEIDEN WINDS, 16 AUG - 11 SEP 1986

[Speed: m/see]

[Dir: "True"]

Month	Day	Time	Beach Speed	Beach Direction	Airstrip Speed	Airstrip Direction	Speed Difference	Direction Difference
8	20	1050	1.34	300				
8	20	1150	1.34	250				
8	20	1250	1.79	280	2.06	300	0.27	20
8	20	1350	3.13	310	2.57	330	-0.56	20
8	20	1450	4.02	320				
8	20	1550	2.68	330				
8	20	1650	2.23	360				
8	20	1750	2.23	320				
8	20	1850	3.13	300	3.60	310	0.47	10
8	20	1950	4.47	320				
8	20	2050	3.13	330				
8	20	2150	2.23	300				
8	20	2250	1.79	300				
8	20	2350	1.79	310				
8	21	050	2.23	270				
8	21	150	3.13	270				
8	21	250	3.13	300				
8	21	350	2.68	300				
8	21	450	2.68	330	2.06	320	-0.63	-10
8	21	550	2.68	330				
8	21	650	2.23	300	2.06	290	-0.18	-10
8	21	750	3.13	290	1.54	280	-1.59	-10
8	21	850	3.13	290	2.06	290	-1.07	0
8	21	950	4.02	280	2.57	270	-1.45	-10
8	21	1050	4.47	270				
8	21	1150	4.92	270				
8	21	1250	5.81	280	3.60	280	-2.21	0
8	21	1350	4.92	290				
8	21	1450	5.36	300				
8	21	1550	4.92	300	3.60	210	-1.32	-90
8	21	1650	4.47	300				
8	21	1750	4.47	280				
8	21	1850	5.81	270	4.11	270	-1.70	0
8	21	1950	6.70	285				
8	21	2050	6.26	280				
8	21	2150	6.70	280				
8	21	2250	6.70	280				
8	21	2350	7.60	290				
8	22	050	7.15	270				
8	22	150	7.60	270				
8	22	250	8.05	270				
8	22	350	8.49	270				
8	22	450	8.05	270				
8	22	550	8.49	270	5.65	270	-2.84	0
8	22	650	9.83	270	6.17	270	-3.67	0
8	22	750	11.18	270	6.17	260	-5.01	-10
8	22	850	11.18	270	6.17	280	-5.01	10
8	22	950	10.28	280	7.71	280	-2.57	0
8	22	1050	11.18	270				
8	22	1150	8.94	270				
8	22	1250	9.83	280	8.22	280	-1.61	0
8	22	1350	10.73	290				
8	22	1450	9.39	290				

PORT HEIDEN WINDS, 16 AUG - 11 SEP 1986

[Speed: m/see]

[Dir: "True"]

Month	Day	Time	Beach Speed	Beach Direction	Airstrip Speed	Airstrip Direction	Speed Difference	Direction Difference
8	22	1550	8.94	280	5.65	270	-3.29	-10
8	22	1650	7.60	270				
8	22	1750	8.94	280				
8	22	1850	7.60	280	4.63	280	-2.97	0
8	22	1950	8.05	280				
8	22	2050	8.05	280				
8	22	2150	7.60	270				
8	22	2250	8.94	250				
8	22	2350	9.83	250				
8	23	050	10.28	250				
8	23	150	10.73	255				
8	23	250	11.18	255				
8	23	350	10.28	260				
8	23	450	11.18	255	4.11	230	-7.06	-25
8	23	550	7.15	240				
8	23	650	6.70	240	4.11	180	-2.59	-60
8	23	750	4.92	180	4.63	200	-0.29	20
8	23	850	6.70	210	5.65	220	-1.05	10
8	23	950	8.94	240	5.14	220	-3.80	-20
8	23	1050	8.05	255				
8	23	1150	7.15	250				
8	23	1250	4.92	260	4.63	250	-0.29	-10
8	23	1350	3.58	240				
8	23	1450	5.81	285				
8	23	1550	4.47	270				
8	23	1650	5.81	280				
8	23	1750	1.79	240				
8	23	1850	4.47	315	2.06	240	-2.41	-75
8	23	1950	1.34	270				
8	23	2050	2.23	210				
8	23	2150	2.68	160				
8	23	2250	3.13	150				
8	23	2350	2.23	160				
8	24	050	1.79	190				
8	24	150	0.00	120				
8	24	250	0.89	45				
8	24	350	0.00	40				
8	24	450	1.34	30				
8	24	550	1.79	140				
8	24	650	0.00	145				
8	24	750	0.45	150				
8	24	850	0.00	155	3.60	170	3.60	15
8	24	950	4.47	160	5.65	160	1.18	0
8	24	1050	7.15	170				
8	24	1150	8.05	170				
8	24	1250	7.60	170	6.68	170	-0.92	0
8	24	1350	7.15	170				
8	24	1450	9.83	160				
8	24	1550	10.73	160	10.28	160	-0.45	0
8	24	1650	11.62	160				
8	24	1750	11.18	150				
8	24	1850	11.18	150	9.77	160	-1.41	10
8	24	1950	11.18	150				

PORT HEI DEN WINDS, 16 AUG - 11 SEP 1986

[Speed: m/sec]

[Dir: 'True]

Month	Day	Time	Beach Speed	Beach Direction	Airstrip Speed	Airstrip Direction	Speed Difference	Direction Difference
8	24	2050	10.73	150				
8	24	2150	11.18	150				
8	24	2250	11.18	150				
8	24	2350	9.39	150				
8	25	050	9.83	165				
8	25	150	11.62	160				
8	25	250	11.18	160				
8	25	350	8.05	155				
8	25	450	9.39	150				
8	25	550	7.60	140				
8	25	650	12.52	165	9.25	160	-3.26	-5
8	25	750	4.47	130	9.25	160	4.78	30
8	25	850	8.49	150	8.74	150	0.25	0
8	25	950	9.83	155	8.22	150	-1.61	-5
8	25	1050	10.28	150				
8	25	1150	12.52	150				
8	25	1250	5.81	120	6.68	140	0.87	20
8	25	1350	4.02	120				
8	25	1450	8.94	115				
8	25	1550	9.39	95				
8	25	1650	10.28	90				
8	25	1750	7.60	75				
8	25	1850	7.15	55	7.20	70	0.04	15
8	25	1950	6.70	55				
8	25	2050	7.15	60				
8	25	2150	11.62	60				
8	25	2250	12.07	60				
8	25	2350	9.83	60				
8	26	050	10.28	60				
8	26	150	9.83	60				
8	26	250	12.52	70				
8	26	350	11.18	80				
8	26	450	11.62	90	2.57	90	-9.05	0
8	26	550	3.58	85	6.68	150	3.11	65
8	26	650	3.58	85	10.80	160	7.22	75
8	26	750	7.60	120	9.77	150	2.17	30
8	26	850	9.83	150	10.80	160	0.96	10
8	26	950	11.18	160				
8	26	1050	11.18	165				
8	26	1150	11.18	150				
8	26	1250	11.62	155	8.74	160	-2.88	5
8	26	1350	12.07	165				
8	26	1450	11.18	160				
8	26	1550	10.73	170	9.25	170	-1.48	0
8	26	1650	12.07	170				
8	26	1750	10.73	175				
8	26	1850	9.39	175	9.77	170	0.38	-5
8	26	1950	8.49	160				
8	26	2050	8.94	165				
8	26	2150	10.73	165				
8	26	2250	11.62	165				
8	26	2350	10.28	165				
8	27	050	9.83	170				

PORT HEIDEN WINDS, 16 AUG - 11 SEP 1986

[Speed: m/sec]

[Dir: "True"]

Month	Day	Time	Beach Speed	Beach Direction	Airstrip Speed	Airstrip Direction	Speed Difference	Direction Difference
8	27	150	8.05	170				
8	27	250	7.60	165				
8	27	350	8.94	165				
8	27	450	8.94	165				
8	27	550	6.70	165	8.74	160	2.03	-5
8	27	650	7.15	160	8.74	160	1.59	0
8	27	750	10.28	165				
8	27	850	8.05	165	8.22	160	0.18	-5
8	27	950	11.18	160	8.22	160	-2.95	0
8	27	1050	10.28	160				
8	27	1150	11.18	155				
8	27	1250	11.18	165	8.22	160	-2.95	-5
8	27	1350	11.62	180				
8	27	1450	11.62	175				
8	27	1550	11.18	170	8.74	160	-2.44	-10
8	27	1650	9.83	170				
8	27	1750	12.07	165				
8	27	1850	8.94	170	7.71	180	-1.23	10
8	27	1950	8.05	180				
8	27	2050	5.81	180				
a	27	2150	6.70	180				
8	27	2250	4.47	195				
8	27	2350	4.47	210				
8	28	050	4.02	225				
8	28	150	3.58	185				
8	28	250	2.23	135				
8	28	350	3.58	155				
8	28	450	1.79	150				
8	28	550	2.23	145				
8	28	650	2.23	160	4.11	170	1.88	10
8	28	750	5.36	175	3.60	160	-1.77	-15
8	28	850	4.47	165	5.14	170	0.67	5
8	28	950	4.92	165	6.17	170	1.25	5
8	28	1050	5.81	150				
8	28	1150	6.26	170				
8	28	1250	4.92	190	2.57	210	-2.35	20
8	28	1350	3.13	230				
8	28	1450	2.23	310				
8	28	1550	4.47	10	5.14	160	0.67	150
8	28	1650	4.92	35				
8	28	1750	3.13	35				
8	28	1850	2.68	60	6.17	150	3.49	90
8	28	1950	0.89	150				
8	28	2050	6.26	150				
8	28	2150	6.26	160				
8	28	2250	4.02	145				
8	28	2350	9.39	150				
8	29	050	10.73	150				
8	29	150	8.49	140				
8	29	250	10.73	140				
8	29	350	13.86	140				
8	29	450	7.60	135	10.28	150	2.68	15
8	29	550	12.07	150				

PORT HEI DEN WINDS, 16 AUG - 11 SEP 1986

[Speed: m/see]

[Dir: 'True]

Month	Day	Time	Beach Speed	Beach Direction	Airstrip Speed	Airstrip Direction	Speed Difference	Direction Difference
8	29	650	8.05	145	9.77	140	1.72	-5
8	29	750	6.70	120	8.22	130	1.52	10
8	29	850	9.83	100	7.71	120	-2.12	20
8	29	950	14.75	105	12.85	130	-1.90	25
8	29	1050	12.96	115				
8	29	1150	13.41	110				
8	29	1250	12.52	120				
8	29	1350	9.83	145				
8	29	1450	8.49	135				
8	29	1550	7.60	130	14.91	140	7.31	10
8	29	1650	9.39	120				
8	29	1750	8.94	135				
8	29	1850	8.94	150	10.28	150	1.34	0
8	29	1950	8.05	150				
8	29	2050	8.05	150				
8	29	2150	10.73	135				
8	29	2250	4.47	145				
8	29	2350	6.70	150				
8	30	050	5.36	140				
8	30	150	8.94	135				
8	30	250	6.70	140				
8	30	350	7.15	125	7.20	140	0.04	15
8	30	450	5.36	120				
8	30	550	4.47	150				
8	30	650	6.26	140	5.65	140	-0.60	0
8	30	750	6.26	135	6.17	130	-0.09	-5
8	30	850	2.23	125	5.14	120	2.91	-5
8	30	950	4.47	125	5.65	140	1.18	15
8	30	1050	3.13	120				
8	30	1150	3.13	135				
8	30	1250	5.36	145				
8	30	1350	7.15	135	7.71	140	0.56	5
8	30	1450	8.49	120				
8	30	1550	7.60	145				
8	30	1650	7.60	140				
8	30	1750	6.70	125				
8	30	1850	5.36	150	4.11	150	-1.25	0
8	30	1950	7.15	140				
8	30	2050	6.26	125				
8	30	2150	6.70	125				
8	30	2250	5.36	120				
8	30	2350	3.13	120				
8	31	050	3.13	120				
8	31	150	1.34	90				
8	31	250	3.13	145				
8	31	350	2.68	135				
8	31	450	4.92	85				
8	31	550	3.13	140				
8	31	650	0.89	165				
8	31	750	3.58	150				
8	31	850	2.23	80	2.06	100	-0.18	20
8	31	950	0.89	45				
8	31	1050	2.23	360				

PORT HEIDEN WINDS, 16 AUG - 11 SEP 1986

[Speed: m/sec]

[Dir: "True"]

Month	Day	Time	Beach Speed	Beach Direction	Airstrip Speed	Airstrip Direction	Speed Difference	Direction Difference
8	31	1150	4.02	300				
8	31	1250	4.47	310	2.57	320	-1.90	10
8	31	1350	3.58	300				
8	31	1450	2.23	350				
8	31	1550	4.02	360	2.06	10	-1.97	-350
8	31	1650	3.58	360				
8	31	1750	3.58	360				
8	31	1850	3.13	315	1.03	170	-2.10	-145
8	31	1950	2.23	310				
8	31	2050	2.23	270				
8	31	2150	4.92	270				
8	31	2250	5.36	255				
8	31	2350	5.36	250				
9	1	050	7.15	255				
9	1	150	5.36	255				
9	1	250	5.81	255				
9	1	350	4.92	225				
9	1	450	4.47	225				
9	1	550	4.02	220				
9	1	650	5.36	235				
9	1	750	6.26	235				
9	1	850	6.70	240				
9	1	950	5.36	240	3.08	240	-2.28	0
9	1	1050	3.58	285				
9	1	1150	3.58	285				
9	1	1250	4.92	290	4.11	280	-0.80	-10
9	1	1350	4.47	290				
9	1	1450	7.60	300				
9	1	1550	7.15	300	5.65	300	-1.50	0
9	1	1650	7.60	300				
9	1	1750	7.15	285				
9	1	1850	7.15	280	4.63	290	-2.53	10
9	1	1950	5.36	300				
9	1	2050	2.68	250				
9	1	2150	8.05	280				
9	1	2250	9.39	295				
9	1	2350	9.83	280				
9	2	050	11.62	300				
9	2	150	10.73	300				
9	2	250	10.28	300				
9	2	350	10.73	290				
9	2	450	7.15	315	4.11	290	-3.04	-25
9	2	550	5.81	295				
9	2	650	4.92	330	4.11	290	-0.80	-40
9	2	750	6.26	300	3.60	290	-2.66	-10
9	2	850	6.26	260	5.14	270	-1.12	10
9	2	950	7.15	320				
9	2	1050	7.15	285				
9	2	1150	7.60	310				
9	2	1250	5.36	290				
9	2	1350	4.02	295				
9	2	1450	4.47	285				
9	2	1550	4.02	275	3.08	240	-0.94	-35

PORT HEIDEN WINDS, 16 AUG - 11 SEP 1986

[Speed: m/see]

[Dir: 'True]

Month	Day	Time	Beach Speed	Beach Direction	Airstrip Speed	Airstrip Direction	Speed Difference	Direction Difference
9	2	1650	3.58	270				
9	2	1750	3.13	285				
9	2	1850	3.13	300				
9	2	1950	2.23	315				
9	2	2050	1.34	290				
9	2	2150	1.34	140				
9	2	2250	2.68	145				
9	2	2350	3.58	140				
9	3	050	3.58	150				
9	3	150	3.13	150				
9	3	250	3.13	150				
9	3	350	3.58	125				
9	3	450	3.13	110	1.03	10	-2.10	-100
9	3	550	1.34	150	1.03	340	-0.31	190
9	3	650	1.34	100	2.57	180	1.23	80
9	3	750	2.23	140				
9	3	850	3.58	150	3.60	170	0.02	20
9	3	950	5.36	165				
9	3	1050	5.36	170				
9	3	1150	4.92	180				
9	3	1250	4.47	180	4.63	180	0.16	0
9	3	1350	6.26	165				
9	3	1450	5.36	140				
9	3	1550	6.70	165	6.68	180	-0.02	15
9	3	1650	7.15	150				
9	3	1750	6.70	160				
9	3	1850	4.47	210	5.14	170	0.67	-40
9	3	1950	1.79	230				
9	3	2050	5.36	150				
9	3	2150	5.36	165				
9	3	2250	7.15	165				
9	3	2350	5.36	155				
9	4	050	8.05	165				
9	4	150	9.39	160				
9	4	250	8.05	160				
9	4	350	7.15	165				
9	4	450	5.81	170				
9	4	550	5.81	180	8.22	170	2.41	-10
9	4	650	11.18	180				
9	4	750	8.94	165	8.74	150	-0.20	-15
9	4	850	9.83	150	5.14	170	-4.69	20
9	4	950	7.60	170				
9	4	1050	8.94	165				
9	4	1150	12.96	150				
9	4	1250	12.52	165	7.71	150	-4.81	-15
9	4	1350	9.83	150				
9	4	1450	12.07	160				
9	4	1550	10.73	165	7.71	160	-3.02	-5
9	4	1650	9.83	155				
9	4	1750	9.83	165				
9	4	1850	10.28	150	9.25	160	-1.03	10
9	4	1950	10.73	155				
9	4	2050	11.18	150				

PORT HEIDEN WINDS, 16 AUG - 11 SEP 1986

[Speed: m/sec]

[Dir: 'True']

Month	Day	Time	Beach Speed	Beach Direction	Airstrip Speed	Airstrip Direction	Speed Difference	Direction Difference
9	4	2150	10.28	150				
9	4	2250	10.28	150				
9	4	2350	7.15	150				
9	5	050	4.92	145				
9	5	150	6.70	150				
9	5	250	8.94	150				
9	5	350	7.60	150				
9	5	450	8.05	150				
9	5	550	8.49	150				
9	5	650	8.94	155	7.71	170	-1.23	15
9	5	750	8.05	160	8.22	170	0.18	10
9	5	850	11.18	165	10.80	160	-0.38	-5
9	5	950	12.07	150				
9	5	1050	11.18	150				
9	5	1150	14.30	165				
9	5	1250	11.62	155	10.80	160	-0.83	5
9	5	1350	14.30	155				
9	5	1450	14.75	150				
9	5	1550	15.20	160				
9	5	1650	16.09	165				
9	5	1750	11.62	165				
9	5	1850	16.09	165				
9	5	1950	12.07	165				
9	5	2050	12.96	165				
9	5	2150	11.18	165				
9	5	2250	11.18	165				
9	5	2350	12.07	160				
9	6	050	6.70	150				
9	6	150	11.18	150				
9	6	250	9.39	150				
9	6	350	11.18	135				
9	6	450	9.39	135	14.39	160	5.01	25
9	6	550	11.18	145	14.39	160	3.22	15
9	6	650	10.73	140				
9	6	750	9.83	135	13.88	160	4.05	25
9	6	850	11.62	135	13.37	160	1.74	25
9	6	950	11.18	140				
9	6	1050	9.83	150				
9	6	1150	8.94	150				
9	6	1250	8.94	150	7.20	160	-1.74	10
9	6	1350	5.81	150				
9	6	1450	5.36	165				
9	6	1550	4.47	260				
9	6	1650	4.02	270				
9	6	1750	7.60	280				
9	6	1850	8.05	310	5.14	310	-2.91	0
9	6	1950	8.94	315				
9	6	2050	8.94	315				
9	6	2150	6.26	310				
9	6	2250	7.60	315				
9	6	2350	5.81	315				
9	7	050	6.26	325				
9	7	150	7.15	320				

PORT HEI DEN WINDS, 16 AUG - 11 SEP 1986

[Speed: m/sec]

[Dir: "True]

Month	Day	Time	Beach Speed	Beach Direction	Airstrip Speed	Airstrip Direction	Speed Difference	Direction Difference
9	7	250	8.05	335				
9	7	350	6.26	335				
9	7	450	6.70	335	2.57	350	-4.13	15
9	7	550	6.26	350				
9	7	650	6.70	345				
9	7	750	6.26	340				
9	7	850	6.70	320	3.08	320	-3.62	0
9	7	950	7.60	310	3.60	320	-4.00	10
9	7	1050	8.05	300				
9	7	1150	7.60	300				
9	7	1250	9.83	285	6.68	280	-3.15	-5
9	7	1350	11.62	290				
9	7	1450	15.20	285				
9	7	1550	15.64	280				
9	7	1650	11.18	310				
9	7	1750	16.54	315				
9	7	1850	19.22	310				
9	7	1950	13.41	315				
9	7	2050	16.09	310				
9	7	2150	15.64	320				
9	7	2250	15.20	315				
9	7	2350	14.75	300				
9	8	050	14.75	300				
9	8	150	12.96	300				
9	8	250	14.30	300				
9	8	350	13.41	300				
9	8	450	11.18	300	10.80	300	-0.38	0
9	8	550	12.07	300	10.80	290	-1.27	-10
9	8	650	10.73	300	8.74	300	-1.99	0
9	8	750	10.73	300	8.22	310	-2.50	10
9	8	850	8.94	300				
9	8	950	10.28	310				
9	8	1050	9.39	315				
9	8	1150	11.18	305				
9	8	1250	9.39	300	7.71	320	-1.68	20
9	8	1350	14.30	315				
9	8	1450	13.41	310				
9	8	1550	13.41	310	10.28	310	-3.13	0
9	8	1650	14.30	300				
9	8	1750	13.41	315				
9	8	1850	12.07	300	8.74	300	-3.33	0
9	8	1950	12.96	300				
9	8	2050	12.52	300				
9	8	2150	12.52	310				
9	8	2250	13.86	300				
9	8	2350	13.41	300				
9	9	050	11.18	300				
9	9	150	11.18	300				
9	9	250	11.62	285				
9	9	350	12.52	285				
9	9	450	9.83	285	6.17	360	-3.67	75
9	9	550	11.18	285	6.68	310	-4.49	25
9	9	650	10.73	300				

PORT HEIDEN WINDS, 16 AUG - 11 SEP 1986

[Speed: m/see]

[Dir: "True]

Month	Day	Time	Beach Speed	Beach Direction	Airstrip Speed	Airstrip Direction	Speed Difference	Direction Difference
9	9	750	9.39	300	4.11	310	-5.27	10
9	9	850	9.39	300	4.63	290	-4.76	-10
9	9	950	8.94	290				
9	9	1050	7.60	290				
9	9	1150	6.70	290				
9	9	1250	6.26	280	5.65	300	-0.60	20
9	9	1350	6.70	280				
9	9	1450	7.15	270				
9	9	1550	8.05	270	6.17	280	-1.88	10
9	9	1650	7.15	270				
9	9	1750	6.26	275				
9	9	1850	7.60	270	6.17	280	-1.43	10
9	9	1950	7.60	270				
9	9	2050	8.49	300				
9	9	2150	8.94	285				
9	9	2250	6.70	280				
9	9	2350	7.15	280				
9	10	050	6.70	270				
9	10	150	8.05	270				
9	10	250	8.49	270				
9	10	350	10.28	270				
9	10	450	8.94	265	2.57	260	-6.37	-5
9	10	550	5.81	260	4.11	280	-1.70	20
9	10	650	7.60	260	4.11	220	-3.49	-40
9	10	750	7.60	250				
9	10	850	6.70	255	4.11	240	-2.59	-15
9	10	950	5.81	240				
9	10	1050	5.36	240				
9	10	1150	6.70	260				
9	10	1250	6.26	270	3.08	280	-3.17	10
9	10	1350	5.81	265				
9	10	1450	4.47	285				
9	10	1550	4.47	285	1.03	330	-3.44	45
9	10	1650	1.34	290				
9	10	1750	1.34	355				
9	10	1850	1.79	360	3.08	50	1.30	-310
9	10	1950	3.58	15				
9	10	2050	3.13	30				
9	10	2150	4.47	40				
9	10	2250	1.79	60				
9	10	2350	3.13	90				
9	11	050	3.13	105				
9	11	150	1.34	75				
9	11	250	1.79	120				
9	11	350	1.34	100				
9	11	450	1.79	90	2.57	60	0.78	-30
9	11	550	2.23	80	2.57	90	0.34	10
9	11	650	2.23	90				
9	11	750	3.13	100	3.08	100	-0.04	0
9	11	850	3.58	120	1.03	170	-2.55	50
9	11	950	1.34	135	1.03	160	-0.31	25
9	11	1050	1.34	130				
9	11	1150	1.34	255				

PORT HEIDEN WINDS, 16 AUG - 11 SEP 1986

[Speed: m/sec]

[Dir: "True"]

Month	Day	Time	Beach Speed	Beach Direction	Airstrip Speed	Airstrip Direction	Speed Difference	Direction Difference
9	11	1250	1.79	290				
9	11	1350	0.00	285				
9	11	1450	1.79	280				
9	11	1550	3.58	300				

APPENDIX II-F

Results of suspended-sediment samples including corresponding coastal processes and annotation of conditions under which each sample was collected. Samples were collected near Port Heiden (Alaska) by means of an apparatus described in Kana (1976) which collects serial vertical arrays of bulk water samples using swimmers in the surf zone.

**SUSPENDED SEDIMENT SAMPLES
AND
CORRESPONDING COASTAL PROCESS MEASUREMENTS**

Station: PH-10

Date: 11 August 1986

COASTAL PROCESSES

Observation number:	1	Visual wave type:	Plunging
Date (month, day, year):	08/11/86	Longshore current velocity (cm/s):	93
Time (24-hour clock):	1530	Longshore current direction viewed from shore:	to right
Wind velocity (mph):	12	Breaker angle/degree:	—
Wind azimuth (degrees True):	160	Distance to inner surf line (m):	—
Breaker height (cm):	70	Distance to outer surf line (m):	—
Breaker depth (cm):	70	Width of surf zone (m):	20
Wave period (seconds):	6.6		

SUSPENDED SEDIMENT

Series #: (A1)	1	Time: 1625
Distance from front stake:	107 m	
Depth of breaking:	70 cm	
Breaker type:	Plunging	
Notes:	Taken approximately 2 seconds after breaking, inside bore, 3 m inside break point. $H_b = 80$ cm. $T = 6.5$ s.	

<u>Height above bottom (cm)</u>	<u>SS concentration (g/l)</u>
40	0.202
10	0.204

Series #: (A2)	2	Time: 1642
Distance from front stake:	108 m	
Depth of breaking:	60 cm	
Breaker type:	Plunging	
Notes:	Taken 1 second after breaking at break point. $H_b = 90$ cm.	

<u>Height above bottom (cm)</u>	<u>SS concentration (g/l)</u>
40	0.868
10	16.9

**SUSPENDED SEDIMENT SAMPLES
AND
CORRESPONDING COASTAL PROCESS MEASUREMENTS**

Station: PH-10

Date: 11 August 1986

Series #: (A3) 3 Time: 1650
 Distance from front stake: 105 m
 Depth of breaking: 40 cm
 Breaker type: Plunging
 Notes: Between breakers, in bore, approximately mid-surf position. $T = 6.5$ s.

<u>Height above bottom (cm)</u>	<u>SS concentration (g/l)</u>
40	0.278
10	0.833

Series #: (A4) 4 Time: 1659
 Distance from front stake: 108 m
 Depth of breaking: 60 cm
 Breaker type: Plunging
 Notes: Right at break point, inner swash zone now at +90 m. $H_b = 80$ cm.

<u>Height above bottom (cm)</u>	<u>SS concentration (g/l)</u>
10	3.44

Series #: (A5) 5 Time: 1710
 Distance from front stake: 106 m
 Depth of breaking: 70 cm
 Breaker type: Plunging
 Notes: Right at break point, as it crested before breaking. $H_b = 80$ cm. $T = 6.5$ s.

<u>Height above bottom (cm)</u>	<u>SS concentration (g/l)</u>
10	1.81

Series #: (A6) 6 Time: 1716
 Distance from front stake: 108 m
 Depth of breaking: 80 cm
 Breaker type: Plunging
 Notes: Right as wave crested. $H_b = 110$ cm.

<u>Height above bottom (cm)</u>	<u>SS concentration (g/l)</u>
40	0.138
10	5.51

**SUSPENDED SEDIMENT SAMPLES
AND
CORRESPONDING COASTAL PROCESS MEASUREMENTS**

Station: PH-10

Date: 13 August 1986

COASTAL PROCESSES

Observation number:	3	Visual wave type:	Spilling
Date (month, day, year):	08/13/86	Longshore current velocity (cm/s):	60
Time (24-hour clock):	1400	Longshore current direction viewed from shore:	to right
Wind velocity (mph):		Breaker angle/degree:	10
Wind azimuth (degrees True):	250	Distance to inner surf line (m):	160
Breaker height (cm):	80	Distance to outer surf line (m):	300
Breaker depth (cm):	100	Width of surf zone (m):	140
Wave period (seconds):	5.5		

SUSPENDED SEDIMENT

Series #: (B1-a) 12 Time: 1445
 Distance from front stake: 190 m
 Depth of breaking: 70 cm in middle of bore
 Breaker type: Spilling
 Notes: Close to mid-surf position, inner swash is at 150, outer swash is at 250. $H_L = NA$. $T = 5.5$ s. LS current = 1.25 m/s." Taken in bore.

<u>Height above bottom (cm)</u>	<u>SS concentration (g/l)</u>
40	0.276
10	1.29

Series #: (B1-b) 13 Time: 1445
 Distance from front stake: 170 m
 Depth at sampler: 40 cm
 Breaker type: Spilling
 Notes: In bore of inner surf zone, synoptic with Series #12.

<u>Height above bottom (cm)</u>	<u>SS concentration (g/l)</u>
10	1.12

**SUSPENDED SEDIMENT SAMPLES
AND
CORRESPONDING COASTAL PROCESS MEASUREMENTS**

Station: PH-10

Date: 13 August 1986

Series #: (B2-a) 14 Time: 1508
 Distance from front stake: 180 m
 Depth at sampler: 90 cm
 Breaker type: Spilling
 Notes: Water depth varying 70-120 close to mid-surf position.

<u>Height above bottom (cm)</u>	<u>SS concentration (g/l)</u>
40	0.206

Series #: (B2-b) 15 Time: 1508
 Distance from front stake: 170 m
 Depth of breaking: 60 cm
 Breaker type: Spilling
 Notes: Synoptic with Series #14.

<u>Height above bottom (cm)</u>	<u>SS concentration (g/l)</u>
10	0.701

Series #: (B3-a) 16 Time: 1523
 Distance from front stake: 180 (A) 160 m (B)
 Depth at sampler: 110 cm (A) Taken just after bore passed
 80 cm (B) Between bores
 Breaker type: Spilling
 Notes: Swash zone, up to 100 m from F. S., outer breaker line 250 m.

<u>Height above bottom (cm)</u>	<u>SS concentration (g/l)</u>
(A) 40	0.284
(B) 10	0.319

Series #: (B3-b) 17 Time: 1523
 Distance from front stake: 155 m
 Depth at sampler: 70 cm
 Breaker type: Spilling
 Notes: Synoptic with Series #16.

<u>Height above bottom (cm)</u>	<u>SS concentration (g/l)</u>
10	0.329

SUSPENDED SEDIMENT SAMPLES
AND
CORRESPONDING COASTAL PROCESS MEASUREMENTS

Station: PH-10

Date: 13 August 1986

Series #: (B4-b) 18 Time: 1535
 Distance from front stake: 180 m
 Depth at sampler: 100 cm
 Breaker type: Spilling
 Notes: Between bores, inner surf line at 120. outer surf line at 250.

<u>Height above bottom (cm)</u>	<u>SS concentration (g/l)</u>
40	0.339

Series #: (B4-b) 19 Time: 1535
 Distance from front stake: 145 m
 Depth at sampler: 50 cm
 Breaker type: Spilling
 Notes: In bore. synoptic with Series #18.

<u>Height above bottom (cm)</u>	<u>SS concentration (g/l)</u>
10	0.206

Series #: (B5-a) 20 Time: 1550
 Distance from front stake: 160 m
 Depth at sampler: 130 cm
 Breaker type: Spilling
 Notes: Inner swash zone at 120, outer surf zone at 230, primary breakers increasing, now 1.5 m. $H_b = 150$ cm: taken in inner surf zone after bore passed.

<u>Height above bottom (cm)</u>	<u>SS concentration (g/l)</u>
40	0.173
10	1.65

**SUSPENDED SEDIMENT SAMPLES
AND
CORRESPONDING COASTAL PROCESS MEASUREMENTS**

Station: PH-10

Date: 15 August 1986

COASTAL PROCESSES

Observation number:	5	Visual wave type:	Spilling
Date (month, day, year):	08/15/86	Longshore current velocity (cm/s):	60
Time (24-hour clock):	1430	Longshore current direction viewed from shore:	to left
Wind velocity (mph):	9	Breaker angle/degree:	—
Wind azimuth (degrees True):	310	Distance to inner surf iine (m):	220
Breaker height (cm):	110	Distance to outer surf iine [m]:	350
Breaker depth (cm):	120	Width of surf zone (m):	130
Wave period (seconds):	8.0		

SUSPENDED SEDIMENT

Series #: (C1)	22	Time: 1545
Distance from front stake:	205 m	
Depth at sampler:	130 cm	
Breaker type:		
Notes:	Taken in runnel outlet. turbid plume running out. T = 8.0 s. LS current = 60 cm/s.	

Height above bottom (cm)SS concentration (g/l)

10

0.627

**SUSPENDED SEDIMENT SAMPLES
AND
CORRESPONDING COASTAL PROCESS MEASUREMENTS**

Station: PH-10

Date: 22 August 1986

COASTAL PROCESSES

Observation number:	12	Visual wave type:	Spilling
Date (month, day, year):	08/22/86	Longshore current velocity (cm/s):	26
Time (24-hour clock):	1600	Longshore current direction viewed from shore:	to right
Wind velocity (mph):	20	Breaker angle/degree:	10
Wind azimuth (degrees True):	280	Distance to inner surf line (m):	95
Breaker height (cm):	100	Distance to outer surf line (m):	120
Breaker depth (cm):	120	Width of surf zone (m):	25
Wave period (seconds):	-		

SUSPENDED SEDIMENT

Series #: (D1) 2 3 Time: 1445
Distance from front stake: 115 m
Depth at sampler: 140 cm
Breaker type: Spilling
Notes: Sample taken in bore just after wave broke.
 $H_b = 120$ cm. $T = 6.0$ s. Wave cycle = 0.

<u>Height above bottom (cm)</u>	<u>SS concentration (g/l)</u>
10	0.832

Series #: (D2) 24 Time: 1500
Distance from front stake: 115 m
Depth at sampler: 150 cm
Breaker type: Spilling
Notes: Just as wave broke. $H_b = 150$ cm. Probably
 spurious-sampling bed layer.

<u>Height above bottom (cm)</u>	<u>SS concentration (g/l)</u>
40	0.181
10	244.0 ?

**SUSPENDED SEDIMENT SAMPLES
AND
CORRESPONDING COASTAL PROCESS MEASUREMENTS**

Station: PH-10

Date: 22 August 1986

Series #: (D7) 29 Time: 1555
 Distance from front stake: 115 m
 Depth at sampler:
 Breaker type: Spilling
 Notes: Crest just prior to break. Lower sample
 possibly spurious.

<u>Height above bottom (cm)</u>	<u>SS concentration (g/l)</u>
40	0.201
10	49.7 ?

COASTAL PROCESSES

--Observation number:	12	Visual wave type:	Spilling
Date (month, day, year):	08/22/86	Longshore current velocity (cm/s):	26
Time (24-hour clock):	1600	Longshore current direction viewed from shore:	to right
Wind velocity (mph):	20	Breaker angle/degree:	10
Wind azimuth (degrees True):	280	Distance to inner surf line (m):	95
Breaker height (cm):	100	Distance to outer surf line (m):	120
Breaker depth (cm):	120	Width of surf zone (m):	25
Wave period (seconds):	-		

**SUSPENDED SEDIMENT SAMPLES
AND
CORRESPONDING COASTAL PROCESS MEASUREMENTS**

Station: PH-10

Date: 27 August 1986

COASTAL PROCESSES

Observation number:	17	Visual wave type:	Plunging
Date (month, day, year):	08/27/86	Longshore current velocity (cm/s):	—
Time (24-hour clock):	1530	Longshore current direction viewed from shore:	to right
Wind velocity (mph):	25	Breaker angle/degree:	3
Wind azimuth (degrees True):	170	Distance to inner surf line (m):	115
Breaker height (cm):	75	Distance to outer surf line (m):	160
Breaker depth (cm):	90	Width of surf zone (m):	45
Wave period (seconds):	6.0		

SUSPENDED SEDIMENT

Series #: (E1)	30	Time: 2010
Distance from front stake:	100 m	
Depth at sampler:	NA	
Breaker type:	Plunging	
Notes:	In trough, before breaking, narrow surf zone. Inner swash = 90 m: outer break = 95 m. H_b = 60 cm. $T = 4.0$ s. Wave angle = 5-10°right.	

<u>Height above bottom (cm)</u>	<u>SS concentration (g/l)</u>
40	0.144
10	0.297

Series #: (E2)	31	Time: 2025
Distance from front stake:	100 m	
Depth of breaking:	NA	
Breaker type:	Plunging	
Notes:	At crest, just before breaking. $H_b = 60$ cm. $T = 4.0$ s.	

<u>Height above bottom (cm)</u>	<u>SS concentration (g/l)</u>
40	0.0927
10	24.6

**SUSPENDED SEDIMENT SAMPLES
AND
CORRESPONDING COASTAL PROCESS MEASUREMENTS**

Station: PH-10

Date: 27 August 1986

Series #: (E3) 32 Time: 2033
 Distance from front stake: 105 m
 Depth at sampler: NA
 Breaker type: Plunging
 Notes: At crest before breaking. $H_b = 60$ cm. $T = 4.0$ s.

<u>Height above bottom (cm)</u>	<u>SS concentration (g/l)</u>
40	0.14
10	0.26

Series #: (E4) 33 Time: 2040
 Distance from front stake: 100 m
 Depth at sampler: NA
 Breaker type: Plunging
 Notes: Crest before breaking. $H_b = 60$ cm. $T = 4$ s.

<u>Height above bottom (cm)</u>	<u>SS concentration (g/l)</u>
40	0.132
10	0.781

Series #: (E5) 34 Time: 2050
 Distance from front stake: 100 m
 Depth at sampler: NA
 Breaker type: Plunging
 Notes: Crest before breaking. $H_b = 60$ cm. $T = 4.0$ s.

<u>Height above bottom (cm)</u>	<u>SS concentration (g/l)</u>
40	0.166

**SUSPENDED SEDIMENT SAMPLES
AND
CORRESPONDING COASTAL PROCESS MEASUREMENTS**

Station: PH-10

Date: 27 August 1986

Series #: (E6) 35 Time: 2055
 Distance from front stake: 100 m
 Depth at sampler: NA
 Breaker type: Plunging
 Notes: Crest before breaking.

<u>Height above bottom (cm)</u>	<u>SS concentration (g/l)</u>
40	0.112
10	0.36

Series #: (E7) 36 Time: 2102
 Distance from front stake: 80 m
 Depth at sampler: —
 Breaker type: Plunging
 Notes: At break.

<u>Height above bottom (cm)</u>	<u>SS concentration (g/l)</u>
10	31.7

Series #: (E8) 37 Time: 2106
 Distance from front stake: 95 m m
 Depth at sampler: NA
 Breaker type: Plunging
 Notes: Crest before breaking.

<u>Height above bottom (cm)</u>	<u>SS concentration (g/l)</u>
10	2.2

Series #: (E9) 38 Time: 2114
 Distance from front stake: 110 m
 Depth at sampler: NA
 Breaker type: Plunging
 Notes: Crest before break.

<u>Height above bottom (cm)</u>	<u>SS concentration (g/l)</u>
40	0.12

**SUSPENDED SEDIMENT SAMPLES
AND
CORRESPONDING COASTAL PROCESS MEASUREMENTS**

Station: PH-10

Date: 27 August 1986

Series #: (E10) 39 Time: 2120
 Distance from front stake: 100 m
 Depth at sampler: NA
 Breaker type: Plunging
 Notes: Crest at breaking.

<u>Height above bottom (cm)</u>	<u>SS concentration (g/l)</u>
40	0.201
10	0.601

Series #: (En) 40 Time: 2127
 Distance from front stake: 110 m
 Depth at sampler: NA
 Breaker type: Plunging
 Notes: Trough before breaking.

<u>Height above bottom (cm)</u>	<u>SS concentration (g/l)</u>
40	0.0848
10	18.6

Series #: (E12) 41 Time: 2133
 Distance from front stake: 105 m
 Depth at sampler: NA
 Breaker type: Plunging
 Notes: Crest before breaking.

<u>Height above bottom (cm)</u>	<u>SS concentration (g/l)</u>
40	0.0946
10	2.84

SUSPENDED SEDIMENT SAMPLES
AND
CORRESPONDING COASTAL PROCESS MEASUREMENTS

Station: PH-10

Date: 27 August 1986

Series #: (E13)	42	Time: 2140
Distance from front stake:	115 m	
Depth at sampler:	NA	
Breaker type:	Plunging	
Notes:	Trough before breaking. Inner swash = 90 m: outer break = 95 m cm. $H_b = 60$ cm. $T =$ 4.0 s. Wave angle = 5-1 OR.	

Height above bottom (cm)SS concentration (g/l)

10

0.475

**SUSPENDED SEDIMENT SAMPLES
AND
CORRESPONDING COASTAL PROCESS MEASUREMENTS**

Station: PH-10

Date: 3 September 1986

COASTAL PROCESSES

Observation number:	24A	Visual wave type:	Plunging
Date (month, day, year):	09/03/86	Longshore current velocity (cm/s):	25
Time (24-hour clock):	0945	Longshore current direction viewed from shore:	to right
Wind velocity (mph)	12	Breaker angle/degree:	8
Wind azimuth (degrees True):	165	Distance to inner surf line (m):	100
Breaker height (cm):	75	Distance to outer surf line (m):	130
Breaker depth (cm):	140	Width of surf zone (m):	30
Wave period (seconds):	5.5		

SUSPENDED SEDIMENT

Series #: (F1) 43 Time: 1015
 Distance from front stake: 122 m
 Depth of breaking:
 Breaker type:
 Notes: Crest of breaking wave.

<u>Height above bottom (cm)</u>	<u>SS concentration (g/l)</u>
40	0.15
10	0.379

Series #: (F2) 44 Time: 1035
 Distance from front stake: 125 m
 Depth of breaking:
 Breaker type:
 Notes: Trough southward of breaking wave.

<u>Height above bottom (cm)</u>	<u>SS concentration (g/l)</u>
40	0.139
10	4.61

**SUSPENDED SEDIMENT SAMPLES
AND
CORRESPONDING COASTAL PROCESS MEASUREMENTS**

Station: PH-10

Date: 3 September 1986

Series #: (F3) 45 Time: 1040
 Distance from front stake: 115 m
 Depth of breaking: —
 Breaker type: —
 Notes: Foam after break - at breakpoint.

<u>Height above bottom (cm)</u>	<u>SS concentration (g/l)</u>
10	1.79

Series #: (F4) 46 Time: 1045
 Distance from front stake: 130 m
 Depth of breaking: —
 Breaker type: —
 Notes: Taken outside breakpoint.

<u>Height above bottom (cm)</u>	<u>SS concentration (g/l)</u>
40	0.248
10	0.0406

Series #: (F5) 47 Time: 1110
 Distance from front stake: 110 m
 Depth of breaking: —
 Breaker type: —
 Notes: Foam 5 m inside breakpoint.

<u>Height above bottom (cm)</u>	<u>SS concentration (g/l)</u>
40	0.143
10	41.0

Series #: (F6) 48 Time: 1115
 Distance from front stake: 125m
 Depth of breaking: —
 Breaker type: —
 Notes: Outside breakpoint.

<u>Height above bottom (cm)</u>	<u>SS concentration (g/l)</u>
40	0.0466
10	1.22

**SUSPENDED SEDIMENT SAMPLES
AND
CORRESPONDING COASTAL PROCESS MEASUREMENTS**

Station: PH-10

Date: 3 September 1986

Series #: (F7) 49 Time: 1125
 Distance from front stake: 120 m
 Depth of breaking:
 Breaker type:
 Notes: At breaker crest.

<u>Height above bottom (cm)</u>	<u>SS concentration (g/l)</u>
40	0.219
10	80.671

Series #: (F8) 50 Time: 1130
 Distance from front stake: 118 m
 Depth of breaking:
 Breaker type:
 Notes: At. plunge point.

<u>Height above bottom (cm)</u>	<u>SS concentration (g/l)</u>
40	0.0509
10	1.389

Series #: (F9) 51 Time: 1145
 Distance from front stake: 115 m
 Depth of breaking:
 Breaker type:
 Notes: Inside plunge point a few meters.

<u>Height above bottom (cm)</u>	<u>SS concentration (g/l)</u>
40	0.0624
10	2.126

COASTAL PROCESSES

Observation number:	24B	Visual wave type:	Plunging
Date (month, day, year):	09/03/86	Longshore current velocity (cm/s):	0
Time (24-hour clock):	1155	Longshore current direction viewed from shore:	-
Wind velocity (mph):	11	Breaker angle/degree:	0
Wind azimuth (degrees True):	180	Distance to inner surf line (m):	100
Breaker height (cm):	100	Distance to outer surf line (m):	140
Breaker depth (cm):	80	Width of surf zone (m):	40
Wave period (seconds):	5.0		

**SUSPENDED SEDIMENT SAMPLES
AND
CORRESPONDING COASTAL PROCESS MEASUREMENTS**

Station: PH-10

Date: 4 September 1986

COASTAL PROCESSES

Observation number:	25A	Visual wave type:	Plunging
Date (month, day, year):	09/04/86	Longshore current velocity (cm/s):	37
Time (24-hour clock):	1120	Longshore current direction viewed from shore:	to right
Wind velocity (mph):	25	Breaker angle/degree:	10
Wind azimuth (degrees True):	160	Distance to inner surf line (m):	90
Breaker height (cm):	60	Distance to outer surf line (m):	130
Breaker depth (cm):	120	Width of surf zone (m):	40
Wave period (seconds):	9.5		

SUSPENDED SEDIMENT

Series #: (G1)	52	Time: 1140
Distance from front stake:	118 m	
Depth of breaking:	—	
Breaker type:	—	
Notes:	Outside breaker crest.	

<u>Height above bottom (cm)</u>	<u>SS concentration (g/l)</u>
40	0.117
10	0.367

Series #: (G2)	53	Time: 1145
Distance from front stake:	110 m	
Depth of breaking:	—	
Breaker type:	—	
Notes:	At breaker crest.	

<u>Height above bottom (cm)</u>	<u>SS concentration (g/l)</u>
40	0.146
10	0.577

**SUSPENDED SEDIMENT SAMPLES
AND
CORRESPONDING COASTAL PROCESS MEASUREMENTS**

Station: PH-10

Date: 4 September 1986

Series #: (G3) **54** Time: 1150
Distance from front stake: 108 m
Depth of breaking:
Breaker type:
Notes: **Near plunge point.**

<u>Height above bottom (cm)</u>	<u>SS concentration (g/l)</u>
40	0.106
10	17.96

Series #: (G4) **55** Time: 1200
Distance from front. stake: 105 m
Depth of breaking:
Breaker type:
Notes: **In bore a few meters landward of plunge point.**

<u>Height above bottom (cm)</u>	<u>SS concentration (g/l)</u>
40	0.122
10	10.607

Series #: (G5) **56** Time: 1210
Distance from front stake: 110 m
Depth of breaking:
Breaker type:
Notes: **Outside breaker crest.**

<u>Height above bottom (cm)</u>	<u>SS concentration (g/l)</u>
40	0.441
10	1.055

COASTAL PROCESSES

Observation number:	25B	Visual wave type:	Plunging
Date (month, day, year):	09/04/86	Longshore current velocity (cm/s):	53
Time (24-hour clock):	1230	Longshore current direction viewed from shore:	to right
Wind velocity (mph):	28	Breaker angle/degree:	10
Wind azimuth (degrees True):	160	Distance to inner surf line (m):	95
Breaker height (cm):	80	Distance to outer surf line (m):	140
Breaker depth (cm):	90	Width of surf zone (m):	45
Wave period (seconds):	7.5		

**SUSPENDED SEDIMENT SAMPLES
AND
CORRESPONDING COASTAL PROCESS MEASUREMENTS**

Station: PH-10

Date: 6 September 1986

COASTAL PROCESSES

Observation number:	27A	Visual wave type:	Collapsing
Date (month, day, year):	09/06/86	Longshore current velocity (cm/s):	22
Time (24-hour clock):	1335	Longshore current direction viewed from shore:	to right
Wind velocity (mph):	13	Breaker angle/degree:	18
Wind azimuth (degrees True):	150	Distance to inner surf line (m):	90
Breaker height (cm):	60	Distance to outer surf line (m):	100
Breaker depth (cm):	30	Width of surf zone (m):	10
Wave period (seconds):	8.0		

SUSPENDED SEDIMENT

Series #: (Hi-a) 57 Time: 1410
 Distance from front stake: 105 m
 Depth at sampler: 1 m
 Breaker type: —
 Notes: Outside breaker crest.

<u>Height above bottom (cm)</u>	<u>SS concentration (g/l)</u>
90	0.188
40	0.193
10	0.242

Series #: (Hi-b) 58 Time: 1410
 Distance from front stake: 99 m
 Depth at sampler: 0.40 m
 Breaker type: —
 Notes: Synoptic with Series #57. Trough before breaking.

<u>Height above bottom (cm)</u>	<u>SS concentration (g/l)</u>
10	0.518

**SUSPENDED SEDIMENT SAMPLES
AND
CORRESPONDING COASTAL PROCESS MEASUREMENTS**

Station: PH-10

Date: 6 September 1986

Series #: (H2) 59 Time: 1415
 Distance from front stake: 99 m
 Depth at sampler: 0.4 m
 Breaker type:
 Notes: In breaker crest.

<u>Height above bottom (cm)</u>	<u>SS concentration (g/l)</u>
10	0.877

Series #: (H3) 60 Time: 1420
 Distance from front stake: 120 m
 Depth at sampler: 1.5 m
 Breaker type:
 Notes: Outside breaker crest.

<u>Height above bottom (cm)</u>	<u>SS concentration (g/l)</u>
90	0.0995
40	0.116
10	0.145

Series #: (H4) 61 Time: 1430
 Distance from front stake: 99 m
 Depth at sampler: 0.4 m
 Breaker type:
 Notes: 3 seconds after break in bore.

<u>Height above bottom (cm)</u>	<u>SS concentration (g/l)</u>
10	0.441

Series #: (H5-a) 62 Time: 1440
 Distance from front stake: 110 m
 Depth at sampler: 1.2 m
 Breaker type:
 Notes: Outside breaker crest.

<u>Height above bottom (cm)</u>	<u>SS concentration (g/l)</u>
90	0.177
40	0.125
10	0.204

**SUSPENDED SEDIMENT SAMPLES
AND
CORRESPONDING COASTAL PROCESS MEASUREMENTS**

Station: PH-10

Date: 6 September 1986

Series #: (H5-b) 63 Time: 1440
 Distance from front stake: 99 m
 Depth of breaking:
 Breaker type:
 Notes: Synoptic with Series #62. Near plunge point.

<u>Height above bottom (cm)</u>	<u>SS concentration (g/l)</u>
10	7.194

Series #: (H6) 64 Time: 1445
 Distance from front stake: 99 m
 Depth at sampler: 0.3 m
 Breaker type:
 Notes: Taken just before wave collapse. Sampling backrush and upwell near plunge point.

<u>Height above bottom (cm)</u>	<u>SS concentration (g/l)</u>
10	11.33

Series #: (H7) 65 Time: 1450
 Distance from front stake: 140 m
 Depth at sampler: 2.20 m
 Breaker type: —
 Notes: Beyond breaker line. Representative of background concentration.

<u>Height above bottom (cm)</u>	<u>SS concentration (g/l)</u>
200	0.047
40	0.084
10	0.165

**SUSPENDED SEDIMENT SAMPLES
AND
CORRESPONDING COASTAL PROCESS MEASUREMENTS**

Station: PH-10

Date: 6 September 1986

Series #: (H8) 66 Time: 1455
 Distance from front stake: 95 m
 Depth of breaking:
 Breaker type:
 Notes:

<u>Height above bottom (cm)</u>	<u>SS concentration (g/l)</u>
10	58.439

Series #: (H9) 67 Time: 2505
 Distance from front stake: 96 m
 Depth at sampler: 0.20 m
 Breaker type: -
 Notes: Taken after bore passed.

<u>Height above bottom (cm)</u>	<u>SS concentration (g/l)</u>
10	2.882

Series #: (H10) 68 Time: 1515
 Distance from front stake: 95 m
 Depth at sampler: 0.10 m
 Breaker type:
 Notes: Just after bore passed.

<u>Height above bottom (cm)</u>	<u>SS concentration (g/l)</u>
10	0.289

COASTAL PROCESSES

Observation number:	27B	Visual wave type:	Collapsing
Date (month, day, year):	09/06/86	Longshore current velocity (cm/s):	
Time (24-hour clock):	1520	Longshore current direction viewed from shore:	to right
Wind velocity (mph):	10	Breaker angle/degree:	14
Wind azimuth (degrees True):	260	Distance to inner surf line (m):	90
Breaker height (cm):	70	Distance to outer surf line (m):	100
Breaker depth (cm):		Width of surf zone (m):	10
Wave period (seconds):	—		

SUSPENDED SEDIMENT SAMPLES
AND
CORRESPONDING COASTAL PROCESS MEASUREMENTS

Station: PH-10

Date: 7 September 1986

COASTAL PROCESSES

Observation number:	28A	Visual wave type:	Spilling
Date (month, day, year):	09/07/86	Longshore current velocity (cm/s):	0
Time (24-hour clock):	1345	Longshore current direction viewed from shore:	-
Wind velocity (mph):	26	Breaker angle/degree:	0
Wind azimuth (degrees True):	290	Distance to inner surf line (m):	-
Breaker height (cm):	130	Distance to outer surf line (m):	-
Breaker depth (cm):	160	Width of surf zone (m):	-
Wave period (seconds):	7.2		

SUSPENDED SEDIMENT

Series #: (11) 69 Time: 1420
Distance from front stake: 110 m
Depth at sampler: 140 cm secondary breaker
Breaker type: Spilling
Notes: sample in bore approximately 5 m landward of
break point. $H_b = 120$ cm.

<u>Height above bottom (cm)</u>	<u>SS concentration (g/l)</u>
90	0.161
40	0.14
10	2.582

Series #: (12) 70 Time: 1425
Distance from front stake: 105 m
Depth at sampler: 0.90 m
Breaker type: Spilling
Notes: Sampled 8 m landward of break point in bore
approximately 4 seconds after wave passed. H_b
= 120 cm.

<u>Height above bottom (cm)</u>	<u>SS concentration (g/l)</u>
90	0.176
40	0.273
10	1.636

**SUSPENDED SEDIMENT SAMPLES
AND
CORRESPONDING COASTAL PROCESS MEASUREMENTS**

Station: PH-10

Date: 7 September 1986

Series #: (13) 71 Time: 1435
 Distance from front stake: 110 m
 Depth at sampler: 120 cm
 Breaker type: Bore
 Notes: Inner surf, secondary breaker, depth sampled
 120 cm, taken 10 m inside break point. $H_b =$
 140 cm.

<u>Height above bottom (cm)</u>	<u>SS concentration (g/l)</u>
90	0.132
40	0.128
10	25.466

Series #: (14) 72 Time: 1445
 Distance from front stake: 110 m
 Depth at sampler: 110 cm
 Breaker type: Spill at crest
 Notes: Taken at break point as crest passed the
 sampler, total water depth approximately 220
 cm. $H_b = 110$ cm.

<u>Height above bottom (cm)</u>	<u>SS concentration (g/l)</u>
90	0.118
40	0.24
10	1.804

Series #: (15) 73 Time: 1506
 Distance from front stake: 104 m
 Depth at sampler: 110 cm
 Breaker type: Spilling
 Notes: Primary waves breaking approximately 140 m
 mark, inner swash up to 80 m mark (berm
 crest). $H_b = 100$ cm. $d_b = 120$ cm.

<u>Height above bottom (cm)</u>	<u>SS concentration (g/l)</u>
90	0.0473
40	0.138
10	2.263

SUSPENDED SEDIMENT SAMPLES
AND
CORRESPONDING COASTAL PROCESS MEASUREMENTS

Station: PH-10

Date: 7 September 1986

Series #: (16)	74	Time: 1515
Distance from front stake:	105 m	
Depth of breaking:	140 cm	
Breaker type:	Spilling	
Notes:	Taken in bore approximately 5 m inside break point after bore passed. $H_b = 130$ cm.	

<u>Height above bottom (cm)</u>	<u>SS concentration (g/l)</u>
90	0.085
40	0.165
10	0.26

COASTAL PROCESSES

Observation number:	28B	Visual wave type:	Spilling
Date (month, day, year):	09/07/86	Longshore current velocity (cm/s):	0
Time (24-hour clock):	1525	Longshore current direction viewed from shore:	-
Wind velocity (mph):	35	Breaker angle/degree:	0
Wind azimuth (degrees True):	280	Distance to inner surf line (m):	80
Breaker height (cm):	180	Distance to outer surf line (m):	150
Breaker depth (cm):	-	Width of surf zone (m):	70
Wave period (seconds):	6.8		

SUSPENDED SEDIMENT SAMPLES
AND
CORRESPONDING COASTAL PROCESS MEASUREMENTS

Station: PH-10

Date: 8 September 1986

COASTAL PROCESSES

Observation number:	29	Visual wave type:	Spilling
Date (month, day, year):	09/08/86	Longshore current velocity (cm/s):	0
Time [24-hour clock]:	1355	Longshore current direction viewed from shore:	-
Wind velocity (mph):	32	Breaker angle/degree:	0
Wind azimuth (degrees True):	315	Distance to inner surf line (m):	80
Breaker height (cm):	120	Distance to outer surf line (m):	250
Breaker depth (cm):	150	Width of surf zone (m):	170
Wave period (seconds):	6.0		

SUSPENDED SEDIMENT

Series #: (J1-a) 75 Time: 1415
 Distance from front stake: 120 m
 Depth of breaking: 170 cm
 Breaker type: Spilling
 Notes: Depth of water in bore 190 cm, 120-220 range
 of bore 10 m inside break point after bore. H_b
 = 120 cm.

<u>Height above bottom (cm)</u>	<u>SS concentration (g/l)</u>
90	1.795
40	0.179
10	14.829

Series #: (J1-b) 76 Time: 1415
 Distance from front stake: 125 m
 Depth of breaking: 210 cm
 Breaker type: Spilling
 Notes: One bore at 200 cm, synoptic with Series #75.

<u>Height above bottom (cm)</u>	<u>SS concentration (g/l)</u>
10	0.184

SUSPENDED SEDIMENT SAMPLES
AND
CORRESPONDING COASTAL PROCESS MEASUREMENTS

Station: PH-10

Date: 8 September 1986

Series #: (J2) 77 Time: 1430
 Distance from front stake: 115 m
 Depth of breaking: 150 cm
 Breaker type: Spilling
 Notes: 180 cm (depth at 5 m inside wave after bore),
 bottom (10 cm) sampler not closed because of
 pea gravel. Concentration should be higher at
 10 cm above bed. $H_b = 120$ cm.

<u>Height above bottom (cm)</u>	<u>SS concentration (g/l)</u>
90	0.121
40	0.10
10	8.974

Series #: (J3-a) 78 Time: 1440
 Distance from front stake: 110 m
 Depth of breaking: 170 cm
 Breaker type: Spilling
 Notes: Broke 5 m seaward, sampled as bore passed.
 170 cm at sample. $H = 130$ cm: middle
 sample leaked.

<u>Height above bottom (cm)</u>	<u>SS concentration (g/l)</u>
90	0.888
40	0.0475
10	12.429

Series #: (J3-b) 79 Time: 1440
 Distance from front stake: 118 m
 Depth of breaking: 220 cm
 Breaker type: Spilling
 Notes: 2 m after wave broke, synoptic with Series
 #78. $H_b = 180$ cm.

<u>Height above bottom (cm)</u>	<u>SS concentration (g/l)</u>
10	57.826

SUSPENDED SEDIMENT SAMPLES
AND
CORRESPONDING COASTAL PROCESS MEASUREMENTS

Station: PH-10

Date: 8 September 1986

Series #: (J4-a) 80 Time: 1452
 Distance from front stake: 100 m
 Depth of breaking: 150 cm
 Breaker type: Spilling
 Notes: 80 cm at sample, inner swash 20 m inside
 break point/wave. Not same wave as J4-b.

<u>Height above bottom (cm)</u>	<u>SS concentration (g/l)</u>
40	0.0812
10	0.945

Series #: (J4-b) 81 Time: 1452
 Distance from front stake: 103 m
 Depth of breaking: 90 cm
 Breaker type: Spilling
 Notes: - 5" m past (landward) of break, synoptic with
 Series #80. $H_b = 80$ cm.

<u>Height above bottom (cm)</u>	<u>SS concentration (g/l)</u>
10	0.572

Series #: (J5-a) 82 Time: 1505
 Distance from front stake: 105 m
 Depth of breaking: 150 cm
 Breaker type: Spilling
 Notes: in bore at 150 cm, 80 cm over bore, 110 cm
 under bore.

<u>Height above bottom (cm)</u>	<u>SS concentration (g/l)</u>
90	0.130
40	0.151
10	11.649

SUSPENDED SEDIMENT SAMPLES
AND
CORRESPONDING COASTAL PROCESS MEASUREMENTS

Station: PH-10

Date: 8 September 1986

Series #: (J5-b) 83 Time: 1505
Distance from front stake: 100 m m
Depth of breaking: 120 cm
Breaker type: Spilling
Notes: 5 m landward of break, synoptic with Series
#82.

Height above bottom (cm)SS concentration (g/l)

10

13.692
